Copy 1

Joint Program:
Woods Hole Oceanographic Institution
Dokuz Eylül University

Temporal and Spatial Variability in Sedimentation in the Black Sea:

Cruise Report

R/V *Knorr* 134-8, Black Sea Leg 1
April 16 - May 7, 1988

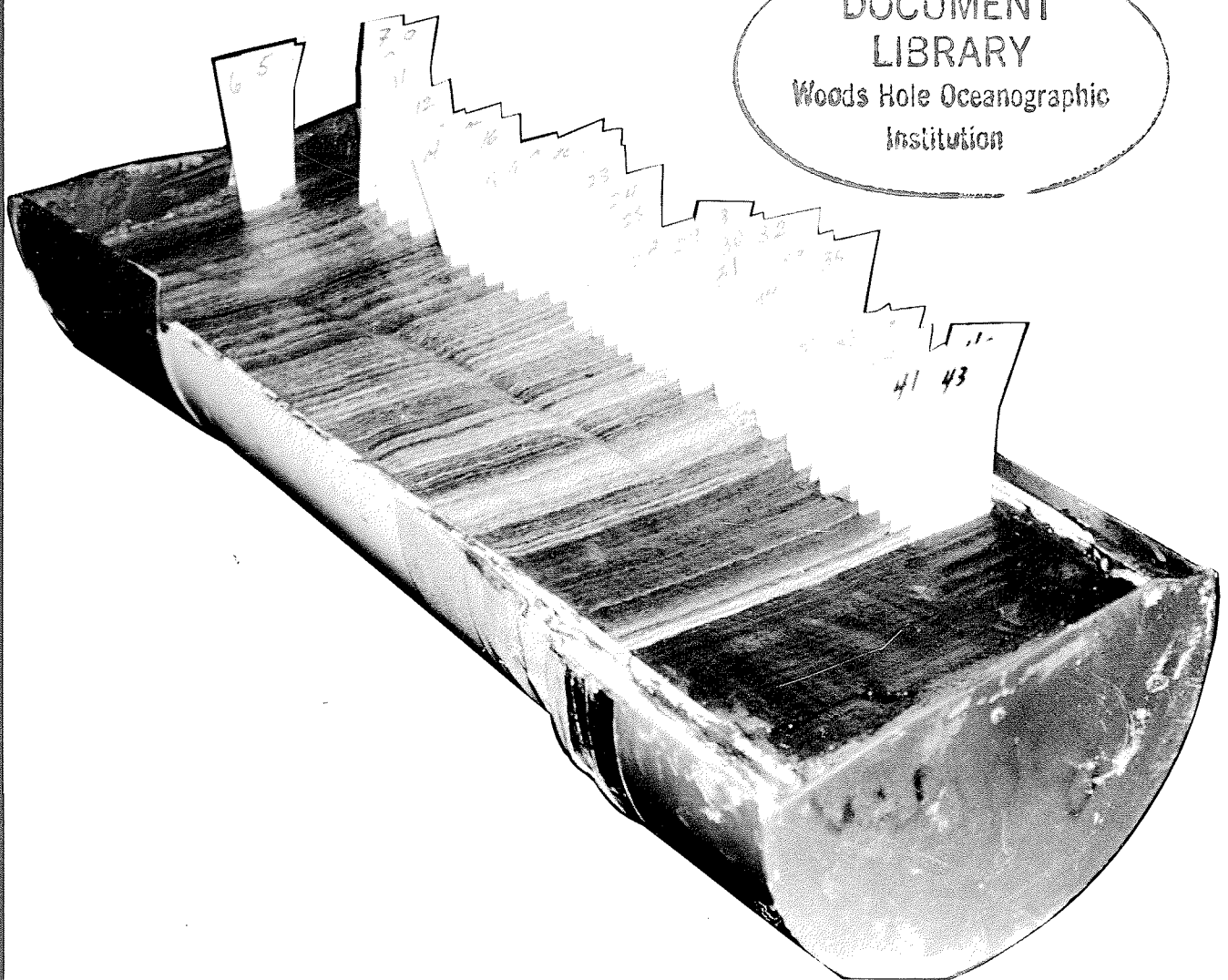

Sponsored by the National Science Foundation, Washington, D.C.

WHOI-88-35

Temporal and Spatial Variability in Sedimentation in the Black Sea:

Cruise Report R/V Knorr 134-8, Black Sea Leg 1 April 16 - May 7, 1988

by

S. Honjo, B. J. Hay, and Members of the Scientific Shipboard Party

Woods Hole Oceanographic Institution
Woods Hole, Massachusetts 02543

Dokuz Eylül University
Institute of Marine Science and Technology
35213 Izmir, Turkey

October 1988

Technical Report

Funding was provided by the National Science Foundation under various grants to shipboard participants

Approved for publication: distribution unlimited.

Approved for Distribution:

David A. Ross, Chairman
Geology and Geophysics Department

TEMPORAL AND SPATIAL VARIABILITY IN SEDIMENTATION IN THE BLACK SEA:

CRUISE REPORT
R/V *Knorr* 134-8, Black Sea Leg 1
April 16 - May 7, 1988

(complete edition)

Woods Hole Oceanographic Institution Technical Report WHOI-88-35.
Piri Reis International Contribution Series Number 6.

Photo on front page: Well-preserved varves in recent Black Sea sediment collected with a Mark III box corer near station BSK3 (BC 55). This site is located near site 1474 of the R/V *Atlantis* cruise in 1969 (e.g. Degens and Ross, 1974). The surface "fluff" layer of this box core was recovered intact. This subcore is in the process of being prepared for very detailed subsampling. Sample number 43 marks the boundary between the older Unit II (sapropel) and the younger Unit I (coccolith ooze). Notice that the transition from Unit II to Unit I is not abrupt; instead there was a period of roughly 50 years (assuming annual deposition of one varve couplet) of coccolith deposition followed by another period of possibly several hundert years of sapropel deposition before finally coccoliths became the dominant biogenic particles in the sediment. *(Photo by John Porteous)*

JOINT PROGRAM

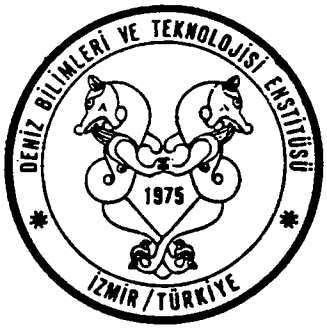

DOKUZ EYLÜL ÜNIVERSITESI
Institute of Marine Science & Technology
P.O. Box 478
35213 Izmir, Turkey
Telephone: 25-43-38
Telex: 52889 dbte

Woods Hole Oceanographic Institution
Woods Hole, Massachusetts 02543 USA
Telephone: (508) 548-1400
Telex: 951679 oceaninst wooh

Editorial Comments

The focus of Leg 1 of the R/V Knorr cruise to the Black Sea was to study the biogeochemical variability in sedimentation in the present and throughout the anoxic history of the Black Sea with high spatial and temporal resolution. This involved research on the particulate matter in the water column as well as research on the particle deposition in the recent past by investigating the laminated bottom sediments by taking high-quality box and gravity cores with ideally well-preserved core tops. This cruise report is organized to reflect this division between water column work (presented in cruise report section IV) and bottom sediment work (presented in cruise report section V). Projects related to these two sampling environments are listed within these two main sections. Most projects were multidisciplinary; this is reflected by the multiple authors of the individual cruise report sections.

Drafts of reports included in this cruise report were written by the cruise participants and submitted to the Chief Scientist prior to disembarking from the vessel in Instanbul. All manuscripts were internally reviewed by Drs. M. Arthur, W. Dean, B. Hay, and S. Honjo. Dr. B. Hay dedicated his time as technical editor, assisted by E. Evans, Woods Hole Oceanographic Institution. In this volume we have included only the reports of projects which generated new data and new observations during the cruise.

All numerical data generated during the cruise will be filed at the National Oceanographic Data Center. Inquiry at NODC regarding R/V Knorr 134-8 data can be referred to George Heimerdinger. The navigational data will be filed in the Digital Data Library, Woods Hole Oceanographic Institution. The following three kinds of data have not been included in this cruise report but copies are available by inquiries to designated personnel:

1. "Box core descriptions, R/V Knorr 134-8" by W. Dean and M. Arthur. Available from these authors or from J. Broda, Core Library, Woods Hole Oceanographic Institution.

2. "Navigation Log and Precision Plots, Voyage 134-8, kept by the bridge, R/V Knorr. 41 pages. Available from the Port Office, Woods Hole Oceanographic Institution.

3. "Satellite Navigation Data." Position fixes and depths (uncorrected) taken at every one minute. Available from M. Realander, School of Oceanography, University of Washington, Seattle, WA 98195.

4. "On-board activities, Black Sea Leg 1." Cruise report on video cassette. Produced and edited by M. Arthur. Available from Dr. M.

Arthur, Graduate School of Oceanography, University of Rhode Island, Narragansett, RI 02882.

Results based on the large number of samples and measurements presented in this report were mostly compiled at the end of the cruise leg on the R/V Knorr; conclusions drawn from these data are largely preliminary and will be widely expanded over the next months and years. Major results of this cruise leg are summarized in cruise report section II; details on cruise logistics and labeling of samples are presented in cruise report section III.

Acknowledgments

The Turkish-USA joint research expedition in the Black Sea on the R/V Knorr, Woods Hole Oceanographic Institution, was sponsored by the National Science Foundation, Washington, D.C. The basic framework of the 3-month long cruise, divided into 6 legs, was originally drafted as an agreement at an executive committee meeting at Dokuz Eylül University, Izmir, Turkey on June 5, 1987. This meeting was chaired by Dr. E. Izdar and the participants were Dr. Neil Andersen (ex. officio), Dr. Turgut Balkas, Dr. Susumu Honjo, Dr. Holgar Jannasch, Dr. James Murray (US Executive Committee Chairman) and Dr. Ümit Ünlüata.

The first leg of the expedition, under the general title "Temporal and Spatial Variability in Sedimentation in the Black Sea," R/V Knorr 134-8, supported by the National Science Foundation, was carried out in the true spirit of international collaboration. First, we heartily thank Dr. E. Izdar, whose leadership caused this expedition to materialize. American and German participants are deeply indebted to the Turkish Government and the Turkish Research Council who granted us permission to pursue oceanographic research work, including long-term, large mooring experiments, in their exclusive economic zone. We also thank the U.S. State Department and the National Science Foundation who smoothly handled the negotiations necessary to gain research permission for this leg.

We thank Dr. T. Konuk and all the members of the Institute of Marine Science and Technology, Izmir, who rendered expert logistic support as well as numerous useful suggestions for organizing this research cruise. They have generously shown their unpublished data on the marine geology of the Black Sea to all of us before and during the cruise which contributed to making this research cruise successful.

Prior to the departure of the cruise, all the scientists and officers who participated on this leg were warmly greeted by a wide range of Turkish scientific colleagues, and state and local officials at a generous reception at the Faculty Club of the University which was sponsored by Dr. Namik Cevik, the Chancellor of Dokuz Eylül University. During the reception, beautiful plaques were presented from the University to Chief

Scientist, Dr. S. Honjo, and the scientific party, to Master R.J. Bowen and the officers and crew of the R/V Knorr, and to Capt. J.L. Coburn for the Woods Hole Oceanographic Institution.

In turn, WHOI sponsored a reception on board the R/V Knorr for Turkish scientific colleagues and officials as a means of thanks for all the support received for this cruise and to encourage further international scientific cooperation. S.M. Lauzon, Manager of Publications and Information, Woods Hole Oceanographic Institution, coordinated the publicity of the R/V Knorr's visit to Turkey. We also thank Dr. Nihal Atuk who participated in the reception representing the Turkish State Planning Organization, Ankara.

All members of the onboard scientific party, and officers and crew of the R/V Knorr warmly thank Consul General Albert N. Williams and his staff who genuinely helped so much in assisting to smooth matters relating to differences in regulations and customs between US and Turkish procedures.

Our sincere thanks goes to Master R. J. Bowen, Boatswain J. M. Cotter, the officers and crew of the R/V Knorr, Woods Hole Oceanographic Institution. Without their dedicated support and hard work around the clock at sea and skilled business acumen in dealing with daily difficulties, this leg would never have been completed successfully.

Last but not least, we thank Paul Dudley-Hart, Woods Hole Oceanographic Institution, who informed us under extremely difficult communications conditions, of mechanical problems with the gravity coring device which occurred during the previous leg, and who remained on board to advise us until our scientific party was able to solve the problem. Our enormous success in collecting excellent gravity cores is partially due to his dedication to making his colleague's leg successful.

Dedication

The onboard scientific party expresses sincere thanks and congratulations to Dr. Egon T. Degens, University of Hamburg, West Germany, an international leader in Black Sea research who joined the R/V Knorr, along with Dr. E. Izdar, for a portion of the first leg from Izmir to Istanbul. Dr. Degens was a co-leader of the well-known R/V Atlantis II trip, Woods Hole Oceanographic Institution, to the Black Sea in 1969 with Dr. D.A. Ross; their cruise firmly established modern oceanography in the Black Sea with new concepts and methodologies. Dr. Degens contributed to the organization of this 1988 leg as a senior advisor since the leg was first planned. He stimulated all of us to participate in vigorous discussions which fueled our enthusiasm throughout the leg. As a means of thanks for his scientific generosity and encouragement to all of us onboard ship, this volume is sincerely dedicated to our friend and colleague, Dr. Egon T. Degens.

Table of Contents

Table of Contents (continued) Page

I. LIST OF PARTICIPANTS AND FUNDING SUPPORT

Chief Scientist		
Susumu Honjo	Woods Hole Oceanographic Institution	OCE8614363
Cruise Coordinator		
Bernward Hay	Woods Hole Oceanographic Institution	OCE8614363
Steering Committee		
Arthur, Michael, Dr.	University of Rhode Island	OCE8711741
Kempe, Stephan, Dr.	University of Hamburg	
Konuk, Y. Tosun, Dr.	Dokuz Eylül University	(†)
Scientific participants		
Algan, Oya	University of Istanbul	
Asper, Vernon, Dr.	University of Southern Mississippi	OCE8619191 OCE8614438
Benli, Huseyin, Dr.	Dokuz Eylül University	(†)
Bilgic, Tayfun	General Directorate of Mineral Research and Exploration, Turkey	
Briskin, Madeleine, Dr.	University of Cincinnati	(**)
Broda, James	Woods Hole Oceanographic Institution	OCE8614363
Dean, Walter, Dr.	U.S. Geological Survey, Denver	(††)
Degens, Egon, T., Dr. *	University of Hamburg	
Derman, A. Sami	Turkish Petroleum Corporation	
Diercks, R. Arne	University of Hamburg	
Duman, Muhammed	Dokuz Eylül University	(†)
Gagnon, Alan	Woods Hole Oceanographic Institution	OCE8712181
Izdar, Erol, Dr. *	Dokuz Eylül University	(†)
Liebezeit, Gerd, Dr.	University of Hamburg	
Lobsiger, Urich, Dr. *	Lobsiger Associates, Inc., Canada	
Neff, Eric, D.	University of Rhode Island	OCE8711741
Nicholson, JoAnn	Cornell University	
Pilskaln, Cynthia H., Dr.	Monterey Bay Aquarium Research Inst.	OCE8614557
Realander, Michael	University of Washington	
Woodward, Bonnie L.	Woods Hole Oceanographic Institution	OCE8614363

* Participated on the subleg from Izmir to Istanbul. Exchanged with Algan, Derman, Duman in Istanbul.

(**) State of Ohio University Fund #: 8-19195-3317-46

(†) Dokuz Eylül University Research Grants No. 0921-83-01-02 and 0921-84-01-01

(††) U.S.G.S. Climate Program and OCE8711741.

II. CRUISE SUMMARY, R/V KNORR CRUISE 134, LEG 8
April 16 to May 7, 1988

Susumu Honjo, Chief Scientist

The 24 scientific members on board the R/V Knorr concluded Cruise 134, Leg 8, in the southern Black Sea with great success. We started from Izmir on April 16, crossing almost the entire east-west section of the Black Sea with three subtransects in a north-south direction along the Anatolian coast, completed a station in the Marmara Sea, and returned to Istanbul on May 7, 1988. We accomplished every goal set for this leg and more during this 3 week cruise. Members of the scientific party on board the ship were always in high spirits. The officers and crew of the ship did everything possible to make this research cruise successful. In addition, we were blessed with quiet seas and fine weather. The international scientific staff of 7 Turkish, 4 German, 1 Canadian, and 14 American scientists composed a multidisciplinary team with many specialities that worked together extremely well to achieve the common objectives of this leg. There was no major loss of time caused by equipment failure or accidents, and no injuries or serious illnesses were reported.

The University of Washington's CTD system proved to be a reliable system for obtaining physical and chemical characteristics of the water column. The software was fast, flexible and user-friendly. All thirty-two CTD profiles taken in the Black Sea showed that the upper 200 m of the water column in the Black Sea is highly structured, both vertically and laterally. The maximum density gradient at about 15 sigma-T, separating the surface water and deep water, occurs at a depth of approximately 50 m in the center of the basin and below 120 m at the edge. The vertical density distribution shows step-like features, suggesting intense layering of the surface water, possibly maintained by shearing of currents. The "pycnocline-induced" suspended particle layer at the interface between the oxic shallow water and anoxic deep water was observed during all stations of transmissometer/CTD or marine snow camera lowerings. The suspended sediment layer varies in structure and actually consists of several peaks that vary in thickness and amplitude. The internal structure appears to be related to the internal layering of water and not simply to chemical processes. The thickness and particle density of a layer increase several-fold toward the coast. Replicated casts at about the same location failed to reproduce the patterns observed even a few hours before, suggesting that there is strong temporal variation in this layer. The vertical distribution of many chemical criteria was examined during this leg including a study to clarify the variability of dissolved sulfide profiles in the upper 300 m in time and space.

The marine snow camera successfully made 14 profiles and took 9,274 particle photographs. Analysis of the results awaits photo development and computerized image analysis on shore. The particle flux camera made an important discovery during this leg. It was deployed at a depth of 400 m for 10 days from April 24 to May 3 at mapsite BSK2. A preliminary onboard examination of time-lapsed camera film revealed the modes and speeds of settling of large particles during these 10 days. Some particles were as large as a few millimeters, often occurring as elongated (comet-shaped) aggregates.

Large particles were also observed by the Mini-Rover TV camera deployed through the shallow oxic water and the suspended sediment layer to a depth of 200 m. The TV camera of the Mini-Rover also was used to obtain a general idea of the water column ecostructure. The Mini-Rover further monitored the fluff layer on top of the bottom sediment.

We completed 6 profiles and 15 surface water suspended-particle stations by filtering 1.3 to 3 liters of water through pre-weighed Nuclepore filters. Particles from the suspended sediment layer were collected by positioning a submersible micro-pump in this layer. Up to 18 liters of water were filtered through a 10 cm diameter membrane filter. Suspended particles collected on the filter were largely fine-grained; particles and larger flocculents included particles covered with manganese oxide minerals. Particles larger than 1 mm in diameter were collected at a rate of less than one particle per liter.

A sediment trap mooring experiment, which has been deployed at mapsite BSC since June, 1986 to monitor the radionuclide fallout into the interior of the Black Sea in the aftermath of the Chernobyl accident, was successfully completed. We will conclude the radionuclide fallout research with this set of samples, combined with an extensive collection of intact bottom surface fluff sediment which is suspected to be anthropogenically hot. Although the results are not conclusive at this time, analysis of sulfide dissolved in the supernatant of the sediment trap sampling cups from mapsite BSC raises the possibility that some dissolved sulfide was lost, possibly during the recovery, although the solid phases were intact. Sediment traps deployed at this Black Sea station have been used continuously for over 6 years, and fatigue of the sealings on the sampler cups is suspected.

We deployed a total of 4 mooring arrays with 8 time-series sediment traps at 4 locations on a quasi-SYNCTISE (synchronized time-series) schedule. Individual samplers on all traps in the Black Sea, starting on August 1, 1988 will by synchronized; the sampling interval will be one month. Two Mark 5-12 traps with 1.2 m^2 openings, are deployed at station BSK2 at two depths to collect samples for about 3 months with close time increments. This array will be recovered during Leg 5 in August and then redeployed at the same location. This summer collection at mapsite BSK2 will provide flux samples for all participants of the international expedition. We deployed 2 traps in the Sea of Marmara on May 7.

The R/V. K. Piri Reis will recover all 3 moorings in the Black Sea in August, 1989; the Marmara Sea mooring will be recovered in October of this year. The successful recovery of all mooring systems will make a significant contribution to J-GOFS by the Turkish marine scientific community. American scientists with skills in mooring recovery will participate on all the R/V K. Piri Reis recovery cruises.

Throughout this leg we collected 62 giant gravity cores, up to 5.2 m long, and 30 box cores. The pelagic Black Sea sediment, in particular in the upper 50 cm of varved sediment of Unit 1 and interbedded turbidite units, are soupy and water-saturated. As a result, the box corer tends to over-penetrate and the gravity corer sometimes does not retain sediment. We overcame these inherent difficulties by using a newly designed core-catcher for the gravity corer and properly distributed resistant plates on the pedestal of the box corer. The recovery success of the cores during this leg, gravity and box cores combined, was 92%.

Successful recoveries of the intact water-sediment interface provided detailed observation of the surface "fluff" layer and annual varve formation. The fluff layer in our box cores was several millimeters thick. In a few box cores in which the water-sediment interface was extraordinarily well preserved during the recovery, continuous formation of varves within the fluff layer and uppermost Unit 1 sediment was observed; thicker and less clearly defined laminae on the top gradually turned to thinner and well demarcated black-and-white couplets which continued into Unit 1. Comparison of the fluff material with time-series sediment trap material will contribute to an understanding of processes and fate of particles settling to the sea floor.

Distinctive light and dark varve packages were used to correlate Unit 1 sediments across the entire Black Sea basin for a distance of more than 1,400 km. Local disturbances caused by occasional turbidite intrusions expanded the sequences, but apparently were "inserted" with little if any erosion of the varve sequence. This continuity of Unit 1 varve sequences from the western to the eastern extremes of the basin is indeed surprising in light of the heterogeneous source of hemipelagic sediment in the Black Sea. This is the first time that modern or ancient varves have been correlated over such a great distance, although Ross et al. (1970) suggested that such correlation was possible but provided no detailed documentation. The apparent onset of calcareous nannoplankton deposition at the very end of Unit 2 suggests that a coccolith-tolerant environment did become established as one sharp event but there were some reversals to more sapropelic mud deposition before calcareous nannoplankton and chalks finally became dominant in the Black Sea. Preliminary counts of varve couplets by X-radiography indicates an age of 1075 years B.P. for the onset of coccolith sedimentation, assuming annual deposition of one couplet. We will seek confirmation of this age with TAMS ^{14}C dating.

The collected sediment will allow a very detailed paleoflux study. Extension of individual laminae across the entire basin strongly suggests

basin-wide processes in the deposition of particles in this hemipelagic environment. Preservation of the core tops will allow precise age dating by varve counts. The biogeochemical composition can be studied in the characteristic areas as proposed: at key mapsites BSK1-3 as well as one key site each on the eastern slope, western slope, and southern slope; now sufficient sediment is available for a detailed multidisciplinary study. Later, the newly deployed sediment trap samples will allow close comparison with the hemipelagic laminated sediment.

An onboard extruded and split gravity core (GGC71) recovered from a water depth of 411 m on a slope allowed us to estimate the time at which the oxic interface rose to approximately 400 m and above in the far-eastern part of the Black Sea. The upper 170 cm of the core is laminated, with no manganese oxide deposition indicating anoxia. Preliminary laminae counting showed that the estimated beginning of anoxia was 2,040 years ago. This age is older than the age estimated for the base of Unit 1 in the deep basin and suggests that the initiation of anoxia at 400 m occurred during the later part of the Unit 2 sapropel deposition. Below this laminated sequence is a well-bioturbated zone followed by extensive deposition of manganese oxide minerals.

Uncontaminated sediment sampling for C-14 dating was successful. Beside the 20 box core samples of Unit 1 sequences, we also collected wood pieces, fish remains, and other matter within the varves. Some of these samples will be suitable for improved age determinations of sediment Units 1 and 2. Three sediment traps deployed at 400 m below the surface at stations BSK1, 2, and 3 were prepared using C-14-free cleaning preparations. Organic and carbonate carbon to be collected by these sediment traps will also be dated by the TAMS method. Successful dating of the surface fluff layer and settling particles will help to resolve the contradiction between the ages based on varve counting and C-14 ages of laminae in Unit 1 and 2 sequences.

In the basin sediment there is a general lack of benthic activity except for anaerobic bacterial metabolism. Furthermore, high sedimentation rates prevent the usual time-related processes from occurring. Thus, the chemical composition of pore water is largely controlled by the source function. In most box core profiles, silicic acid decreased with depth. Pore waters of turbidite layers generally had considerably less silicic acid content than varved sediments. Stratigraphic units are clearly discernable in silicic acid and in the RDP and TDP profiles in the pore water profiles in two gravity cores which were extruded and opened onboard. Concentration of all dissolved phosphorus in the pore water extracted from the oxygenated sequence below the Unit 1 in GGC66 was extremely low.

Turkish scientists will research the details of turbidite distribution in time and space in the Black Sea. Preliminary conclusions were: 1. turbidite layers are more abundant at the Anatolian side of the Black Sea; 2. the turbidite layers in Unit 1 occur at different stratigraphic

horizons at different locations, even between relatively closely spaced sites, suggesting highly random formation in time and space; 3. a turbidite is exposed (under the surface fluff) at all Amasra and Sakarya transect stations suggesting very recent turbidite intrusion into this area. In addition to the many gravity cores taken by the R/V K. Piri Reis during the last few years, the core collection from our Kizil Irmak transect will add significant data to the existing University of Izmir's turbidite research program in the southern Black Sea.

Of all the onboard accomplishments, our most significant, collective accomplishment was that we greatly increased sample and data bases for sediment and water column chemistry for the use of international research communities interested in Black Sea studies. These samples also will be examined using new techniques such as nuclear magnetic resonance imagery. Intensive laboratory studies and discussions will continue for many years to come. The first international expedition to the Black Sea by R/V Atlantis II set the standard for the first modern, multifaceted oceanographic research in the Black Sea almost 20 years ago.

The main operational problem during Leg 1 was the lack of instant communication from the ship to a remote outside location. The present onboard Inmarsat satellite system is highly unreliable and practically useless for emergency situations.

The R/V Knorr was escorted constantly by a Soviet ship in the Black Sea. Four ships, the electronic frigate 845, the R/V Okean, the R/V Gidrolog, and the intelligence-collecting ship Ladoga (armed), alternated in following us constantly at a distance of 2 to 4 miles. They were particularly watchful when we deployed sediment trap moorings or the marine snow camera and occasionally came as close as 200 m. We did not seek contact with them throughout the leg and no report-worthy incident occurred.

The R/V Knorr Cruise 134, Leg 8, logged approximately 2600 nautical miles, and occupied 180 stations. The ship berthed at Usukdar, Istanbul, at 18:00 on May 7, 1988, 48 hours earlier than planned.

III. STATION AND TRANSECT INFORMATION

Bernward J. Hay and Muhammed Duman

Daily Activities

All the proposed work could be carried out successfully during this cruise (Figs. 1 and 2). Most of the daily scientific activity involved coring (42%), and was about equally split between box coring and gravity coring (Fig. 3). Sediment trap mooring recoveries (2) and deployments (4) required a total of about 4% of total scientific activity. Hydrocasts and CTD lowerings required a total of 12%, pumping across the interface about 8%. Particle camera work occupied about 22% of the scientific work, of which 19% was occupied by the deep water "Marine Snow Camera," 2% for the time-series "Flux Camera," and 1% for the shallow water "Particle Camera." The remaining 12% were occupied by plankton tows (8%) and by the submersible mini-rover (4%) which was used to study the macro-particles in the shallow water.

Scientific activities occupied a total of 212 hours of the entire shiptime (551 hours), which represents 39%. Steaming accounted for 261 hours (47%), and harbor time for 78 hours (14%).

Transects

All station transects were covered, close to the original plan (Figs. 1 and 2). Basin transects along the Anatolian coast were modified in order to accommodate the more complex subsurface topography and additional sample requests from our Turkish colleagues. One station transect was added (Inebolu transect) for a detailed study of the intersection of the chemocline on the slope and its expression in the sedimentary record (Fig. 4). The Amasra transect (Fig. 5), starting at mapsite BS (the 2-1/2 year long feasibility sediment trap study site; e.g., Izdar et al., 1987; Honjo et al., 1987), was extended into a more detailed chemocline transect to better understand the particle supply collected in the traps.

Transects	Mapsite
Bosporus	6-11
Western Black Sea	11-BSK2
Eastern Black Sea	BSK2-BSK3 (and 47, 48)
Findikli	BSK3-30
Kizil Irmak	31-43
Inebolu	44-BSK2
Southwestern	45-36
Amasra	BS-53
Sakarya	36-54

Stations

Most originally planned stations (refered to here as mapsites, see below) were covered (Figs. 1 and 2). Mapsite 23 was not cored, based on information obtained in the previous core. Mapsites 13 and 14, 21 and 22, 25 and 26, and 27 and 28 were each combined into one mapsite. Thirteen additional mapsites were added.

Station nomenclature:

On this cruise, we distinguished between "mapsites," stations," and "activities."

"Mapsites" were used only for the purposes of cruise planning; they are found on most maps (e.g., Figs. 1 and 2) and in research proposals. Mapsites were not used in the labeling of samples.

"Stations" represent the position in the Black Sea each time a piece of equipment was lowered into the water (Table 1). For example, a hydrocast, a box core, a gravity core, and a sediment trap deployment at mapsite BSK1 each represent a new station, a total of 4 stations. This nomenclature appeared sensible given the frequent stops with comparatively short time intervals in conjunction with the considerable drift in the Black Sea.

"Activities" identify the work that was carried out at each individual station. For example, the activities at mapsite BSK1 mentioned in the paragraph above are HC (hydrocast), BC (box core), GGC (gravity core), and TRAP (sediment trap work). The following is the complete list of activities.

PT	Plankton tow
MSC	Marine Snow Camera
ROV	Rover
TRAP	Sediment trap deployment or recovery
HC	Hydrocast or CTD & transmissometer lowering
PUMP	Particle pump
PAC	Particle camera
FC	Fluc camera
GGC	Giant gravity core *
BC	Box core *

(*) Note that all cores were labeeled successively independent of being gravity cores or box cores (see example below).

Sample Label Code: 134-8 Sta. XX (Activity) (Activity number)

134	Voyage number R/V Knorr
8	Leg 8 (Izmir-Istanbul)
Sta. XX	Station number, successively counted. EACH time a new instrument went over the side there was a new station number.

Examples:	134-8 Sta. 1, GGC 1	First station, first core (gravity core)
	134-8 Sta. 2, BC 2	Second station, second core (box core)
	134-8 Sta. 3, GGC 3	Third station, third core
	134-8 Sta. 4, PT 1	Fourth station, first plankton tow
	134-8 Sta. 5, MSC1	Fifth station, Vernon's Camera
	134-8 Sta. 6, BC 4	Sixth staion, fourth core
	etc.	

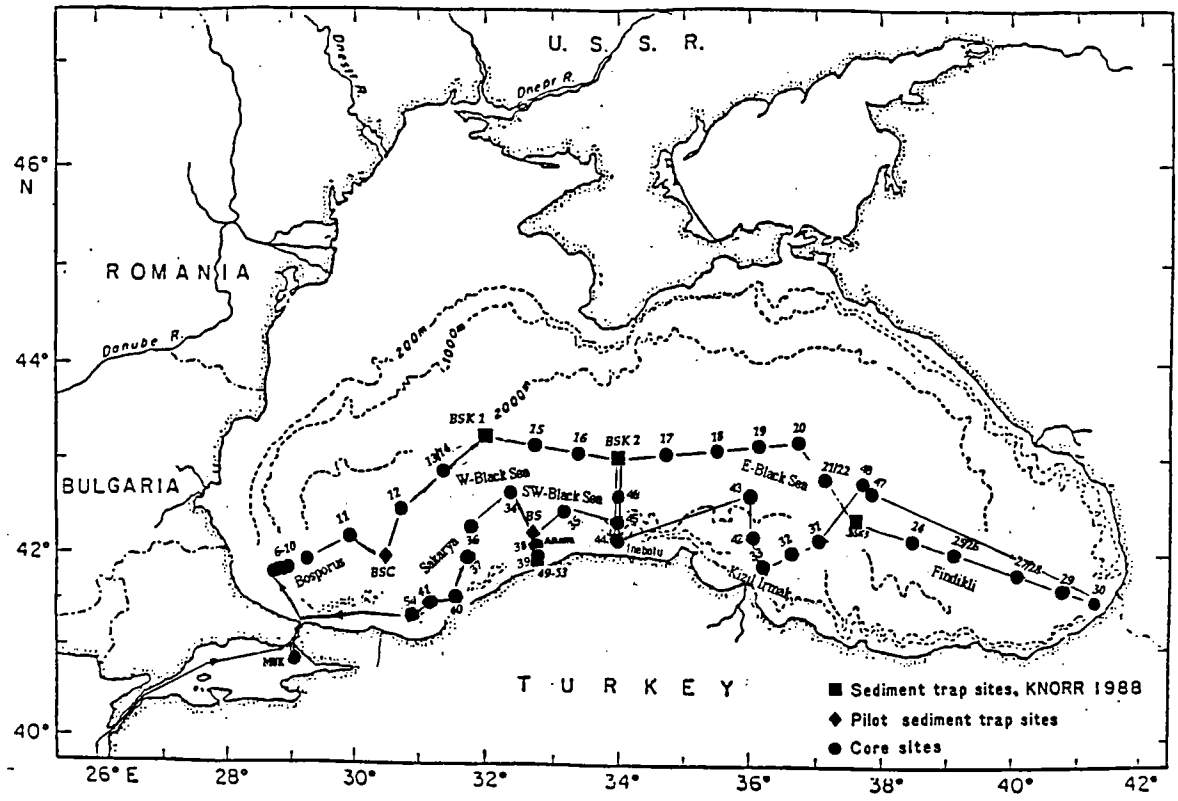

Figure 1: Final cruise track during Leg1 of the R/V Knorr cruise to the Black Sea. (The station numbers are refered to in the text as "mapsites".)

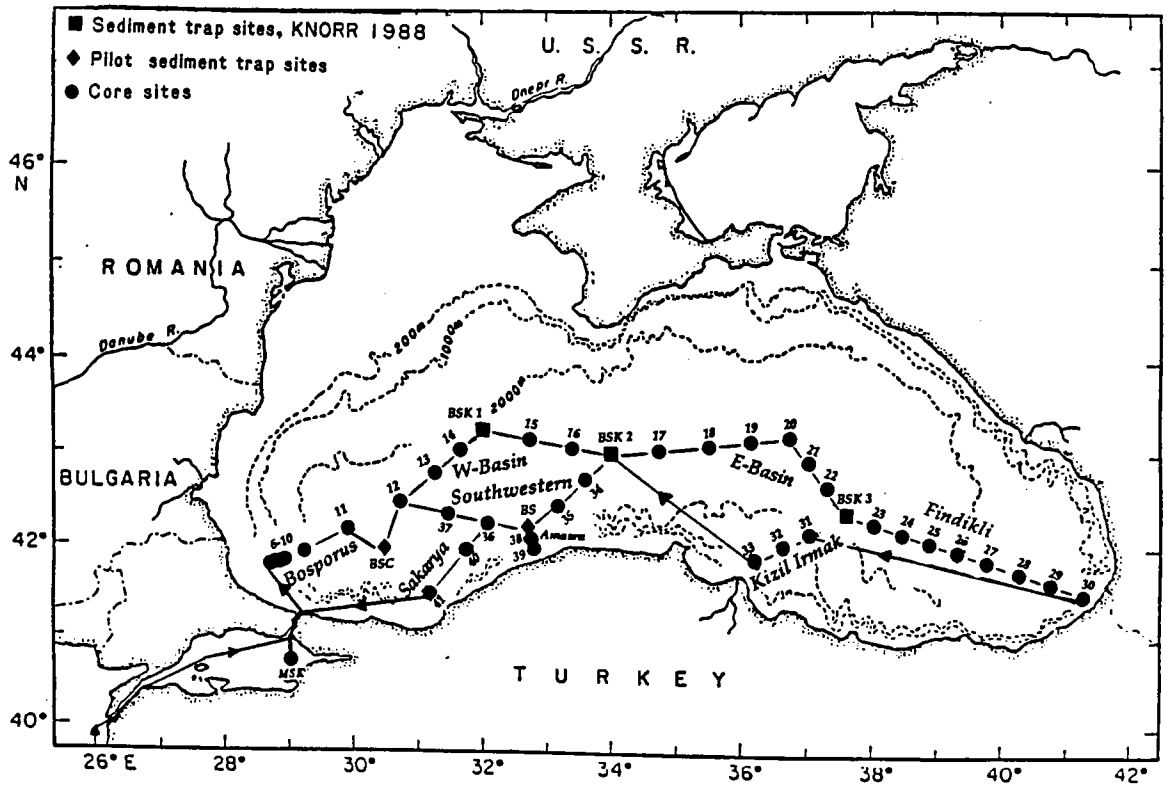

Figure 2: Originally proposed cruise track for Leg 1.

Daily activity, Black Sea Leg 1, *R/V Knorr*

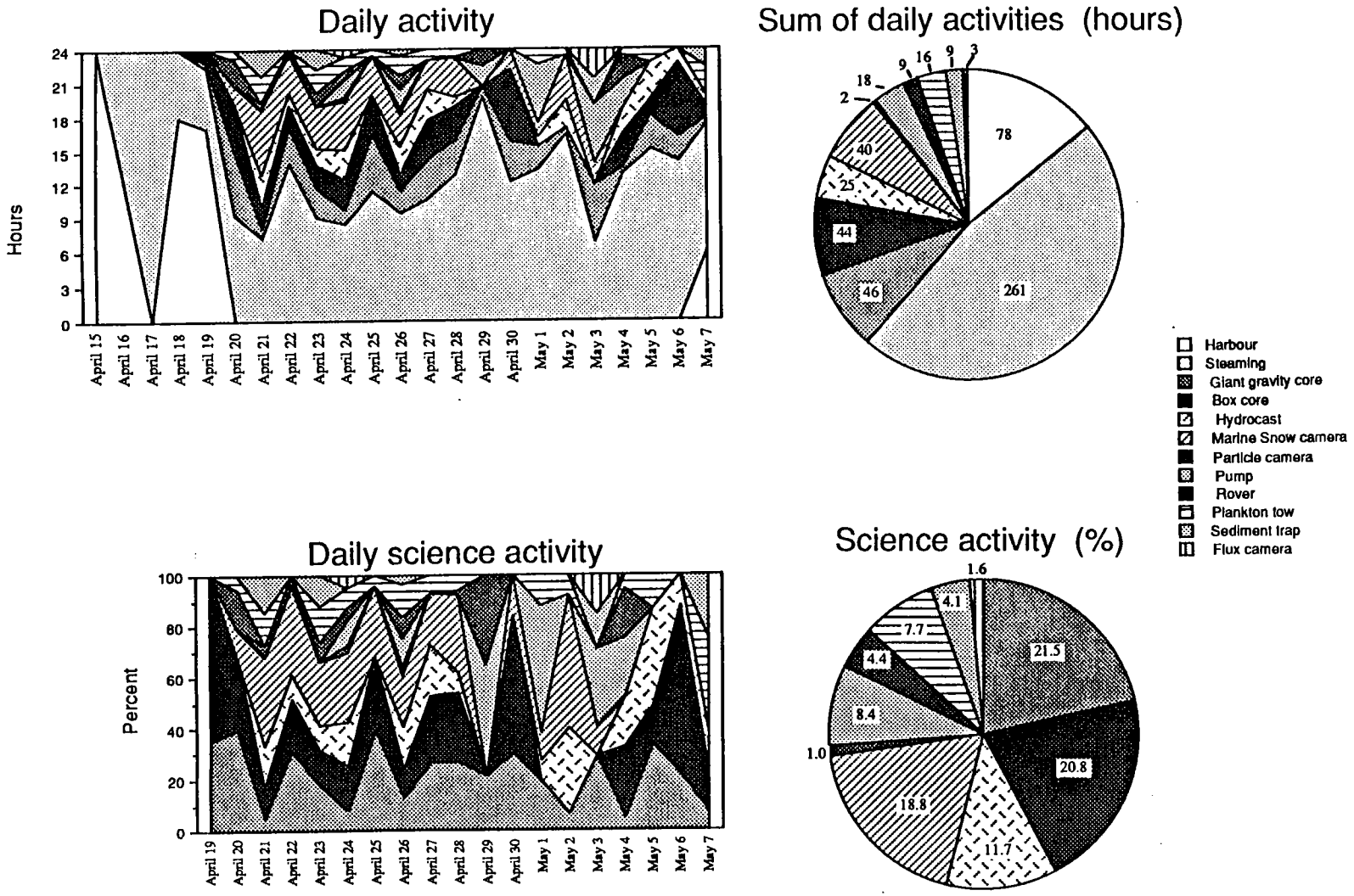

Figure 3: Daily activity during Leg1, broken down into all activities (incl. steaming and harbour time and daily science activities. Both types of daily charts are summarized in a pie chart for the entire cruise.

INEBOLU CHEMOCLINE TRANSECT

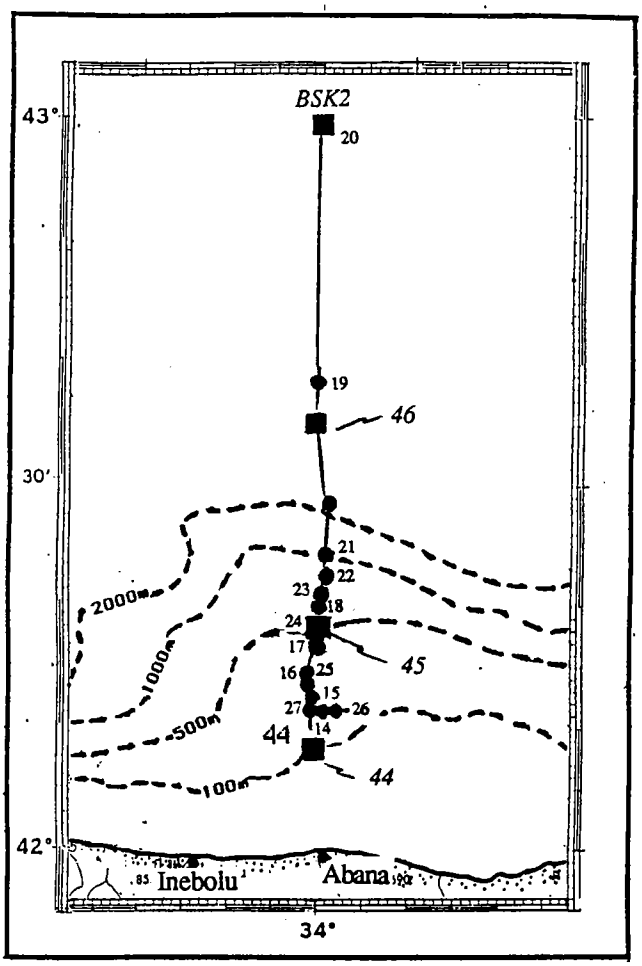

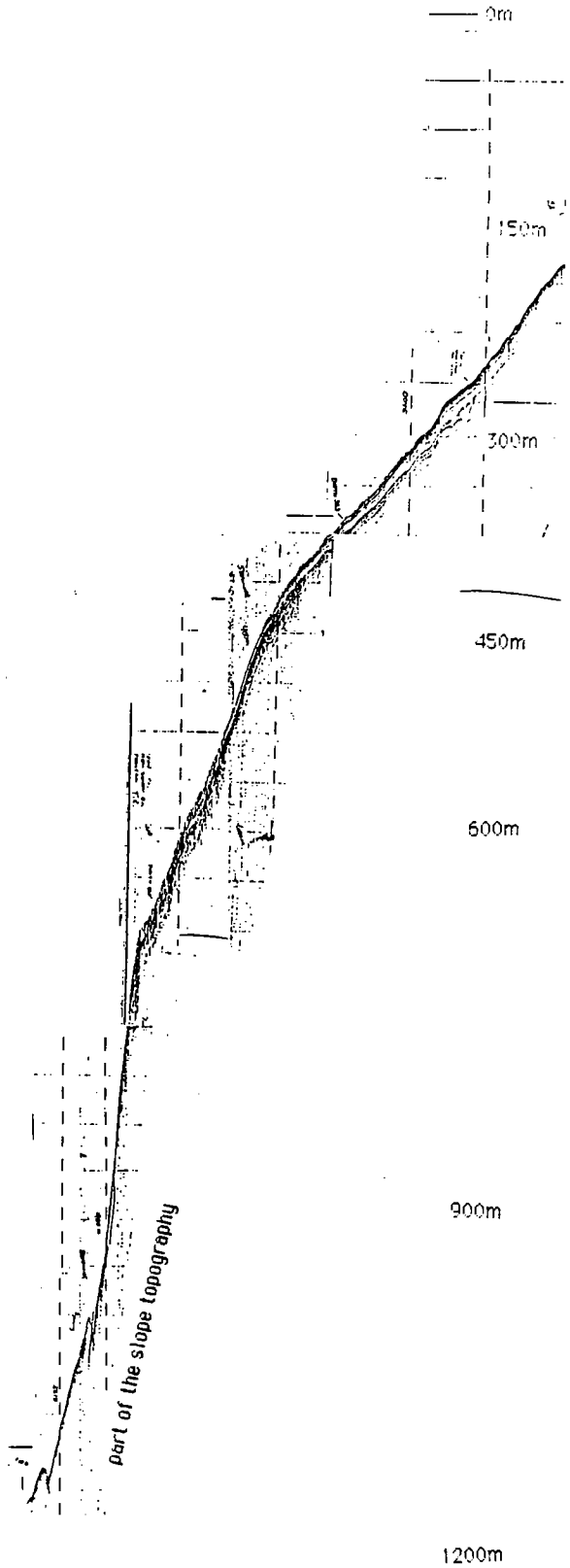

Inebolu Transect I

Mapsite	Stn. no.	HC No.	Depth (m)	Lat.	Long.
44	123	HC14	154	42 10.57	33 59.96
44	125	HC15	189	42 11.40	33 58.45
44	126	HC16	303	42 13.99	33 58.83
45	127	HC17	554	42 17.71	34 00.04
45/46	129	HC18	811	42 20.36	34 01.05
45/46	130	HC19	---	42 38.30	33 59.06

Inebolu Transect II

Mapsite	Stn. no.	HC No.	Depth (m)	Lat.	Long.
BSK2	135	HC20	2186	43 03.33	34 04.96
46/45	142	HC21	1550	42 24.35	34 01.94
46/45	143	HC22	1035	42 22.04	34 01.47
45	144	HC23	675	42 20.15	34 01.95
45	145	HC24	512	42 18.57	34 02.26
45/44	146	HC25	257	42 13.60	34 02.74
44	147	HC26	171	42 11.75	34 03.20
44	148	HC27	199	42 12.03	34 02.58

Figure 4: "Inebolu Chemocline Transect" detailed map, upper slope topography, and station locations. This transect was covered on May 2 (transect I) and May 4 (transect II). Numbers on the map refer to the hydrocast number. Mapsites 44-46 and BSK2 are identified for reference.

AMASRA CHEMOCLINE TRANSECT

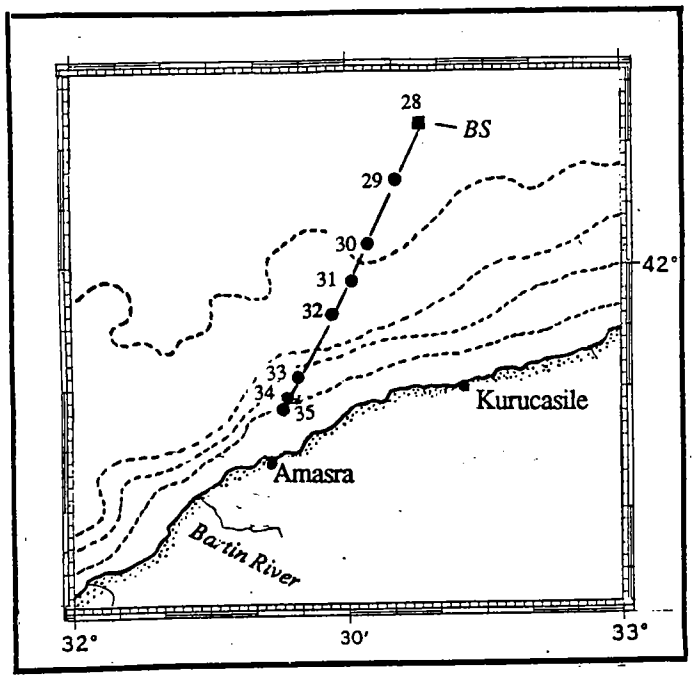

Mapsite	Stn. no.	HC No.	Depth (m)	Lat.	Long.
BS	165	HC28	2200	42 14.72	32 43.94
38	166	HC29	2169	42 07.30	32 36.37
39	167	HC30	2106	42 02.01	32 33.46
49	168	HC31	1980	41 57.97	32 31.25
50	169	HC32	1323	41 55.92	32 29.46
51	170	HC33	400	41 50.01	32 26.80
52	171	HC34	177	41 49.70	32 26.92
53	172	HC35	107	41 49.38	32 24.34

Figure 5: "Amasra Chemocline Transect" detailed map, topography, and station locations. The numbers on the map refer to the hydrocast number. Mapsite BS is identied for reference.

Table 1

Station list

R/V Knorr 134-8
Black Sea Leg 1

DATE	MAPSITE	STN.NR	START	END	LAT(N)	LONG(E)	DEPTH(m)	ACTIVITY
April 19	8	1	22.10	22.45	41 53.32	28.49.21	549	GGC1
"	8	2	23.06	23.52	41 51.08	28 50.12	667	BC2
April 20	7	3	00.50	01.10	41 51.54	28 43.07	394	GGC3
"	7	4	01.30	02.00	41 50.40	28 43.22	317	PT1
"	7	5	02.40	03.40	41 49.93	28 44.68	405	MSC1
"	7	6	03.45	04.19	41 49.12	28 44.96	403	GGC4
"	7	7	04.31	05.06	41 49.02	28 45.00	404	BC5
"	6	8	06.05	07.30	41 49.37	28 40.62	167	ROV1
"	6	9	07.35	08.20	41 48.58	28 40.62	154	ROV2
"	6	10	08.41	09.25	41 50.34	28 41.22	211	GGC6
"	6	11	09.35	09.55	41 50.11	28 41.45	211	GGC7
"	9	12	11.12	11.45	41 55.91	28 55.17	897	GGC8
"	10	13	12.48	13.17	41 56.24	29 02.11	1259	GGC9
"	10	14	13.51	15.14	41 57.71	29 05.24	1503	BC10
"	10	15	15.39	16.35	41 56.96	29 06.32	1490	GGC11
"	11	16	21.02	22.02	42 14.63	29 58.98	2139	GGC12
"	11	17	22.16	00.15	42 15.39	30 00.15	2137	BC13
April 21	11	18	00.43	04.21	42 16.74	30 00.62	2137	MSC2
"	BSC	19	08.24	10.50	41 47.64	30 28.48	1924	TRAP1
"	BSC	20	11.51	13.05	41 48.37	30 25.98	1920	PT2
"	BSC	21	13.14	14.55	41 48.26	30 28.12	1900	HC1
"	BSC	22	15.30	16.15	41 47.49	30 28.88	1916	GGC14
"	BSC	23	16.26	17.05	41 46.92	30 28.42	1908	PAC1
"	BSC	24	17.18	18.52	41 46.52	30 28.42	1938	BC15
"	BSC	25	19.47	21.08	41 45.74	30 26.83	1914	MSC3
"	BSC	26	21.30	22.03	41 46.75	30 30.03	1920	HC2
"	BSC	27	22.10	23.03	41 46.25	30 30.50	1935	PT3
April 22	12	28	03.45	07.13	42 26.48	30 40.25	2170	MSC4
"	12	29	07.24	08.25	42 26.27	30 39.60	2170	GGC16
"	13/14	30	13.15	15.15	42 58.20	31 25.26	2066	BC17
"	13/14	31	16.40	17.40	42 52.53	31 23.29	2091	GGC18
"	13/14	32	17.50	18.40	42 52.48	31 22.46	2098	GGC19
"	BSK1	33	22.15	22.40	43 11.00	31 59.49	2067	PAC2
"	BSK1	34	23.00	00.35	43 09.73	31 59.92	2067	HC3
April 23	BSK1	35	01.00	01.40	43 09.55	32 00.23	2065	PT4
"	BSK1	36	01.45	02.40	43 08.10	32 00.23	2065	PT5
"	BSK1	37	02.57	06.18	43 07.77	32 01.03	2079	MSC5
"	BSK1	38	06.25	07.14	43 06.98	32 00.85	2088	GGC20
"	BSK1	39	07.28	09.20	43 05.52	32 01.56	2092	BC21
"	BSK1	40	10.20	12.10	43 10.57	32 01.22	2100	TRAP2
"	BSK1	41	13.15	14.28	43 02.38	31 59.43	2100	ROV3
"	BSK1	42	14.55	15.20	43 01.97	31 59.27	2110	HC4
"	15/16	43	18.48	19.31	43 06.63	31 59.43	2151	GGC22
"	16	44	22.47	23.50	43 02.00	33 16.48	2219	GGC23
April 24	BSK2	45	03.30	07.02	42 59.92	34 00.49	2220	MSC6
"	BSK2	46	07.12	08.17	42 59.00	34 00.37	2195	GGC24
"	BSK2	47	08.26	10.15	42 58.69	34 00.55	2219	HC5
"	BSK2	48	10.46	11.32	42 58.26	34 00.14	2217	FC1
"	BSK2	49	12.13	13.25	43 00.14	34 00.33	2217	PT6
"	BSK2	50	14.10	16.50	42 55.58	34 01.03	2217	BC25
"	BSK2	51	18.00	18.45	42 54.72	34 00.70	2218	ROV4
"	BSK2	52	18.55	20.15	42 56.02	34 01.73	2217	PUMP1
"	BSK2	53	20.30	20.55	42 53.20	34 01.46	2217	HC6
"	BSK2	54	20.55	21.23	42 54.32	34 01.24	2218	PAC3
April 25	17	55	00.15	01.05	43 02.16	34 35.45	2177	GGC26
"	17	56	01.10	02.05	43 02.28	34 35.67	2178	GGC27
"	17/18	57	05.05	08.38	43 05.84	35 17.30	2206	MSC7
"	18	58	09.28	10.25	43 05.09	35 24.57	2204	GGC28
"	18	59	10.33	11.48	43 03.59	35 26.55	2205	BC29
"	19	60	16.10	16.55	43 09.30	36 10.55	2194	GGC30
"	20	61	19.55	22.05	43 04.89	36 41.10	2184	BC31
"	20	62	22.25	23.30	43 05.92	36 35.72	2184	GGC32
April 26	20	63	23.39	00.10	43 06.42	36 41.13	2183	PT7
"	20	64	00.15	01.22	43 07.30	36 38.23	2184	MSC8
"	21/22	65	04.41	05.27	42 43.30	37 12.48	2162	GGC33
"	BSK3	66	09.07	10.57	42 23.50	37 35.49	2137	HC7
"	BSK3	67	11.15	11.58	42 21.08	37 35.58	2133	PT8
"	BSK3	68	12.45	13.15	42 20.85	37 34.33	2133	TRAP3
"	BSK3	69	14.57	16.38	42 16.01	37 32.03	2060	BC34
"	BSK3	70	16.55	17.43	42 15.01	37 31.60	2060	GGC35
"	BSK3	71	18.01	19.18	42 15.00	37 31.29	2060	PUMP2
"	BSK3	72	19.24	19.52	42 14.23	37 32.76	2049	HC8
"	BSK3	73	20.05	21.09	42 14.64	37 33.03	2046	ROV5
"	BSK3	74	21.11	21.40	42 14.44	37 34.11	2043	PAC4
"	BSK3	75	21.45	22.20	42 13.26	37 34.08	2038	PT9
"	BSK3	76	22.40	01.53	42 12.64	37 35.39	2038	MSC9
April 27	BSK3	77	03.14	05.10	42 22.56	37 35.39	2038	BC36
"	BSK3	78	06.10	07.40	42 22.56	37 35.39	2030	BC37

"	BSK3	79	08.03	08.56	42 21.32	37 30.01	2030	GGC38
"	24	80	13.45	14.30	42 11.33	38 35.17	2089	GGC39
"	24	81	14.35	15.16	42 10.21	38 34.81	2089	GGC40
"	25/26	82	18 .44	21.28	42 00.80	39 17.71	2039	HC9
"	25/26	83	21.55	22.25	42 01.23	39 08.07	2038	PT10
"	25/26	84	22.32	23.13	42 01.23	39 13.60	2037	GGC41
April 28	25/26	85	23.26	02.34	42 00.09	39 13.81	2037	MSC10
"	27/28	86	07.11	07.38	41 48.54	40 11.82	1868	HC10
"	27/28	87	07.43	08.25	41 49.33	40 11.41	1864	GGC42
"	27/28	88	08.41	10.08	41 49.38	40 12.82	1861	BC43
"	29	89	13.36	14.07	41 40.58	40 55.44	1665	GGC44
"	29	90	14.10	14.46	41 40.75	40 55.35	1670	GGC45
"	30a	91	17.36	17.55	41 27.04	40 25.66	195	GGC46
"	30a	92	18.00	18.30	41 27.01	41 21.55	184	BC47
"	30a	93	18.37	18.52	41 26.66	41 21.78	205	GGC48
"	30b	94	19.17	19.33	41 25.14	41 23.10	101	GGC49
"	30b	95	20.03	20.17	41 26.46	41 26.04	101	BC50
"	30c	96	21.05	21.32	41 25.78	41 20.41	234	HC11
"	30c	97	21.40	22.10	41 25.33	41 16.04	242	PT11
"	30c	98	22.17	22.55	41 26.67	41 17.23	255	MSC11
April 29	30c	99	23.46	01.30	41 25.18	41 18.24	174	ROV6
"	30c	100	02.00	03.20	41 26.69	41 18.07	569	PUMP3
"	30d	101	05.21	05.52	41 28.23	41 15.44	1406	GGC51
"	30	102	09.09	09.31	41 25.19	41 13.31	990	GGC52
April 30	47	103	02.22	04.27	42 39.73	37 36.98	2154	BC53
"	47	104	04.40	05.33	42 40.73	37 45.59	2157	GGC54
"	48	105	06.35	08.35	42 44.91	37 34.80	2164	BC55
"	48	106	08.38	09.23	42 45.77	37 33.99	2162	GGC56
"	31	107	13.40	14.40	42 07.75	36 54.70	1979	GGC57
"	31	108	14.45	17.00	42 08.15	36 54.00	1980	BC58
"	32	109	19.20	20.00	41 58.54	36 33.30	600	GGC59
May 1	31	110	22.10	01.10	42 06.73	36 52.73	1977	MSC12
"	31	111	01.15	01.45	42 06.75	36 52.33	1963	PT12
"	33	112	06.54	07.25	41 49.07	36 17.51	1170	GGC60
"	33	113	08.06	09.25	41 47.80	36 17.20	1159	PUMP4
"	33	114	09.44	11.03	41 47.20	36 16.41	1127	PUMP5
"	33	115	11.22	12.45	41 46.75	36 16.44	1118	PUMP6
"	42	116	16.36	17.22	42 16.99	36 17.48	1750	GGC61
"	42	117	17.35	17.58	42 14.55	36 17.48	1735	HC12
"	43	118	20.43	21.00	42 34.21	36 00.74	2034	HC13
"	43	119	21.03	21.46	42 34.85	36 00.30	2034	GGC62
"	43	120	22.00	22.30	42 33.97	36 01.91	2033	PT13
May 2	43/44	121	04.00	06.15	42 15.79	34 51.00	746	MSC13
"	44	122	10.49	10.54	42 10.34	33 59.97	155	GGC63
"	44	123	11.08	11.19	42 10.57	33 59.96	154	HC14
"	44	124	11.35	11.43	42 11.54	35 59.94	203	GGC64
"	44	125	11.52	12.10	42 11.40	33 58.45	189	HC15
"	44	126	12.51	13.09	42 13.99	33 58.83	303	HC16
"	45	127	13.58	14.22	42 17.71	34 00.04	554	HC17
"	45	128	14.25	14.40	42 17.78	33 59.92	563	GGC65
"	45/46	129	15.14	15.41	42 20.36	34 01.05	811	HC18
"	45/46	130	17.50	18.17	42 38.30	33 59.06	727	HC19
"	BSK2	131	21.46	22.20	43 01.78	34 06.65	2189	PT14
May 3	BSK2	132	22.39	01.58	43 04.50	34 06.10	2189	MSC14
"	BSK2	133	02.08	02.55	43 03.25	34 04.66	2190	GGC66
"	BSK2	134	03.05	03.53	43 03.21	34 04.91	2186	GGC67
"	BSK2	135	04.10	06.40	43 03.33	34 04.96	2186	HC20/Pump7
"	BSK2	136	07.30	10.08	42 59.07	34 00.42	2172	FC2
"	BSK2	137	10.51	11.42	42 59.21	34 00.30	2221	GGC68
"	BSK2	138	12.11	13.04	42 57.88	33 59.18	2221	GGC69
"	BSK2	139	13.14	15.27	42 57.98	33 59.00	2220	PUMP8
"	BSK2	140	16.37	17.48	42 57.25	33 59.41	2223	TRAP4
"	46	141	21.40	22.30	42 34.33	34 00.09	2220	GGC70
May 4	46/45	142	00.30	00.50	42 24.35	34 01.94	1550	HC21
"	46/45	143	01.27	01.47	42 22.04	34 01.47	1035	HC22
"	45	144	02.13	02.35	42 20.15	34 01.95	675	HC23
"	45	145	02.56	03.15	42 18.57	34 02.26	512	HC24
"	45/44	146	03.52	04.09	42 13.60	34 02.74	257	HC25
"	44	147	04.25	04.35	42 11.75	34 03.20	171	HC26
"	44	148	04.49	04.59	42 12.03	34 02.58	199	HC27
"	44/45	149	05.45	05.52	42 12.02	34 06.33	411	GGC71
"	45	150	06.13	06.24	42 12.42	34 03.23	435	GGC72
"	44	151	07.09	07.31	42 12.84	34 05.83	194	BC73
"	44	152	08.01	08.14	42 13.85	34 05.96	147	BC74
"	44	153	09.15	09.22	42 11.00	33 59.21	174	GGC75
"	44	154	09.40	11.50	42 10.27	33 59.85	172	ROV7
"	44	155	12.10	12.31	42 10.91	34 00.69	130	BC76
"	44	156	13.46	14.05	42 12.69	33 59.38	253	BC77
"	44	157	14.25	15.54	42 12.95	34 00.66	250	BC78
"	45	158	16.01	16.10	42 19.39	34 00.94	707	GGC79
"	45	159	16.25	18.43	42 19.46	34 01.20	706	PUMP9
"	35	160	23.24	00.08	42 30.10	33 07.44	2215	PT15
May 5	35	161	00.24	01.15	42 30.74	33 13.20	2215	GGC80
"	BS	162	04.46	05.50	42 12.81	32 40.11	2199	PT16
"	BS	163	06.08	06.55	42 13.69	32 43.69	2199	GGC81
"	BS	164	07.02	08.07	42 14.48	32 42.61	2199	BC82
"	BS	165	09.19	09.37	42 14.72	32 43.94	2200	HC28
"	38	166	11.00	11.22	42 07.30	32 36.37	2169	HC29
"	39	167	12.15	12.27	42 02.01	32 33.46	2106	HC30
"	49	168	12.53	13.07	41 57.97	32 31.25	1980	HC31

"	50	169	13.38	13.53	41 55.92	32 29.46	1323	HC32
"	51	170	14.45	15.01	41 50.01	32 26.80	400	HC33
"	52	171	15.10	15.20	41 49.70	32 26.92	177	HC34
"	53	172	15.26	15.35	41 49.38	32 24.34	107	HC35
"	34	173	21.15	21.30	42 43.61	32 19.76	2194	HC36
"	34	174	21.41	22.29	42 52.07	32 19.40	2196	GGC83
May 6	36	175	01.25	03.20	42 22.00	31 53.19	2203	BC84
"	36	176	03.29	04.21	42 21.87	31 54.65	2202	GGC85
"	37	177	06.52	09.03	42 00.31	31 52.50	2140	BC86
"	40	178	12.15	12.54	41 35.14	31 30.13	1758	GGC87
"	41	179	15.19	15.50	41 29.72	31 00.47	1368	GGC88
"	41	180	15.56	17.14	41 30.16	31 01.49	1328	BC89
"	54	181	19.15	19.24	41 11.03	30 47.60	122	BC90
"	54	182	19.45	19.59	41 08.16	30 42.55	258	HC 37
"	54	183	20.19	20.37	41 12.88	30 52.13	641	HC38
May 7	MSK	184	09.00	09.30	40 41.08	29 09.31	1225	GGC91
"	MSK	185	09.38	10.30	40 55.25	29 04.28	1225	HC39
"	MSK	186	10.36	11.36	40 47.80	29 01.85	1215	BC92
"	MSK	187	11.55	14.04	40 48.26	29 03.53	1194	PT17
"	MSK	188	14.34	15.44	40 46.38	29 01.39	1200	TRAP5

IV. SCIENTIFIC INVESTIGATIONS IN THE WATER COLUMN

IV. A. SEDIMENT TRAP WORK

Bernward J. Hay, Susumu Honjo, and Tosun Konuk

Sediment trap work on R/V Knorr Black Sea Leg 1 consisted of 3 parts:

1. Deployment of three sediment trap moorings in the characteristic central regions of the Black Sea.

The objective of the sediment trap moorings at three central sites in the Black Sea is to monitor the intra-annual variability in the particle flux in the eastern, central, and western Black Sea. The selected sites are:

BSK1:	43°11.07'N	32°01.37'E	western Black Sea	Fig. 1
BSK2:	43°00.13'N	34°00.73'E	central Black Sea	Fig. 2
BSK3:	42°20.85'N	37°34.33'E	eastern Black Sea	Fig. 3

There will be a short summer deployment and a 1-year deployment (Fig. 4). At all three mapsites there will be samples from the deep water at around 1,300 m (about 800 m from the basin floor). At mapsites BSK1 and BSK2 there will be samples from a shallow water depth at about 400 m (about 1,700 m from the basin floor).

Sampling will be synchronized for all traps (Figs. 5-7). During the 2 1/2-month long summer deployment, 12 high-resolution samples will be collected at mapsite BSK2 (sampling period: 5.75 days) in both the shallow and deep traps (Fig. 6). The sampling periods of the traps will be synchronized. On about July 14, the array will be recovered and redeployed by V. Asper on Leg 5 (Chief Scientist: Dr. Reeburgh). During the summer deployment, traps at mapsites BSK1 and BSK3 will collect one sample each (Fig. 5). The timer will then automatically switch to a sampling period of 30.5 days for the 1-year deployment on August 1. The time of the redeployed traps at mapsite BSK2 will be adjusted to the identical sampling interval. Thus, the sampling periods in all traps will be precisely synchronized during the 1-year deployment. All moorings will be recovered finally in August, 1989, by the R/V K. Piri Reis from the Dokuz Eylül University of Izmir, Turkey.

At mapsite BSK1, the summer sample will be collected by the first cup of the 13-cup Mark 6 sediment traps, and the 1-year samples by the subsequent 12 cups. At mapsite BSK3, the summer sample will be collected by the single-cup Mark 6 at 1,300 m, and the 1-year samples will be collected by the 12-cup Mark 5 trap at 1,172 m.

2. Recovery of the "Chernobyl sediment trap mooring" BSC.

This mooring (Fig. 8) was first deployed at mapsite BSC in June, 1986, shortly after the Chernobyl nuclear accident (e.g., Buesseler et al., 1987; Hay et al., in prep). The mooring was recovered for the third time during this leg; it had been redeployed in May, 1987 (see cruise report, section IV.C., for details on trap samples). The particle flux study of material collected by the sediment traps at this site was carried out in collaboration with the Dokuz Eylül University in Izmir, Turkey, the University of Hamburg, West Germany, and the Woods Hole Oceanographic Institution.

3. Redeployment of the BSC mooring array in the Sea of Marmara.

The sediment trap mooring array from mapsite BSC was redeployed with a modified design in the Sea of Marmara, mapsite MSK (Figs. 9, 10). Sampling intervals of the shallow and deep sediment traps were synchronized. Samples will be collected from May 7, 1988 to October 25, 1988; the sampling period is 14 days (Table 1). This array will be recovered by the R/V K. Piri Reis in November, 1988 and the experiment will be administered by the Dokuz Eylül University.

Table 1. Programmed schedule for shallow and deep traps at mapsite MSK:

Created 05/07/88 08:41
MSK May 1988
Events = 15

Event	Date 1988	Time	
# 00	05/07	10:00	
# 01	05/07	10:30	(test)
# 02	05/10	00:00	(rotation to first sample cup)
# 03	05/24	00:00	(rotation to second sample cup)
# 04	06/07	00:00	(rotation to third sample cup)
# 05	06/21	00:00	(rotation to fourth sample cup)
# 06	07/04	00:00	(rotation to fifth sample cup)
# 07	07/19	00:00	(rotation to sixth sample cup)
# 08	08/02	00:00	(rotation to seventh sample cup)
# 09	08/16	00:00	(rotation to eighth sample cup)
# 10	08/30	00:00	(rotation to ninth sample cup)
# 11	09/13	00:00	(rotation to tenth sample cup)
# 12	09/27	00:00	(rotation to eleventh sample cup)
# 13	10/11	00:00	(rotation to twelfth sample cup)
# 14	10/25	00:00	(closing of last sample cup; rotation to open hole)

----------End of Data----------

Figure 1

BSK-1 Mooring System

Western Black Sea

(Lat. 43°11.07'N Long.: 32°01.37'E)

April 23, 1988

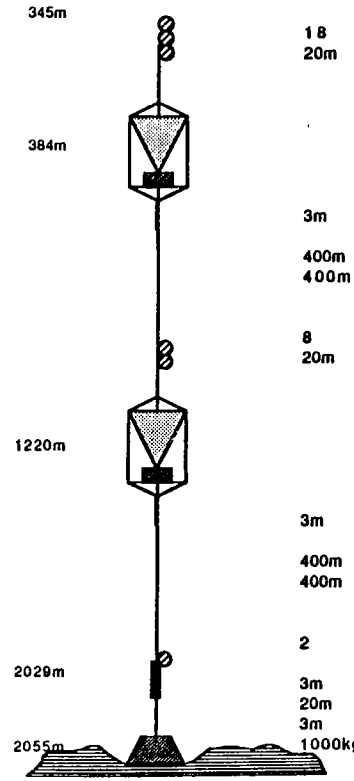

	Mooring components	Deployment time
18	17" glassballs	10:29
20m	3/4" nylon rope	
	Coated nylon bridles, with stainless steel shackles	
	Sediment trap (MARK 6)	10:31
	Coated nylon bridles, with galvanized steel shackles	
3m	chain	
400m	3/16" wire	
400m	3/16" wire	
8	17" glassballs	10:39
20m	3/4" nylon rope	
	Coated nylon bridles, with stainless steel shackles	
	Sediment trap (MARK 6)	
	Coated nylon bridles, with galvanized steel shackles	
3m	chain	
400m	3/16" wire	
400m	3/16" wire	
2	17" glassballs	
	Release	11:00
3m	chain	
20m	3/4"nylon	
3m	chain	11:10
1000kg	Anchor	

Sediment Trap Mooring Deployment
R/V Knorr Cruise134, Leg 8

BSK-1

(Black Sea, Knorr station 1)

General area: base of the Danube Fan, western Black Sea

Mooring description

Total length:	1710m
Main instrumentation:	2 time-series sediment traps, Mark 6, 13 cups.
Total buoyancy:	800 lbs.
Taut line:	3/16" jacketed wire
Release:	Benthos 865-A, serial number 240 Battery volt.: new (9.5V)
Mooring design:	P. Clay, WHOI

Deployment

Date:	April 23, 1988
Platform:	R/V Knorr, Woods Hole Oceanographic Institution
Deployment in charge:	B. J. Hay
Chief Scientist:	S. Honjo
Bosun:	J. Cotter, WHOI
Support:	2 AB and 1 OS, a few science hands
Equipment:	Stern winch for haul. Hand intake and hand spooling
Release armed witness:	J. Broda, B.J. Hay
Deployment position:	43°11.07'N, 32°01.37'E
Depth:	2055m, Raytheon PDD
Trap ID:	BSKS-1 (shallow trap, summer sample & 1-year depl., Depth 384m) BSKD-1 (deep trap, summer sample & 1-year depl., Depth 1220m)
Trap water fixation:	4% buffered Formalin, NaCl content: 50‰
Sea state:	1
Weather:	overcast/sunny, Temp.: 66°F, Wind NE, breezing

Satellite positioning

	Latitude	Longitude	Transducer reading
Anchor drop	43°11.07'N	32°01.37'E	
Fix 1	43°10.18'N	32°00.39'E	2070m
Fix 2	43°10.64'N	32°00.96'E	2340m
Fix 3 (12:03h)	43°10.94'N	32°01.24'E	2690m

Figure 2

BSK-2 Mooring System

Central Black Sea

(Lat. 43°00.13'N Long.: 34°00.73'E)

May 3, 1988

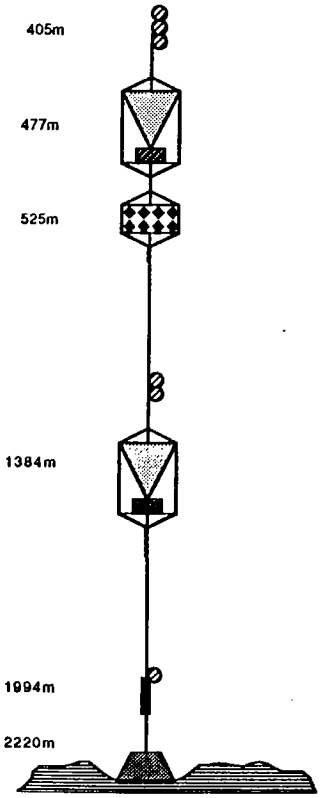

	Mooring components	Deployment time
21	17" glassballs	16:25
50m	3/4" nylon rope Coated nylon bridles	
	Sediment trap (MARK 5)	17:00
	Coated nylon bridles	
25m	3/16" wire	
15m	3/4" nylon Flux camera	
3m	chain	17:16
400m	3/16" wire	
400m	3/16" wire	
3	17" glassballs	17:30
50m	3/4" nylon rope Coated nylon bridles	
	Sediment trap (MARK 5)	17:33
	Coated nylon bridles	
3m	chain	
400m	3/16" wire	
400m	3/16" wire	
2	17" glassballs	
	Release	17:45
3m	chain	
20m	3/4"nylon	
3m	chain	17:50
1000 kg	Anchor	

Sediment Trap Mooring Deployment
R/V Knorr Cruise134, Leg 8

BSK-2

(Black Sea, Knorr station 2)

General area: central Black Sea

Mooring description

Total length:	1815m
Main instrumentation:	2 time-series sediment traps, Mark 5, 12 cups.
Net buoyancy:	1000 lbs.
Taut line:	3/16" jacketed wire
Release:	Benthos 865-A, serial number 284 Battery volt.: new (9.5V)
Mooring design:	P. Clay, WHOI

Deployment

Date:	May 3, 1988
Platform:	R/V Knorr, Woods Hole Oceanographic Institution
Deployment in charge:	B. J. Hay
Chief Scientist:	S. Honjo
Bosun:	J. Cotter, WHOI
Support:	2 AB and 1 OS, a few science hands
Equipment:	Stern winch for hauling, hand spooling of wire
Release arming witness:	V. Asper, J. Broda
Deployment position:	43°00.13'N, 34°00.73'E
Depth:	2220m, Raytheon PDD
Trap ID:	BSKS-2a (shallow trap, summer depl. (a), Depth 477m) BSKD-2a (deep trap, summer depl. (a), Depth 1384m)
Trap water fixation:	4% buffered Formalin, NaCl content: 50‰
Sea state:	1
Weather:	sunny, Temp.: 68°F, Wind NE, slightly breezing

Satellite positioning

	Latitude	Longitude	Transducer reading	
Anchor drop	43°00.13'N	34°00.73'E		17:45h
Fix 1 (anchor at bottom)	43°00.43'N	34°00.53'E	2386m	18:05h

Figure 3

BSK-3 Mooring System

Eastern Black Sea

(Lat. 42°20.85'N; Long. 37°34.22'E)

April 26, 1988

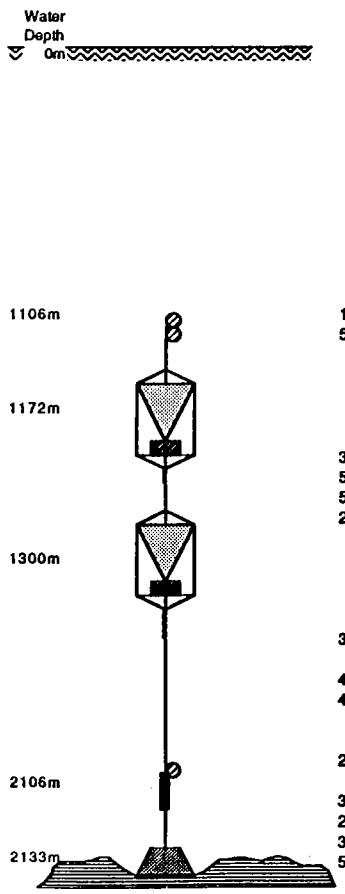

	Mooring components	Deployment time
12	17" glassballs	12:48
50m	3/4" nylon rope	
	Coated nylon bridles	
	Sediment trap (Mark 5)	12:55
	Coated nylon bridles	
3m	Chain	
50m	3/16" wire	
50m	3/16" wire	
20m	3/4" nylon rope	
	Coated nylon bridles	
	Sediment trap (MARK 6) (single cup)	13:00
	Coated nylon bridles	
3m	chain	
400m	3/16" wire	
400m	3/16" wire	
2	17" glassballs	
	Release	
3m	chain	
20m	3/4"nylon	
3m	chain	
500 kg	Anchor	13:17

Sediment Trap Mooring Deployment
R/V Knorr Cruise134, Leg 8

BSK-3

(Black Sea, Knorr station 2)

General area: eastern Black Sea
(station identical with station 1474, R/V Atlantis II cruise in 1969)

Mooring description

Total length:	1027m
Main instrumentation:	1 time-series sediment traps, Mark 5, 12 cups 1 sediment trap Mark 6, single-cup
Net buoyancy:	500 lbs.
Taut line:	3/16" jacketed wire
Release:	Benthos 865-A, serial number 271 Battery volt.: new (9.5V)
Mooring design:	P. Clay, WHOI

Deployment

Date:	April 26, 1988
Platform:	R/V Knorr, Woods Hole Oceanographic Institution
Deployment in charge:	B. J. Hay
Chief Scientist:	S. Honjo
Bosun:	J. Cotter, WHOI
Support:	2 AB and 1 OS, a few science hands
Equipment:	Stern winch for hauling, hand spooling of wire
Release arming witness:	J. Broda, B.J. Hay
Deployment position:	42°20.85'N, 37°34.33'E
Depth:	2133m, Raytheon PDD
Trap ID:	BSKD-3 (Mark 6 single cup trap (summer-deployment sample), Depth 1300m) BSKD-3 (Mark 5 time-series trap (1-year deployment samples) Depth 1172m)
Trap water fixation:	4% buffered Formalin, NaCl content: 50‰
Sea state:	1
Weather:	sunny, Temp.: 65°F, Wind NE, breezing

Satellite positioning

	Latitude	Longitude	Transducer reading	
Anchor drop	42°20.85'N	37°34.33'E		13:16h
Fix 1	42°20.85'N	37°32.82'E	3150m	13:54h
Fix 2	42°20.06'N	37°32.26'E	3660m	14:14h

Sediment trap sampling schedule

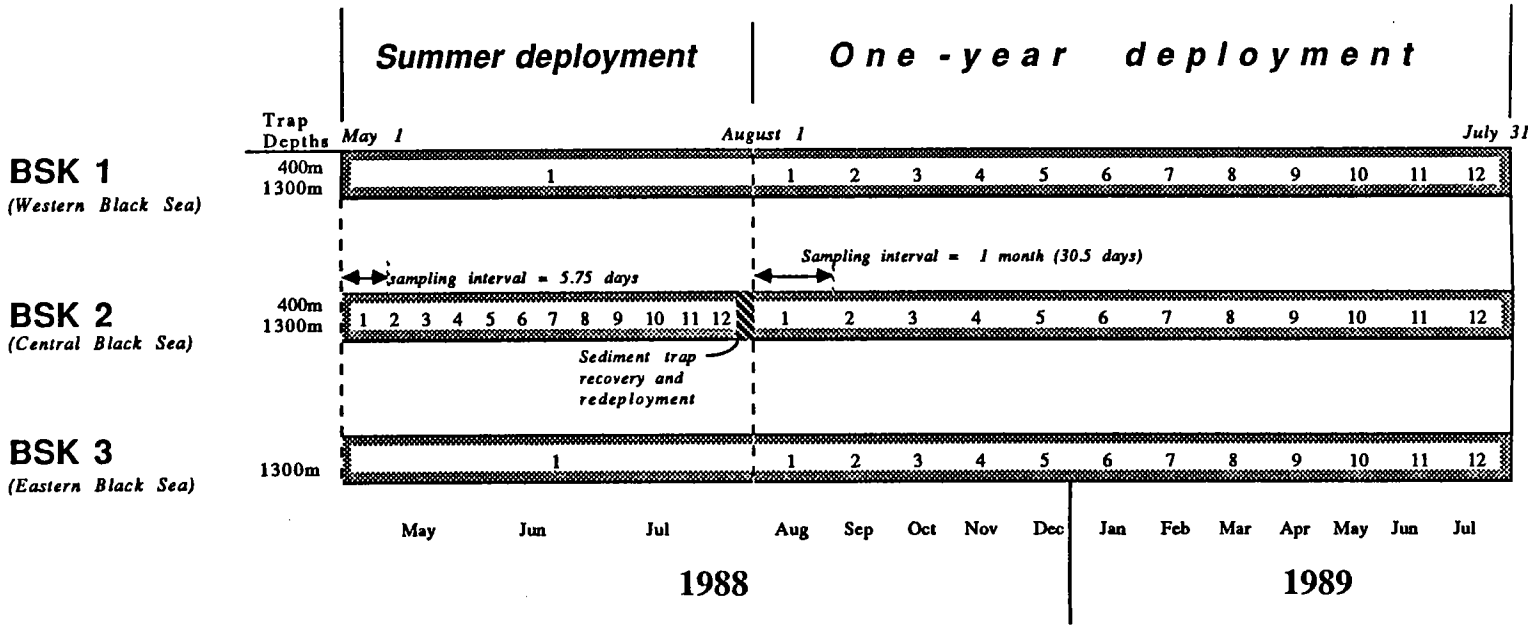

Fig. 4: Diagram of number of samples collected at the different sediment trap sites in the Black Sea throughout the short summer deployment and the one-year deployment. At sites BSK1 and BSK2, time-series samples will be collected at about 350 m and 1,300 m; at site BSK3 samples will collected only at 1,300 m. The summer sample of the traps at site BSK1 will be collected by the first cup of the 13-cup time-series trap Mark-6. The summer sample at site BSK3 will be collected by a single-cup Mark-5 trap; the subsequent 12 samples of the one-year deployment will be collected by a 12-cup time-series Mark-5 trap, positioned 100 m above the single-cup trap. Sample collection between all trap samples in the Black Sea is precisely synchronized.

SCHEDULE OF ROTATION FOR TIME-SERIES SEDIMENT TRAP TIMERS

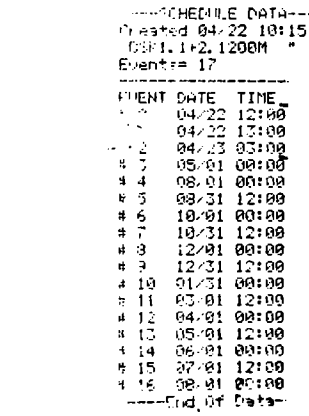

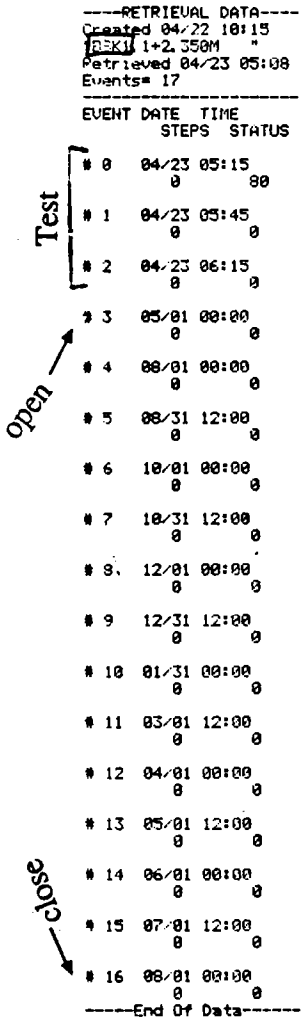

Fig. 5: Programmed schedule for shallow and deep traps at site BSK1 (summer and one-year deployment).

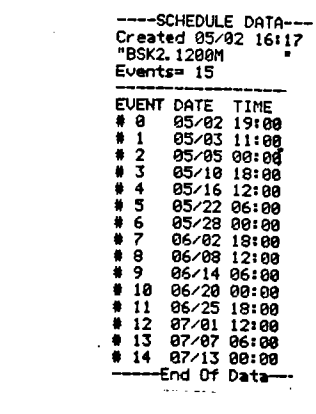

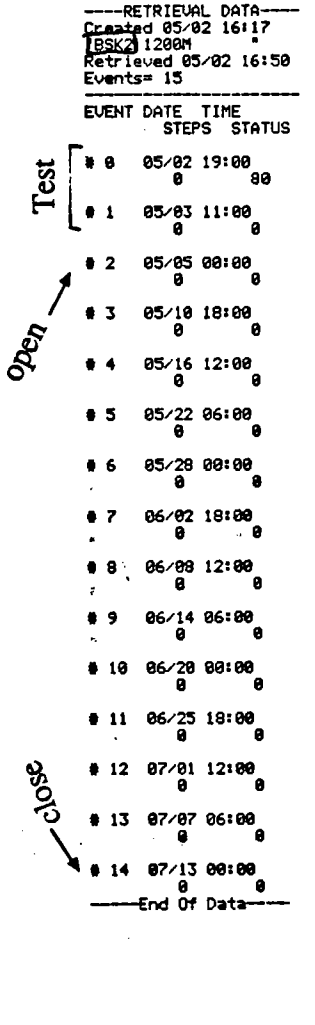

Fig. 6: Programmed schedule for shallow and deep traps at site BSK2 (summer deployment only; the one-year deployment will be scheduled before redeployment in July).

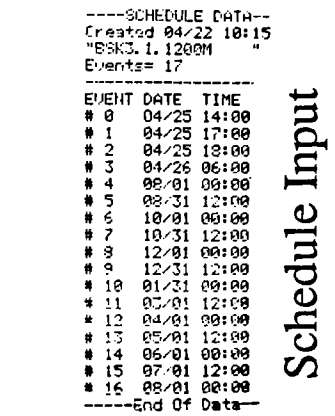

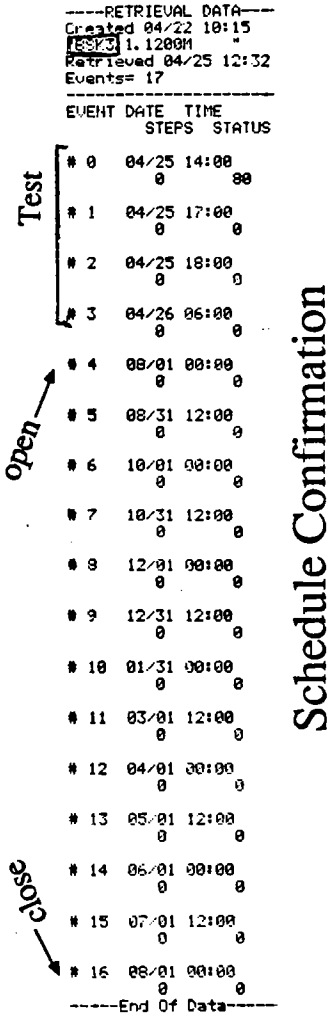

Fig. 7: Programmed schedule for the deep trap at site BSK3 (one-year deployment only; the summer sample will be collected separately with a single-cup trap).

Schedule Input

Schedule Confirmation

Figure 8

BSC Mooring System

Southwestern Black Sea

(Lat. 41°48.49'N Long.: 30°26.27'N)

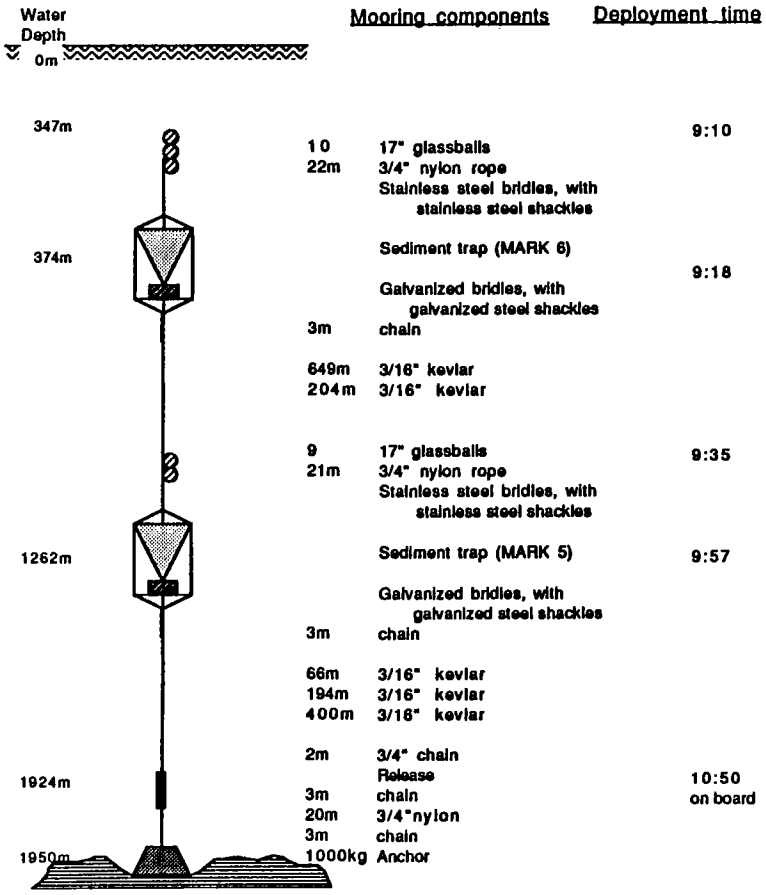

Sediment Trap Mooring Recovery
R/V Knorr Cruise134, Leg 8

BSC

(Black Sea, Chernobyl station)

General area: southwestern Black Sea, north of the mouth of the Sakarya Nehri

Deployment

Date:	May 13, 1987
Platform:	R/V Koca Piri Reis, Dokuz Eylül Universitesi, Izmir, Turkey
Deployment in charge:	T. Konuk, B.J. Hay
Chief Scientist:	T. Konuk
Deployment position:	41°48.48.6'N, 30°26.265'E
Depth:	1924m, Raytheon PDD
Trap ID:	BSCS.3 (shallow trap, 3rd deployment, Depth 374) BSCD.3 (deep trap, 3rd deployment, Depth 1262m)
Trap water fixation:	4% buffered Formalin, NaCl content: 50‰

Mooring description

Total length:	1503m
Main instrumentation:	1 time-series sediment traps Mark 6 1 time-series sediment trap Mark 5
Total buoyancy:	800 lbs.
Taut line:	3/16" kevlar
Release:	Benthos 865-A, serial number 271
Mooring design:	P. Clay, WHOI

Recovery

Date:	April 21, 1988
Platform:	R/V Knorr, Woods Hole Oceanographic Institution
Recovery in charge:	B. J. Hay
Chief Scientist:	S. Honjo
Bosun:	J. Cotter, WHOI
Support:	2 AB and 1 OS, a few science hands
Equipment:	Stern winch for haul., Hand intake and hand spooling
Sea state:	1
Weather:	overcast, Temp.: 60°F

Figure 9

MSK Mooring System

Marmara Sea

(Lat. 40°48.38'N Long.: 29°01.39'E)

Experiment for Dokuz Eylül University, Izmir, Turkey

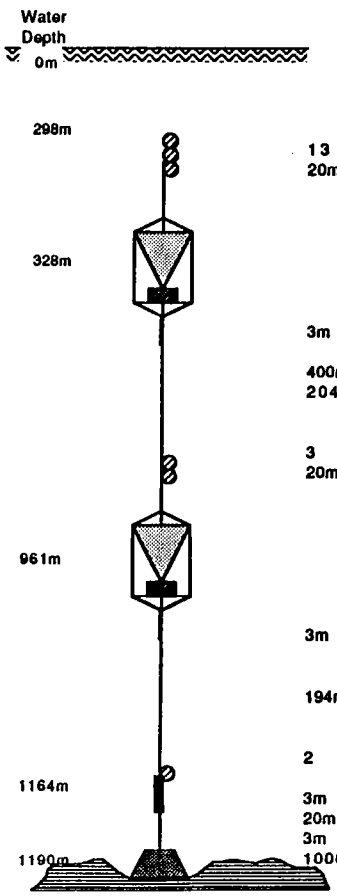

	Mooring components	Deployment time
13	17" glassballs	
20m	3/4" nylon rope	14:34
	Coated nylon bridles, with stainless steel shackles	
	Sediment trap (MARK 5)	14:45
	Coated nylon bridles, with galvanized steel shackles	
3m	chain	
400m	3/16" kevlar	
204m	3/16" kevlar	
3	17" glassballs	
20m	3/4" nylon rope	
	Coated nylon bridles, with stainless steel shackles	
	Sediment trap (MARK 5)	15:25
	Coated nylon bridles, with galvanized steel shackles	
3m	chain	
194m	3/16" kevlar	
2	17" glassballs	
	Release	15:35
3m	chain	
20m	3/4"nylon	
3m	chain	
1000kg	Anchor	15:44

Sediment Trap Mooring Deployment
R/V Knorr Cruise134, Leg 8

MSK

(Marmara Sea)

General area: Northeastern Marmara Sea

Mooring description

Total length:	900m
Main instrumentation:	1 time-series sediment trap, Mark 6, 12 cups
	1 time-series sediment trap, Mark 5, 12 cups
Net buoyancy:	750 lbs.
Taut line:	3/16" kevlar
Release:	Benthos 865-A, serial number 079, Battery volt.: new (9.5V)
Mooring design:	P. Clay, WHOI

Deployment

Date:	May 7, 1988
Platform:	R/V Knorr, Woods Hole Oceanographic Institution
Deployment in charge:	B. J. Hay
Chief Scientist:	S. Honjo
Bosun:	J. Cotter, WHOI
Support:	2 AB and 1 OS, a few science hands
Equipment:	Stern winch for hauling, hand spooling of wire
Release arming witness:	T. Konuk, J. Broda, B.J. Hay
Deployment position:	40°48.38'N 29°01.39'E
Depth:	1190m, Raytheon PDD
Trap ID:	MSKS (Mark 6, shallow trap, depth 328m)
	MSKD (Mark 5 deep trap, depth 961m)
Trap water fixation:	4% buffered Formalin, NaCl content: 50‰
Sea state:	1
Weather:	overcast, Temp.: 64°F, breezing

Satellite positioning

	Latitude
Anchor drop	40°48.38'N
	Longitude
	29°01.39'E
	Transducer reading
	1260

Figure 10

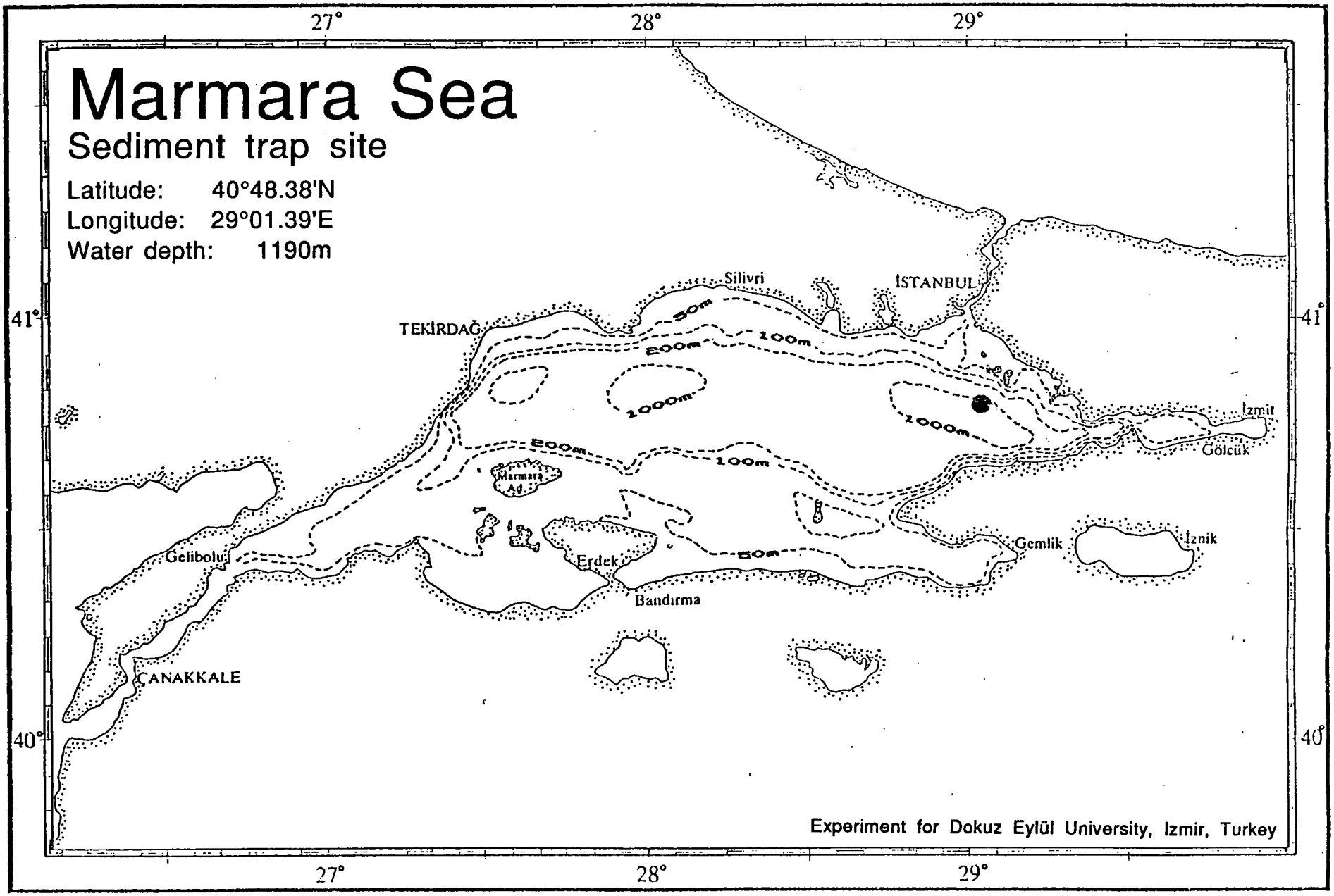
Marmara Sea
Sediment trap site
Latitude: 40°48.38'N
Longitude: 29°01.39'E
Water depth: 1190m
27°
28°
29°
41°
40°
Silivri
İSTANBUL
TEKİRDAĞ
50m
100m
200m
1000m
İzmit
Gölcük
Marmara Ad.
Gelibolu
Erdek
Bandırma
Gemlik
İznik
ÇANAKKALE
Experiment for Dokuz Eylül University, Izmir, Turkey

IV. B. WATER COLUMN ANALYSIS

Stephan Kempe, Gerd Liebezeit, Arne Diercks,
JoAnn Nicholson, Alan Gagnon, Bonnie Woodward
and Michael Realander

Objective

The 1988 R/V Knorr Black Sea Cruise Leg 1 provided a unique opportunity to look at the chemistry of dissolved and particulate phases throughout the entire southern Black Sea. None of the following legs will have such a wide geographic scope. Several groups, therefore, pooled their analytical resources to analyze the collected water and particulate samples for various parameters and to document the distribution of particulate matter in the water by in-situ photography, in-situ video inspection, and in-situ pumping.

Because the Black Sea is the only large-scale anaerobic marine water body on earth, the study of its chemistry, particulate matter, and sediments allows the only contemporary chance to study "euxinic" processes which have prevailed in the world oceans for substantial periods of geologic history. An extensive literature exists describing various aspects of the Black Sea chemistry.

Procedures and Instrumentation

A 12-Niskin-bottle (each 30 liters in volume) rosette sampler was used in connection with a Seastar-CTD (see CTD report section) to obtain samples from various depths and to describe the physicochemical properties of the water column.

Aliquots were drawn from Niskin bottles. H_2S, pH, Eh, NH_4, R-PO_4 (RDP = reactive dissolved phosphorus), T-PO_4 (TDP = total dissolved phosphorus), and $Si(OH)_4$ were determined onboard from the dissolved phase. P-PO_4 (TPP = total particulate phosphorus) was determined on the particulate phase. Analysis followed the standard procedures as, for example, published by Grasshoff. Samples for later determination of ^{14}C, O_2, alkaliniity, DOC and DIC were drawn and conserved. Glass fiber, membrane, and Nuclepore filters were used to collect the particulate phase for later analysis of POC (particulate organic carbon), PN (particulate nitrogen), TSM (total suspended matter), manganese, and SEM/EDX inspection. On one profile samples to determine dissolved manganese were taken independently with a Go-Flo bottle deployed on a Kevlar line.

C-14 Analysis

Water samples were collected at mapsites BSK1 (Table 3) and BSK3 (Table 7) utilizing the rosette sampler with twelve 30-liter Niskin bottles. Prior

to each cast, the Niskin bottles were cleaned with a soap solution, rinsed with 10% HCl, and finally rinsed with Methanol just before deployment.

Water samples for ^{14}C analysis were drawn off before other water samples were taken, using pre-cleaned silicon tubing and pre-baked 1 µm quartz-fiber in-line filters. Surgical rubber gloves and plastic bags (to create clean surfaces) were used at all times. Two samples were taken from each Niskin bottle; a 4-liter sample was collected in a 4-liter pre-cleaned glass bottle and immediately frozen at -12°C. A 1-liter sample was collected in a 1-liter pre-cleaned glass bottle and was poisoned with a 6.9g/100ml solution of mercuric chloride and stored at ambient temperatures.

The dissolved inorganic and organic carbon will be dated by Tandem Accelerator Mass Spectroscopy (TAMS). CO_2 gas will be stripped from these samples and converted to graphite at the Woods Hole Graphite Preparation Facility. The graphite targets will then be analyzed at the TAMS facility in Tucson, Arizona.

Results

All hydrochemical results are listed in Tables 1 to 14. NH_4 and $Si(OH)_4$ data still need to be corrected for the salinity effect, which will result in a 10% increase in values.

The following figures (Figs. 1-4) give a first view of the data. Figure 1 shows the concentration of RDP of all shallow water casts. Depending on the geographical location and therefore on the depth of the chemocline (see CTD report section), we found the sharp increase of RDP concentrations coupled to the onset of anoxia at depths between 45 m and 170 m. A remarkable feature of the RDP curve is the maximum just below the concentration increase, as already noticed by Fonselius (1974). Figures 2a and 4a depict the deep profiles of RDP and TDP measurements and show the further increase of the dissolved phosphorus with depth. Figure 3a also plots the TPP (particulate phosphorus; units in nM/1), showing its sharp decrease at the chemocline and rather stable concentrations in the deep water body.

Figures 2b, 3b, and 4b show the distribution of NH_4+ with depth. Its increase starts below the chemocline and is more gradual than the increase in RDP. Below a depth of 600 m concentrations tend to be rather stable at 45 to 50 µM/1.

Figures 2c, 2d, 3c, and 4c give the distribution of dissolved silica with depth. The silica concentration increase starts immediately below the spring thermocline where diatoms have already depleted its concentration. The following increase is even slower than that of ammonia and continues all the way to the sea bottom. This increase shows a rather remarkable correlation with the increase of pH (Fig. 2e) if one excludes the silica-depleted surface waters. Remineralization of organics (producing CO_2 and lowering the pH) and of siliceous debris may thus follow similar kinetics.

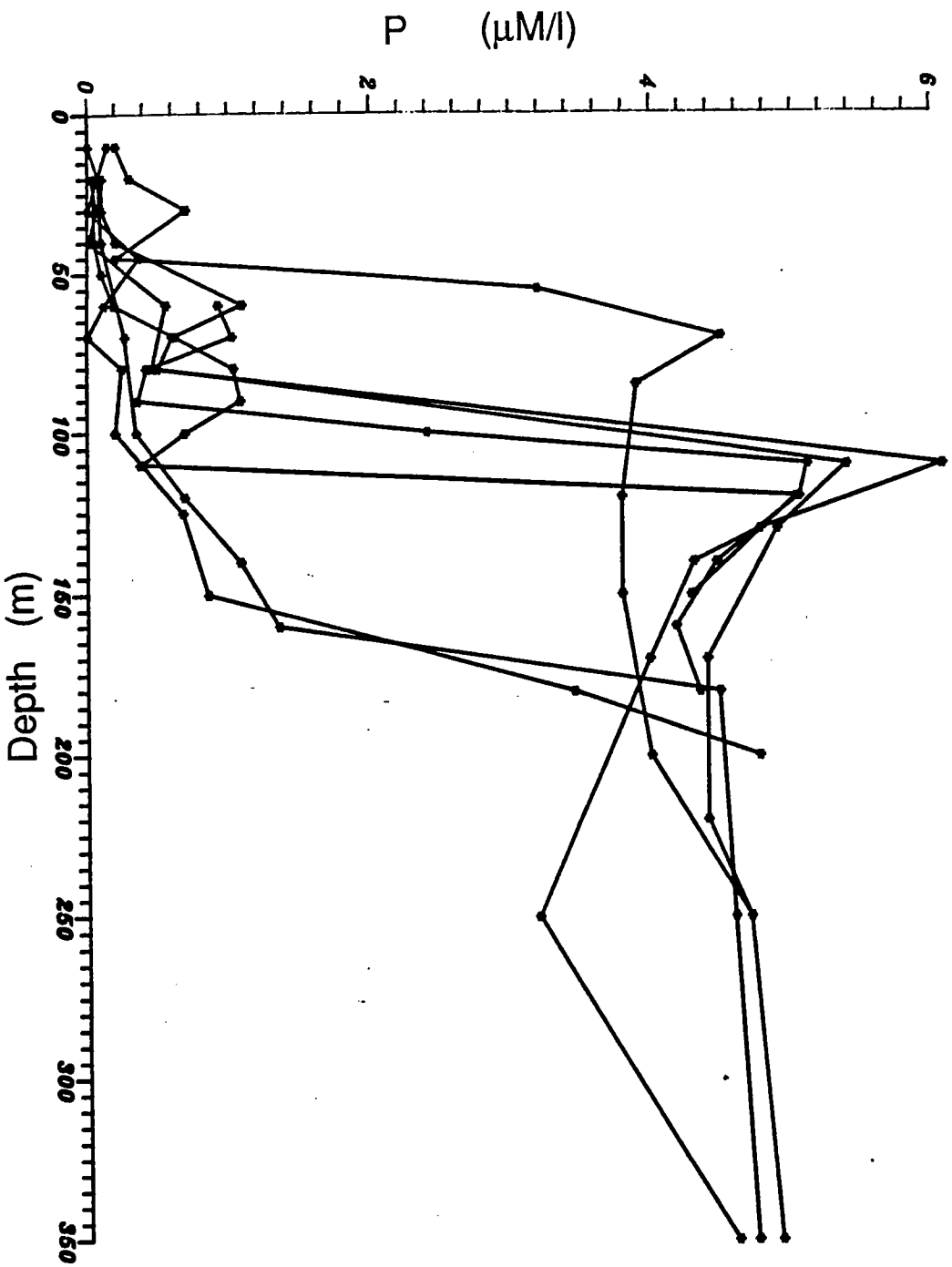

Fig. 1: Concentration of RDP of all shallow water casts

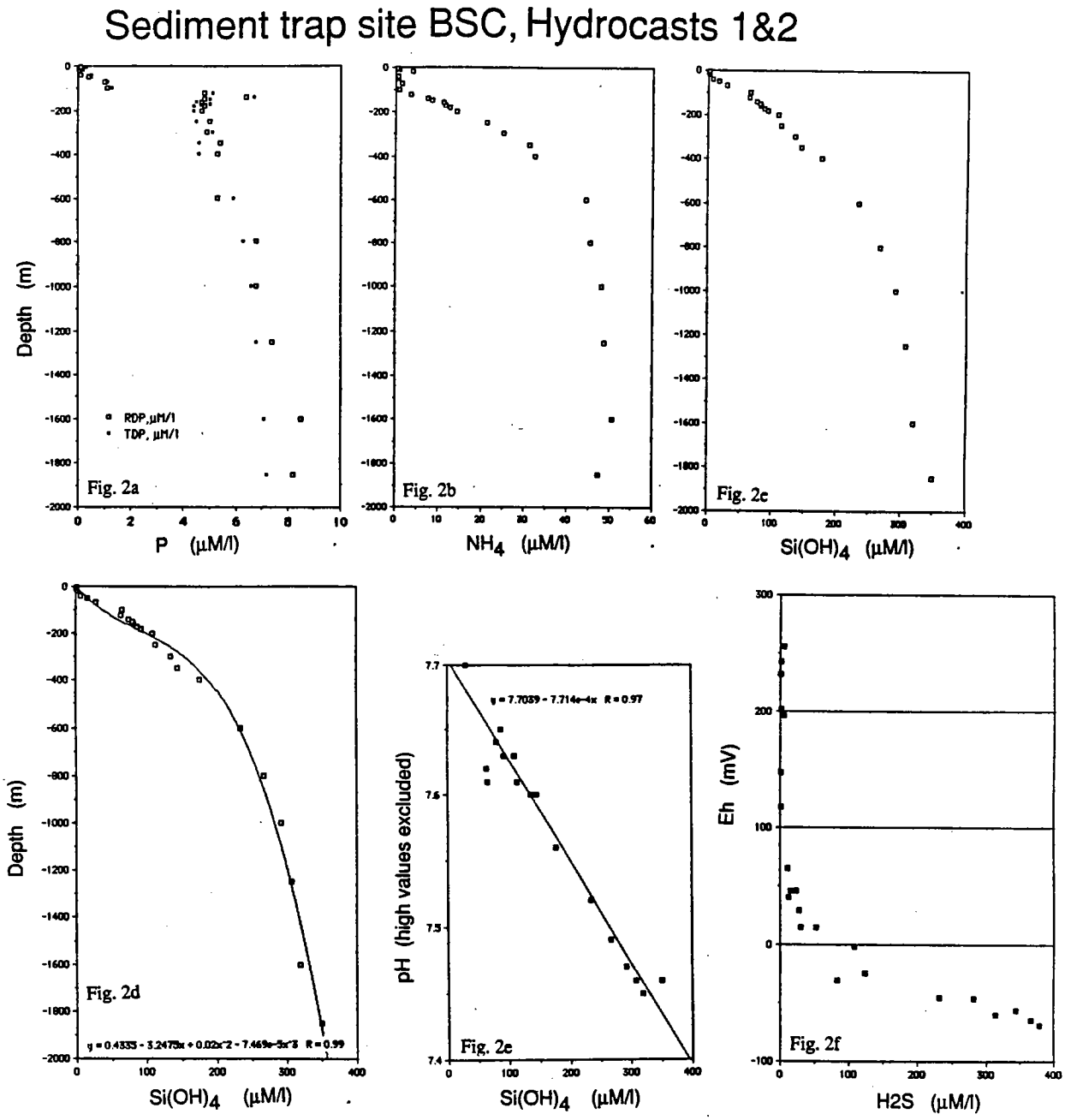

Fig. 2: Hydrochemical results from sediment trap site BSC.

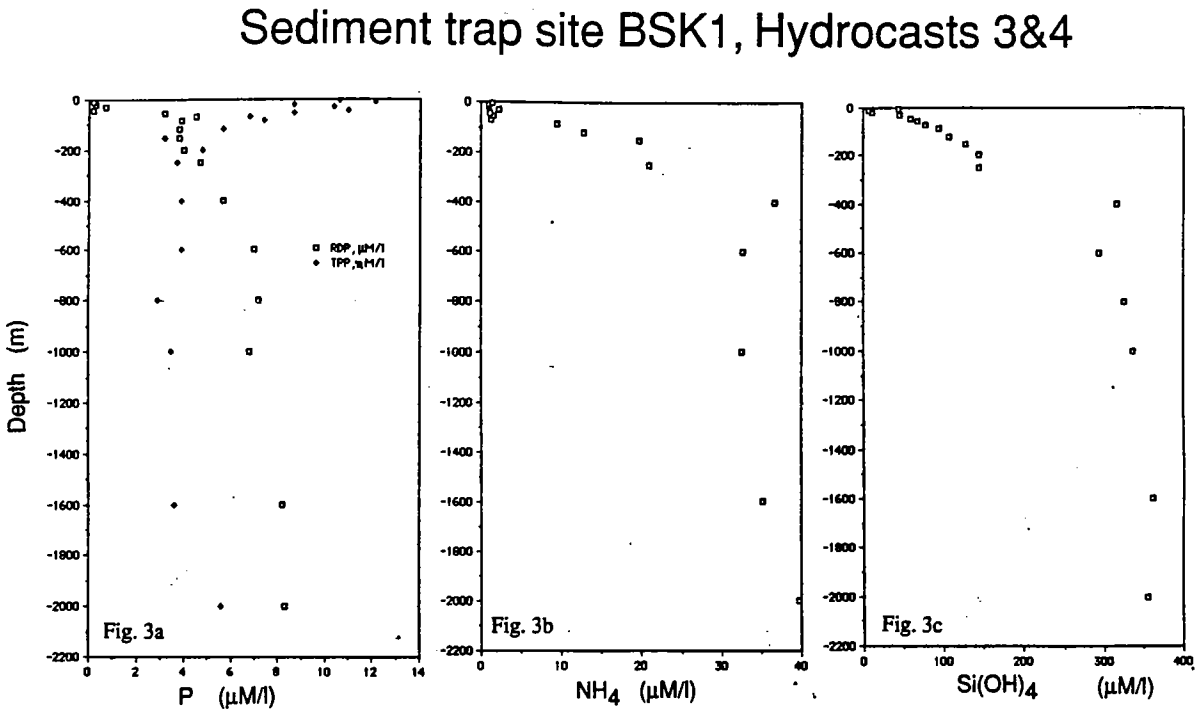

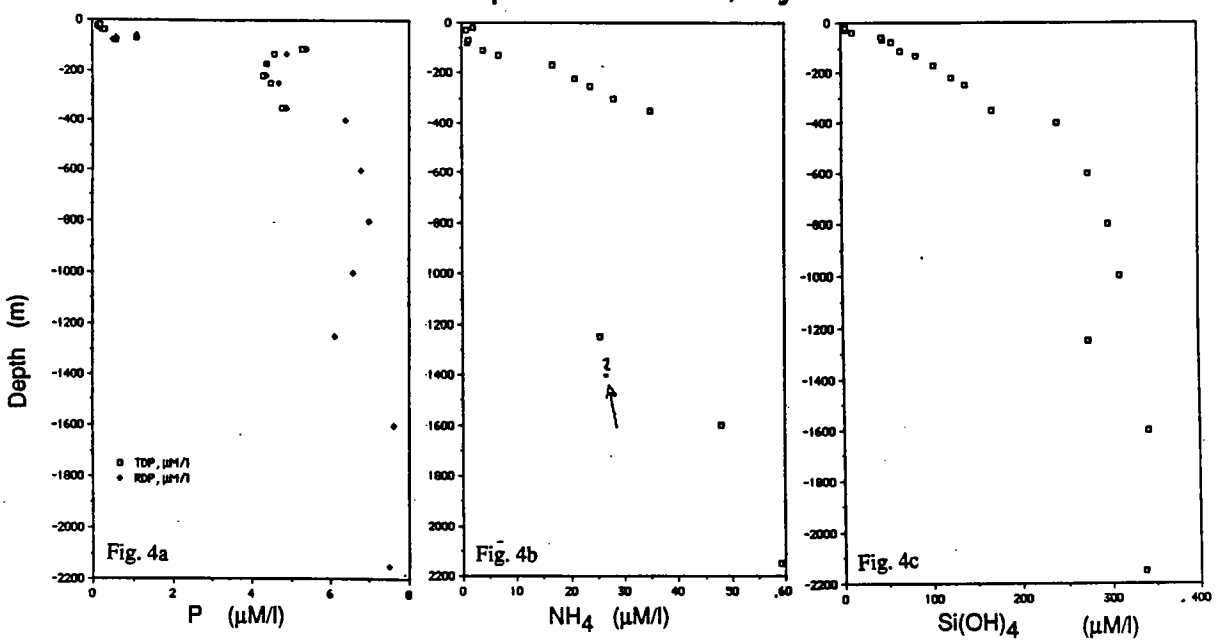

Figs. 3&4: Hydrochemical results from sediment trap sites BSK1 and BSK2, respectively.

Table 1
Station 21 (BSC), Hydrocast 1, April 21st, 1988, Black Sea, 41 46.26N,

Niskin	Depth m	Pressure db	Temp. oC	Salinity per mil	pH	Eh mV
1	1850	1856,0	9,094	22,320	7,46	-70
2	1600	1588,6	9,054	22,324	7,45	-65
3	1250	1227,5	8,999	22,309	7,46	-57
4	1000	978,5	8,958	22,279	7,47	-61
5	800	782,4	8,923	22,227	7,49	-47
6	600	592,2	8,899	22,127	7,52	-46
7	400	392,9	8,870	21,917	7,56	-25
8	300	299,9	8,835	21,755	7,60	-31
9	200	202,2	8,721	21,407	7,63	15
10	100	103,4	8,266	20,517	7,61	147
11	50	54,3	6,784	18,718	7,99	202
12	5	7,3	8,698	18,311	8,16	232

Table 2
Station 25 (BSC), Hydrocast 2, April 21, 1988, Black Sea, 41 46.98N, 3

Niskin No	Depth m	Pressure db	Temp. oC	Salinity per mil	pH	Eh mV
1	350	351,1	8,848	21,853	7,60	-2
2	250	252,1	8,795	21,616	7,61	15
3	180	180,9	8,707	21,369	7,63	40
4	170	172,9	8,685	21,319	7,65	29
5	160	163,2	8,657	21,258	7,67	46
6	150	153,5	8,631	21,184	7,64	46
7	140	143,5	8,576	21,073	7,67	65
8	120	123,2	8,436	20,771	7,62	117
9	70	74,7	7,327	19,378	7,77	196
10	40	44,5	7,151	18,476	8,06	232
11	20	24,3	8,436	18,298	8,16	243
12	10	10,9	8,527	18,281	8,19	256

30 27.43E

HS- mymol/l	RDP mymol/l	TDP mymol/l	Si(OH)4 mymol/l	NH4 mymol/l	TPP nmol/l	Deep water contamina.
378,7	8,2	7,2	350,0	47,3		
366,7	8,5	7,1	319,2	50,7		
344,9	7,4	6,8	307,4	48,9		
313,3	6,8	6,6	292,4	48,3		
281,8	6,8	6,3	267,0	45,5		
231,6	5,3	5,9	234,0	44,4		
124,0	5,3	4,6	176,1	32,4		
83,1	4,9	5,1	135,8	25,3		
30,7	4,7	4,4	109,3	14,3		conta.
0,8	1,1	1,3	65,5	0,9		conta.
0,9	0,4	0,5	15,8	0,7	3,8	conta.
0	0,1	0,3	1,6	0,5		conta.

0 30.88E

HS- mymol/l	RDP mymol/l	TDP mymol/l	Si(OH)4 mymol/l	NH4 mymol/l	TPP nmol/l
109,0	5,4	4,6	144,7	31,2	1,2
53,3	5,0	4,5	113,4	21,3	2,5
12,9	4,8	4,4	92,2	12,6	
28,0	4,7	5,0	87,6	11,5	1,5
24,0	4,7	4,5	82,5	11,1	1,7
15,1	4,8	5,0	80,4	8,4	0,4
10,7	6,4	6,7	74,8	7,5	1,2
1,8	4,8	5,1	64,3	3,6	1,2
4,9	1,0	1,1	29,2	1,5	1,9
1,8	0,1	0,5	7,3	0,7	4,2
0,9	0,1	0,2	0,9	3,9	4,8
4,9	0,1	0,2	0,6	0,8	0,8

Filter (Dry) [g]	Filter plus material [g]	Weight [g]	Liter
0,1023		-0,1023	3,00
0,1040		-0,1040	5,00
0,0878		-0,0878	4,00
0,1033		-0,1033	6,00
0,0985		-0,0985	6,00
0,1021		-0,1021	6,00
0,1022		-0,1022	5,25
0,0988		-0,0988	5,25
0,0995		-0,0995	7,25
0,0991		-0,0991	6,15
0,1019		-0,1019	13,00
0,0994		-0,0994	7,50

Filter (dry) [g]	Filter plus material [g]	Weight [g]	Liter
0,1028		-0,1028	7,0
0,1044		-0,1044	5,5
0,1049		-0,1049	8,0
0,1020		-0,1020	7,5
0,1036		-0,1036	7,5
0,1028		-0,1028	11,0
0,1015		-0,1015	9,0
0,1015		-0,1015	10,0
0,1040		-0,1040	10,5
0,1036		-0,1036	9,5
0,0881		-0,0881	6,0
0,1055		-0,1055	7,0

Table 3
Station 34 (BSK1), Hydrocast 3, April 22, 1988, Black Sea, 43 09.67N,

Niskin No	Depth m	Pressure db	Temp. oC	Salinity per mil	pH	Eh mV
1	2000	1998,6	9,109	22,326	7,40	-49
2	1600	1598,3	9,054	22,323	7,40	-50
3	1250	1248,7	9,003	22,310	-	-
4	1000	998,7	8,962	22,288	7,42	-52
5	800	797,8	8,929	22,246	7,41	-52
6	600	599,5	8,900	22,161	7,45	-44
7	400	400,8	8,878	22,009	7,46	-43
8	300	301,8	8,852	21,865	7,53	-39
9	200	202,3	8,793	21,687	7,56	-14
10	100	130,5	8,577	21,252	7,57	-10
11	50	54,1	7,871	20,801	7,61	42
12	5	9,4	8,826	18,298	7,54	100

Table 4
Station 42, Hydrocast 4, April 23, 1988, Black Sea, 43 01.97 N, 31 59.

Niskin No	Depth m	Pressure db	Temp. oC	Salinity per mil	pH	Eh mV
1	250	252,5	8,830	21,768	7,59	-35
2	200	202,9	8,796	21,636	7,64	4
3	150	153,5	8,725	21,455	7,64	-17
4	120	123,8	8,659	21,292	7,63	15
5	85	89,3	8,521	20,943	7,65	32
6	70	74,5	8,405	20,741	7,63	99
7	55	59,7	8,163	20,348	7,61	123
8	45	49,5	7,455	19,681	7,59	144
9	30	34,9	7,190	18,769	7,60	208
10	20	25,1	7,848	18,697	8,04	237
11	10	15,1	8,563	18,650	7,96	263

31-59.92E

DOC	Alk.	H2S	HS- mymol/l	RDP mymol/l	Si(OH)4 mymol/l	NH4 mymol/l
1	1	present	340,0	8,3	356,0	39,7
1	1	present	389,3	8,2	361,7	35,2
-	-	-				
1	1	present	396,0	6,8	336,7	32,5
1	1	present	313,3	7,2	324,8	
1	1	present	286,7	7,0	294,1	32,6
1	1	present	238,7	5,7	315,4	36,7
1	1	present	138,7	5,5	204,7	36,8
1	1	present	90,7		163,2	24,4
1	1	present	54,6	4,7	128,3	21,0
1	1	absent	5,3	5,1	78,6	77,3
1	1	absent	0,0	1,1	44,0	1,4

27 E

DOC	Alk.	H2S	HS- mymol/l	RDP mymol/l	Si(OH)4 mymol/l	NH4 mymol/l
1	1	present	48,00	4,7	144,2	20,9
1	1	present	78,70	4,0	144,2	
1	1	present	53,30	3,8	126,8	19,6
1	1	present	29,30	3,8	106,9	12,7
1	1	present	18,70	3,9	94,0	9,4
1	1	absent	1,33	4,5	77,3	1,2
1	1	absent	2,67	3,2	67,9	1,5
1	1	absent	2,67	0,2	60,1	1,1
1	1	absent	2,67	0,7	45,7	2,2
1	1	absent	1,33	0,3	11,2	1,0
1	1	absent	2,67	0,2	6,7	0,9

TPP nmol/l	Deep water contamin.	Filter	Filter (dry) [g]	Filter plus material [g]	Weigth	Liter
5,6		13				1
3,6				0	0	0
				0	0	0
				0	0	0
3,5				0	0	0
2,9				0	0	0
3,9				0	0	0
3,9				0	0	0
3,8				0	0	0
3,2	contam.			0	0	0
6,1	contam.			0	0	0
5,4	contam.			0	0	0
10,6	contam.			0	0	

TPP nmol/l	Filter No.	Filter (dry) [g]	Filter plus material [g] weight	Liter
3,7	27	0,0883	-0,0883	6,0
4,8	28	0,1030	-0,1030	5,5
3,2	29	0,1027	-0,1027	6,0
5,7	30	0,1041	-0,1041	9,0
7,4	31	0,0985	-0,0985	6,0
6,8	32	0,1000	-0,1000	7,0
8,7	33	0,1048	-0,1048	6,0
11,0	34	0,1042	-0,1042	8,5
10,4	35	0,1053	-0,1053	6,0
8,7	36	0,0874	-0,0874	6,0
12,1	37	0,1011	-0,1011	6,0

Table 5
Station 47 (BSK2), Hydrocast 5, April 24, 1988, Black Sea, 42 58.79N,

Niskin No	Depth m	Pressure db	Temp. oC	Salinity per mil	pH	Eh mV
1	2150	2144,8	9,128	22,325	7,46	-114
2	1600	1597,7	9,053	22,320	7,43	-104
3	1250	1245,4	9,001	22,306	7,47	-82
4	1000	991,9	8,959	22,228	7,51	-56
5	800	795,8	8,925	22,227	7,49	-77
6	600	598,9	8,901	22,134	7,49	-74
7	400	399,3	8,877	21,951	7,52	-64
8	300	300,3	8,842	21,796	7,57	-51
9	200	202,2	8,760	21,523	7,61	-32
10	100	102,9	8,426	20,762	7,61	30
11	50	54,0	7,239	19,321	7,61	89
12	5	9,1	9,586	18,292	7,72	164

34 00.31E

DOC	Alk.	H2S	HS- mymol/l	TDP mymol/l	RDP mymol/l	Si(OH)4 mymol/l
		present	369,3		7,3	337,8
		present	366,7		7,5	341,0
		present	253,3		6,1	273,9
		present	330,7		6,6	309,9
		present	300,0		7,0	298,2
		present	273,3		6,6	275,2
		present	220,0		6,4	240,0
		present	136,0		5,4	184,3
1	1	present	90,7		5,1	123,4
1	1	absent	42,7		4,5	116,3
1	1	absent	5,3		3,5	71,0
1	1	absent	0,0		0,8	36,0

NH4 mymol/l	Deep water contamina.	Filter No.	Filter (dry) [g]	Fulilter plus [g]	Material Weight	Liter
59,2						
48,0						
25,4						
28,1	contam.					
23,0	contam.	41	0,1025		-0,1025	6
16,3	contam.	40	0,0992		-0,0992	6
	contam.	39	0,1021		-0,1021	6
	contam.	38	0,1036		-0,1036	6

Table 6
Station 6 (BSK2), Hydrocast 6, April 24, 1988, Black Sea, 42 54.25N, 3

Niskin No.	Depth m	Pressure db	Temp. oC	Salinity per mil	pH	Eh mV
1	350	353,2	8,865	21,889	7,63	-25
2	250	254,2	8,816	21,701	7,65	-10
3	220	224,2	8,786	21,608	7,65	-9
4	170	174,5	8,711	21,402	7,66	4
5	130	134,8	8,612	21,136	7,62	38
6	110	114,5	8,505	20,904	7,65	67
7	80	85,1	8,223	20,436	7,63	98
8	70	75,7	8,069	20,228	7,61	136
9	60	65,5	7,773	20,062	7,62	157
10	40	45,9	6,404	18,591	8,04	208
11	30	36,2	6,711	18,499	8,13	256
12	20	25,9	7,428	18,421	8,17	274

4 01.43E

DOC	Alk.	H2S	HS- mymol/l	TDP mymol/l	RDP mymol/l	Si(OH)4 mymol/l
1	1	present	108,0	4,8	4,9	168,2
1	1	present	8,0	4,5	4,7	136,0
1	1	present	54,7	4,3	4,4	123,4
1	1	present	29,3	4,4	4,4	103,5
1	1	present	5,3	4,6	4,9	83,8
1	1	present	6,7	5,3	5,4	65,8
1	1	absent	4,0	0,6	0,5	56,2
1	1	absent	4,0	1,1	0,6	45,8
1	1	absent	4,0		1,1	44,8
1	1	absent	6,7	0,3	0,2	12,7
1	1	absent	6,7	0,2	0,1	4,7
1	1	absent	6,7	0,2	0,1	4,8

NH4 mymol/l	Filter No.	Filter (dry g	Filter plus material g	Weight	Liter filtered
35,0	47	0,0995		-0,0995	6,0
23,8	48	0,0989		-0,0989	8,5
20,9	49	0,1033		-0,1033	7,0
16,8	50	0,1030		-0,1030	7,0
6,9	42	0,1055		-0,1055	7,5
4,0	43	0,0989		-0,0989	7,5
1,1	44	0,0994		-0,0994	8,5
1,3	45	0,1035		-0,1035	8,5
	46	0,1038		-0,1038	7,5
	51	0,1051		-0,1051	7,5
0,9	52	0,1038		-0,1038	7,0
2,1	53	0,1040		-0,1040	7,0

Table 7
Station 66 (BSK3), Hydrocast 7, April 26, 1988, Black Sea, 42 23.50N,

Niskin No	Depth m	Pressure db	Temp. oC	Salinity per mil	pH	Eh mV
1	2100	2094,8	9,121	22,325	7,51	-94
2	1600	1580,8	9,050	22,320	7,51	-85
3	1250	1227,1	8,999	22,305	7,53	-82
4	1000	983,1	8,956	22,275	7,53	-78
5	800	787,5	8,926	22,227	7,54	-72
6	600	601,2	8,901	22,129	7,58	-71
7	400	401,9	8,876	21,947	7,57	-58
8	300	302,9	8,842	21,786	7,64	-49
9	200	203,9	8,755	21,492	7,67	-43
10	100	105,1	8,352	20,678	7,72	-1
11	50	54,9	7,271	19,282	7,69	119
12	5	10,1	11,002	18,129	7,86	199

37 35.49E

DOC	Alk.	HS- mymol/l	RDP mymol/l	Si(OH)4 mymol/l	NH4 mymol/l	TPP nmol/l
1	1	314,7	7,7	312,7	56,7	4,4
1	1	352,0	7,8	308,1	57,9	2,6
1	1	292,0	7,6	293,0	34,9	3,5
1	1	232,0		286,8	46,7	4,1
1	1	301,3	7,2	263,8	30,8	3,1
1	1	180,0	6,2	210,3	43,4	6,3
1	1	216,0	5,8	203,8	45,1	3,3
1	1	121,3	5,4	164,0	27,7	2,2
1	1	72,0		117,7	24,6	3,6
1	1	32,0	4,8	119,3	11,4	3,7
1	1	1,3	2,5	62,2	0,9	3,4
1	1	1,3	1,0	25,3	0,3	3,9

Deep water contamina.	Filter No.	Filter (dry) g	Filter plus material g	Weight	Liter filtered
	49	0,0920	-0,0920		1,8
	48	0,0952	-0,0952		1,8
		0,0000	0,0000		
		0,0000	0,0000		
		0,0000	0,0000		
	43	0,0934	-0,0934		2,0
		0,0000	0,0000		
		0,0000	0,0000		
	44	0,0953	-0,0953		2,1
contam.	45	0,0953	-0,0953		1,8
contam.	46	0,0924	-0,0924		2,0
contam.	47	0,0941	-0,0941		2,0

Table 8
Station Station 72 (BSK3), Hydrocast 8, April 26, 1988, Black Sea, 42

Niskin No	Depth m	Pressure db	Temp. oC	Salinity per mil	pH	Eh mV
1	350	350,5	8,862	21,876	7,46	26
2	250	251,2	8,812	21,674	7,47	48
3	170	171,8	8,710	21,377	7,52	75
4	140	142,7	8,628	21,176	7,47	78
5	130	132,4	8,589	21,083	7,60	91
6	120	122,1	8,553	21,014	-	-
7	110	112,5	8,499	20,898	7,75	173
8	80	82,5	8,145	20,351	7,69	206
9	60	62,8	7,482	19,544	7,79	216
10	40	42,8	6,906	18,600	8,06	246
11	30	33,2	7,201	18,317	8,09	273
12	20	22,9	7,940	18,250	8,11	282

14.66N, 37 32.78E

DOC	Alk.	HS- mymol/l	RDP mymol/l	Si(OH)4 mymol/l	NH4 mymol/l	TPP nmol/l
1	1	202,7	4,6	173,7		4,3
1	1	118,7		117,7	24,6	3,6
1	1	49,3	4,0	103,7	8,8	7,1
1	1	1,3	4,3	93,1	9,5	1,6
1	1	13,3	4,8	87,3	8,4	
1	1	4,0				
1	1	2,7	6,1	69,5	0,0	3,2
1	1	2,7	0,5	52,2	6,2	0,8
1	1	0,0	0,6	31,4	3,3	1,9
1	1	8,0	0,0	11,5	1,7	0,6
1	1	2,7	0,1	3,1	2,6	2,3
1	1	2,7	0,0	2,6	1,2	

Filter No	Filter (dry) g	Filter plus material g	Weight	Liter filtered
55	0,1037		-0,1037	6
56	0,1028		-0,1028	7
57	0,1027		-0,1027	6
58	0,1015		-0,1015	6,5
59	0,1042		-0,1042	8
60	0,0986		-0,0986	6
62	0,1039		-0,1039	7,5
63	0,1041		-0,1041	7,5
64	0,1045		-0,1045	7,5
65	0,1041		-0,1041	7,5
25	0,0877		-0,0877	4,5
24	0,0887		-0,0887	4

Table 9
Station 82, Hydrocast 9, April 27, 1988, Black Sea, 42 02.39N, 39 15.29E

GoFlo Sample	Depth m	pH	Eh mV	RDP mymol/l	Si(OH)4 mymol/l	NH4 mymol/l	H2S smell	Manganese
1	20	8,21	266	0,04	5,15	0,15	absent	1
2	40			0,05	9,40	1,65	absent	1
3	50			0,10	10,11	0,60	absent	1
4	60			0,19	16,45	1,02	absent	1
5	70			0,62	30,05	2,13	absent	1
6	80			1,04	39,78	1,68	absent	1
7	90			1,09	52,84	5,58	absent	1
8	100			0,69	58,47	2,28	absent	1
9	110			0,38	44,97	2,48	absent	1
10	120	7,61	196	5,04	73,99	2,83	present	1
11	130	7,64	226				present	1
12	150	7,64	234	4,29	97,10	8,23	present	1

Table 10
Station 86, Hydrocast 10, April 28, 1988, Black Sea, 41 48.50N, 40 12.80 E

Niskin No	Depth m	Pressure dB	Temp. oC	Salinity per mil	pH	Eh mV	RDP mymol/l	Si(OH)4 mymol/l	NH4 mymol/l
1	350	348,3	8,845	21,792	7,54	5	4,73	162,56	28,53
2	250	249,0	8,737	21,458	7,59	65	4,59	117,89	17,63
3	180	179,6	8,467	20,870	7,57	130	4,49	79,06	1,93
4	160	160,3	8,264	20,521	7,62	191	1,36	66,23	7,73
5	140	140,6	7,820	19,947	7,65	205	1,09	52,45	4,03
6	malfunctio								
7	120	120,9	7,336	19,306	7,81	248	0,69	33,48	8,48
8	100	100,7	7,044	18,719	7,96	269	0,35	17,98	5,63
9	70	70,8	6,734	18,354	8,10	284	0,27	5,74	3,15
10	40	41,2	7,289	18,180	8,16	294	0,10	3,20	1,30
11	20	21,3	7,738	18,128	8,21	300	0,08	2,06	0,10
12	10	11,6	9,612	17,956	8,25	304	0,00	2,04	2,10

Table 11
Station 96, Hydrocast 11, April 28, 1988, Black Sea, 41 25.66N, 41 18.52E

Niskin No	Depth m	Press. db	Temp. oC	Sal. per mil	pH	Eh mV	RDP mymol/l	Si(OH)4 mymol/l	NH4 mymol/l	DOC HgCl2	Alk. HgCl2
1	200	201,4	8,520	20,974	7,52	135	4,77	88,36	3,74	1	1
2	180	181,1	8,430	20,810	7,56	165	3,46	74,16	1,67	1	1
3	150	151,7	8,098	20,286	7,60	222	0,86	57,23	0,51	1	1
4	125	127,5	7,471	19,504	7,71	246	0,68	36,04	0,59	1	1
5	100	102,1	7,046	18,707	7,91	282	0,20	19,99	0,47	1	1
6	malfunction										
7	80	82,4	7,066	18,467	8,01	289	0,25	9,83	1,57	1	1
8	70	72,5	7,009	18,356	8,05	303	0,00	6,17	0,45	1	1
9	60	62,5	7,102	18,297	8,08	309	0,12	4,48	0,29	1	1
10	45	47,4	7,319	18,188	8,08	316	0,37	1,47	1,40	1	1
11	30	33,0	7,745	18,048	8,11	334	0,00	0,66	0,29	1	1
12	10	12,1	12,511	17,884	8,16	338	0,14	0,66	0,64	1	1

Table 12
Station 115, Pump 6, May 1, 1988, Black Sea, 41 46.75N, 36 16.46E

Niskin No	Depth m	Pressure dB	Temp. oC	Salinity per mil	pH	Eh mV	Filter No	New Weight g	Liter filtered
8	185	184,4	8,529	20,974	7,68	328	13	0,6621	13,68
9	173	173,6	8,512	20,914	7,67	387	58	0,6689	13,77
10	168	168,7	8,430	20,825	7,65	362	30		14,44
11	163	164,2	8,377	20,748	7,65	363	31	0,6554	19,91
12	150	149,8	8,200	20,463	7,66	366	57	0,7190	13,61

(10cm membrane filter, Seastar pump)

Table 13
Station 135 (BSK2), Hydrocast 20/Pump 7, May 3, 1988, Black Sea, 43 03.33N, 34 04.96E

Niskin No	Depth m	Pressure dB	Temp. oC	Salinity per mil	pH	Eh mV	HS- mymol/l	Alk. (HgCl2)	Ca2+ (pH2)	TDP mymol/l	RDP mymol/l	Si(OH)4 mymol/l	NH4 mymol/l
1	200	201,2	8,756	21,511				1	1	Sample contaminated with water from shallower depth			
2	180	182,0	8,729	21,439	7,65	19	15,33	1	1	4,35	3,72	22,06	16,45
3	160	162,0	8,687	21,331	7,65	31	12,00	1	1	4,18	3,59	18,58	13,70
4	140	142,6	8,636	21,208	7,65	54	3,33	1	1	4,47	4,38	18,90	11,40
5	120	118,6	8,567	21,026	7,67	64	2,00	1	1	5,06	5,13	16,76	4,50
7	110	108,9	8,495	20,843	7,65	118	1,33	1	1	5,12	5,63	15,48	5,05
8	100	99,0	8,407	20,709	7,66	157	0,00	1	1	2,41	2,26	13,85	5,88
9	90	88,7	8,28	20,523	7,63	179	0,67	1	1	0,36	0,23	12,91	3,55
10	80	79,3	8,149	20,336	7,62	182	1,33	1	1	0,42	0,42	11,46	5,90
11	70	69,3	7,848	19,958	7,63	196	0,00	1	1	1,03	0,84	9,60	2,40
12	60	59,3	7,426	19,523	7,72	226	0,00	1	1	0,93	0,71	6,90	0,88

Table 14
Station 165, Hydrocast 28, May 5, 1988, Black Sea, 42 14.36N 32 43.16

Niskin No	Depth m	Pressure dB	Temp. oC	Salinity per mil	pH	Eh mV
1	200	199,8	8,726	21,464	7,60	26
2	160	160,9	8,633	21,253	7,61	20
3	120	121,6	8,504	20,902	7,62	14
4	100	101,6	8,321	20,585	7,62	31
5	80	81,7	8,021	20,164	7,61	85
7	50	52,0	6,751	18,627	7,58	152
8	10	12,1	9,138	18,202	7,57	169

IV. C. SEDIMENT TRAP SUPERNATANT CHEMISTRY WITH COMPARISONS TO WATER COLUMN CHEMISTRY

J. M. Nicholson, S. Kempe, G. Liebezeit, and B. Woodward

1. DESCRIPTION OF SAMPLING CUP CONTENTS

Black Sea-Chernobyl Deployment 3 (BSC3), May 15, 1987 - April 21, 1988 (12 intervals of 30.5 days) (see Fig. 8 in cruise report section IV.A. for mooring design).

Shallow Trap (371 m).

Sediment trap Mark 6, 0.5 m^2 cone diameter, twelve 250-ml cups preserved with 4% formaldehyde solution in a 34°/$_{oo}$ NaCl solution, buffered with sodium borate.

Cup	Date	Particle Vol.; ml	Description
1	5/15-6/14	50	Greenish grey, fluffy matter, rather coarse aggregates swimming in a finer matrix, supernatant cloudy, some creamy whitish matter at bottom (ZnS ?), (at recovery some material was spilled from cup 1 incidentally).
2	06/14-07/15	0.5	Very few light greenish brown aggregates.
3	07/15-08/14	0.4	Same as cup 2.
4	08/14-09/14	0.4	Same as cup 2.
5	09/14-10/14	1	Same as cup 2.
6	10/14-11/14	0.7	Same as cup 2.
7	11/14-12/14	1	Same as cup 2.
8	12/14-01/14	0.7	Same as cup 2, three particles, possibly contamination.
9	01/14-02/13	0.7	Same as cup 2.
10	02/13-03/15	1	Same as cup 2, more whitish
11	03/15-04/14	1	Same as cup 2.
	Trap was recovered with cup 12 open (see note below)		
12	04/14-05/15	10	Greenish coarse grained aggregates (cup contained cotter pin and large particles of rust which fell into the trap accidentally during mooring recovery since this cup was still open).

(Note: Cup 12 of both traps were open because the mooring had to be recovered earlier than planned during the deployment due to schedule changes of the R/V Knorr cruise.)

Deep Trap (1,257 m)

Sediment trap Mark 5, 1.2 m^2 cone diameter, twelve 1000-ml cups preserved with 4% formaldehyde solution in a 34°/$_{oo}$ NaCl solution, buffered with sodium borate.

Cup	Date	Particle Vol.; ml	Description
1	5/15-6/14	400	Greenish grey fluffy mass of aggregates, very sticky. White creamy mass on bottom (possibly ZnS), one well preserved, 5-cm medusa. Supernatant cloudy and grey.
2	06/14-07/15	10	Some buoyant greenish clouds of smaller aggregates, possible fecal pellets. Supernatant clear.
3	07/15-08/14	10	Same as cup 2, less fecal pellets.
4	08/14-09/14	5	Some buoyant light greenish clouds of aggregates, and a creamy white more dense mass (ZnS ?). Supernatant clear.
5	09/14-10/14	3	Very little buoyant greenish matter, some creamy but more dense mass (ZnS ?). Supernatant clear.
6	10/14-11/14	3	Same as cup 5.
7	11/14-12/14	2	Same as cup 5.
8	12/14-01/14	3	Same as cup 5 but less of the greenish matter and more of the possible ZnS, some fecal pellets. Supernatant clear.
9	01/14-02/13	2	Same as cup 5.
10	02/13-03/15	2	Same as cup 5.
11	03/15-04/14	8	More darker greenish very buoyant fluff, some darker fecal pellets.
	Trap was recovered with cup 12 open (see note above)		
12	04/14-05/15	250	Darkish, greenish fluffy matter, containing rather dark aggregates, possible fecal pellets, in total more coarsely structured than cup 1 material. Some creamy white more dense mass (ZnS ?) and particles. Supernatant cloudy.

2. CHEMICAL ANALYSIS OF TRAP SUPERNATANT

Both traps at mapsite BSC were deployed in May, 1987, containing supernatant whose pH was buffered to between 7.5 and 8.0. The other components of the supernatant were: 4% formadehyde in distilled water, 34°/$_{oo}$ sodium chloride, and sodium borate as buffer. The supernatant was prepared by boiling distilled water and bubbling nitrogen gas through it, and was allowed to cool with nitrogen gas bubbling through it. The other ingredients were added during this cooling stage, and then trap cups containing this solution were stored under nitrogen in a glove bag until deployment of the traps took place. After retrieval of the traps at mapsite BSC, the supernatant in each cup of both shallow (371 m) and deep (1,262 m) traps was analyzed on board ship for the following:

pH, Eh -- S. Kempe, B. Woodward
Dissolved sulfide (HS^-) -- J. Nicholson
Total dissolved phosphorus (TDP), reactive dissolved phosphorus (RDP) and dissolved silicate (H_4SiO_4) -- G. Liebezeit

The results of these analyses for both shallow and deep traps are briefly summarized below.

pH: The trap cups upon recovery probably reflect the original pH of the supernatant used, although differences exist (Fig. 1). For example, the shallow trap has lower pH's than the deep trap (in one case dropping below 7.0), although the deep trap has more uniform values than the shallow trap.

pE: In order to compare the redox behavior of the solution on a logarithmic scale, and also to compare with other published pE-pH diagrams, we converted Eh (mV) to pE, a measure of the electron activity, using the following formula:

$$pE = -\log \{e^-\} = Eh/\ 2.303\ RTF^{-1}$$

where Eh = equilibrium redox potential (volts)
R = gas constant (8.314 $J\text{-}mol^{-1}\,°K^{-1}$)
T = absolute temperature in °K
F = 96,490 coulombs/mol
$2.303\ RF^{-1}$ = 0.19844 mV/mol.

For more reducing environments, pE is more negative, while under more oxidizing conditions, pE is more positive. pE values of the trap cups is around +3 (Fig. 2), placing it within an oxidized pH-pE regime. For most cups, pE is uniform, except for the first and last cups in the deep trap which are indicated to be more oxidizing. There are no consistent differences between deep and shallow traps.

Table 1. Chemical Analyses of Supernatant

Cup	pH	Eh(mV) mV	HS^- µmol/l	RDP µmol/l	TDP µmol/l	$Si(OH)_4$ µmol/l
BSC3 Shallow:						
1	7.72	239	16.0	36.7	40.9	69.7
2	7.47	174	14.7	6.9	6.8	266.5
3	7.35	186	14.7	6.6	6.9	245.2
4	7.14	184	13.3	5.5	5.4	222.3
5	7.19	182	9.3	4.9	5.0	259.4
6	7.29	148	13.3	4.4	4.5	211.9
7	7.27	155	12.0	4.9	4.8	216.7
8	7.31	151	17.3	4.1	4.2	154.5
9	6.91	164	10.7	3.2	3.2	136.0
10	7.11	163	16.0	3.3	3.6	158.9
11	7.07	159	10.7	2.8	3.1	179.1
12	7.81	160	14.7	1.5	1.4	93.9
BSC3 Deep:						
1	7.97	398	13.3	1.3	1.5	36.0
2	8.04	180	14.7	0.2	0.5	17.5
3	7.88	158	26.7	3.7	5.1	333.9
4	8.05	150	26.3	3.3	4.5	307.2
5	7.86	147	33.3	3.0	3.8	253.4
6	7.90	170	20.0	1.6	2.2	242.5
7	7.94	155	29.3	2.9	3.8	240.0
8	8.11	163	28.0	1.4	1.5	103.5
9	8.25	216	17.3	0.6	0.5	81.4
10	8.22	232	18.7	0.2	0.2	15.8
11	8.18	210	17.3	0.8	1.0	62.5
12	8.09	111	16.0	1.1	1.4	32.5

(Note: We are aware of the fact that Eh readings are not in accordance with the measured HS^- concentrations; the Eh readings are far too positive. This may be due to either a faulty Eh electrode, or to the failure of the Eh measurement or HS^- measurements to yield correct values in a formaldehyde solution. We could not decide aboard ship which of the above causes was responsible for the discrepancy in the data. We advise, therefore, that the results above be treated as preliminary only.)

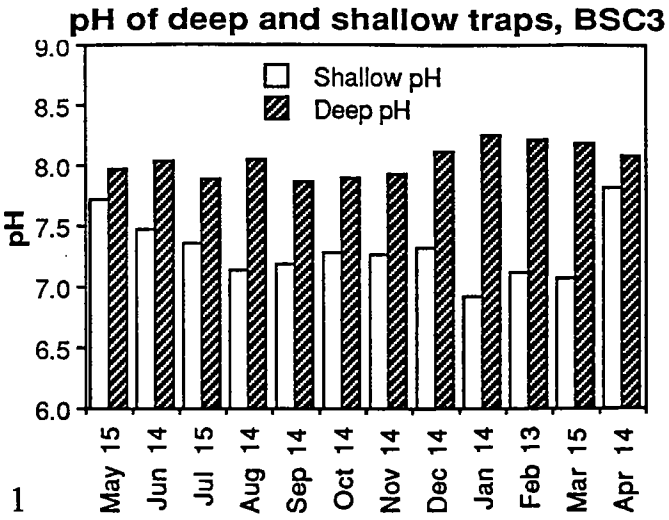

Fig. 1

Fig. 1 The pH of both deep (1,262 m) and shallow (371 m) traps retrieved at Site BSC (trap designation BSC 3) is shown for each of 12 cups. Opening date for each cup is shown at the bottom.

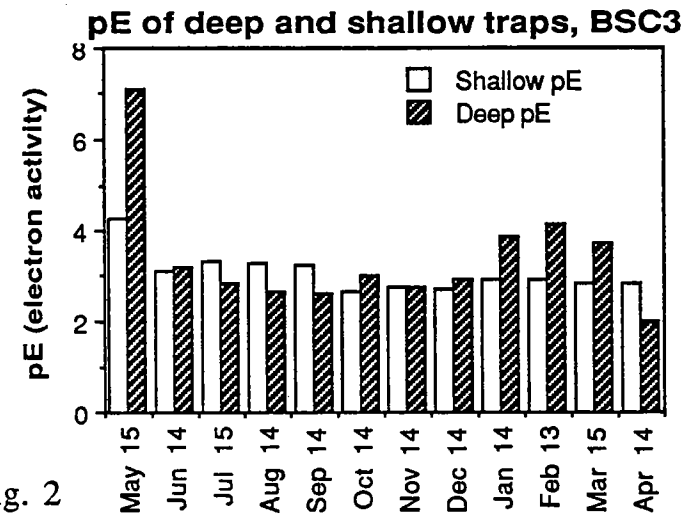

Fig. 2

Fig. 2 pE of both deep and shallow traps are plotted (see text for conversion of Eh to pE, a measure of electron activity) for each cup.

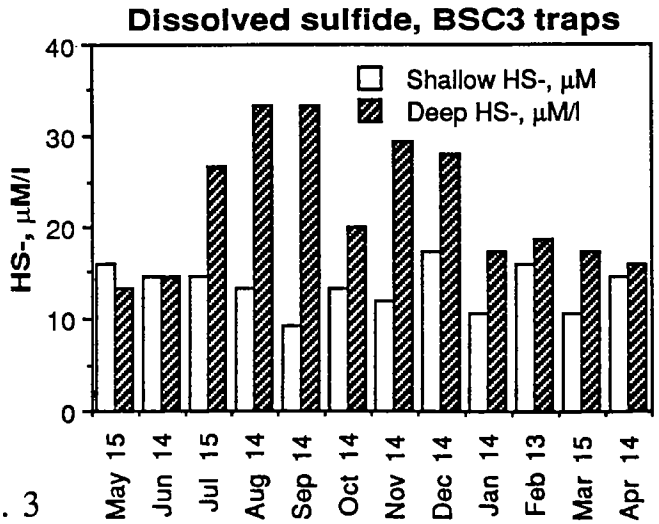

Fig. 3

Fig. 3 Dissolved sulfide (HS-) for both deep and shallow traps at Site BSC is shown plotted for each cup. Note that the highest levels of sulfide in the deep trap are found in cups whose pE tends to be lower.

Dissolved sulfide, HS^-: The shallow trap has average dissolved sulfide levels of about 15 μM/l, whereas the deep trap has usually higher levels (30 μM/l), but shows a more variable pattern (Fig. 3). For the deep trap, dissolved sulfide is highest in those cups which also have the lowest pE (more reducing), which is consistent. The values of sulfide we obtained are low compared to the water column sulfide content, as will be discussed below.

Total dissolved and reactive dissolved phosphorus (TDP, RDP): TDP of the trap cups appears moderately uniform (Fig. 4), with the exception of the first cup (possibly a typographical error in the data). The shallow trap has consistently more TDP than the deep trap. RDP (Fig. 5) in the shallow trap is more uniform over time than in the deep trap. In most cases, the amount of RDP in the shallow trap is greater than in the deep trap.

Dissolved silicate (H_4SiO_4): Dissolved silicate is lowest during the May-June and March-April periods, and rises during the summer and autumn months, as can be seen in Fig. 6. This peak occurs after the late spring diatom bloom commonly observed in previous sediment trap experiments in the southwestern Black Sea (PARFLUX sites BS and BSC), and may reflect the rise in dissolved silicate which is available after the annual peak in diatom production has passed.

3. COMPARISON OF TRAP SUPERNATANT CHEMISTRY WITH WATER COLUMN CHEMISTRY

In order to see how the trap supernatant compares with the water column, we combined data from the four sites for which complete depth profiles of water column chemistry were made (mapsites BSC, BSK1, BSK2/station S3, BSK3, and BSK2/station 135, with the data from the traps moored at 371 m and 1,262 m. For all data plotted, points representing the trap values can be distinguished from data from nearly equivalent depths at 350, 400, 1,200, and 1,250 m.

pH: Both shallow and deep traps differ in pH behavior from the ambient water column (Fig. 7). The main features of the differences are:

- Trap cups exhibit a greater range of pH values than do water column samples from comparable depths.

- The shallow trap has a lower mean pH than the water column at that depth; conversely the deep trap has a higher mean of pH than the ambient water. Values of pH in the shallow trap are like those of deep water, and are lower than those of the original supernatant, whereas pH's in the deep trap are more like those of surface water, and are a little higher than the pH of the original supernatant.

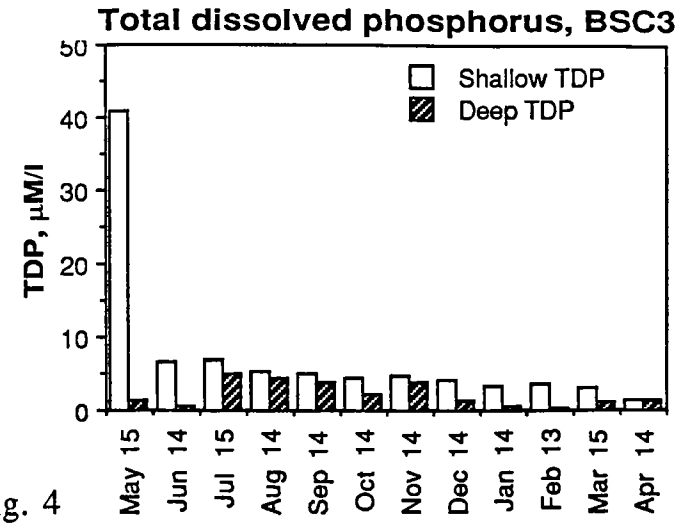

Fig. 4

Fig. 4 Shown here is total dissolved phosphorus (TDP) for both shallow and deep traps over the year-long deployment at Site BSC.

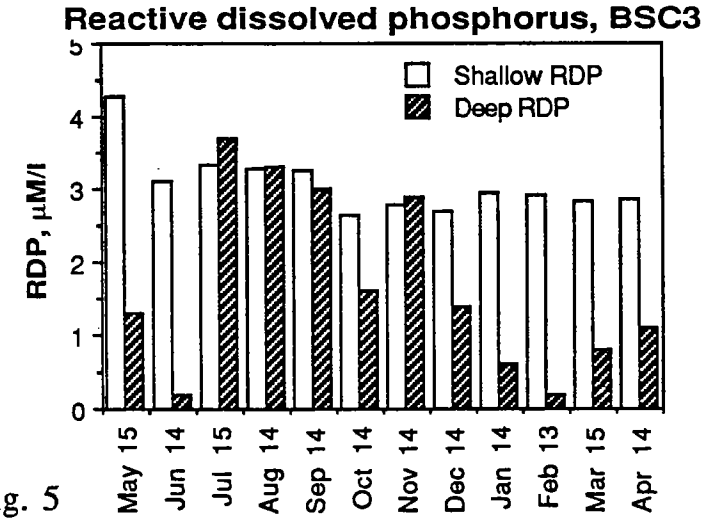

Fig. 5

Fig. 5 Reactive dissolved phosphorus (RDP) for both deep and shallow traps is shown plotted for each cup. Note that values in the shallow trap are more uniform, whereas values in the deep trap are less so.

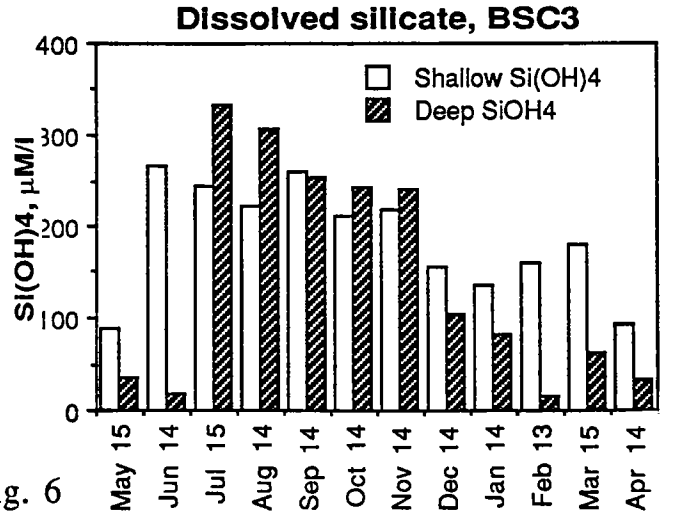

Fig. 6

Fig. 6 Dissolved silicate (H_4SiO_4) in both shallow and deep traps. Note the low levels of dissolved silicate in both traps, but especially the deep trap, during the months of February-June, a time during which the spring diatom bloom has been observed to occur in the Black Sea using sediment trap data. Higher levels of dissolved silicate appear during the late summer and autumn months.

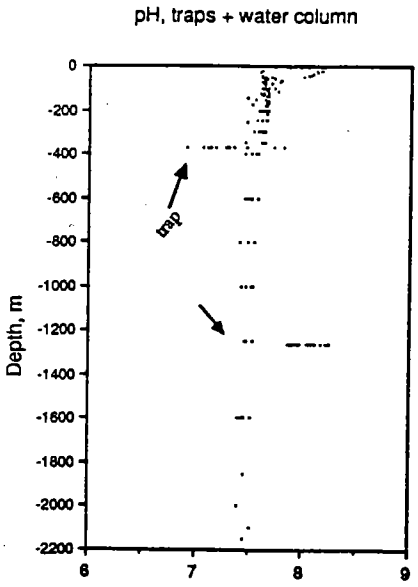

Fig. 7

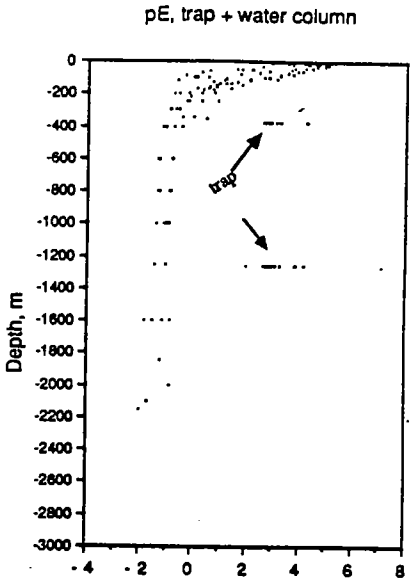

Fig. 8

Fig. 7 Shown here are all pH data for sediment trap supernatant in deep and shallow traps at Site BSC and all other hydrocast stations for which both sulfide and Eh were measured (Sites BSC, BSK 1, BSK 2, BSK 3, and BSK 2/Station 135, which was Site BSK 2 revisited 9 days later). Trap values stand out at 371 m and 1,262 m.

Fig. 8 Shown here are all values of pE, a measure of electron activity, for sediment trap supernatant and hydrocast stations as explained above. All values for the traps are above pE = 2.

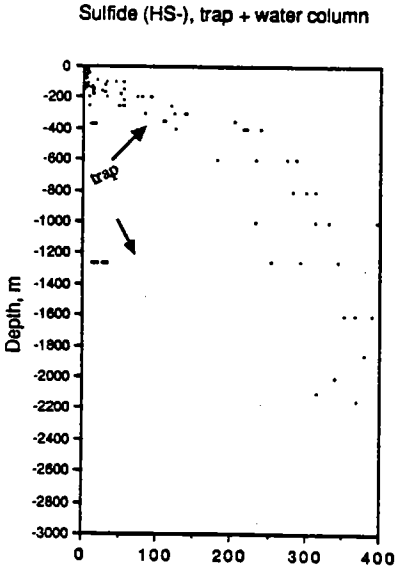

Fig. 9

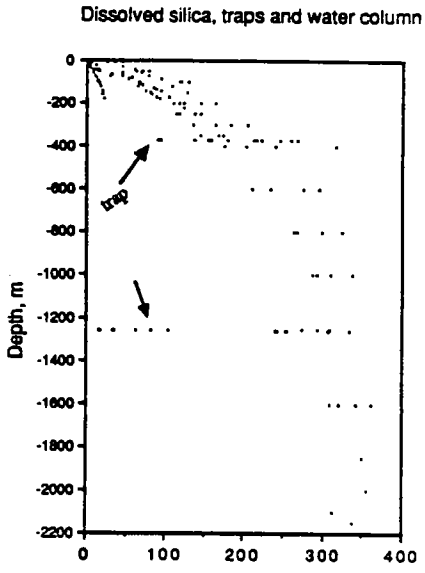

Fig. 10

Fig. 9 Dissolved sulfide (HS-) in the water column at hydrocast stations and in sediment traps at Site BSC. All values for the deep and shallow traps are less than 40 µM/l, and form two tight clusters at 371 m and 1,262 m.

Fig. 10. Dissolved silica in the sediment traps and hydrocast stations. Although values for the shallow sediment trap overlap values found in the water column at a nearly equivalent depth, they can be distinguished by being at a slightly different level. Likewise, only a few values for the deep trap overlap the range found in the water column at 1,250 m depth.

pE: The redox potential (shown as electron activity, pE) of the trap cups is quite different from that of the ambient water column at the relevant depths (Fig. 8); trap cups have more oxidizing (more positive pE) conditions than water samples taken from nearly equivalent depths.

Dissolved sulfide (HS^-): The dissolved sulfide values for the deep and shallow traps form two tight clusters of unresolved points at concentrations less than 50 µM/l, and that sulfide concentration is less than that in water samples from ambient depths (Fig. 9).

Dissolved silicate, H_4SiO_4: The shallow trap has levels of dissolved silicate that are consistent with the depth of this trap, but the deep trap has less silicate than expected (Fig. 10).

TDP and RDP: For both TDP and RDP, the shallow trap is similar to the water column values, although there is a wider range of values (Figs. 11 and 12). However, the deep trap is different from deep water; lower values of TDP and RDP characterize the deep trap supernatants.

DISCUSSION

The general characteristics of trap supernatant chemistry are as follows:

1) The deep trap tends to be depleted in nutrients and sulfide, and higher in pH and pE, relative to the ambient water column.

2) The shallow trap has higher pE and lower sulfide values than the ambient water, but otherwise nutrient levels and pH are consistent with ambient conditions.

3) Both shallow and deep traps have greater variations in pH, pE, TDP, RDP, and H_4SiO_4 than does the water column at the respective depths.

At this preliminary stage, we can only suggest several possibilities for the behavior of the trap supernatant under conditions existing in the Black Sea. First, since the deep trap appears more out of equilibrium with deep water and resembles surface water, the first question might be whether it has somehow been contaminated with surface water. For trap cups which have already closed, the only possible means of contamination might be via loose gaskets or O-rings at the mouth of the cup. Assuming that complete equilibration of cup supernatant with the ambient water occurred during the 1-month period that each cup was open, then each trap cup upon closing should have had a concentration of dissolved silicate equal to about 300 µM/l. Upon retrieval, the trap is brought to the surface where the hypothesized leakage/contamination occurred, and where silicate values are nil to less than 100 µM/l. A three-hundredfold decrease, or even a threefold decrease in silicate concentrations (dilution factors of 300 and 3) calls for a significant amount of water exchanged; essentially the entire amount of supernatant (to go from 300

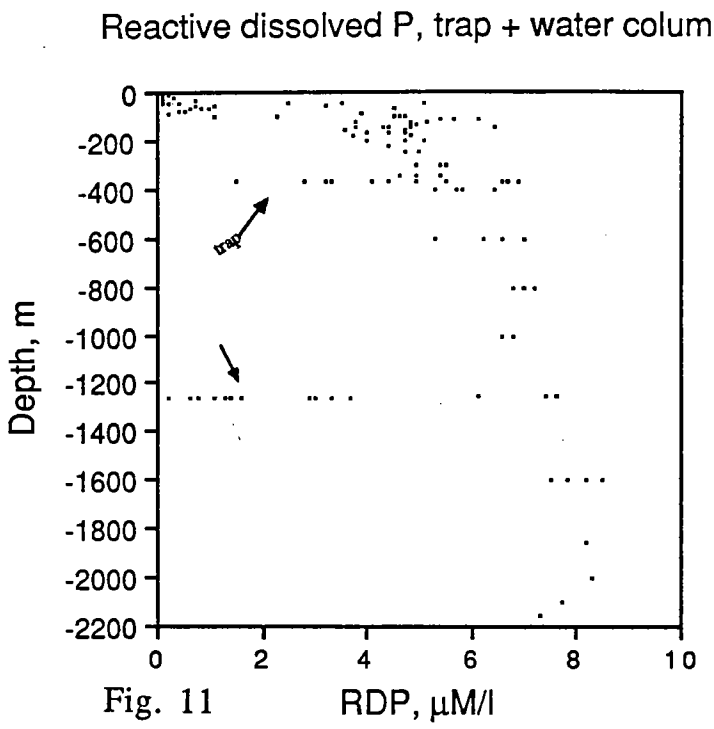

Fig. 11

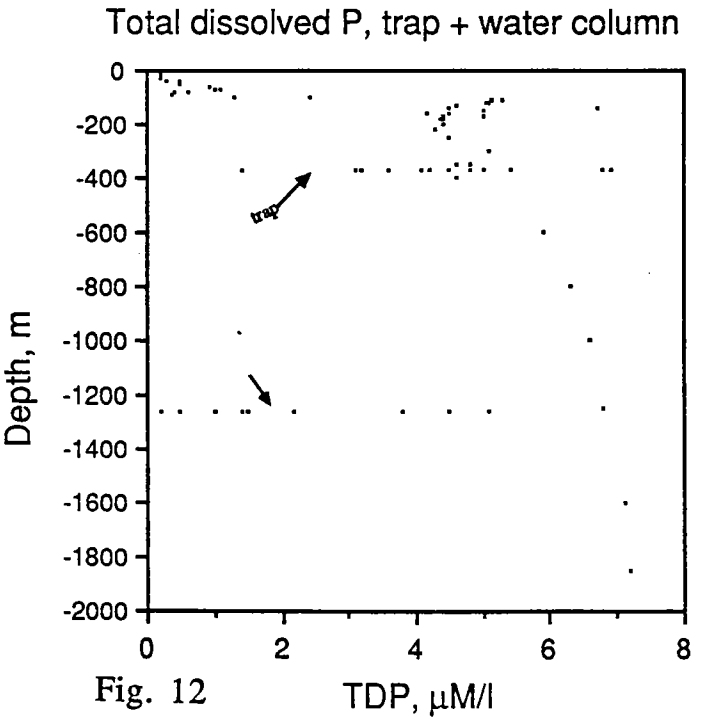

Fig. 12

Figs. 11, 12. Shown here are reactive dissolved phosphorus (RDP) and total dissolved phosphorus (TDP) for hydrocast stations and deep and shallow sediment traps at mapsite BSC. Both RDP and TDP show similar patterns in that the shallow trap has mean values similar to those of the water column, although greater variation exists, while the deep trap generally has less phosphorus than the water column, but also shows a large degree of variability. No trap samples have values greater than the water column which is a good indicator that the cellular material in the particulate matter of the traps has not yet begun to significantly lyse and release dissolved phosphorus.

to zero μM/l) or two-thirds of the supernatant (to go from 300 to 100 μM/l) must be replaced by surface water leaking in. This is highly improbable. Also, even if passive diffusion across a concentration gradient were another possibility rather than replacement of part of the cup supernatant by seawater, the time scale over which the traps are in surface waters is only about one hour.

Second, depletion of nutrients, raising of pE and change in pH could be due to microbial activity inside the closed cups. Some arguments for microbial activity exist for these traps. First, lowering of pH might occur due to sulfate reduction (release of carbon dioxide), and depletion of dissolved nutrients such as phosphate might well occur due to microbial growth. Second, even though formadehyde was present (4% original concentration), it does not prevent all microbial growth, as observed empirically during a one-week lowering of V. Asper's sediment trap/camera system, in which one trap contained formalin and the other did not; both trap chambers exhibited microbial growth on the side walls, although there was much less in the trap containing formalin. Phase-contrast microscopy of formalin-preserved sediment trap samples by one of us (J. Nicholson, unpublished results) has shown that live bacteria are still present in formadehyde-preserved trap material. In a closed environment such as a closed trap cup, depletion of nutrients might occur. However, silicate depletion by such a mechanism, to the levels observed here in the deep trap, probably is not occurring, since active growth and incorporation of silica by diatoms, for example, requires light. Therefore this explanation does not explain the silica distribution observed here, although it is not inconsistent with the nutrient values observed.

Incomplete diffusion of dissolved substances into the trap cups during open cup intervals is the third possibility, and perhaps the most probable. Because the trap supernatant was prepared from distilled water + salt + formalin + sodium borate, any other dissolved substances present after trap recovery would have diffused in or advected during the month-long period that a cup remains open. Incomplete diffusion or mixing could explain the fact that most of the values for dissolved nutrients are less than or equal to the water column values at that depth, and are never greater. Incomplete mixing might be due to the higher salinity of the supernatant than ambient water salinities (34 vs. 24°/$_{oo}$, respectively). One good test of this suggestion will be the short-term traps which will be retrieved in August, which were deployed with 40°/$_{oo}$ salinity supernatant.

The oxidizing nature of the supernatant despite anoxic precautions, indicated by both pE and the low levels of sulfide observed in the trap cups, might be due to inefficacy of the anoxic precautions used. However, previous measurements of sulfide in trap cups made during the PARFLUX experiment in the Black Sea (Nicholson et al., in preparation), were higher (up to 300 μM/l) and were furthermore made on supernatant which had not been anoxically prepared. One possible reason for low sulfide and high pE values might be the use of some hitherto unrecognized oxidizing agent; sodium borate ($Na_2B_4O_7$:10 H_2O), used for the first time during this trap deployment is a conceivable culprit. If this is so, then carbonate may be a better buffer ($CaCO_3$).

IV. D. REDUCED SULFUR IN THE BLACK SEA WATER COLUMN AND SEDIMENT TRAPS

Jo Ann M. Nicholson

General Description

As part of a research program by J. M. Nicholson and J. L. Cisne to investigate reduced sulfur fluxes in the water column and reduced sulfur content composition of bottom sediments, work aboard ship included the following elements:

1. Subsampling the sediment trap supernatant (mapsite BSC) for sulfide analysis.
2. Obtaining profiles of dissolved sulfide in the water column.
3. Water sampling for later lab analyses of dissolved oxygen and sulfate.
4. Subcoring of box cores for later studies of reduced sulfur species, sulfur isotope analyses, and iron in sediments.
5. Sampling of uppermost "fluff" layer for later analyses of reduced sulfur and iron.
6. Filtration of water column samples for later particle analysis and sulfur analysis.
7. Anoxic subsampling sediment trap particulate material (mapsite BSC) for later particulate reduced sulfur species.
8. Recovery of a clay experiment deployed on the deep trap at mapsite BSC in May of 1987 (trap designation BSC3).

Of this work, results from items 2 and 8 will be described here. Sulfide analyses of the trap supernatant (item 1 above) are discussed in the previous section dealing with comparison of trap supernatant chemistry with water column chemistry.

Methods

1. Water sampling

Sulfide analyses: Water samples were collected from the rosette sampler fitted with Niskin bottles (30 liter capacity). Nitrogen gas was used to provide head pressure and to prevent oxidation of water while sampling. Sampling for sulfide was done using brown glass bottles prefilled with argon gas and filled to half volume with 10% zinc acetate (made up in deionized water and deoxygenated previously by gassing with argon gas for several hours), to directly preserve the sulfide in the water as it flowed into the sample bottles. This set of samples was designated S1. A secondary set of water samples was collected using brown glass bottles prefilled with argon gas, but without any preservative zinc acetate solution. This set of samples was designated S2, and later in the ship's

lab, 50 mls of subsample from each bottle was mixed with 50 mls of deaerated zinc acetate and stored preserved.

Oxygen bottles: We used 250 ml glass bottles for oxygen determination. Unfortunately, one reagent needed was in a glass container that broke on board ship. All samples for oxygen were collected and preserved for later titration using 1.0 ml of $MnSO_4$ solution, followed by 1.0 ml of alkaline iodide solution, shaken and stored in the dark tightly capped, with no head space.

Sulfate: Samples for later sulfate analyses were collected using glass 250 ml bottles previously filled with argon gas, with no head space.

Water Filtration: Filtration of water samples from water column profiles at mapsites BSC and BSK1 for later SEM studies of sulfur and iron content of the particulate material. One-half liter of seawater was used for filtration. Preweighed "A"-type 0.45 μm Nuclepore membrane filters were used. Samples were stored in desiccant jars under an argon atmosphere.

2. Measurement of dissolved sulfide

Reagents used:

10% zinc acetate (100 g/liter deionized water)
02% zinc acetate (20 g/1)
Diamine dye reagent: 3.726 g of n,n-dimethyl-p-phenylene diamine hydrochloride dye, together with 6.0 g of $FeCl3{:}6H_2O$, were made up in one liter of 6N hydrochloric acid.

Dissolved sulfide standards were made up on board ship using sodium sulfide ($Na_2S{:}9H_2O$). From this a set of photometric standards was prepared and a curve for absorbence vs. concentration prepared. This was used for all subsequent work on board ship. A spectrophotometer set at 650 nm was used for determination of absorbence (normally a wavelength of 670 nm would have been used if available, but the filter available with the spectrophotometer was 650 nm). Blanks were prepared using both surface seawater and distilled water.

The procedure for analysis was as follows: 1.0 ml of the sample (Set S1, previously preserved in 10% zinc acetate) was pipetted into scintillation vials already containing 10 ml of 2% zinc acetate solution. After addition of the sample, 10 ml of diamine dye reagent was added, and the vial quickly capped. These vials were then stored in the dark for an hour before measurement of the absorbence. Replicates using S1 and S2 (preserved after collection of water samples) were run for mapsites BSC and BSK2, in order to determine the experimental standard deviation.

3. Anoxic subsampling of sediment trap supernatant and particulate material

All subsampling of trap cup contents was carried out in a glove bag under an argon atmosphere. For dissolved sulfide, two 10-ml aliquots of supernatant were sampled from each cup, and preserved in an equal amount of 10% zinc acetate. For later analyses of reduced sulfur content and elemental analysis of trap material, 10 ml of suspended particulate material was sampled from cups 1, 2, and 12 using syringes filled with argon. These samples were subsequently filtered, rinsed, and dried on preweighed filters in a glove bag, under an argon atmosphere.

4. Subcores and sampling of uppermost "fluff" layer

Three-inch diameter subcores were taken (number 4) for later studies of sulfur species and iron content. Whenever possible, samples of the "fluff" layer were taken and preserved in formaldehyde and kept refrigerated in vials containing an argon atmosphere.

Results

1. Profiles of dissolved sulfide in the water column

Profiles of dissolved sulfide in the water column were taken at mapsites BSC, BSK1, BSK2, and BSK3, as well as a second shallow watercast at mapsite BSK2 when we returned to this site on May 3. These sites represent all the sites where sediment traps were either recovered or deployed. For mapsite BSC, two different sets of samples (S1 and S2, which vary in the way that zinc acetate preservative was added) were taken and analyzed in order to obtain sample standard deviations. Similar replicates for the other sites will be run at a later date, upon return to Woods Hole.

For the most part, the sulfide profiles are generally similar in that sulfide begins to appear in the water column by about 100 m depth, although the pattern here is generally very noisy (Figs. 1-5). Sulfide increases gradually to about 350-400 μM/l at the bottom. For an example of the amount of noise in the data, figure 1 shows the mean value plus and minus 1 s.d., although the amount of noise may or may not be typical. Interestingly enough, when these profiles are compared to the sulfide profiles obtained previously by Brewer and Spencer (1974), there is no increase in sulfide near the bottom of the kind they found. Although replicates need to be run before anything more definitive can be said, there is the suggestion that the values may decrease slightly nearer the bottom, or at least not increase.

For the purpose of better defining the oxic-anoxic interface at mapsite BSK2, a second shallow watercast was taken upon our return to this site on May 3 (HC 135). Sampling intervals were 10 m apart, starting from a depth of 70 m and continuing down to 200 m (Fig. 5). Although I

Mean dissolved sulfide, Site BSC

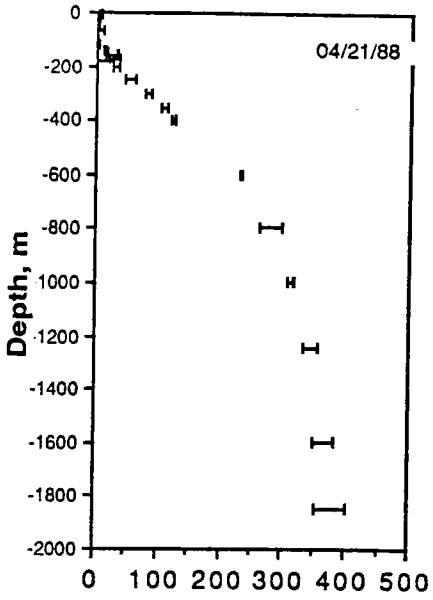

Fig. 1 Mean HS^-, μM/l

Dissolved sulfide, Site BSK 1

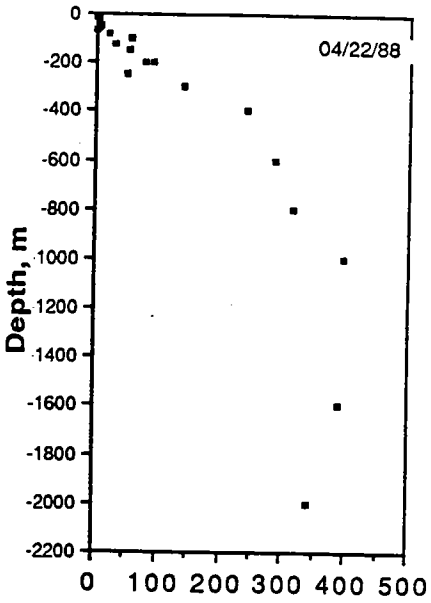

Fig. 2 HS^-, μM/l

Dissolved sulfide, Site BSK 2

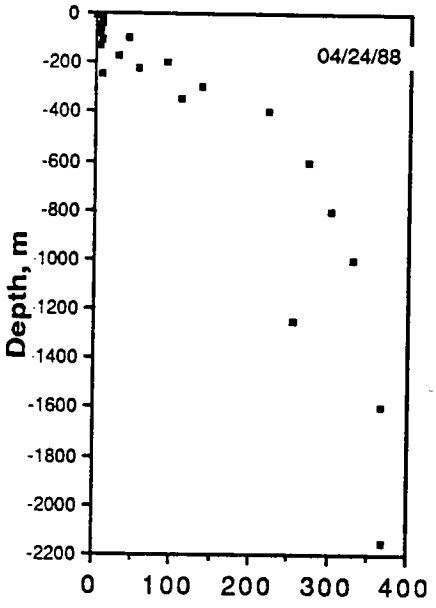

Fig. 3 HS^-, μM/l

Dissolved sulfide, Site BSK 3

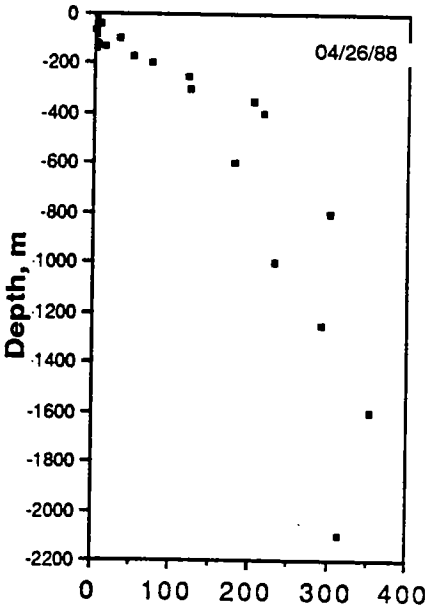

Fig. 4 HS^-, μM/l

Fig. 1 Shown here is a depth profile of dissolved sulfide taken at Site BSC, showing 1 s.d. error bars for the mean of triplicate measurements.

Figs. 2–4 Three other depth profiles were taken at sites BSK 1, BSK 2, and BSK 3, respectively, shown in these three plots. Sulfide is significantly established by 100 m depth in all of these profiles.

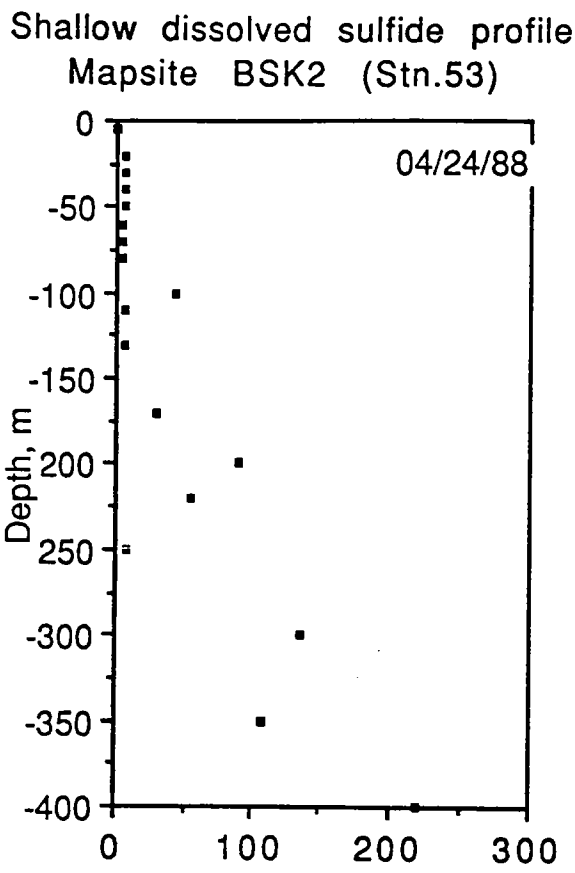

Fig. 5

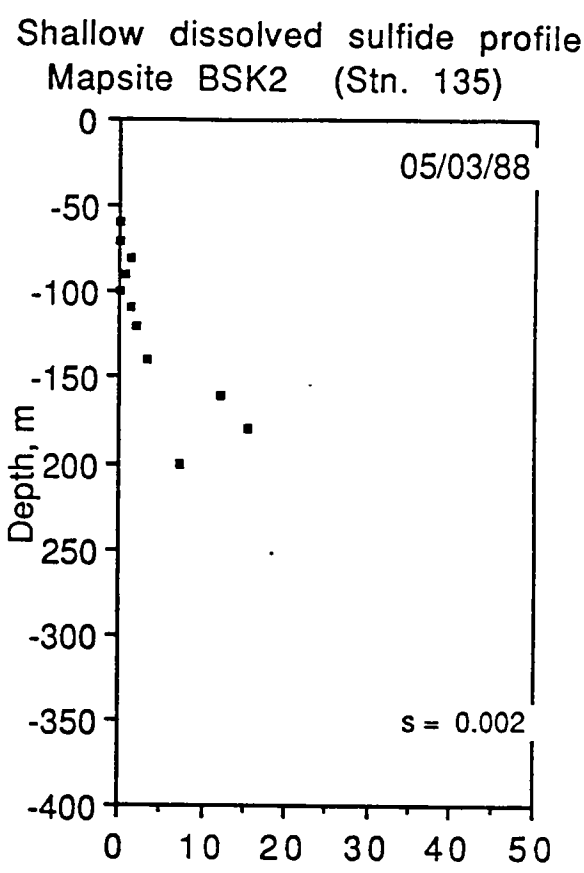

Fig. 6

Fig. 5 An enlargement of the depth profile taken on April 24 at mapsite BSK2.

Fig. 6 A shallow profile of dissolved sulfide, taken upon return to mapsite BSK2 nine days later on May 3 (station 135). Note how levels of sulfide are depressed relative to the April 24 profile, so that much lower values (about 1/5) of dissolved sulfide are found. The sampling and analytical procedures for both were identical, save for the use of argon-filled LPE bottles during the second profile, and the use of argon-filled glass bottles during the first profile, so that experimental procedure may be one reason for the difference; however, other hydrological data presented elsewhere in this cruise report by S. Kempe and others supports the depression of the oxic-anoxic interface at this time as a real phenomenon.

initially thought these values were too low, compared to the previous watercast at this site, closer comparison with other data on dissolved components and salinity (discussed in full by S. Kempe elsewhere in this report) showed these values are entirely reasonable, especially considering the fluctuations in sulfide between 100 and 200 m observed at other sites.

In summary, the sulfide water-column profiles at the trap sites were taken for the purpose of later comparison with dissolved and particulate sulfide content of material hopefully to be collected by traps moored at these sites. For mapsite BSC, we already have sampled the particulates, the dissolved sulfide in the cups, and done a water-column profile. All of these profiles show that sulfide generally increases in a fluctuating pattern below about 100 m, and increases with depth to 350-400 μM/1. There is no increase observed near the bottom for these sites. Dissolved sulfide in the traps will be discussed in a later section, but our results indicate that perhaps the supernatant in the trap cups is either not in equilibrium with the ambient water and/or there is significant loss of sulfide upon recovery of traps, although we sampled for sulfide within 1/2 hour of the traps arriving on deck. The amount of sulfide in the trap cups for both deep and shallow traps is roughly 1/10 of the "ambient" sulfide observed in the water column at this time.

2. Clay experiment on a deep trap at mapsite BSC, May 1987

In May, 1987, a clay experiment was attached to the deep trap (1,262 m) being deployed at mapsite BSC in the southwestern Black Sea. The purpose of the experiment was: 1) to test whether clay minerals are capable of acting as sources of iron for iron sulfide precipitation and thus to experimentally address the question of whether clay input to the Black Sea has an effect on sedimentation of iron sulfide minerals; and 2) to test for precipitation of iron sulfides on surfaces of various clay and other minerals using a moored sediment trap in the Black Sea. This kind of experiment involving materials attached to the sediment trap to investigate ambient vs. sediment trap conditions, has been utilized before, and a similar experiment has been suggested for coccoliths, diatoms, and clay materials by N. Caraco and J. Cole in order to compare iron and sulfide removal by biogenic versus nonbiogenic fluxes in the water column.

Treatment of clay and mineral samples:

Between 0.1 and 0.5 grams of sample were weighed out (Table 1). A replicate portion of certain clay samples were soaked in 5 ml of 0.1 Molar ferric chloride solution ($FeCl_3 \cdot 6H_2O$, F.W. = 270.32 g/mol) overnight. (Note: samples from the Filyos River had a very orange supernatant in the morning.) Samples were then placed in plastic BEEM capsules whose ends had been replaced with 15 μm NITEX Nylon mesh. These in turn were taped with glass tape and then enclosed in large-mesh NITEX Nylon mesh.

Table 1. Description of clay samples deployed at 1262 m, Black Sea, May 1988.

Sample Number	Description	Weight of sample deployed
1	Mt. St. Helens ash	0.50081 g
2	Filyos R., 15-63 um	0.50053 g
3	Filyos R., < 15 um	0.50556 g
4	Montmorillonite/bentonite, Osage, Wyoming	0.50687 g
5	Montmorillonite, API 11, Santa Rita, N.M.	0.40122 g
6	Montmorillonite, API 25, Upton, Wyoming	0.40080 g
7	Montmorillonite, API 26, Suc, Wyoming, < 63 um	0.40155 g
8	Montmorillonite, API 11, < 63 um	0.23086 g
9	Illite, API 35, Fithian, Ill.	0.41537 g
10	Illite, API 36, < 63 um, Morris, Ill.	0.30810 g
11	Kaolinite, API 17, Lewiston, Montana	0.40194 g
12	SiO_2, SPEX pure	0.05046 g
13	Chlorite, < 63 um, Michigan	0.14807 g
14	Chlorite, cryst., Ishpeming, Mich.	0.37280 g
15	Biotite	0.26860 g
16	Pyrite	0.40693 g
17	*Mont. API 25, Upton, WY	0.10798 g
18	*Mt. St. Helens ash	0.18486 g
19	* Filyos R., 15-63 um	0.10075 g
20	* Filyos R., < 15 um	0.04860 g
21	* Mont. API 11, Santa Rita, N.M.	0.09459 g
22	* Mont. API 26, Su, WY, < 63 um	0.02480 g
23	* Kaolinite, API 7,< 63 um	0.15045 g
24	* Illite, API 36, Morris, Ill., < 63 um	0.03512 g
25	* Illite, API 35, Fithian, Ill.	0.15109 g
26	* Kaolinite, API 17, Lewiston, Mont.	0.09582 g

Upon recovery, the samples were retrieved and anoxic technique was used thereafter for handling. Samples were rinsed with deoxygenated distilled water, and allowed to dry under vacuum under an argon atmosphere in a glove bag. Samples were then stored under argon in glass jars containing desiccant, a method found previously to be satisfactory for keeping small samples anoxic for a long time. Samples later will be analyzed for sulfides and elemental composition, together with untreated control samples.

IV. E. CTD OBSERVATIONS

Michael Realander, Stephan Kempe, Arne Diercks,
and Bernward J. Hay

Objectives

The anaerobic chemistry of the Black Sea deep water is caused by a lack of significant vertical mixing. Mixing is inhibited by a very strong pycnocline between the surface water of low salinity (18°/$_{oo}$) and the high-salinity deep water (22°/$_{oo}$). This pycnocline is kept permanent by a large surplus of fresh water from rivers and precipitation entering the Black Sea each year (320 and 230 km^3/yr, respectively) as compared to the rate of evaporation (350 km^3/yr) and by the injection of heavy Mediterranean water through the Bosporus into the deep Black Sea (200 km^3/yr). The interface among the two bodies of water is on the order of 2 σ/200 m and is the most pronounced pycnocline found in any ocean.

Associated with this pycnocline is a chemocline. Along the chemocline oxygen is quickly depleted and the redox potential falls to values well below zero. At oxygen levels of less than 0.5 mg/l most higher life is terminated and in the following deeper zone only a few kinds of bacteria thrive. Along this redox gradient, dissolved manganese and iron upwelled from the reducing water below, is oxidized and precipitates to form a pronounced zone of turbidity (in the following called, in short, the "Mn-layer").

The CTD work on this cruise was designed to define the hydrophysical structure of the water column and its vertical and lateral variances. Furthermore, the structure of the manganese/iron turbidity zone was to be resolved with a transmissometer and its depth and thickness recorded relative to the distance from shore. The contribution of the phytoplankton in the oxygenated zone to the turbidity signal was to be investigated with a fluorometer.

Instrumentation

The SEABIRD CTD system used included a model SBE-9 underwater unit, a model SBE-11 deck unit, an IBM-AT clone data logging desk-top computer, and a hydrowinch with 0.322' armored cable. The conductivity, temperature, and pressure sensors are digitized in the underwater unit (fish) at 24 scan per second. Resultant data in Manchester code is transmitted to the deck unit via the single conductor cable. The power for the fish is supplied by the deck unit through the same cable. Standard sensors are a SBE 3-01/F thermometer, SBE 4-10/0 conductivity meters, and paroscientific digiquartz model 4-6000K. A temperature

sensor within the pressure transducer permits compensation for most of the ambient temperature related pressure errors. The fish further carried a SeaTech 25 cm transmissometer (5000 m) and a SeaTech fluorometer (500 m). The external sensors are connected to the underwater unit. The signals are digitized and transmitted up the cable along with the CTD data. All underwater units were mounted on or underneath the Niskin bottle rosette sampler. The following table gives the technical specifications of the employed electrodes:

Measurement Range:	
Temperature	-5 to +35°C
Conductivity	0 to 7 S/m (= to 70 mmho/cm)
Depth	0 to 6000 m (depends on range selected)
Accuracy:	
Temperature	0.004 °C/year (typical, 0.01 per 6-months guaranteed)
Conductivity	0.0003 S/m/month (typical, 0.001/month guaranteed)
Depth	0.05% of full scale over the ambient temperature range of 0 to 25°C (typical, 0.1% guaranteed 0.02%) with temperature compensation feature installed
Resolution:	
Temperature	0.0003°C
Conductivity	0.000045 S/m
Depth	0.004% of full scale
Response time:	
Temperature	0.082 sec (0.5 m/sec drop)
	0.070 (1.0 m/sec drop)
Conductivity	0.084 sec (0.5 m/sec drop)
(pumped)	0.070 sec (1.0 m/sec drop)
Conductivity (no pump)	0.170 sec (1.0 m/sec drop)
Depth	0.001 sec

Results

A total of 38 hydrocasts and 8 pump stations were made during this leg throughout the southern Black Sea (Fig. 1). The detailed printouts of the data collected fill two large volumes and will be available on request from the Chief Scientist. Here we can only reproduce some of the more important results as a synopsis.

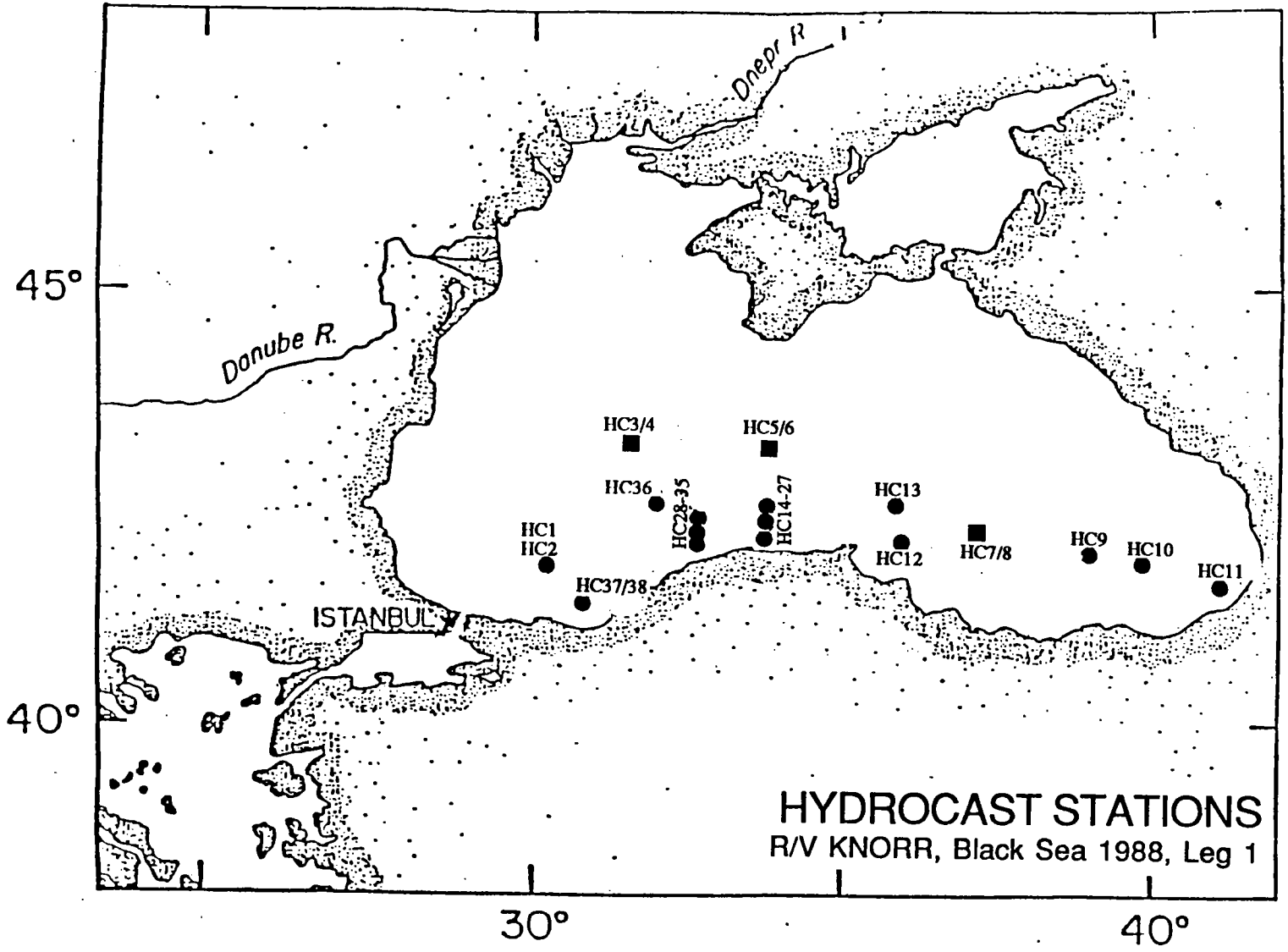

Fig. 1: Location of hydrocast sites. For detailed locations of hydrocasts of the Inebolu Transects and Amasra Transect see Figs. 4 & 5 in cruise report section III.

1. SHALLOW WATER BODY

Stations can be grouped into four general transects:

a) the longitudinal Black Sea W-E transect (April 21 to 26: Hydrocasts 1 to 11)
b) the first Inebolu Transect perpendicular to the Turkish coast (May 2: Hydrocasts 14 to 19)
c) the second Inebolu Transect (May 4: Hydrocasts 21 to 26), and
d) the Amasra Transect (May 5: Hydrocasts 28 to 35).

The remaining stations fall into other areas of the Black Sea and will not be reported in detail here.

a) The Black Sea W-E Transect

Figure 2 gives the density structure of the upper 200 m of the Black Sea. At the onset of the cruise, a series of cold and cloudy days led to the mixing of the upper 40 m in the western part of the basin, possibly ending the first spring diatom plankton bloom in the Black Sea. Sea surface temperatures dropped and showed values of only 8°C at the onset of our cruise even though at the end of March and the beginning of April warm and fair weather had already occurred. During the following days of our cruise renewed warming and lack of wind formed a second shallow and warmer mixed layer at the surface, well established by April 26 at HC 11.

The main pycnocline seems to be centered at around the 15σ level, and it is significantly higher in the center of the Black Sea than in the west and east of the basin. The 15σ level occurred at less than 50 m at mapsite BSK1 and at below 120 m at HC 11/mapsite 30. This lateral slope of the pycnocline is upheld by the counterclockwise rotation of the surface water in the Black Sea. It is interesting to note that many steps occurred in the density curves, especially pronounced in the lower section of the pycnocline. These steps probably represent individual layers of water, mixed internally but bordered by sharp density gradients against each other.

Figures 3 and 4 plot the transmissivity curves for hydrocasts 1 to 11. In general, we observe a fast decline of the transmissivity in the surface layer, interrupted by a peak most pronounced at station BSK3 (HC 7 and 8) representative of phytoplankton at depths between 30 and 60 m. At HC 11, we also see a very pronounced peak at a depth of 120 m which coincides with the massive occurrence of arrowworms (Sagitta) as observed directly with the Mini-Rover (see cruise report section IV.G.).

Below the biologically caused turbidity in the oxygenated zone we always find a more or less prominant peak or series of peaks. These peaks are produced by particulate manganese/iron oxides as shown by our in-situ pumping (see cruise report section IV.F.). At mapsite BSC this peak occurs at a depth of 100 m, then rises to 50 m at BSK1, and falls to 80 m

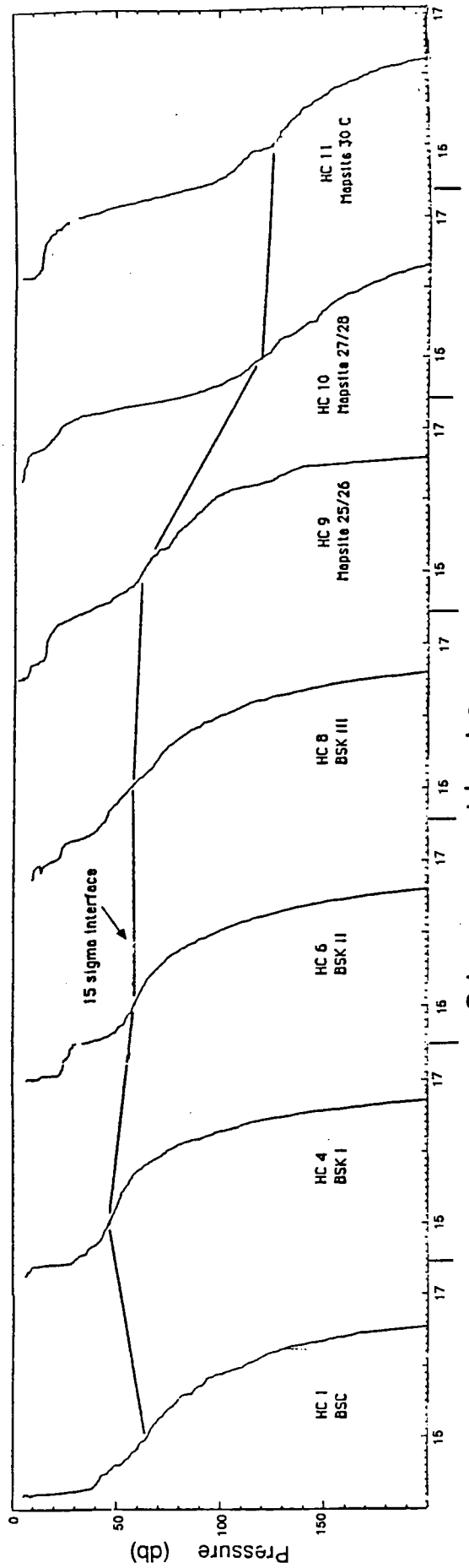

Fig. 2: Vertical density structure of the upper 200 m of the Black Sea along an east-west transect from April 21-28. (Pressure corresponds roughly to depth.)

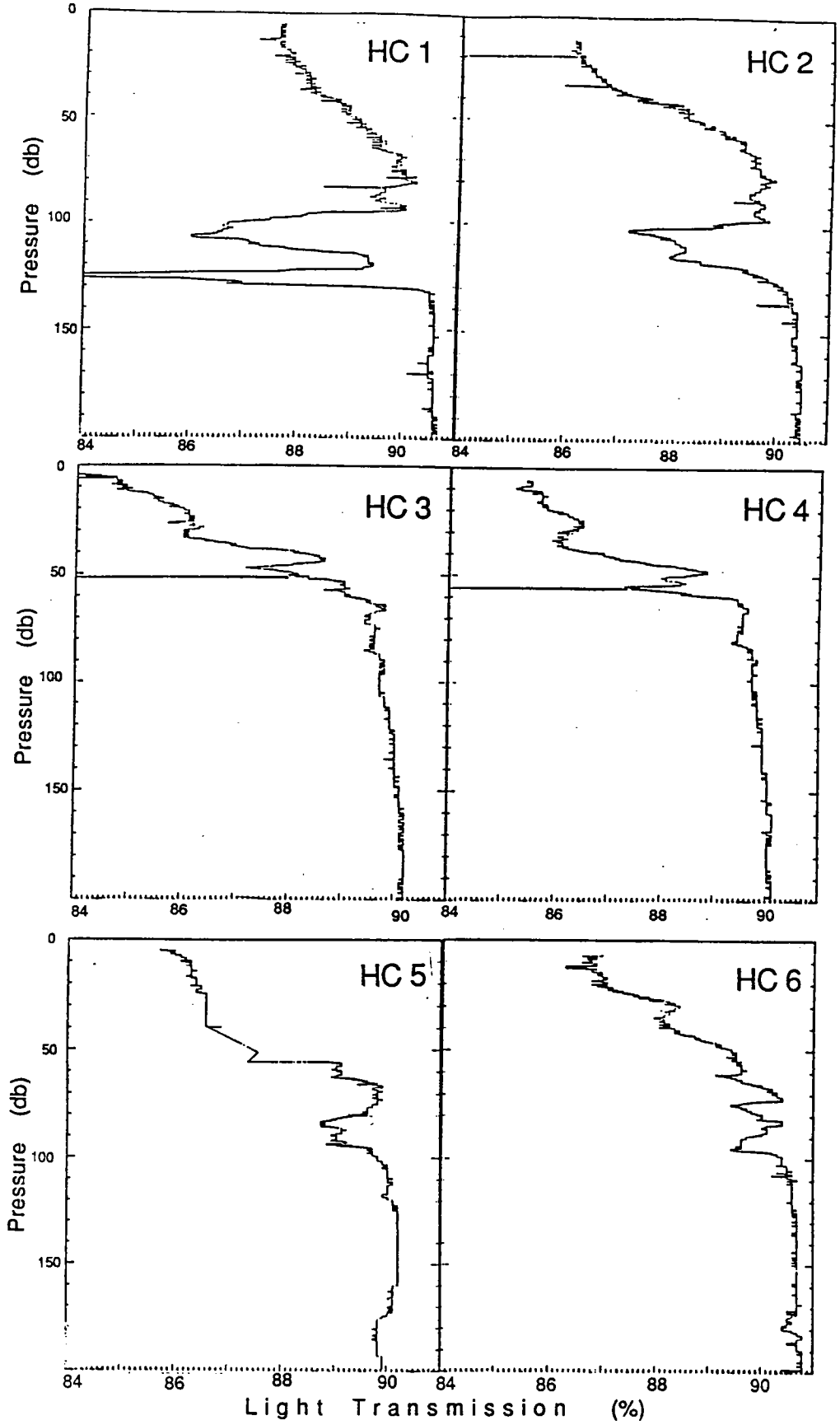

Fig. 3: Transmissivity of the upper 200 m of the Black Sea water column for mapsites BSC (HC 1 and 2), BSK1 (HC 3 and 4) and BSK2 (HC 5 and 6). (Pressure corresponds roughly to depth.)

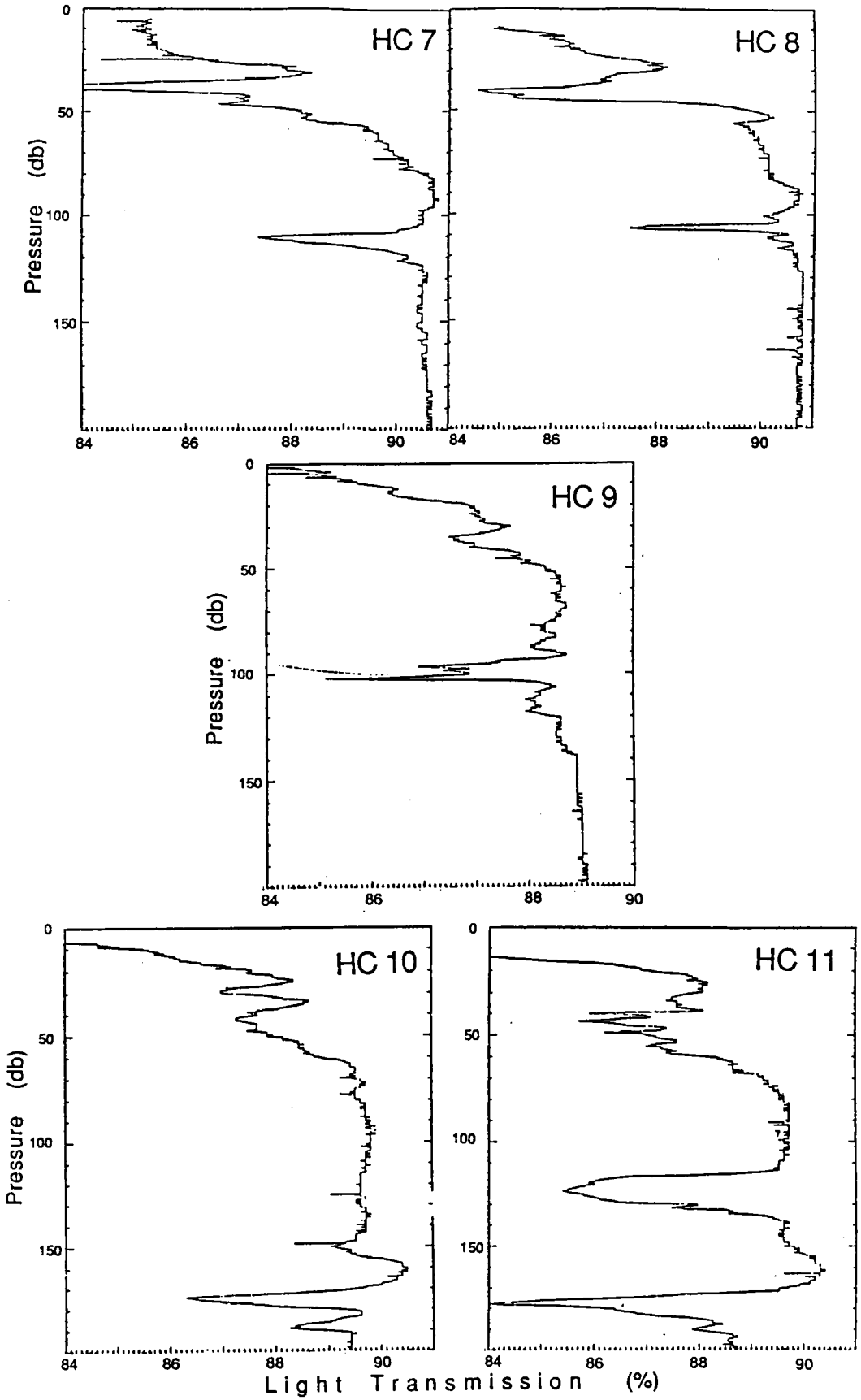

Fig. 4: Transmissivity of the upper 200 m of the Black Sea water column for mapsites BSK3 (HC 7 and 8), mapsites 25/26 (HC 9), 27/28 (HC 10) and 30 C (HC 11).

at BSK2 and to 110 m at BSK3. Towards the east it falls to 170 m at HC 11. Compared to the 15σ interface, the Mn-layer peak is depressed much further down (120 m as compared to 70 m) and bends much more strongly down towards the coast than does the pycnocline.

Since at mapsites BSC, BSK1, BSK2, and BSK3 both deep and shallow hydrocasts were made, we have repetitive measurements, just a few hours apart. Comparison of these double casts (Figures 3 and 4) shows that the internal structure of the Mn-layer peak is changing fast. HC 1, for example, shows a large and pronounced double peak, while HC 2 shows a much smaller peak hardly showing two maxima (Fig. 3, top). In BSK1 (HC 3 and HC 4) we find an extremely thin Mn-layer layer, probably less than 1 m thick. If it were not for the double recording, one would dismiss this peak altogether as an instrument failure.

b) First Inebolu Transect

Figure 5 shows the density curves of the 6 stations occupied during the first Inebolu transect (for station locations, see figure 4 in cruise report section III). The 15σ level declines from about 60 m at the basin-most station HC 19 to about 90 m at the most coastward station, HC 14. Some of the curves show pronounced stepping, which, however, may also be induced by the relatively rough weather the leg was experiencing during the transect. The corresponding transmissivity measurements (Fig. 6) show that the layer is first depressed toward the shore and then rises a few meters to intersect the sea bottom. At this transect, the sea bottom intercepted the Mn-layer at about 140 m depth. These peaks have been transformed into a contour graph in Figure 7. Highest light absorbences occur about 7 nautical miles off the coast and the layer declines both in thickness and in intensity rapidly toward the basin. At HC 19 only a small peak can be noticed above the background.

c) Second Inebolu Transect

The Inebolu transect was repeated two days later in order to obtain data on the stability of the Mn-layer (for station locations, see figure 4 in cruise report section III). At this time, the sea was very smooth so that the step-structure of the density curves (Fig. 8) was observed again. Therefore, it is a real feature. Most striking are the differences between the two transects in the transmissivity curves. The original double layer has parted into a quadruple peak and is now significantly deeper (180 m) than it was two days earlier (150 m). If one closely inspects both the density and the transmissivity traces one comes to the conclusion that the structure observed in the transmissivity is linked to the internal layering of the water mass. This would explain the fast alteration of the peak structure, which could hardly be a consequence of alterations in the general redox-gradient (which should exclude the generation of multiple layers).

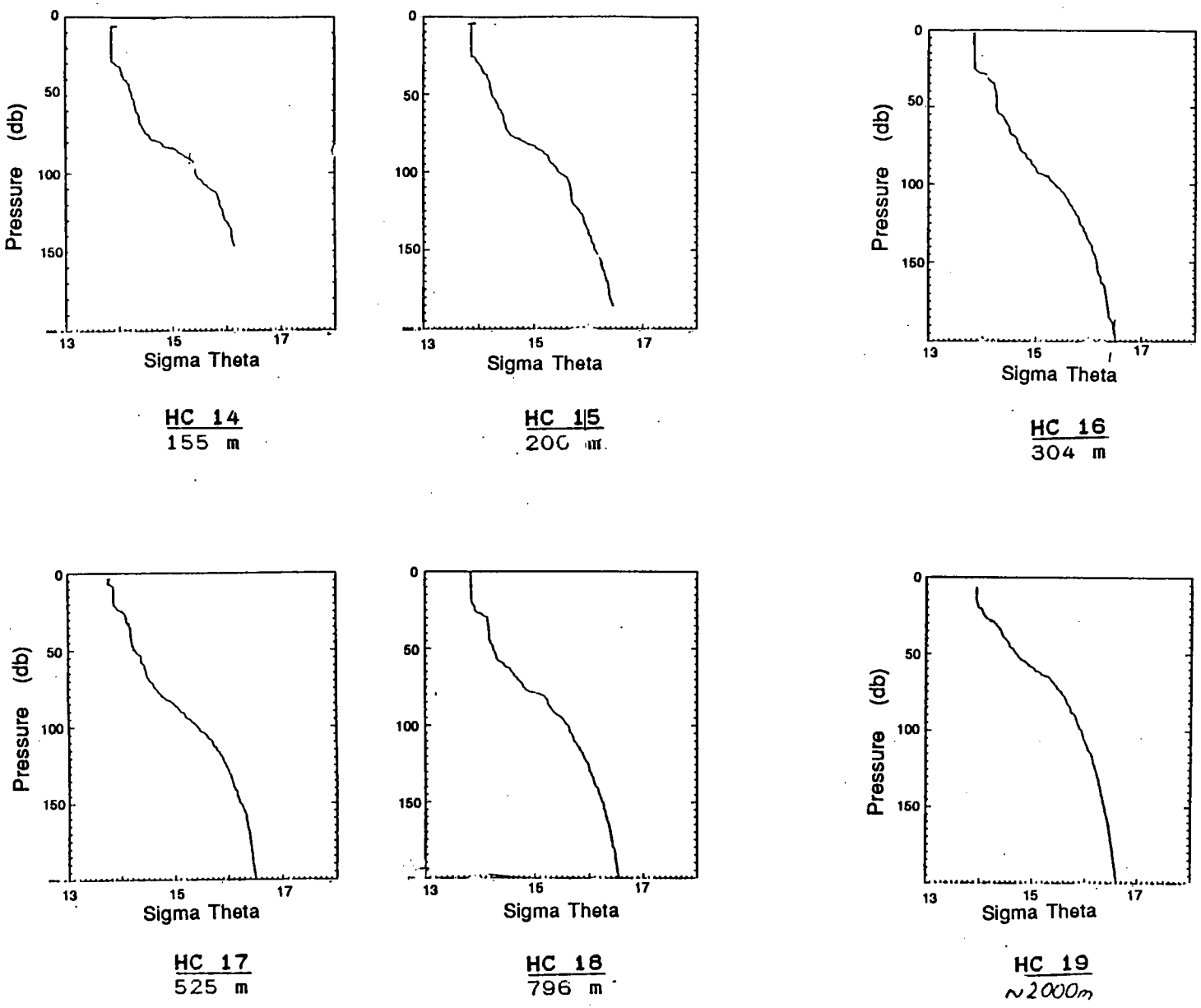

Fig. 5: Density curves of the first Inebolu transect (HC 14 to HC 19). (Pressure corresponds roughly to depth.)

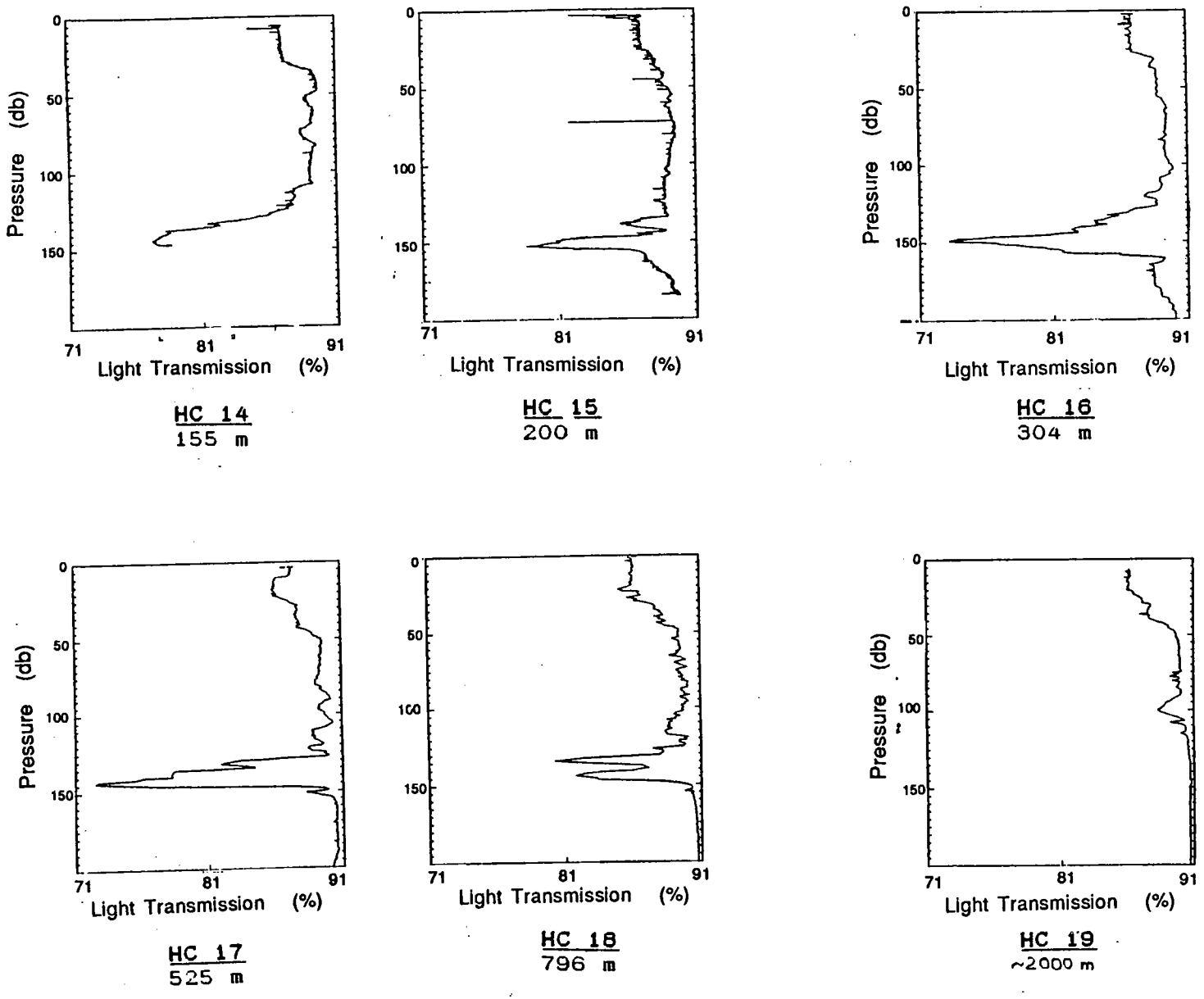

Fig. 6: Transmissivity curves of the first Inebolu transect (HC 14-HC 19).

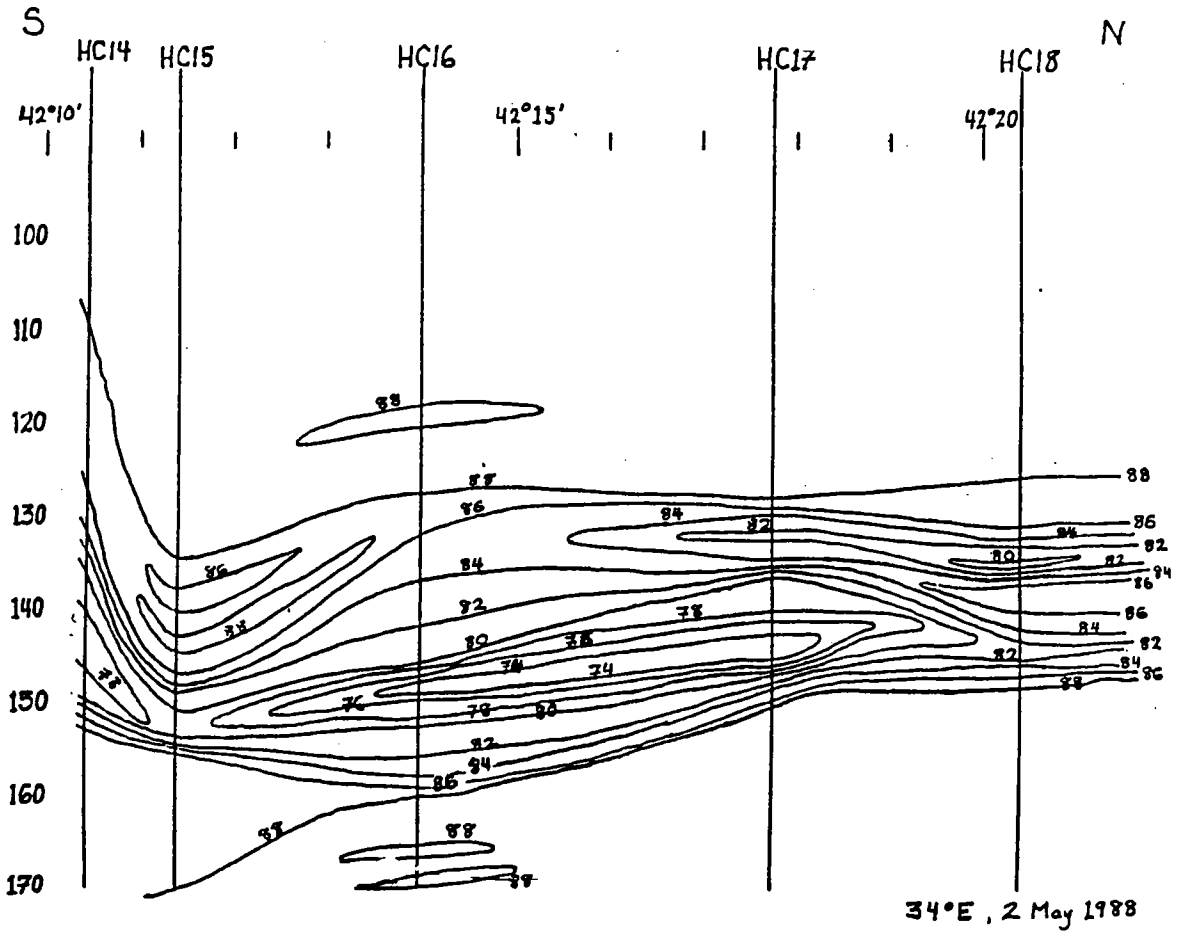

Fig. 7:

Vertical section through the Mn-particle layer presented as contours of light transmission for the first Inebolu transect. Note the uplift of the layer at the very intersection of the Mn-layer with the sea bottom (HC 14, left side of diagram). (Pressure corresponds roughly to depth.)

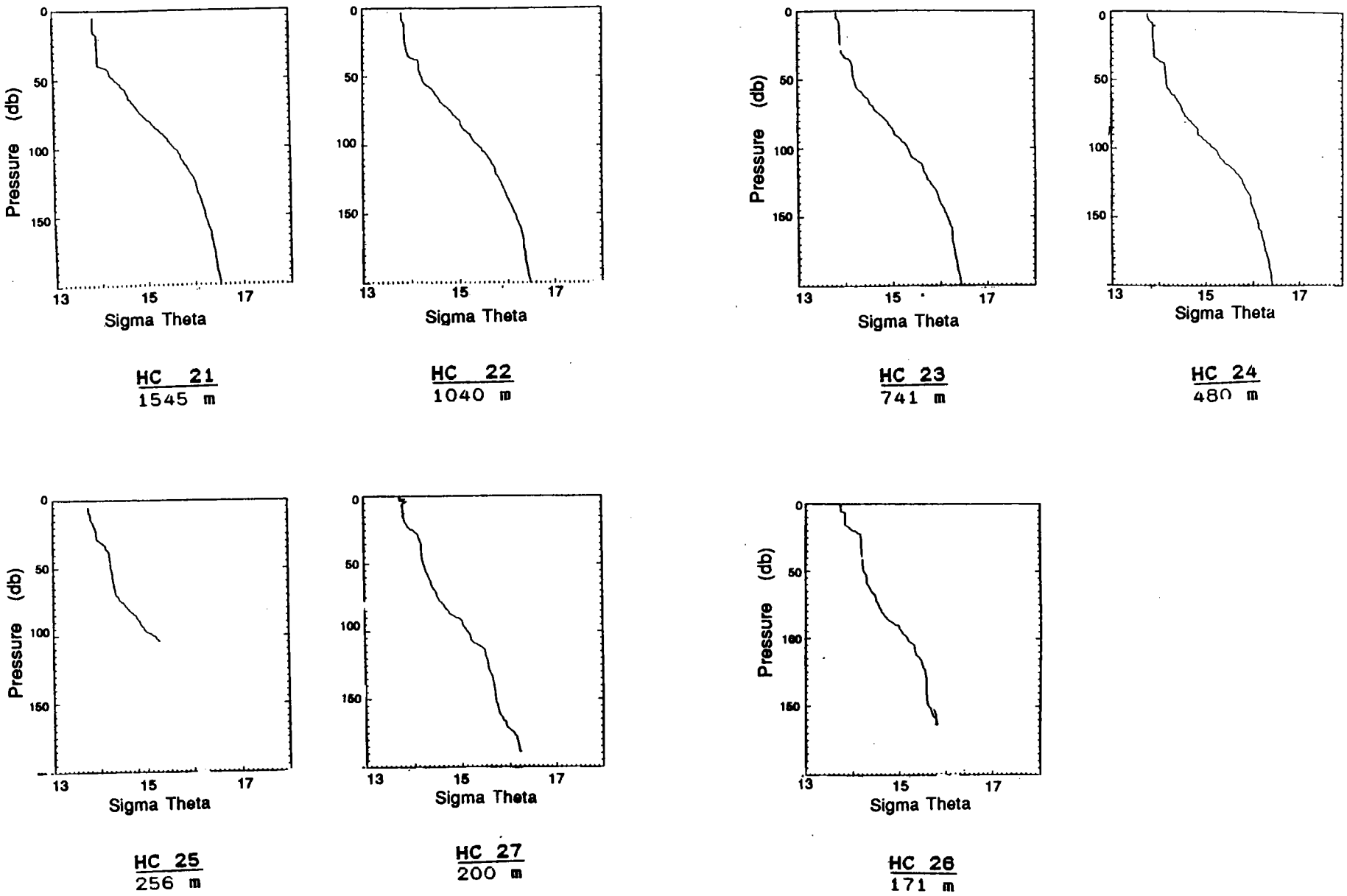

Fig. 8: Density profiles of second Inebolu transect, May 4. Stations are ordered from basin (top left) to coast (bottom right).

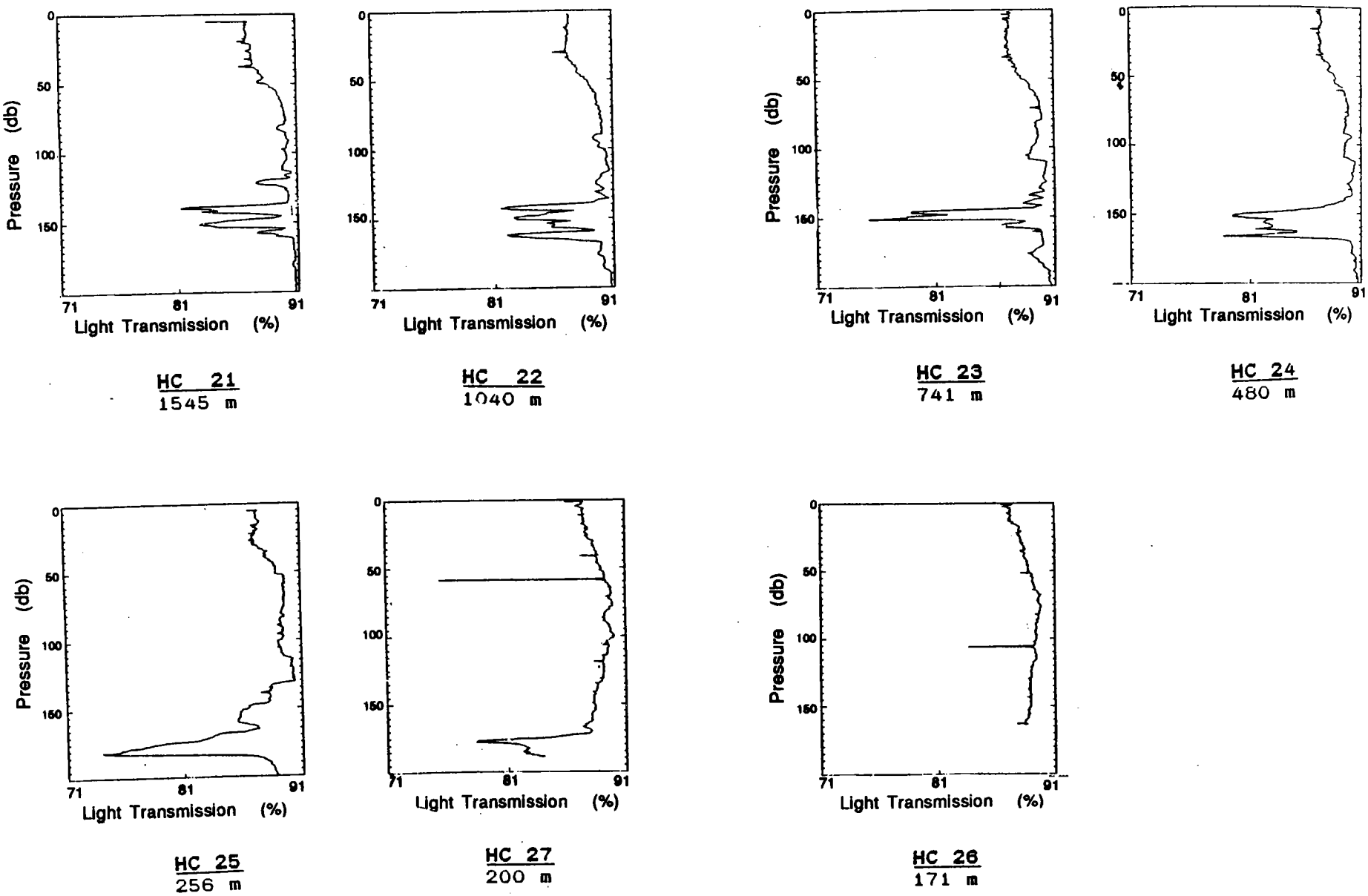

Fig. 9: Transmissivity profiles of the second Inebolu transect.

d) Amasra Transect

The density profiles of the Amasra transect tell a story similar to that of the Inebolu transect (for station locations, see figure 5 in cruise report section III). Again we observe the depression of the 15σ level from 60 m at the basin-most station (HC 28) to 105 m at the coastal station. Steps are a common feature in these curves, bearing witness to intense internal shear due to currents. In the Amasra profile the peak associated with the Mn-layer is not as pronounced as in the data of the Inebolu transects; it reaches high intensities only very near the coast (HC 33). The intersection of the Mn-layer with the sediment surface is at about a depth of 160 m.

2. DEEP WATER BODY

At mapsites BSC, BSK1, BSK2, and BSK3 deep CTD lowerings were made (HC 1, 3, 5, 7, respectively). These lowerings showed the expected slight increase of temperature, salinity, and density with depth. Figure 12 gives an example of one of the deep water casts (HC 7).

More interesting was the transmissometer curve which found two mid-water turbidity events (Figs. 13 and 14) (HC 1 at a depth of about 200 m and HC 5 at a depth of about 350 m). Similar events were recorded by the transmissometer mounted on Vernon Asper's deep particle camera. The recorded peaks may derive from tongues of resuspended shelf sediments.

Conclusions

1) As previous published, the pycnocline in the Black Sea is domed toward the center of the Black Sea gyres.

2) The associated chemocline is also domed, but to an amount about twice as high as the pycnocline.

3) A distinct turbidity event is found throughout the Black Sea which can be associated with the Mn-layer reported previously.

4) This layer is very variable as to its depth (in consequence to the doming of the chemocline), its thickness, and its internal structure both on temporal and spatial short scales. This variability is tentatively attributed to current-induced small scale stratification.

5) Along the coast the intersect of the Mn-layer can move up and down by at least 30 m within 2 days, thus bearing witness to abrupt changes in the coastal currents or to large scale internal waves.

6) Sporadic mid-water turbidity maxima may be associated with lateral advection of resuspended slope sediments.

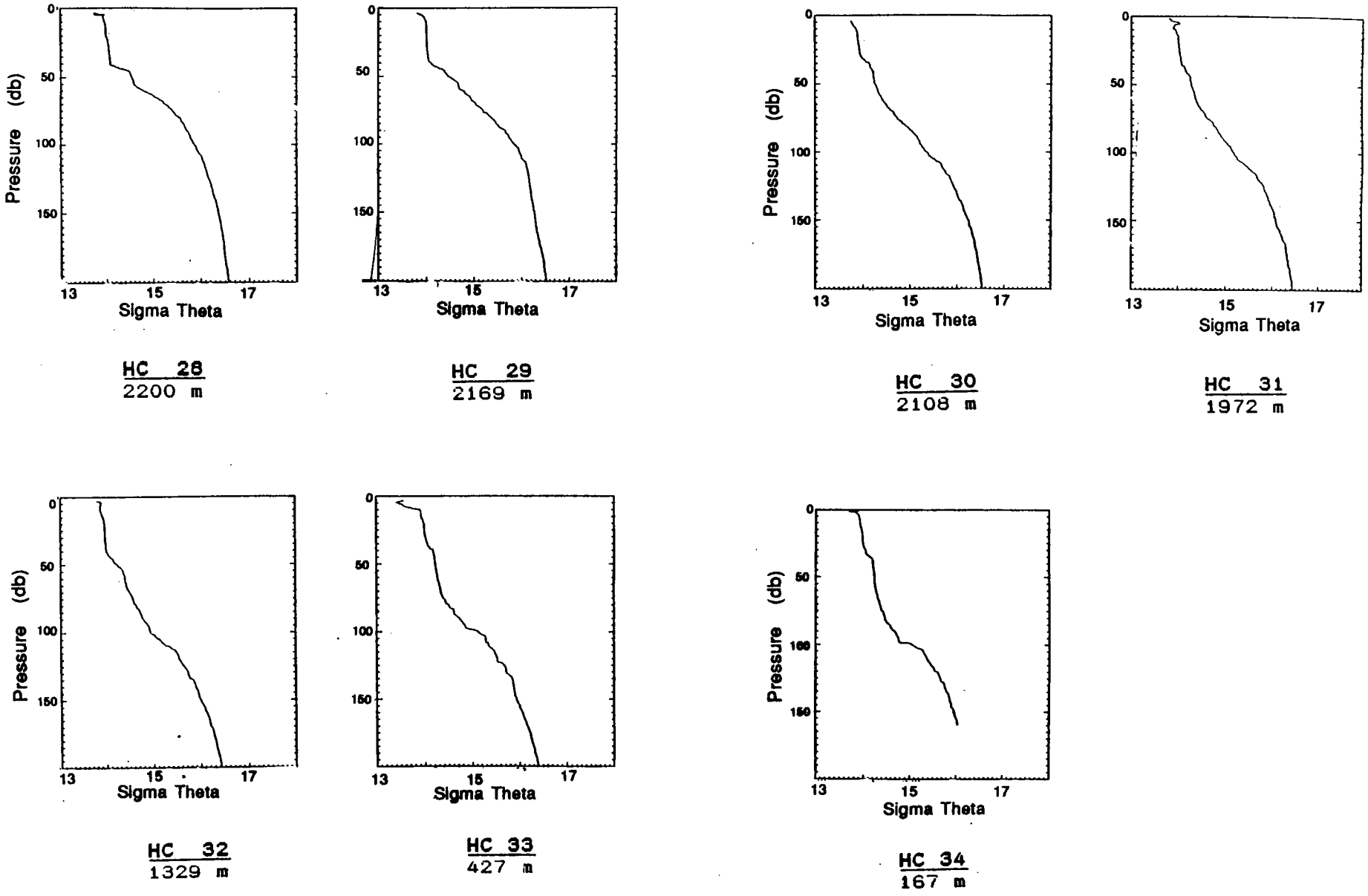

Fig. 10: Density profiles of Amasra transect (May 5). Stations are ordered from basin (top left) to coast (bottom right).

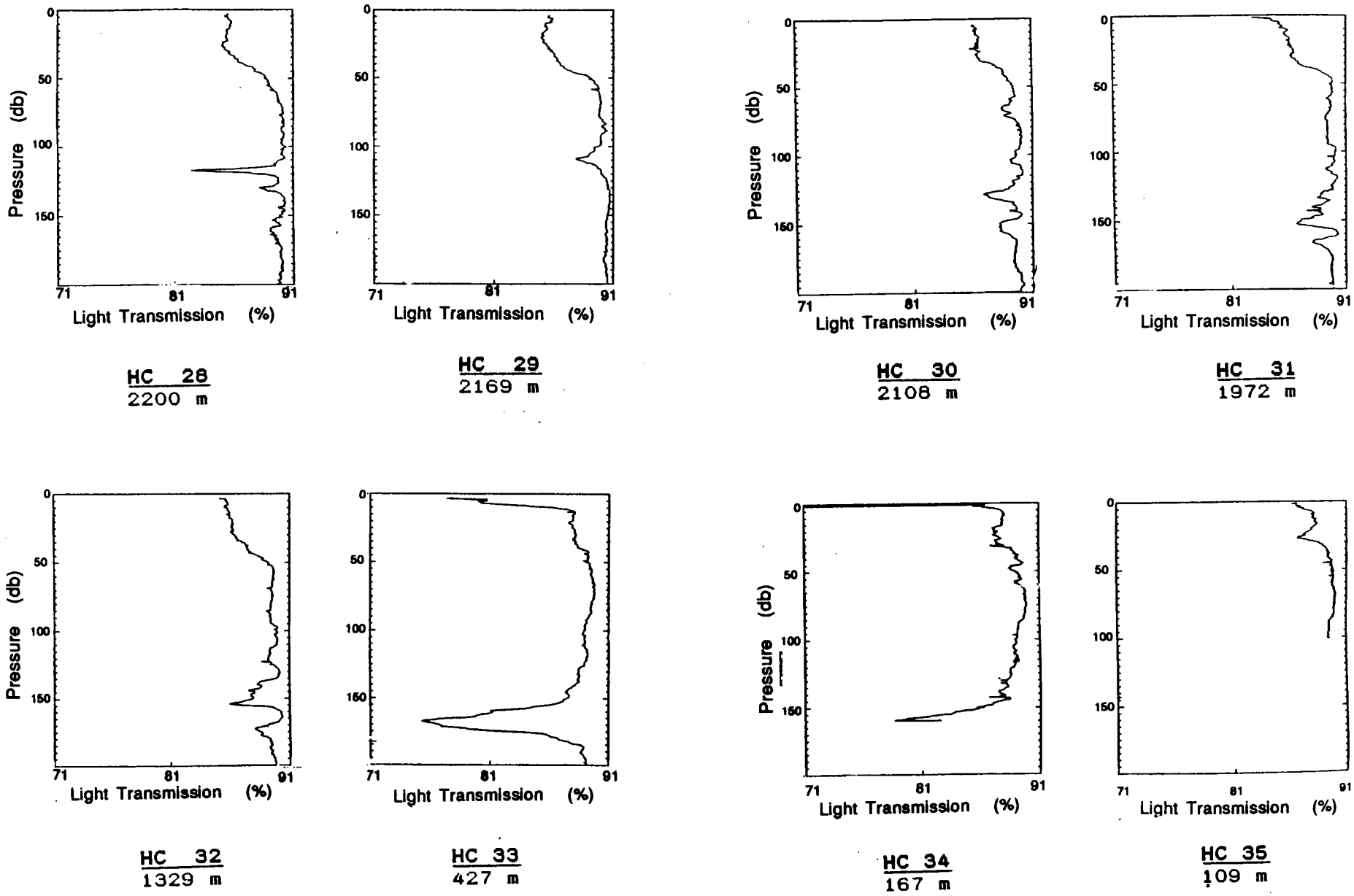

Fig. 11: Transmissivity profiles of Amasra transect. (Pressure corresponds roughly to depth.)

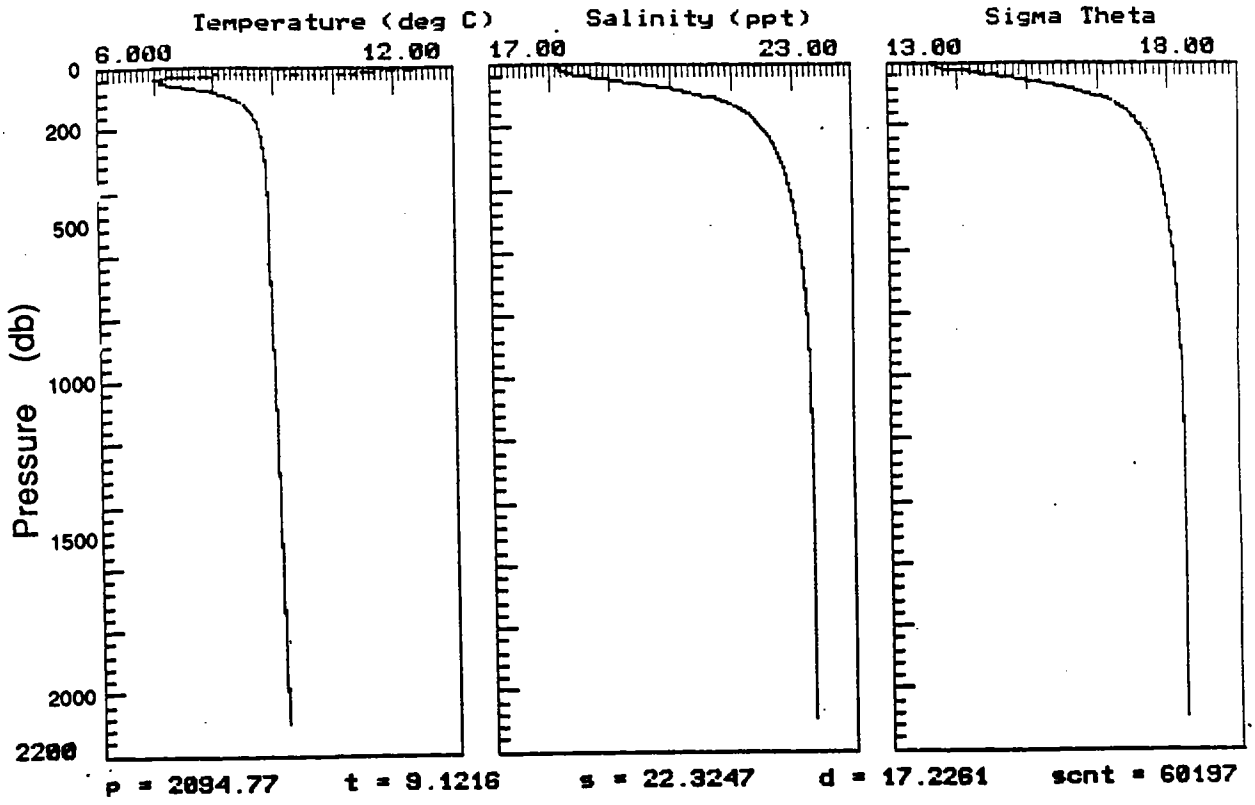

Figure 12: Temperature, salinity and density (sigma theta) plot of the deep water cast HC 7 at site BSK3.

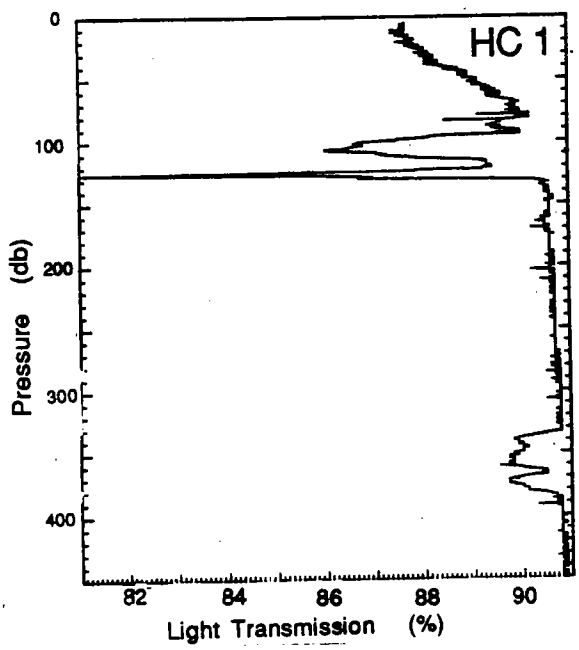

Fig. 13: Plot of transmissometer readings at mapsite BSC (HC 1) recording a mid-water turbidity event at a depth of 200 m, well below the Mn-layer transmissometer peak. This peak may be induced by laterally advected resuspended slope sediments.

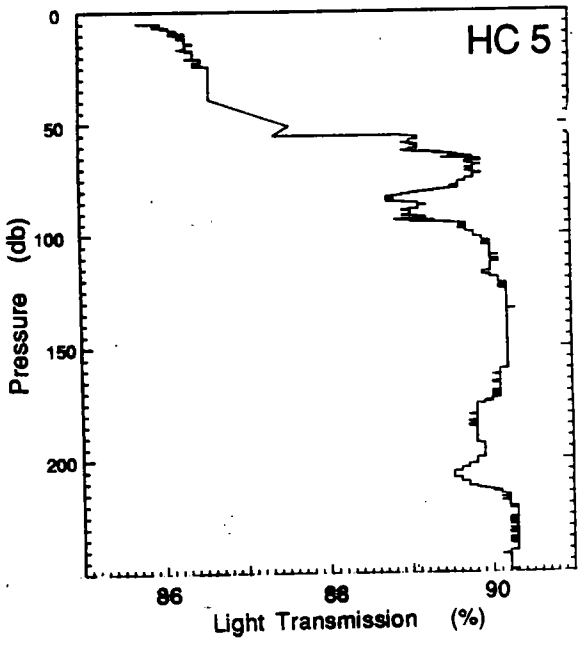

Fig. 14: Plot of transmissometer readings at mapsite BSK2 (HC 5) recording a mid-water turbidity event at a depth of 350 m, well below the Mn-layer transmissometer peak. This peak may be induced by laterally advected resuspended slope sediments.

IV. F. IN-SITU PUMPING AT THE Mn-LAYER IN THE BLACK SEA

Stephan Kempe and Arne Diercks

Objectives

The Mn-layer in the Black Sea is an integral feature of the chemocline between the anaerobic and deep water and the aerobic surface water. Its existence was first described by Brewer and Spencer (1974) who measured the concentration of particulate manganese and iron. Nothing, however, is known about the internal structure of this layer, the in-situ grain size distribution, or the exact chemistry and mineralogy of the particles.

We therefore employed an in-situ filtration unit to collect enough material from this layer for a more detailed study of the particles with regard to their grain size, chemistry, and morphology.

Instrumentation

The SEASTAR deep sea pump (depth limitation: 400 m) is controlled by magnetically coupled external knobs (Figs. 1 and 2) which allow various time delays to start the pump and which give access to various modes of pumping (Table 1) and to three flow modes of the two-gear pump (50, 100, and 150 ml/min). The resolution of the flow meter is 0.01 liters with a maximal capacity of 9999.99 liters and a calibration readout accuracy of $\pm$ 2.5. The pumping rate accuracy is $\pm$ 3%. We used pre-washed and pre-weighed 142 mm diameter membrane filters in an all-Teflon filter holder.

The pump was mounted on the frame of the rosette sampler at all except one of the pump stations. It was positioned at the same height as the transmissometer of the CTD. The standard procedure was to lower the CTD down to 200 m, to record the entire Mn-layer transmissometer peak (see also cruise report section IV.E.), and then to position the pump at exactly the height within the transmissometer peak where we wanted to sample. The pump was started with a delay of ten minutes after deployment, an interval which proved just long enough for the necessary CTD maneuvers. Pumping time was either one or two hours (see Table 2 for station details) and pumping mode 4 or 5 was used.

A total of 9 pumping stations were made (Table 2). Of these, numbers 4, 5, and 6 were made at the lower and upper boundary and in the center of the Mn-layer transmissometer peak (Fig. 3a, b, c) at mapsite 33. Station pump 8 was used to pump in the "background" region below the particle layer transmissometer peak (see Fig. 4).

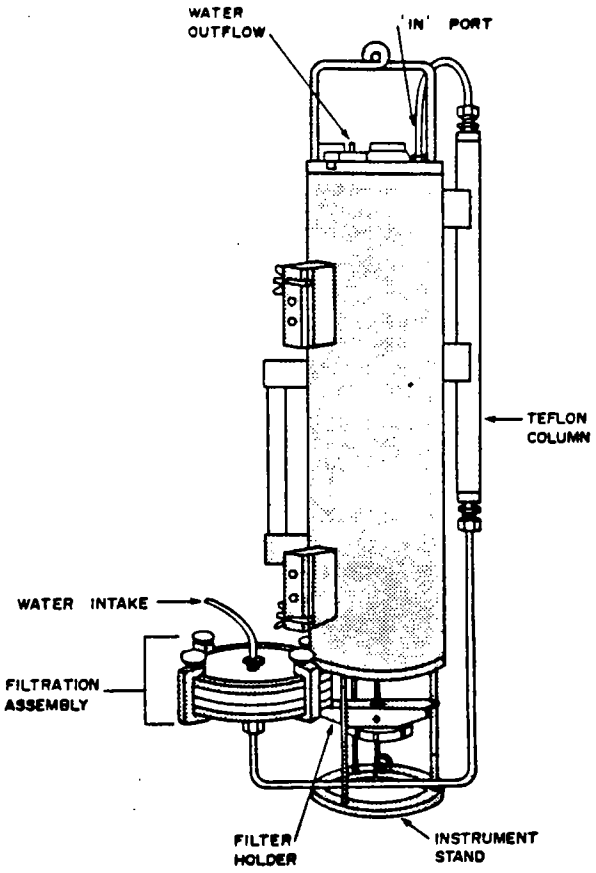

Fig. 1: Diagram of in situ sampler with filtration assembly.

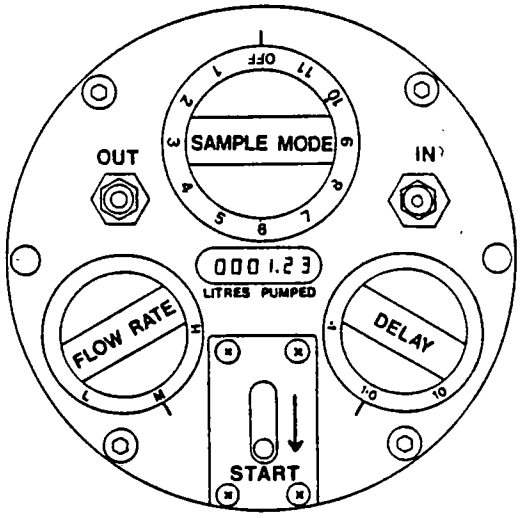

Fig. 2: Diagram of the top plate of the In Situ Sampler. Microprocessor control allows for the selection of flow rate, delay time, and sampling mode. The flow meter readout displays the total volume of water passed through the column in litres.

Table 1

MODE SWITCH SETTINGS

Sample Mode Switch Position	Sampler Pumping Interval	Total Pumping Time	Sampling Interval Ratio (On/Off)	Total Volume Pumped*** (litres) High[1] Flow Rate	Medium[2] Flow Rate	Low[3] Flow Rate
Off	Off	0	-	-	-	-
1	*	*	continuous on	**	**	**
2	15 min.	15 min.	"	2.2	1.5	0.8
3	30 min.	30 min.	"	4.5	3.0	1.5
4	1 hr.	1 hr.	"	9	6	3
5	2 hrs.	2 hrs.	"	18	12	6
6	4 hrs.	4 hrs.	"	36	24	12
7	8 hrs.	8 hrs.	"	72	48	24
8	24 hrs.	12 hrs.	30/30	108	72	36
9	48 hrs.	12 hrs.	15/45	108	72	36
10	72 hrs.	18 hrs.	15/45	162	108	54
11	96 hrs.	24 hrs.	15/45	216	144	72

Table 2: Pumping station list

DATE	MAPSITE	STN.NR	START	END	LAT(N)	LONG(E)	DEPTH(m)	ACTIVITY
April 24	BSK2	52	18.55	20.15	42 56.02	34 01.73	2217	PUMP1
April 26	BSK3	71	18.01	19.18	42 15.00	37 31.29	2060	PUMP2
April 29	30c	100	02.00	03.20	41 26.69	41 18.07	569	PUMP3
May 1	33	113	08.06	09.25	41 47.80	36 17.20	1159	PUMP4
"	33	114	09.44	11.03	41 47.20	36 16.41	1127	PUMP5
"	33	115	11.22	12.45	41 46.75	36 16.44	1118	PUMP6
May 3	BSK2	135	04.10	06.40	43 03.33	34 04.96	2186	HC20/PUMP7
"	BSK2	139	13.14	15.27	42 57.98	33 59.00	2220	PUMP8
May 4	45	159	16.25	18.43	42 19.46	34 01.20	706	PUMP9

Results

All filters recovered visible material. The filters from the depth of the transmissometer peak were light to dark brown and showed much more material than the background station. An estimated 10 mg of sample was recovered from some of the lowerings. Most of the material seemed to be present in the very fine-grained fraction, but a few macroscopically visible particles were always found, even in the background station. This suggests that the transmissometer-active material is a fine-grained suspension and not a layer of rather coarse-grained flocs. The recovered larger particles (macroflocs) may just have been sampled according to their average concentration which is probably in the range of 0.5 per liter. This interpretation would be in accordance with our in-situ video inspection of the upper Black Sea water column (see cruise section IV.G.).

At present, we can only speculate as to the processes which form and stabilize the Mn-layer. In principle, it could come about by the oxidation of upwelled reduced Mn^2 at very low oxygen levels. Measurements of the redox-potential during this cruise tentatively suggest that the layer is stable at about 120 mV Eh. Particles sinking out of this layer or being dragged out by "impacting" macrofloc comets will be reduced and dissolved below in the reducing zone, liberating Mn^2 and Fe^2. Most of the Fe^2 will then be precipitated as sulfide and removed from the water column while Mn^2 cannot be removed and will accumulate in the deeper water, being available for further upwelling events. Such an equilibrium model would call for a relatively wide transmissometer peak similar to a normal distribution function. The peaks observed by the transmissometer, however, have more often than not several peaks which seem to be linked to the internal lamination of the water body caused by current shear. Also, the peak is by no means a stable structure, but undergoes substantial changes in its width, intensity, and internal structure within a few hours or within a few miles. Thus, hydrodynamic advective processes may be even more responsible for the existence and the observed structure of the Mn-layer than chemical processes governed diffusive processes.

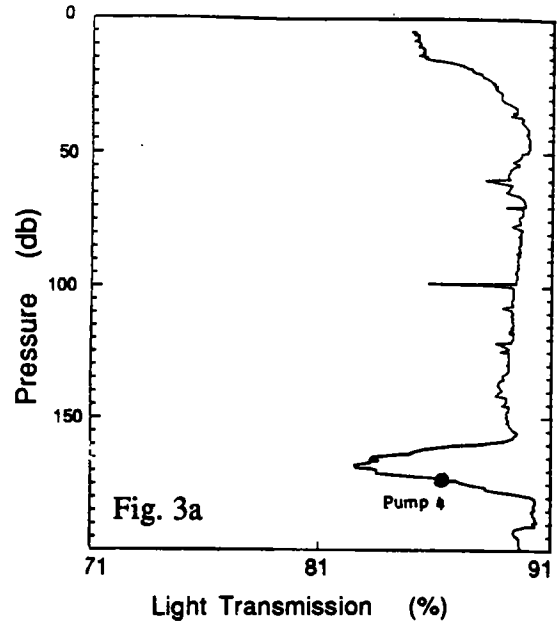

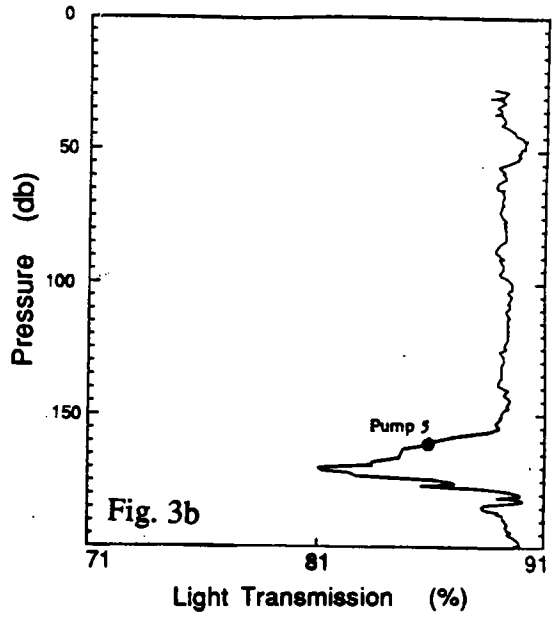

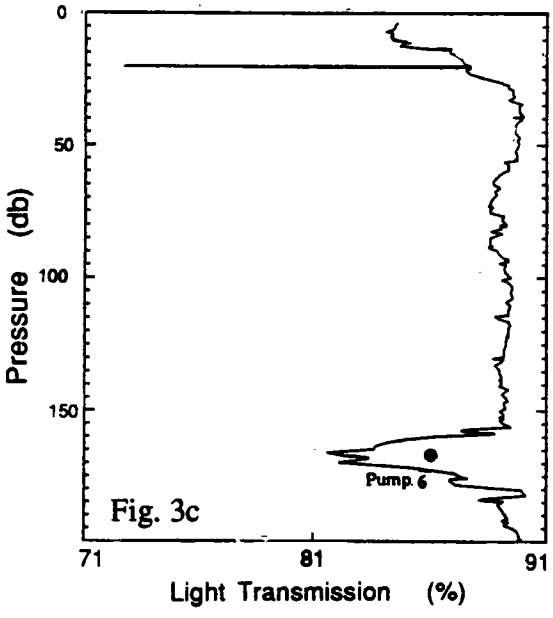

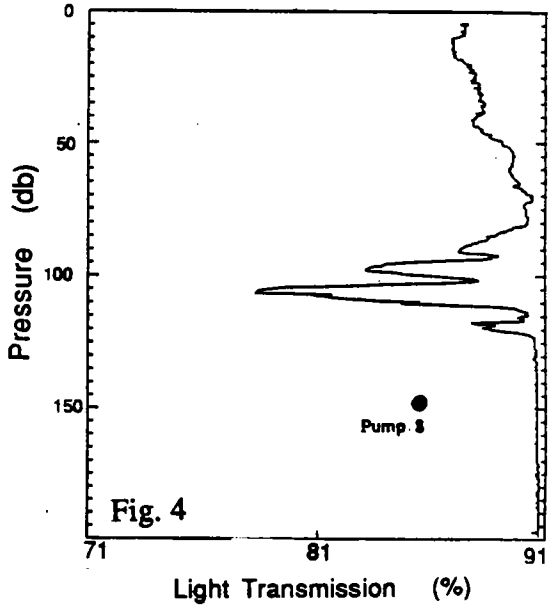

Figs. 3&4: Position of pumping in the water column with respect to the Mn-Layer shown by the light transmission record.
(Pressure corresponds roughly to depth.)

IV. G. VISUAL INSPECTION OF THE WATER COLUMN AND SEA BOTTOM

and of Microplankton and macroflocs in the upper 200 m of the water column with a video camera and photo camera equipped Mini-Rover

Arne Diercks and Stephan Kempe

Objective

Classical oceanographic sampling methods - like plankton tows or coring - give only an incomplete picture of the structure of the planktonic community and of the immediate sediment surface. These can be studied much better in-situ. Video and photo techniques allow remote-controlled inspection of the vertical plankton structure, of the size distribution of macroflocs (marine snow), and of the fluff layer at the sea bottom surface.

Instrumentation

A total of 7 dives (Table 1) were conducted using a Deep-Sea Systems International Inc. Mini-Rover (Remote Operated Vehicle) equipped with a PAL-color video camera and a Benthos underwater camera and flash. The Rover carries two 1000 W lights, a depth gauge, and a compass. The vehicle is driven by three thrusters, two mounted horizontally and one vertically, allowing free movement in all directions. Power (220 V) for the motors and lights is transmitted through an umbilical cable which also carries the signals for the thruster operation, the tilt of the camera, the command for triggering the photo camera, and the returning video signal. All dives were recorded full-length on VHS-Pal cassettes. The photo camera has a depth of focus between 50 and 70 cm and carries a wide-angle lens (28°). The volume theoretically in focus is roughly 0.5 m^3. Small-grained black and white film was used at an exposure time of $1/60^{th}$ of a second.

The Rover was attached to the starboard hydrowire of the R/V Knorr and lowered at 120 m intervals, fixing the umbilical cable to the wire. The operational distance from the cable was kept at between 3 and 5 m. This had the advantage of using the wire as a point of reference both for direction and size. Also, the kinking of the electrical cable by random turns of the rover is thus kept to a minimum.

Results

1) Two of the nine dives reached the bottom of the Black Sea. These dives allowed for the first time an in-situ observation of the fluff layer. Station ROV 1 showed a distinct layer of dark fluff, on top of a

much lighter, very fine-grained sediment. Station ROV 7 showed a much different situation. At this station, the fluff layer was much thicker and graded into the underlying sediment. Also patchiness was observed which was not found at station ROV 1. It seemed as if agglomerates of up to a few millimeters in size had collected in small depressions.

2) Marine snow particles were observed at all depths. Stringers, comets, and globular aggregates were observed, even though an estimate of the proportions of these types will be difficult due to the high current velocities encountered, which tends to blur the shape of the fast-moving particles both on the video and on the photo image. Certain layers showed higher concentrations than others. Careful inspection of the recorded material is needed in order to substantiate this subjective observation. The derivation of semiquantitative data on numbers and sizes of these particles from the camera films is anticipated.

3) In-situ inspection of the Mn-layer did not show a very marked maximum in the number of large particles. It is concluded that the main mass of particles is very fine-grained. This observation is in aggrement with the results of the in-situ pump (see cruise report section IV.F.).

4) Three zones of macro-plankton were found (Fig. 1): a top zone dominated by coelenterata (medusa) Aurelia sp. (Fig. 2, top); these animals were seen during both daytime and nighttime at the surface of the Black Sea. Below this zone a layer dominated by ctenophora Pleurobranchia sp. (Fig. 2, bottom) followed. Between these zones a gradual transition was observed where both animals occurred. The medusa and ctenophora layers were found at all stations, the thickness depending on the local depth of the oxygenated surface layer. This zonation was seen both during the daytime and during nighttime dives and seems to originate from oxygen distribution rather than from light intensity. A third zone was found at stations ROV 6 and 7 which probed the marginal waters of the Black Sea. In these areas a dense population of the chaetognatha (arrowworm) Sagitta setosa was observed below the ctenophora zone. Copepods were seen occasionally; they could be distinguished from marine snow particles by their irregular movement. As expected the macroscopic biota did not penetrate the Mn-layer.

The observed planktonic community is typical for the Black Sea in late spring as a consequence of hetrotroph proliferation after the massive diatom bloom. The population densities of Aurelia, Pleurobranchia, and Sagitta was striking. The first two species occurred at densities of often over one specimen per m^3 while Sagitta showed densities of probably several tens of specimens per m^3 in its respective layer. It will be interesting to discuss the impact of these animals on the production of large aggregates which seem to be the main conveyers of particulate matter to the sea bottom at this time of the year as shown by the results of the in-situ sedimentation camera of Vernon Asper (see cruise report section IV.H.).

Table 1. Location and diving depth of each Mini-River dive.

Date 1988	Map-site	Sta.	Latitude (N)	Longitude (E)	Bottom Depth (m)	Dive Depth (m)	Acti-vity
20 Apr	6	8	41°49.37	28°40.62	167	157	ROV1
20 Apr	6	9	41°48.58	28°40.62	154	150	ROV2
23 Apr	BSK1	41	43°02.38	31°59.43	2100	65	ROV3
24 Apr	BSK2	51	42°54.72	34°00.72	2218	90	ROV4
26 Apr	BSK3	73	42°14.64	37°33.03	2046	120	ROV5
29 Apr	30c	99	41°25.18	41°28.24	174	145	ROV6
04 May	44	154	42°10.27	33°59.85	192	192	ROV7

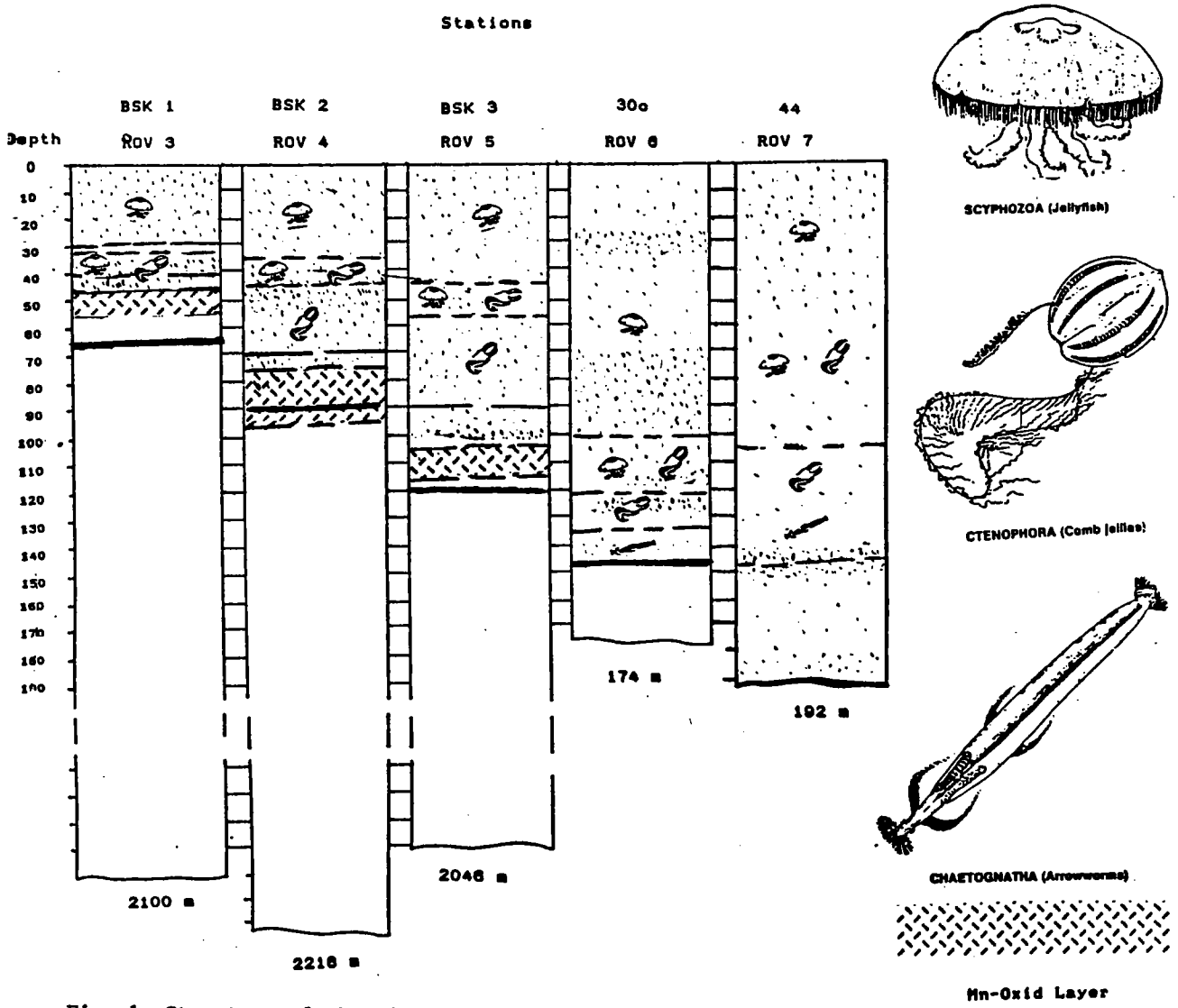

Fig. 1: Structure of the planktonic community in the surface water across the Black Sea in April 1988 as observed by the camera of the submersible mini-rover.

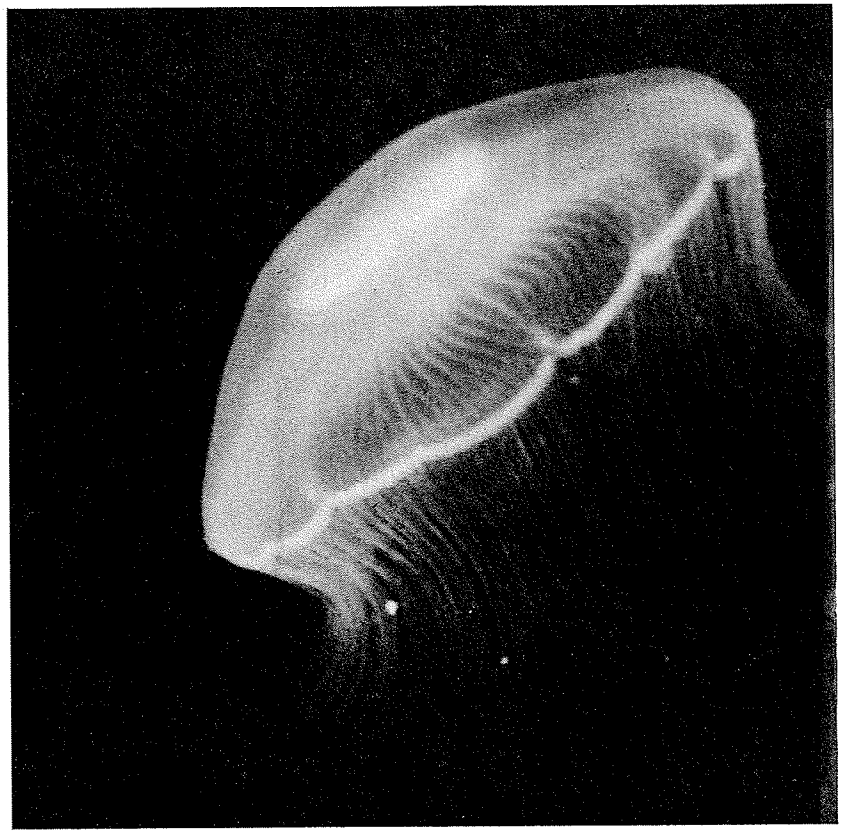

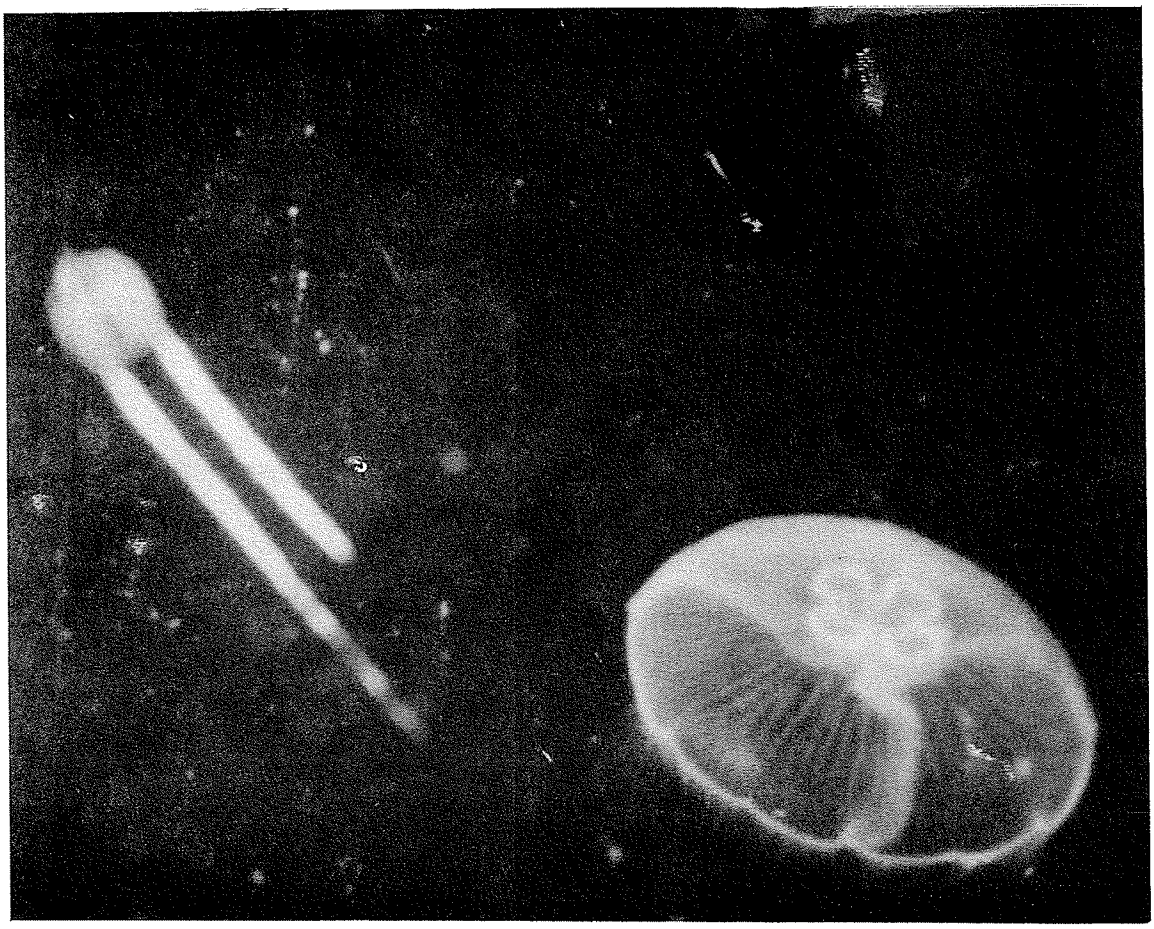

Fig. 2: Examples of the Benthos camera images: Left: Medusa Aurelia, photographed at a depth of 35 m at station ROV 3. Bottom: Aurelia and the ctenophora Pleurobranchia at a depth of 50 m at station ROV 3. Note numerous "marine" snow particles.

IV. H. MARINE SNOW IN THE BLACK SEA: ABUNDANCE, FLUX AND IN-SITU SINKING SPEEDS

Vernon L. Asper

Introduction

In addition to measuring the quantitative mass flux of particles, determining the modes and sedimentation mechanisms can provide useful information. We now realize that most particles in the ocean do not settle as individuals; rather, they settle as constituents of larger aggregated particles. Fecal pellet fluxes can account for some or even the majority of the sedimentation in certain locations, but in most environments other mechanisms are responsible for the bulk of the sediment flux. Marine snow aggregates (large amorphous aggregates of mucus and a variety of other biogenic and non-biogenic particles) have been proposed as one possible mechanism of rapid settling of fine particles and the observed positive correlation between fluxes of all types of particles.

Investigating these large particles has proven to be a considerable challenge because of their extremely fragile nature. Attempts to collect marine snow using pumps, water bottles, or even nets have resulted in a sample of the constituent small particles but the matrix of mucus in which these fine particles were once embedded is always destroyed. Honjo et al. (1984a) developed a photographic system designed to image a well-defined volume of water in which the aggregates can be counted. This non-contact (and therefore non-destructive) technique has proven to be very successful and the existence of aggregates has been documented in many regions of the world's oceans.

Equipment

The equipment used to investigate marine snow consists of two independent but complementary camera systems. The first will be a modified (improved?) version of the original Honjo et al. (1984a) system and the second will be a combination sediment trap/camera similar to that developed during my tenure as graduate student with S. Honjo.

1. Survey Camera

The survey camera consists of a single camera and a strobe light/Fresnel lens system which produces a slab of light (Fig. 1). Photographing this light slab at approximately 90° encloses a volume of water which is defined by the dimensions of the light slab and the camera angle of view. This system was lowered through the water column to produce a vertical profile of aggregate abundance or deployed at a single depth on

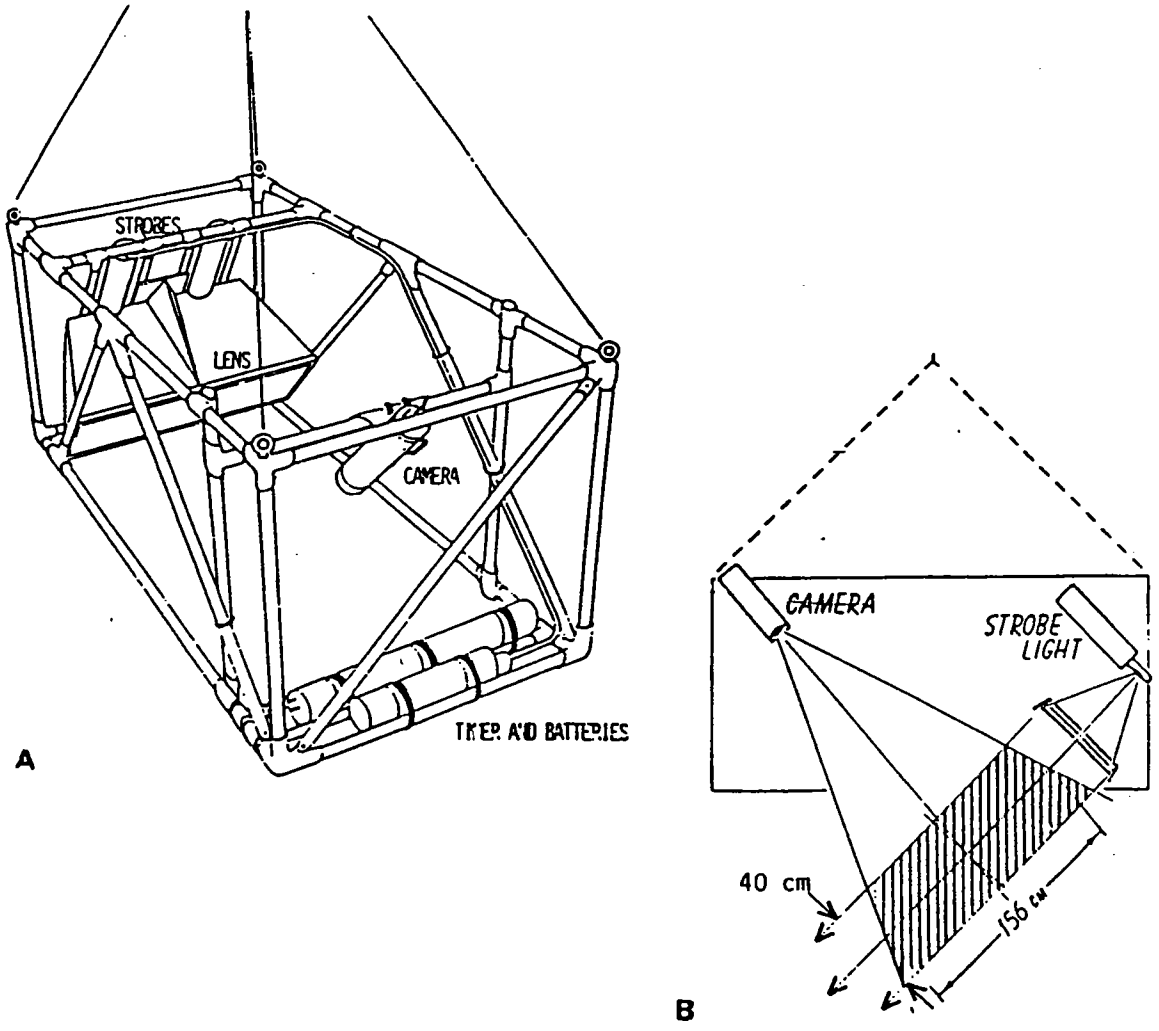

Figure 1. a) Configuration of marine snow photography system. Benthos model 292 strobes (200 watt seconds each) are mounted at the focal point of a pair of compound Fresnel lenses. The Camera, Benthos model 372, is mounted at 90° to the "slab" of light produced by the strobes. b) Diagram showing the dimensions of slab. 600 liters of water are included in the photograph.

a mooring to produce a time-series record of the abundance of aggregates at that depth. Also installed on the frame was a CTD and beam transmissometer to look at the water column structure and the concentration of fine suspended matter for comparison to the profiles of marine snow abundance.

2. "Flux Camera" (ASTAC-2, Aggregate Settling Tube and Collector)

This system consists of a double sediment trap (10 cm diameter opening) with a clear bottom settling chamber comprising the base of each trap (Fig. 2). Cameras are positioned beneath and normal to this clear chamber to photograph particles settling through and lying on the bottom of the chamber. The time-series record of particle arrival (upward looking vertical camera) will yield the flux of aggregates, and the horizontal camera will photograph in burst mode (30 sec-5 min interval) to record the in-situ sinking speeds of aggregates. One trap is fitted with an open/close device triggered by a burn wire. This side of the trap will be pre-charged with a saline formadehyde solution to preserve the sample and investigate the effect of preservatives on trap samples.

Deployments

1. Survey camera

Table 1 and figure 3 list the sites, water depth, and lowering depth of the 14 lowerings of the marine snow survey camera (profiler). Short pieces of several films were developed onboard, showing that the cameras were functioning properly and that the exposure and focus were properly set. All films will be transported back to the U.S. for processing by a professional laboratory. Each of the 9,274 frames will be analyzed using a digital image analysis system which will count the aggregates in the image and group them according to size class. These results will then be compared to profiles of fine suspended particles (or absorbing dissolved substances) obtained from the transmissometer and also to the water column density structure obtained from CTD profiles. Since all instruments were attached to the same structure and were sampling simultaneously, detailed comparisons will be possible.

2. Flux Camera (sediment trap)

This camera system was deployed at 688 m below the surface at station BSK2 (Figure 4) on April 24 and set to open at 20:00. Due to technical problems with the vertical-looking camera, only the horizontal camera was installed. The trap closed at 08:00 on May 3 and was recovered an hour later. All 800 frames of film were exposed with excellent results.

Immediately following recovery, the components of the ASTAC-2 were refurbished, the sample treated (vacuum filtration, Bonnie Woodward), batteries charged, and other preparations made in anticipation of an early evening redeployment. The second camera (removed from the survey

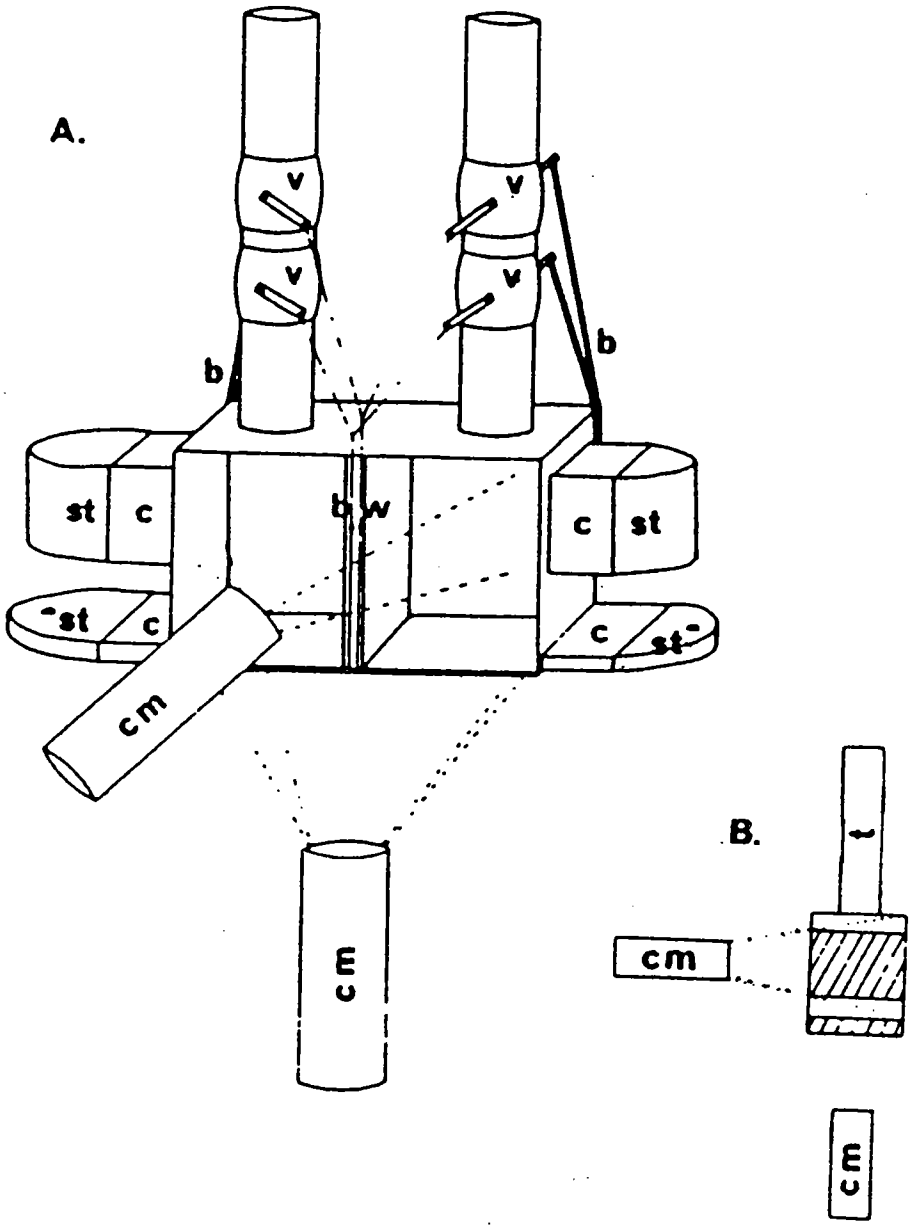

Figure 2. a) Sketch of proposed ASTAC (Aggregate Settling Tube And Collector) showing closing valves (V), burn wire (BW), light source (ST) with collimators (C), and cameras (CM). Particles settling into the device will be photographed as they settle through a quiescent chamber (sinking speed) by the side-mounted camera and again upon their arrival on the clear bottom plate by the bottom-mounted camera (flux). The chambers can be sealed prior to deployment and prior to recovery by ball valves mounted above the settling chamber. Bungee cords (B) pull the valves closed upon release of the burn wires. Activation of the valves is confirmed photographically by observing the burn wire. Duplicate systems are used to provide replicate samples or to evaluate the effects of poisons, baffles, or tube geometry, in which case one tube/chamber is used as a control. b) Diagram of the ASTAC showing illuminated area (hatched) and geometry of the system.

camera frame) was added to photograph in the vertical mode. The CTD/transmissometer was also attached and interfaced to the camera so that time varying concentrations of fine particles as well as conductivity, temperature, and depth will be recorded throughout the 72-day deployment. The latter values will be used to determine the precise depth of the ASTAC-2 beneath the surface as well as to record any vertical excursions the trap may experience due to current action. This mooring will be recovered during Leg 5 of the Black Sea expedition and the two Mark V sediment traps will be redeployed.

Results

1. Survey Camera/CTD

Results from the camera will not be available until the films have been developed and fully analyzed. However, preliminary indications show that marine snow aggregates are extremely abundant in the upper water column and rare below the chemocline. The CTD/transmissometer profiles show several peaks in abundance of fine particles associated with the pycno-chemocline. Comparisons of fine particle and large aggregate abundances will be made later and the results reported at the Izmir conference.

2. Trap Camera (ASTAC-2)

Of the 24 frames developed from this film, it is quite apparent that the flux of material from the surface arrives nearly exclusively in the form of marine snow aggregates. Surprisingly, sinking speed seems to bear no relation to aggregates size; aggregates of similar characteristics observed in the same frame settle at drastically different rates. The large quantity of film exposed (800 frames) will allow determination, with statistical confidence, of the sinking speeds of these aggregates and the variations in speed within each size class. The sample itself will also be analyzed for dry weight, carbon and nitrogen content, and also for content by SEM.

Summary

The data collected here will provide the first direct comparisons between the concentration of fine particles, water column structure, and the abundance of large aggregates ("marine snow"). In addition, the in-situ sinking speeds of these aggregates will be determined directly, providing crucial information pertaining to their importance in the flux of particulate matter to the deep sea. Overall success of these endeavors was extremely high, in spite of frequent technical problems with the camera systems. The addition of the anticipated samples and films from the second deployment will supplement the over 10,000 photographic images acquired on this cruise, bringing the total to nearly 14,000 discrete samples. Coupled with the CTD, transmissometer, core and trap sample analyses, these data will contribute substantially to our understanding of the sedimentation processes active in the Black Sea.

Table 1. Deployment sites and depths of survey camera. The camera was lowered to the basin floor in most cases. Small differences between basin depth and lowering depth are a result of different depth readings. The basin depth was obtained from the 3.5 kHz depth recorder; the lowering depth was obtained from the hydrowire meter.

#	Date	Mapsite	Station number	Latitude (°N)	Longitude (°E)	Basin depth (m)	Lowering depth (m)	Frames exposed	Activity
1	April 20	7	5	41 49.93	28 44.68	394	389	422	MSC1
2	April 21	11	18	42 16.74	30 00.62	2137	2135	700	MSC2
3	"	BSC	25	41 45.74	30 26.83	1914	831	400	MSC3
4	April 22	12	28	42 26.48	30 40.25	2170	2193	800	MSC4
5	April 23	BSK1	37	43 07.77	32 01.03	2079	2055	801	MSC5
6	April 24	BSK2	45	42 59.92	34 00.49	2220	2233	803	MSC6
7	April 25	17/18	57	43 05.84	35 17.30	2206	2225	801	MSC7
8	April 26	20	64	43 07.30	36 38.23	2184	708	431	MSC8
9	"	BSK3	76	42 12.64	37 35.39	2038	2061	810	MSC9 10
	April 28	25/26	85	42 00.09	39 13.81	2037	2039	800	MSC10
11	"	30c	98	41 26.67	41 17.23	366	360	247	MSC11
12	May 1	31	110	42 06.73	36 52.73	1977	1978	800	MSC12
13	May 2	43/44	121	42 15.79	34 51.00	746	865	667	MSC13
14	May 3	BSK2	132	43 04.50	34 06.10	2189	222	792	MSC14

Figure 3. Deployment sites of the survey camera.

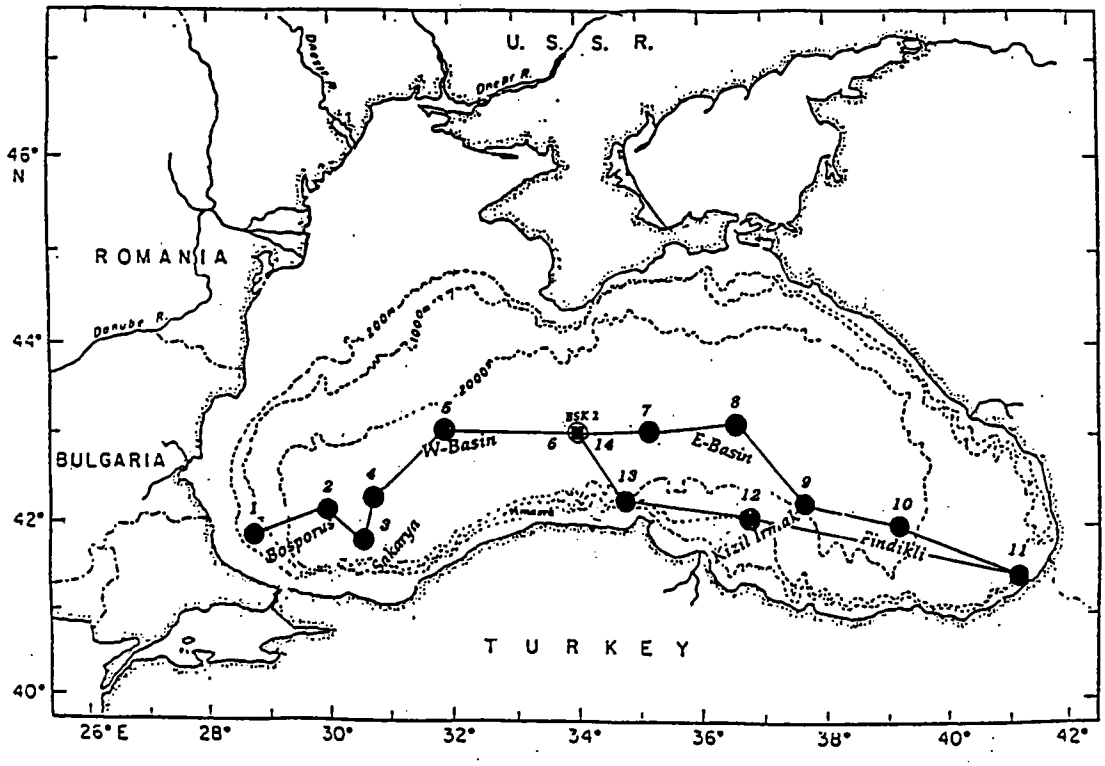

BSK-2 Camera mooring

Central Black Sea

(Lat. 42°59.25'N Long.: 34°00.16E)

April 24, 1988

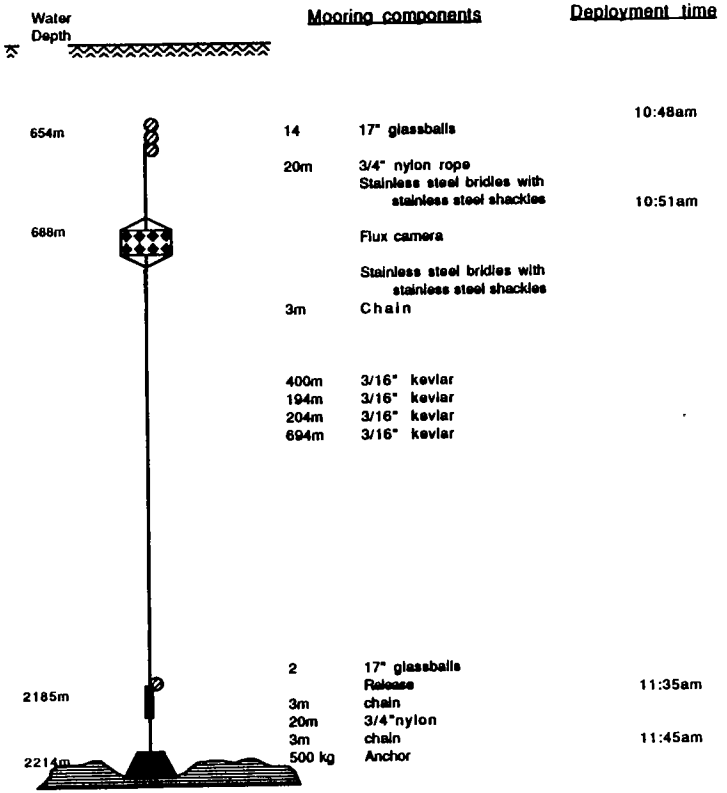

Figure 4: Mooring design of the Flux camera (ASTAC-2) deployment.

Sediment Trap Mooring Deployment/Recovery

R/V Knorr Cruise134, Leg 8

BSK-2 / Camera

(Black Sea, Knorr station 2)

General area: central Black Sea

Mooring description

Total length:	1560m
Main instrumentation:	1 Flux Camera (ASTAC-2)
Net buoyancy:	500 lbs.
Taut line:	3/16" kevlar
Release:	Benthos 865-A, serial number 284 Battery volt.: new (9.5V)
Mooring design:	P. Clay, WHOI

Deployment

Date:	April 24, 1988
Platform:	R/V Knorr, Woods Hole Oceanographic Institution
Deployment in charge:	B. J. Hay, V. Asper
Chief Scientist:	S. Honjo
Bosun:	J. Cotter, WHOI
Support:	2 AB and 1 OS, a few science hands
Equipment:	Stern winch for hauling, hand spooling of wire
Release arming witness:	V. Asper, J. Broda
Deployment position:	42°59.25'N; 34°00.16'E
Depth:	2214m, Raytheon PDD
Sea state:	1
Weather:	overcast

Satellite positioning

	Latitude	Longitude	Transducer reading	
Anchor drop	42°59.25'N	34°00.16'E		11:35h
Fix 1 (anchor at bottom)	43°00.23'N	34°00.32'E	2416m	12:10h
Fix 2	43°01.07'N	34°00.25'E		12:49h

Recovery

Date:	May 3, 1988
Time:	10:50h until 11:42h
Sea state:	1,
Weather:	sunnny, Temp. 68°F
Recovery pers./equip.:	same as for deployment above

IV. I. SUSPENDED PARTICLE COLLECTION

Bonnie L. Woodward

Vertical Profiles

Suspended sediment was collected by filtration onto pre-weighed 0.45 μm Nuclepore membrane filters at selected stations. Samples were collected with 30 liter Niskin bottles.

BSC-Profile 1

HC 01-Sta. 21

Depth, m	mls filtered
5	1000
50	1000
100	1000
200	1000
1000	1000

HC 02-Sta. 26

Depth, m	mls filtered
10	1350
20	2200
120	2000
160	2000
350	1500

BSK1-Profile 2

HC 03-Sta. 34

Depth, m	mls filtered
5	2000
50	1800
100	2000
200	1850
1000	1700

HC 04-Sta. 42

Depth, m	mls filtered
10	2000
20	1500
30	2000
45	1700
85	1500
250	2000

BSK2-Profile 3

HC 05-Sta. 47

Depth, m	mls filtered
5	2000
50	2000
100	2000
200	2000
1000	2000

HC 06-Sta. 53

Depth. m	mls filtered
20	2000
30	2000
70	2000
130	2000
350	2000

BSK3-Profile 4

HC 07-Sta. 66

Depth, m	mls filtered
5	2000
50	2000
100	2000
200	2000
1000	2000

HC 08-Sta. 72

Depth, m	mls filtered
20	2000
80	2000
110	2000
140	2000
350	2000

Mapsite 27/28-Profile 5
HC 10-Sta. 86

Depth, m	mls filtered
10	1500
40	2600
100	3000
120	3000
160	3000
350	2000

Mapsite 30C-Profile 6
HC 11-Sta. 96

Depth, m	mls filtered
10	1000
60	2000
100	2000
150	1000
200	2000

mapsite BS-Profile 7
HC 28-Sta. 165

Depth, m	mls filtered
10	2000
50	2000
100	2000
120	2000
160	2000
200	2000

Surface Water Samples

Suspended sediment was collected from the surface water with a clean bucket for the study of plankton assemblages. The samples were filtered onto 0.45 μm gridded Gelman filters.

No.	Date	Station	Time	Amount, ml
1	4/18	Istanbul	1435	1000
2	4/19	Mapsite 8	2225	600
3	4/20	Mapsite 6	0722	1250
4	4/20	Mapsite 11	2150	1800
5	4/23	Mapsite 16	2305	3000
6	4/25	Mapsite 18	0840	3000
7	4/27	Mapsite 24	1417	2000
8	4/28	Mapsite 29	1415	2000
9	4/30	Mapsite 31	1640	2000
10	5/1	Mapsite 33	0830	2000
11	5/1	Mapsite 43	2100	2000
12	5/2	Mapsite 44	1210	2000
13	5/5	Mapsite 50	1400	2000
14	5/5	Mapsite 34	1850	2000
Box core supernatant:				
15	4/24	Mapsite 47/BC 55	0915	30

IV. J. PLANKTON COMMUNITY

Huseyin A. Benli and Cynthia H. Pilskaln

Introduction

Plankton samples were collected on Leg 1 of the Black Sea cruise with two objectives in mind:

1) Quantification and description (species and genus identification) of the major zooplankton and phytoplankton groups forming the plankton community at depths ranging from 0 m to 120 m. These data will serve to supplement the detailed plankton surveys previously reported by Benli (1987).

2) Collection of fecal pellet material from zooplankton obtained in shallow (25-40 m), horizontal tows for geochemical analyses to be conducted in the laboratory. It is hypothesized that zooplankton fecal pellets represent an important mode of vertical transport of material to the deep anoxic benthos. Minimal degradation of the pellets at the anoxic benthic boundary layer would allow for their preservation and incorporation into the surface sediments. It is necessary to determine and compare the geochemical composition of pellets collected from live organisms, mid-water column sediment traps, and the surface sediments in order to assess the role which these biogenic aggregates play in the flux and deposition of various sediment components in the Black Sea.

Methods

1) For plankton species identification, samples were collected at 1-5 m, 30 m, 60 m, 90 m, and 120 m at mapsites BSC, BSK1, BSK2, BSK3, and BS (Fig. 1). A high-speed (ship speed approximately 4 knots), 10 minute horizontal tow was completed for the 1-5 m depth stations, using a net of mesh size 50 μm. This procedure was followed by 4 vertical tows to the other depths using a net (mesh size 200 μm) which was triggered to close with a messenger. A flow meter set within the frame of the nets allowed for the calculation of total water volume sampled at each tow. All plankton samples were fixed in a 4% formalin solution following collection.

2) Zooplankton fecal pellet material was collected from zooplankton obtained in 20-30 minute horizontal tows made at depths between 25-40 m using a net of mesh size 200 μm. Tows were carried out at mapsites BSC, BSK1, BSK2, BSK3, 7, 20, 30c, 31, 35, 43, and 25/26 (Fig. 1). The zooplankton was immediately placed in a fecal pellet collection apparatus

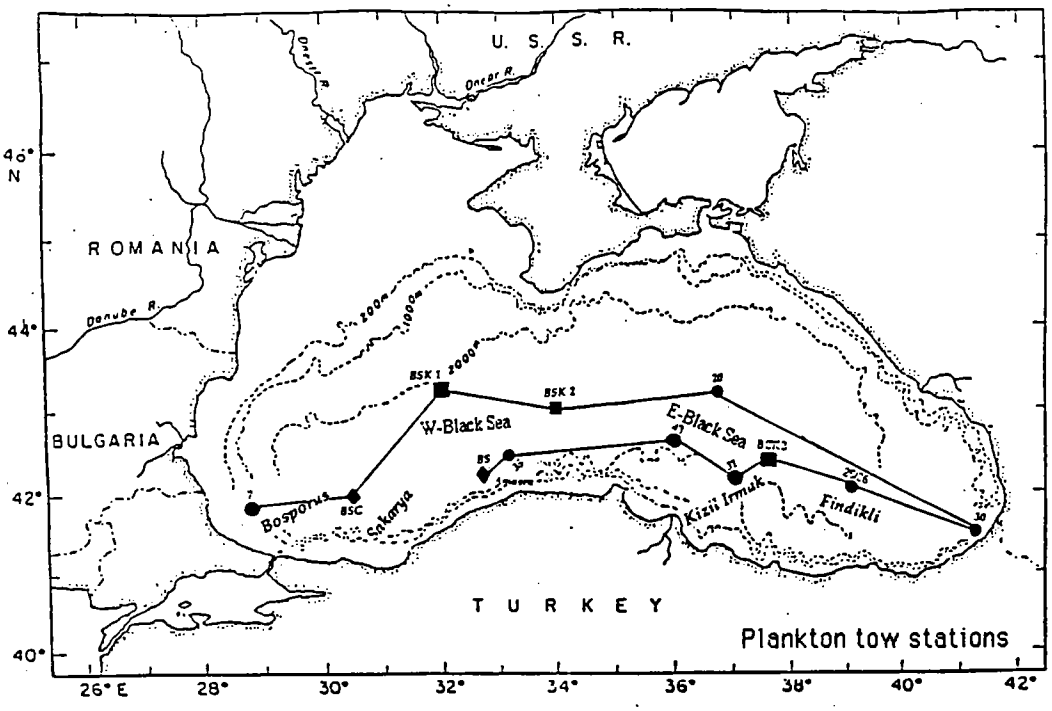

Fig. 1: Locations (mapsites) of the plankton tows in the Black Sea.

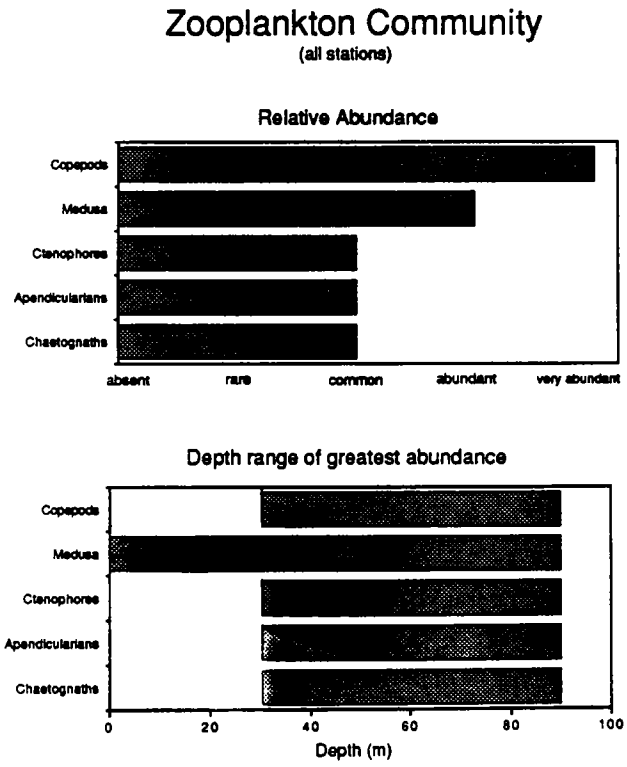

Fig. 2:
Summary of the occurrence of dominant zooplankton groups in terms of abundance and depth.

where it remained for 10-12 hours. Separate zooplankton and fecal pellet samples were then removed and immediately fixed with 4% formalin and refrigerated.

Results

Preliminary onboard examination of the plankton samples provided data on the community structure and depth ranges of greatest abundance for the plankton population observed in the upper 120 m of the Black Sea for the period between mid-April and early May, 1988. These data are summarized in figure 2.

V. SCIENTIFIC INVESTIGATIONS IN THE SEDIMENT

V. A. BLACK SEA SEDIMENTS

M.A. Arthur, J.E. Broda, W.E. Dean, A.S. Derman, A.R. Gagnon,
B.J. Hay, Y.T. Konuk, S. Honjo, E.D. Neff,
C.H. Pilskaln, and M. Briskin

1. CORING AND SEDIMENT PROCESSING

A total of 92 core stations were covered in the Black Sea, 2 in the Sea of Marmara (Fig. 1). Of these core stations, 62 were gravity cores (Table 2) and 30 were box cores (Table 1). Only 9 gravity cores resulted in no recovery but every attempt to obtain a box core was successful (Fig. 2). The cores obtained should allow us to fulfill the multifold research objectives in the Black Sea on Leg 1.

Box Cores

The Ocean Instruments Mark III box corer was used exclusively with excellent results. The Mark III recovers a nominal maximum 50 cm-thick sediment section with a 50 x 50 cm surface area. The high water content of Unit 1 sediments and turbidites, however, frequently allowed over-penetration and recovery of up to 65 cm-thick sections. We attempted to adjust for this tendency by using the lower "limit" plate which was designed to cut penetration by about one-half. In addition, the Mark III was fitted with wooden "paddles" or platforms on the front and back of the lower frame in order to provide a more stable base in contact with the sediment substrate and to reduce sinking of the frame into the mud. The coring device was lowered at a speed of 35 m/min in order to prevent kiting and/or pre-tripping, particularly with the wooden "paddles" attached. At 10-20 m above the bottom, the winch was switched over to "slow mode" and the box core was lowered at 5-10 m/min until wire tension indicated contact with the bottom. The pull-out wire tension typically was 7,500 lbs (3,570 kg). Successful closure of the spade was indicated by a change in the repetition rate of the attached 12 kHz pinger. The corer was returned to the surface as a speed of 50 m/min.

Most coring attempts recovered a brownish-green organic "fluff" or flocculent layer at the sediment/water interface, but only 7 of the box cores actually retained supernatant water above the interface. A number of investigators (M. Arthur, C. Pilskaln, J. Nicholson, S. Honjo) routinely sampled and preserved (formalin, freezing) the fluff samples for later geochemical and textural studies.

Upon recovery, a box core usually was subsampled using custom-cut thin-walled liners (3" and 4" or 7.6 and 10.2 cm thick) according to the sampling plan shown in figure 3. Subcores were recovered after one side of the box was removed. The subcores were capped, sealed, marked, and

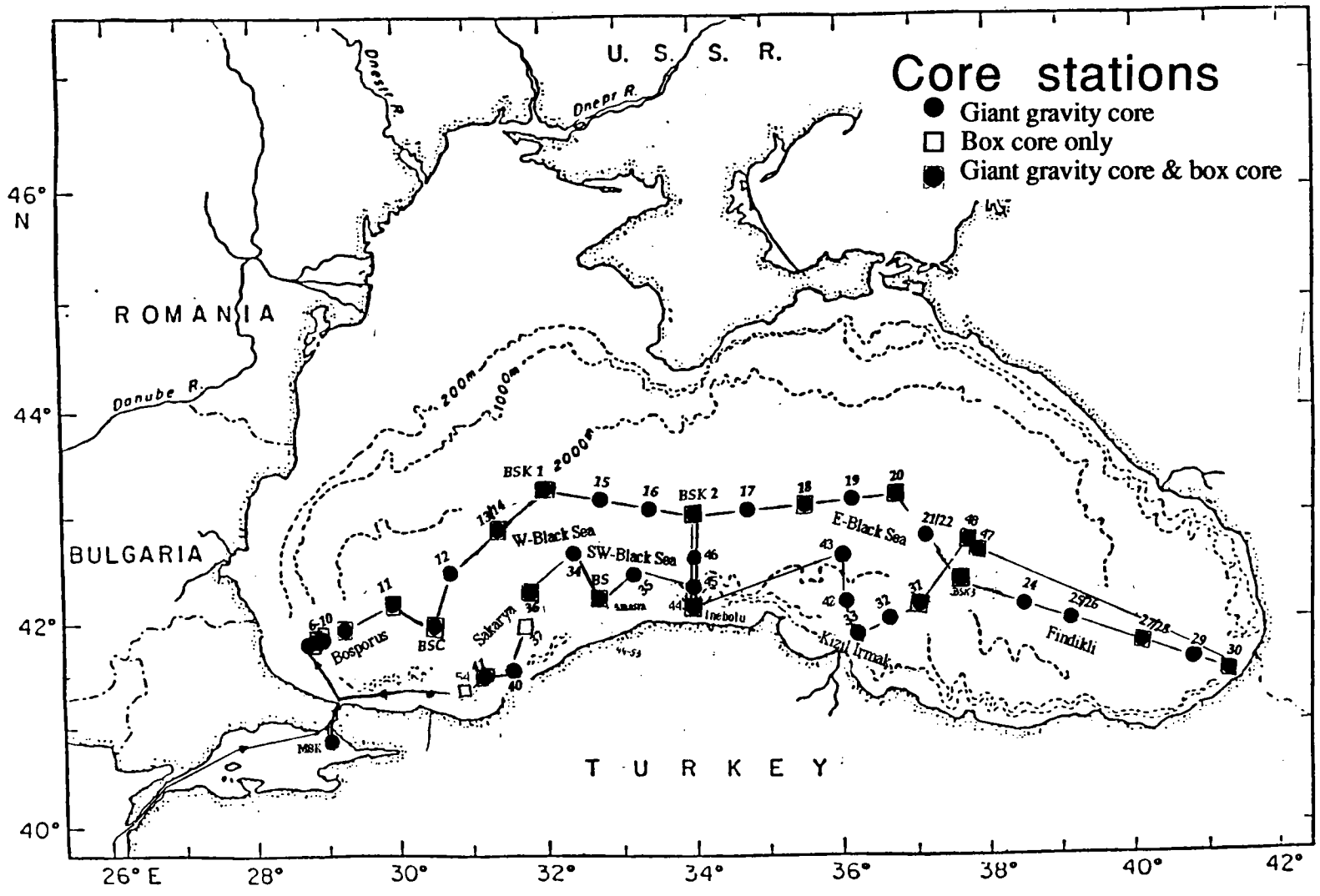

Fig. 1: Locations (mapsites) of gravity and box coring.

Table 1: Box core stations (BC).

Date (1988)	Mapsite	Station number	Latitude (°N)	Longitude (°E)	Water depth	Activity	Core length (cm)	X-ray
April 19	8	2	41°51.08	28°50.12	667	BC2	>60	x
April 20	7	7	41°49.02	28°45.00	404	BC5	>70	x
"	10	14	41°57.71	29°05.24	1503	BC10	43	
"	11	17	42°15.39	30°00.15	2137	BC13	>60	
April 21	BSC	24	41°46.52	30°28.42	1938	BC15	>60	
April 22	13/14	30	42°58.20	31°25.26	2066	BC17	60	x
"	BSK1	39	43°05.52	32°01.56	2092	BC21	60	x
April 24	BSK2	50	42°55.58	34°01.03	2217	BC25	>60	x
April 25	18	59	43°03.59	35°26.55	2205	BC29	>60	x
"	20	61	43°04.89	36°41.10	2184	BC31	>60	x
April 26	BSK3	69	42°16.01	37°32.03	2060	BC34	>60	x
April 27	BSK3	77	42°22.56	37°35.39	2038	BC36	>60	x
"	BSK3	78	42°22.56	37°35.39	2030	BC37	>60	x
April 28	27/28	88	41°49.38	40°12.82	1861	BC43	50	x
"	30a	92	41°27.01	41°21.55	184	BC47	>60	x
"	30d	95	41°26.46	41°26.04	101	BC50	35	x
April 30	47	103	42°39.73	37°36.98	2154	BC53	48	x
"	48	105	42°44.91	37°34.80	2164	BC55	50	x
"	31	108	42°08.15	36°54.00	1980	BC58	50	x
May 1	44	151	42°12.84	34°05.83	194	BC73	27	x
"	44	152	42°13.85	34°05.96	147	BC74	47	x
"	44	155	42°10.91	34°00.69	130	BC76	50	x
"	44	156	42°12.69	33°59.38	253	BC77	50	
"	44	157	42°12.95	34°00.66	250	BC78	55	x
May 5	BS	164	42°14.48	32°42.61	2199	BC82	60	x
May 6	36	175	42°22.00	31°53.19	2203	BC84	62	x
"	37	177	42°00.31	31°52.50	2140	BC86	>67	x
"	41	180	41°30.16	31°01.49	1328	BC89	56	x
"	54	181	41°11.03	30°47.60	122	BC90	26	x
"	MSK	186	40°47.80	29°01.85	1215	BC92	40	

Note: The symbol > indicates overpenetration of the corer slightly.

Fig. 2a: Giant Gravity Core lengths

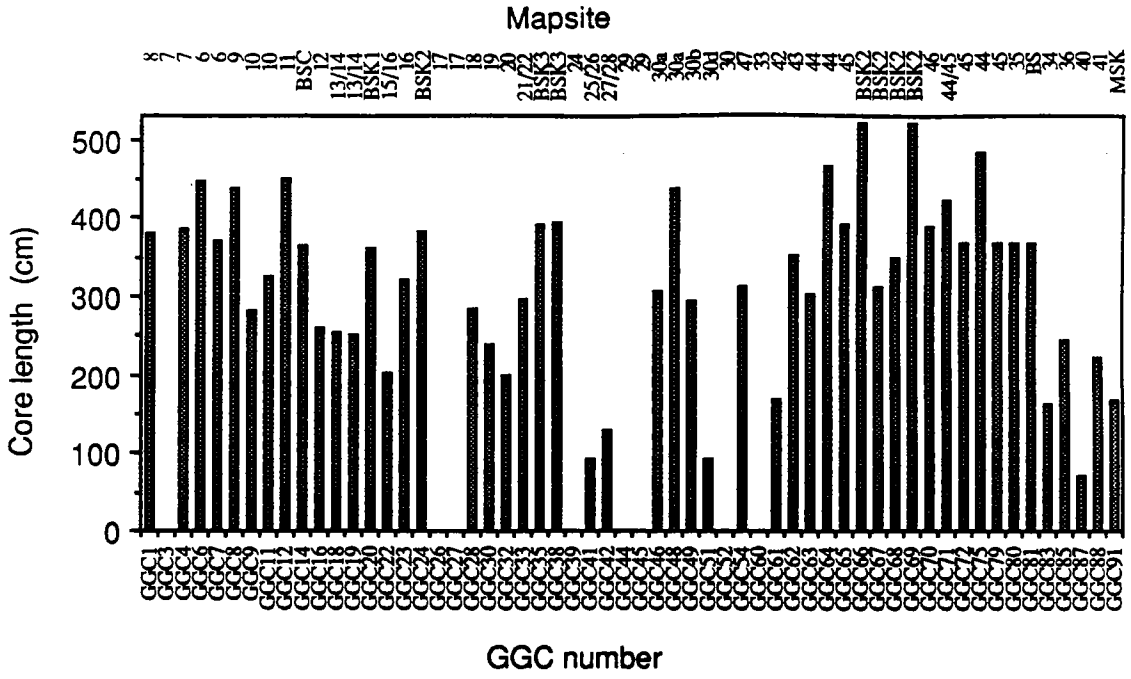

Fig. 2b: Box Core length

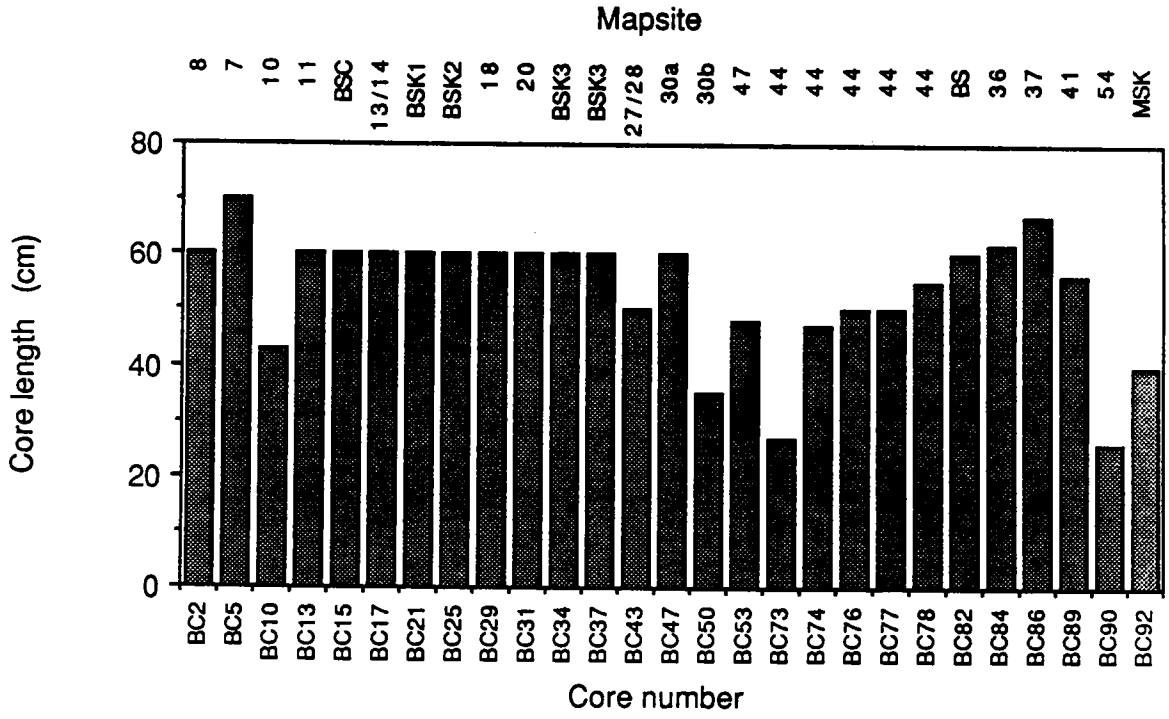

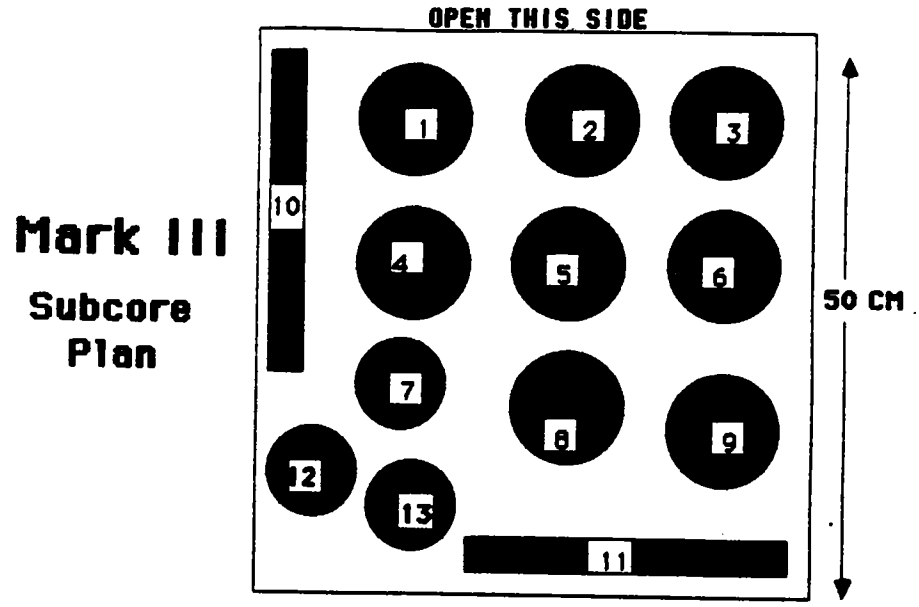

TENTATIVE SUBCORE PLAN AND DISTRIBUTION

1. 4" Subcore--G. Jones/A. Gagnon (Frozen for 14C)
2. 4" Subcore--Arthur/Hay/Dean (Inorg. geochem/isotopes)
3. 4" Subcore--Archive (not to be opened-Hay-Arthur)
4. 3" Subcore--J. Nicholson (sulfur geochemistry)
5. 4" Subcore--WHOI archive (can be split at WHOI)
6. 4" Subcore--Kempe Group (Organic Geochemistry)
7. 3" Subcore--Moore/Todd (Radionuclides-Ra)
8. 4" Subcore--On board split, photograph, sampling
   (Piiskein samples, any others on 1/2)
9. 4" Subcore--Turkish core repository
10. 1.5 cm slab--Arthur et al. (archive); also Briskin NMR)
11. 1.5 cm slab--Arthur et al. (varve studies)
12. 3" Subcore--Liebezeit (Pore water extraction)
13. 3" Subcore--Konuk (sedimentological studies)

Fig. 3: Subsampling scheme for box cores used during the cruise.

stored upright in the refrigerated van. The van is kept at 9°C, the average bottom-water temperature of the Black Sea. One subcore was carefully precleaned, inserted and withdrawn, then sealed in plastic and frozen (A. Gagnon) for later ^{14}C work. One subcore of each box core was usually split in a glovebox under nitrogen atmosphere; the surface was then cleaned with an electro-osmotic knife, photographed, and described (description available upon request to Chief Scientist). One-half of this split core was available for sampling aboard ship. A further subcore was taken for onboard studies of pore-water nutrient distributions (G. Liebezeit).

In general, each box core was also slabbed using 2 plexiglas samplers (25 cm wide, 1.5 cm thick, 50 cm tall), which were then cleaned and sealed at the base using Plexiglas and silicone sealant. Any void space at the top was filled with fomofil, an expanding foam insulator, that generally helped to preserve the sediment/water interface intact. Although we had some problems with foam expansion and artificial compaction of the sediment, these slabs allowed a clear view of sedimentary textures and structures. Each was photographed, described (description available upon request to Chief Scientist), and then used for onboard X-radiography (see subsection below for details). The X-radiographs were developed on board ship and provided a permanent record of the sedimentary structures in cores for reference and varve counting/correlation; fine laminae in Unit 1 were resolved by X-radiography, but those in Unit 2 were too thin and of low contrast.

Gravity Cores

A gravity core was attempted at most mapsites. The gravity core rig used a standard core cutter attached directly to a 4" diameter (10.2 cm), thick-walled PVC liner (water-well casing) cut to an average length of 5 m. The weight-stand contained 350 lbs (167 kg) of lead, and the entire rig weighed approximately 650 lbs (310 kg). A winch speed of 100 m/min was used for raising and lowering the core, but we generally used a winch speed of 125 m/min for penetration. Wire tension on the hydrowinch at pull-out averaged about 1200 lbs (571 kg). Two variants of an iris or sphincter-type core catcher were used with good success, at least in muddy sequences. One was a single, heavy-weight sheet-metal finger sphincter; the other consisted of two nested, light-weight sheet-metal finger catchers with a plastic "sock" in between. Recovery averaged over 2.5 cm per core. Cores were recovered in a vertical position, the overlying water was drained off, and the liner was cut and capped before lowering so that core tops were preserved if present. Cores were cut, capped, labeled and stored vertically in the refrigerated van. We did not plan to open them onboard due to time limitations. Only two cores were extruded on deck (GGC 66 and 71). These cores were sectioned into 50 cm lengths and extruded with a fixed piston device into presplit half-rounds of 4" (10.2 cm) PVC liners. The presplit halves were separated with one-half used for pore-water squeezing and the other described, photographed, and saved as an archive core.

Table 2: Giant gravity core stations (GGC).

Date (1988)	Mapsite	Station number	Latitude (°N)	Longitude (°E)	Water depth (m)	Activity	Core length(cm)
April 19	8	1	41°53.32	28.49.21	549	GGC1	379
April 20	7	3	41°51.54	28°43.07	394	GGC3	0
"	7	6	41°49.12	28°44.96	403	GGC4	386
"	6	10	41°50.34	28°41.22	211	GGC6	447
"	6	11	41°50.11	28°41.45	211	GGC7	370
"	9	12	41°55.91	28°55.17	897	GGC8	439
"	10	13	41°56.24	29°02.11	1259	GGC9	283
"	10	15	41°56.96	29°06.32	1490	GGC11	325
"	11	16	42°14.63	29°58.98	2139	GGC12	450
April 21	BSC	22	41°47.49	30°28.88	1916	GGC14	365
April 22	12	29	42°26.27	30°39.60	2170	GGC16	260
"	13/14	31	42°52.53	31°23.29	2091	GGC18	255
"	13/14	32	42°52.48	31°22.46	2096	GGC19	250
"	BSK1	38	43°06.98	32°00.85	2088	GGC20	360
"	15/16	43	43°06.63	31°59.43	2151	GGC22	203
"	16	44	43°02.00	33°16.48	2219	GGC23	322
April 24	BSK2	46	42°59.00	34°00.37	2195	GGC24	382
April 25	17	55	43°02.16	34°35.45	2177	GGC26	0
"	17	56	43°02.28	34°35.67	2178	GGC27	0
"	18	58	43°05.09	35°24.57	2204	GGC28	284
"	19	60	43°09.30	36°10.55	2194	GGC30	238
"	20	62	43°05.92	36°35.72	2184	GGC32	200
April 26	21/22	65	42°43.30	37°12.48	2162	GGC33	298
"	BSK3	70	42°15.01	37°31.60	2060	GGC35	392
April 27	BSK3	79	42°21.32	37°30.01	2030	GGC38	395
"	24	80	42°11.33	38°35.17	2089	GGC39	0
"	24	81	42°10.21	38°34.81	2089	GGC40	0
"	25/26	84	42°01.23	39°13.60	2037	GGC41	93
April 28	27/28	87	41°49.33	40°11.41	1864	GGC42	130
"	29	89	41°40.58	40°55.44	1665	GGC44	0
"	29	90	41°40.75	40°55.35	1670	GGC45	0
"	30a	91	41°27.04	40°25.66	195	GGC46	307
"	30a	93	41°26.66	41°21.78	205	GGC48	438
"	30b	94	41°25.14	41°23.10	101	GGC49	295
"	30d	101	41°28.23	41°15.44	1406	GGC51	91
"	30	102	41°25.19	41°13.31	990	GGC52	0
April 30	47	104	42°40.73	37°45.59	2157	GGC54	314
"	48	106	42°45.77	37°33.99	2162	GGC56	124
"	31	107	42°07.75	36°54.70	1979	GGC57	300
"	32	109	41°58.54	36°33.30	600	GGC59	457
May 1	33	112	41°49.07	36°17.51	1170	GGC60	0
"	42	116	42°16.99	36°17.48	1750	GGC61	170
"	43	119	42°34.85	36°00.30	2034	GGC62	352
May 2	44	122	42°10.34	33°59.97	155	GGC63	304
"	44	124	42°11.54	35°59.94	203	GGC64	466
"	45	128	42°17.78	33°59.92	563	GGC65	393
May 3	BSK2	133	43°03.25	34°04.66	2190	GGC66	522
"	BSK2	134	43°03.21	34°04.91	2186	GGC67	314
"	BSK2	137	42°59.21	34°00.30	2221	GGC68	348
"	BSK2	138	42°57.88	33°59.18	2221	GGC69	520
"	46	141	42°34.33	34°00.09	2220	GGC70	390
May 4	44/45	149	42°12.02	34°06.33	411	GGC71	422
"	45	150	42°12.42	34°03.23	435	GGC72	369
"	44	153	42°11.00	33°59.21	174	GGC75	484
"	45	158	42°19.39	34°00.94	707	GGC79	369
May 5	35	161	42°30.74	33°13.20	2215	GGC80	367
"	BS	163	42°13.69	32°43.69	2199	GGC81	368
"	34	174	42°52.07	32°19.40	2196	GGC83	161
May 6	36	176	42°21.87	31°54.65	2202	GGC85	244
"	40	178	41°35.14	31°30.13	1758	GGC87	69
"	41	179	41°29.72	31°00.47	1368	GGC88	223
"	MSK	184	40°41.08	29°09.31	1225	GGC91	170

X-Radiography Routine

Procedures were developed onboard for x-radiography of 1.5 cm thick slabs taken with Plexiglas "slicers" from the Mark III box cores. This was done in order to obtain the best possible record of sediment structure within the subcore. X-radiography of the slab cores were taken immediately after removal from the box because many of the cores contained an unconsolidated surface "fluff" layer, the texture of which deteriorated rapidly with handling of the slabs. Table 1 lists the available X-radiography. The X-radiography was performed in the aft side of the reefer van on the 01 deck. We used a specially constructed lead box (30x60x150 cm) with a port at one end to which was affixed the Acoma Portable x-ray unit, Model PX20N. In order to expose a slab (or core) with a vertical dimension of 50 cm, the working distance was set at 110 cm from the focal point of the X-ray tube (with field limit plate no. 1). Shims were installed in the lead box in order to slide the slabs in and hold them steady at the proper distance. After some experimentation, the following settings were found to give the best results:

KV-MA: 50-20
Exposure time: 15-20 secs.

The maximum X-ray exposure setting is only 10 sec, so it was necessary to do a double exposure, allowing 3-5 min between individual exposures for cool-down of the tube. Otherwise tube damage or circuit overload may result. For subcores (9 to 12.5 cm thick) of box cores, rather than thin slabs, the required exposure time was longer. We made certain that the cores did not move at all or blurred images would result. Also, a lead apron was provided and was worn at all times when the X-ray equipment was in use. For safety purposes we stepped outside the van and pushed the hand button then.

We used Kodak Industrex X-ray film, developer, and fixer. Negatives were placed in developer for 5-8 min, rinsed in water for 1 min, placed in fixer for 10 min and rinsed again in water for more than 20 min. A warm (18-30°C) room is necessary for exposure and developing. We cut sheets (being careful not to expose them to light) to size and placed them directly behind the slabs for exposure. The negative was removed from the envelope in safe light only. For this purpose we used the "Damage Control Locker" because it provided more room than the "darkroom."

2. UNIT 1: HOLOCENE COCCOLITH-BEARING VARVED SEDIMENT

Varve couplets of lithologic Unit 1 of Degens and Ross (1974) consist of thin (<1 mm) laminations of white, coccolith-rich material alternating with darker organic-terrigenous material. Variations in amount of carbonate in individual varve couplets and groups of varve couplets has produced distinctive, cyclic cm-scale color bands that are useful for correlation between cores (Fig. 4). These variations in relative carbonate abundance may reflect variation in coccolith productivity and/or dilution by terrigenous material (Hay, 1987). Figure 4a illustrates correlation of these cm-scale color bands between plastic slabs from BC 17 (mapsite 13/14) and BC 21 (mapsite BSK1), a distance of about 40 km. Figure 4b illustrates the correlation between 4"-diameter (10.2 cm) subcores from BC 21 and BC 55, a distance of about 600 km. Although BC 21 a turbidite layer, we used this box core as the reference section for Unit 1 because it was collected at mapsite BSK1 which is one of the major "key" sites in the Black Sea and will be characterized by extensive data on ^{14}C, sediment flux, water chemistry, etc. Note the extremely uniform thickness of the color bands (reflecting uniform thickness of individual varve couplets) over great distances. These distinct color bands occur in, and can be easily correlated among, the following box cores: BC 1, BC 5, 10, 21, 25, 34, 37, 43, 53, and 55. Correlations of key laminae between six of these box cores are illustrated diagrammatically in figure 5. No attempt was made on board ship to count individual varves because of the lack of proper imaging and microscope facilities, but there is no doubt that thicknesses of individual laminae can be measured, and that individual laminations can be correlated across most of the Black Sea with the same uniformity as the color bands produced by distinctive groupings of carbonate-rich and carbonate-poor laminae. Such long-distance correlation of varves over 1000 km across the floor of the Black Sea was unexpected because we anticipated greater interregional differences in influx of terrigenous material and/or coccolith productivity. However, the fact that laminae thicknesses are so uniform suggests that there was a surprising uniformity in depositional processes throughout both the eastern and western Black Sea. This is the first time that modern or ancient varves have been correlated over such great distances, and exceeds the long-distance correlation of distinctive evaporite varves of the Permian Castile and Zechstein Formations (Anderson and Kirkland, 1966).

The laminations recovered in most box cores have been interrupted by one or more fine-grained turbidites (Figs. 4 and 6). By correlation among box cores, it has been possible to demonstrate that in most cases the turbidites have been inserted between varves with little if any removal (erosion) of laminae (Fig. 6).

Figure 4 illustrates the differences in degree of compaction between the plastic-slab subcores and the 4" subcores. In figure 4a, the top of the turbidite in the plastic-slab subcore of BC 21 occurs at about 21 cm,

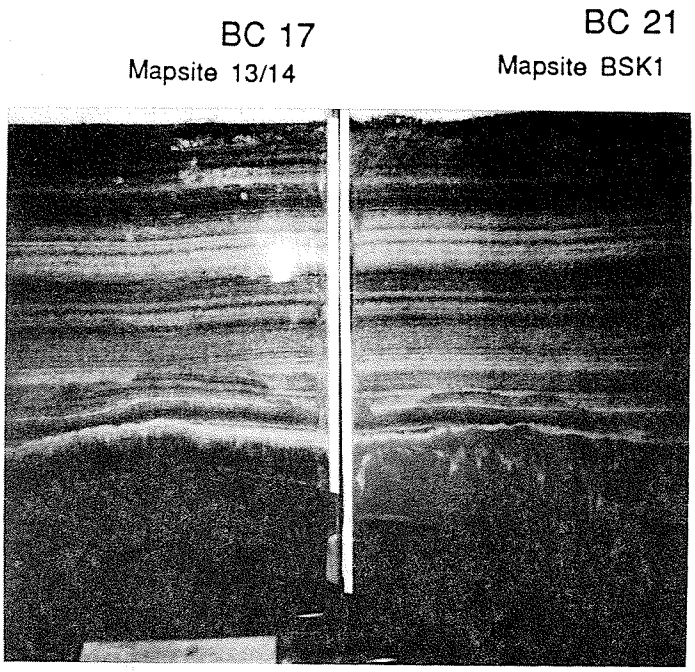

Fig. 4: Laminated box cores (BC 17 and BC 21) from different locations across the Black Sea. Notice that the black and white laminae of Unit I can be well correlated.

Figure 5. Diagrammatic correlation of 20 selected key lamonations in Unit 1 in 6 box cores.

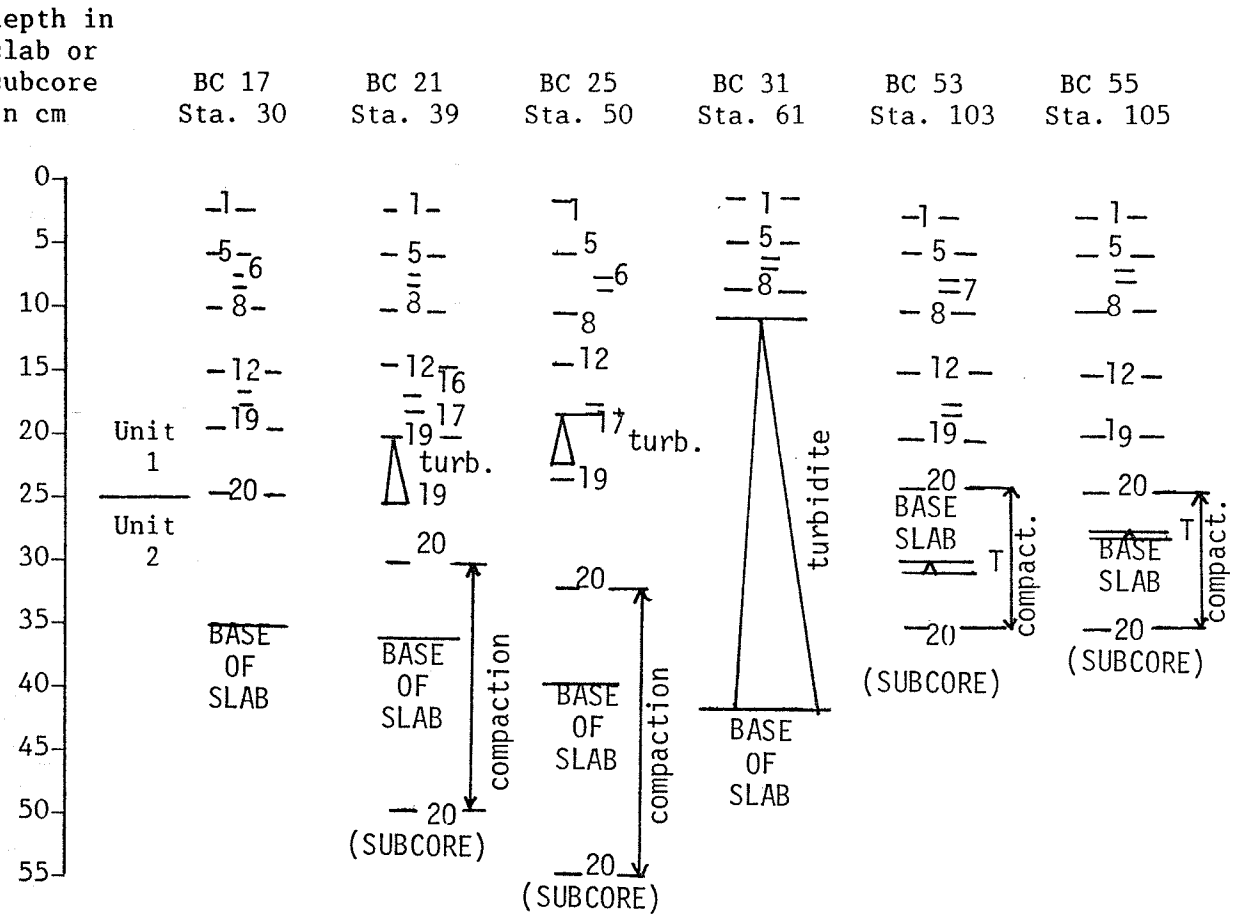

Notes: BC02 and BC05 probably can be correlated
BC10 can be correlated
BC13 contains 4-5 mud turbidites
BC15 contains mostly turbidites but thin (1-2 cm) intervals of Unit 1 laminae might be correlatable
BC29 all turbidite
BC34 and BC37 are mostly turbidites but intervals of Unit 2 laminae probably can be correlated
BC43 contains mostly terrigenous material but has been correlated with BC21
BC47 hemipelagic mud varves (311 in 53 cm)

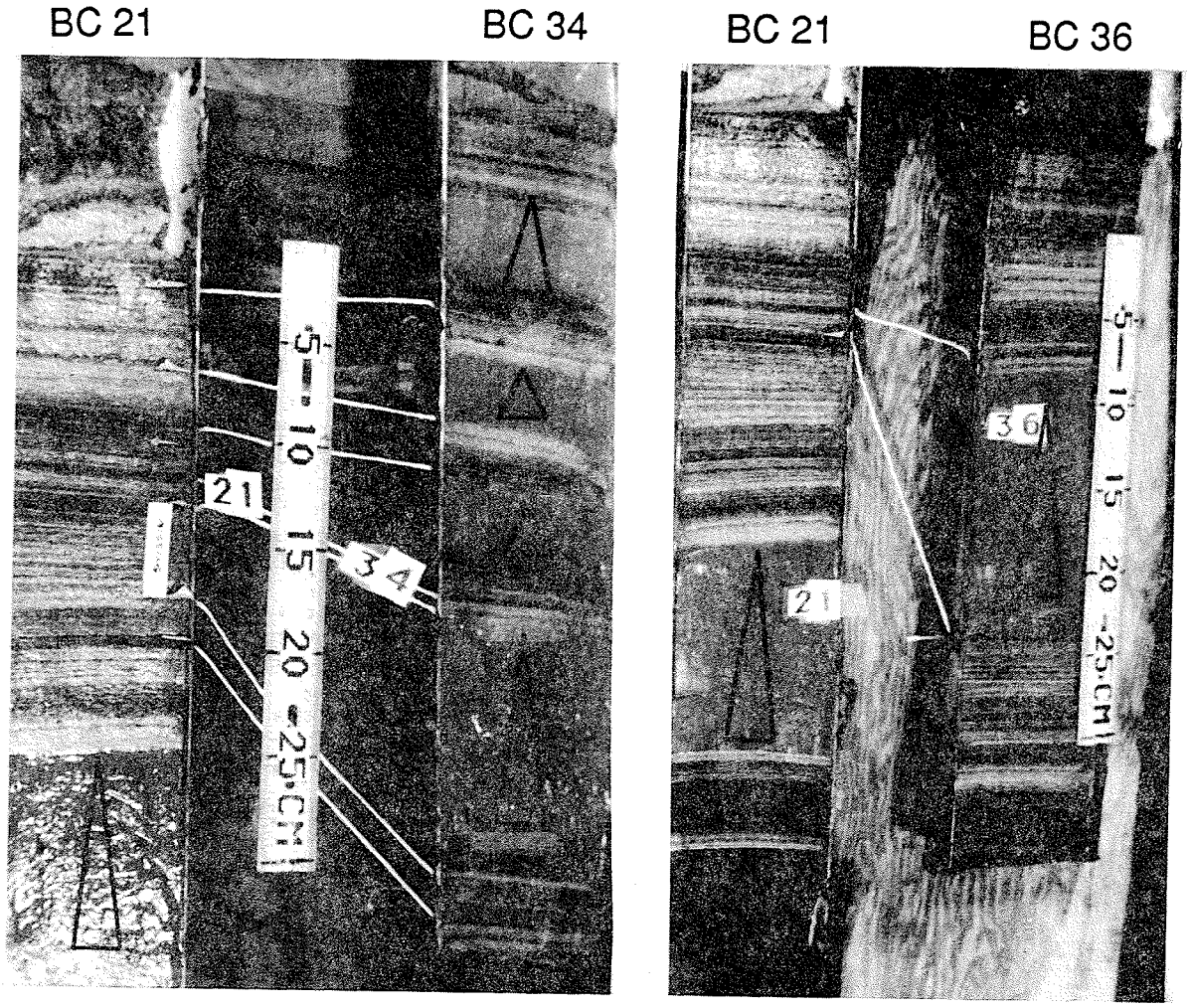

Fig. 6: Correlation between BC21 (mapsite BSK1) and two cores taken at mapsite BSK3 (BC 34, left, and BC 36, right). Turbidite deposition usually occurred without erosion of the laminated sediment. The only exception is the lowest turbidite in BC 34 where a few varves are missing at its base.

whereas in the 4" subcore the top of the turbidite occurs at about 30 cm, a difference in compaction of about 30%. Even with these differences in degree of compaction between types of subcores, the thicknesses of Unit 1 laminae remain remarkably constant as long as one compares thicknesses in the same type of subcore.

Unit 1/2 Boundary and Uppermost Unit 2 Sapropels

The first occurrence of coccolith-rich laminations typical of Unit 1 occurs at about 25 cm in plastic-slab subcores of box cores and at about 45 cm in 4" subcores (key correlation lamina number 20 in Fig. 4). Carbonate-rich sedimentation during this first phase of Unit 1-type sedimentation only lasted roughly about 50 years before returning to Unit 2-type sedimentation that resulted in deposition of no more than 5 cm of sapropel. We place the Unit 1/2 boundary at the base of the lowest band of carbonate-rich sediment because it documents the first occurrence of coccolith accumulation in the Black Sea and, therefore, represents a fundamental change in depositional conditions.

The Unit 1/2 boundary was recovered in six box cores (Table 3), and only a few centimeters of the upper part of Unit 2 are available to characterize the Unit 2 sapropel. This sapropel consists of very finely laminated, dark olive gray to black organic-rich clay. Although the varves in Unit 2 are much thinner than those in Unit 1 and lack the white carbonate marker laminae, they are still grouped into distinctive cyclic color bands that should be extremely useful in correlating Unit 2 from site to site, particularly in the gravity cores. More extensive examination of Unit 2 sediments awaits the opening of the giant gravity cores.

Turbidites

Medium gray to light greenish gray, plastic, fine-grained turbidites are common in box cores that we recovered from both the eastern and western basins of the Black Sea. The number of turbidites is not the same even in box cores from the same general area as was demonstrated by repeated box coring around mapsite BSK3 (BC 34, BC 36, BC 37, BC 53, and BC 55). Also, the turbidites do not occur at the same stratigraphic positions in different localities. Varve correlation shows that the turbidites are "inserted" between laminations (Fig. 6) with little if any erosion even though X-radiographs show distinctive ripple cross lamination in the coarser bases of some turbidites. More extensive information on the occurrence of turbidites over greater stratigraphic intervals and greater geographic areas should be possible from the gravity cores. The distribution and composition of the turbidites should provide valuable information on possible sources and modes of deposition of turbidites throughout the southern Black Sea.

Table 3. Box cores that recovered the Unit 1/Unit 2 boundary.

Core	Station	Mapsite	Water Depth	Depth of 1/2 Boundary*
BC 17	30	13/14	2066	26
BC 21	39	BSK1	2092	36 (49)
BC 25	50	BSK2	2217	33 (49)
BC 37	78	BSK3	2030	(78)
BC 53	103	47	2154	23 (32)
BC 55	105	48	2164	24 (34)

* Depths to the Unit 1/Unit 2 boundary are given in cm within the plastic slab subcore and, in parentheses, for the depth within a 4" thick (10.2 cm) thin-walled tube subcore. Sediment was severely compacted by the plastic slab but very little by the 4" subcore. The difference between depth of the 1/2 boundary within the two types of subcores gives a relative measure of the degree of compaction by the plastic slab.

History of Deepwater Sedimentation in the Black Sea

Core GGC 66 from near mapsite BSK2 (station 133, 2190 m water depth) was extruded, split, photographed, and described onboard. This core (Fig. 6) provides insights into the sedimentation history of the deep Black Sea basins. The core includes a complete sequence of the classic Holocene sediment Units 1, 2, and 3 as defined by Degens and Ross (1974). The laminated coccolith ooze of Unit 1 is compacted and the core top was lost in GGC 66, but Unit 1 was recovered in a box core from a nearby station (BC 25, station 50, 2217 m water depth). The Unit 1/2 boundary occurs at a depth of 27.5 cm in GGC 66, but a 20 cm-thick homogeneous mud turbidite has been "inserted" beginning 1 cm above the contact (Fig. 7). The thinly laminated black to olive gray sapropel of Unit 2 is 47 cm thick in GGC 66. The detailed correlation of Unit 2 across the deep basins of the southern Black Sea awaits the opening of other gravity cores, but there is little doubt that the base of laminated sapropel of Unit 2 in GGC 66 is older than that on the Inebolu slope (see next chapter). A very preliminary estimate of the number of varves in Unit 2 was made by counting varves over a three centimeter section of the upper part of Unit 2 and extrapolating the average number of varves per centimeter (96) over the entire 47 cm section of Unit 2 in GGC 66. This calculation gives an approximate duration of 4,500 years for Unit 2 which, although crude, is in line with previous estimates by Degens et al. (1978; 1980).

Figure 7: Generalized lithology of sediment in GGC 66 at mapsite BSK2 (water depth: 2190 m)

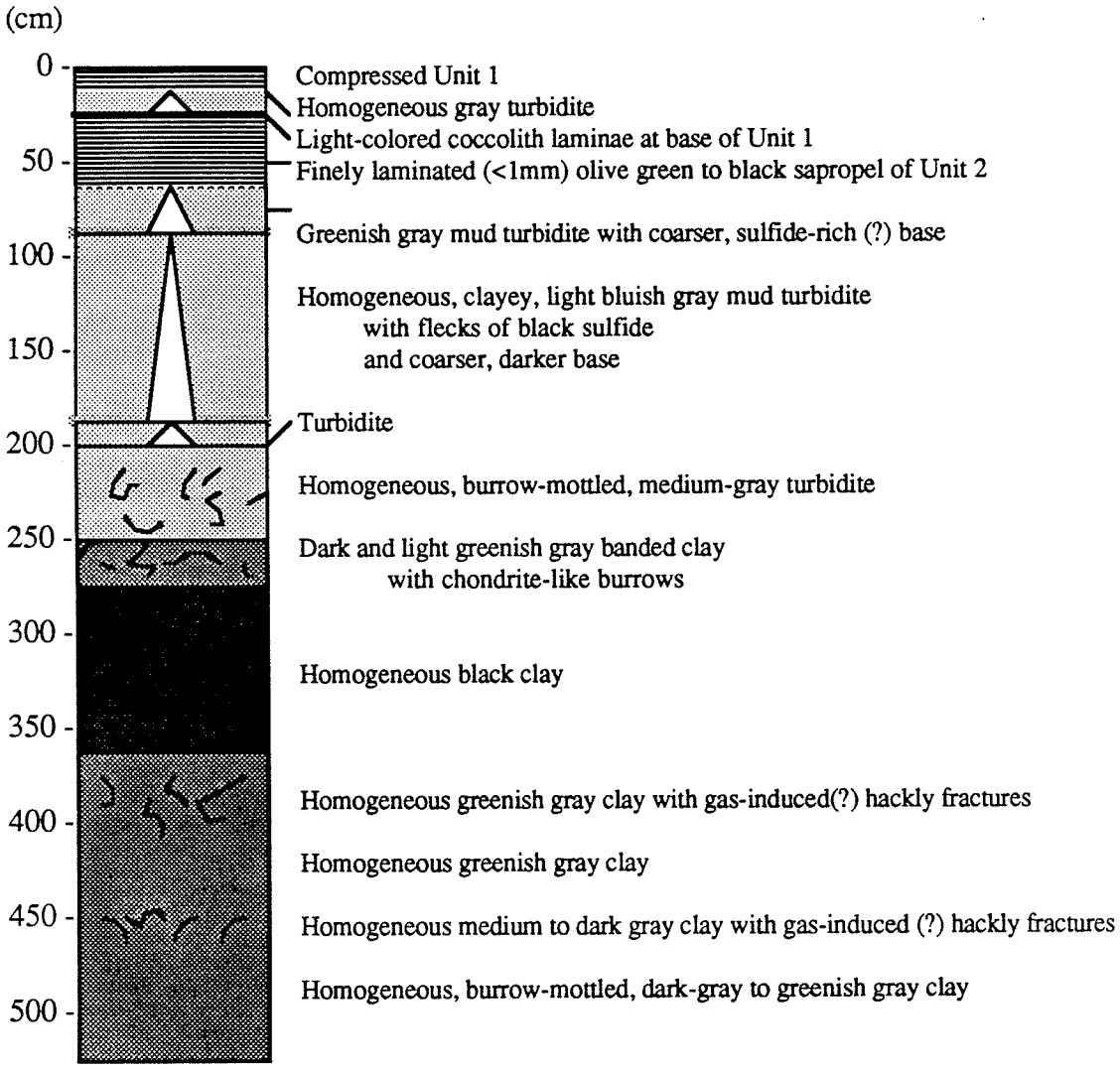

The remainder of GGC 66 consists primarily of a series of thick, gray-green homogeneous, sulfidic mud turbidites characterized by sharp basal contacts and thin silty or sandy basal units. However, homogeneous black clay of classical Unit 3 occurs from about 275 cm to 375 cm in the core (Fig. 7). The black clay is underlain by medium gray, burrow-mottled to homogeneous green-gray clay. The gray color faded rapidly upon exposure to air suggesting the presence of iron monosulfides as the coloring agent.

Although complicated by interbedded turbidites, GGC 66 contains the classical Holocene sequence representing the transition from fresh-water clay sediment, including unlaminated, organic-carbon rich mud and the brackish-water phase of laminated sapropel deposition, which probably mark the onset of anoxia in the deep-water mass as well as high biologic productivity (e.g., Glenn and Arthur, 1985; Calvert et al., 1987; Hay, 1988). The base of Unit 1 probably marks the transition to a water-mass structure much like the present and the first appearance of coccoliths as primary producers.

The coccolith Emiliana huxleyi probably first appeared at the time when surface-water salinity reached the lower limit of its tolerance (Bukry, 1974), although it is not clear how the coccolith found its way into the Black Sea at that time. The change from laminated sapropel to coccolith ooze is not monotonic, however. The initial bloom of coccoliths is marked by a series of relatively thick carbonate laminae, which total perhaps 50 varve years. Above this interval there is a return to carbonate-poor sapropelic sediment 2-3 cm thick, followed by coccolith mud again. These lithologic alternations suggest that significant changes in climate and runoff occurred that influenced the salinity of the surface-water mass after the modern regime was first established. These hypotheses will be tested by our shore-based geochemical and stable isotope studies.

3. THE INEBOLU SLOPE TRANSECT

A series of cores was taken in a transect down the slope south of BSK2 (Inebolu Transect; Fig. 8) in order to document the relationships among the position of the pycnocline, the particle-density maximum, the O_2/H_2S interface and their impingement on the upper slope. A number of CTD casts provided very precise control on the variations with depth and distance of the pycnocline and particle maxima offshore and allowed selection of optimum depths for box and gravity cores in the transect. We obtained four box cores (BC 76, 74, 73, and 78) at depths of 135 m, 150 m, 201 m, and 250 m, respectively. Giant gravity cores were recovered from depths of 155 m, 174 m, 203 m, 411 m, 435 m, 563 m, and 700 m (GGC 63, 75, 64, 71, 72, 65, and 79). GGC 71 and 72 were recovered from approximately 400 m; GGC 71 of 4.22 m length was cut into 50 cm sections and extruded on deck (Fig. 9). One-half was squeezed for pore-water geochemistry and the other was described and photographed. GGC 71 provided important preliminary constraints on the timing of the rise of the anoxic deep-water mass to 400 m on the slope, as well as on the nature of the lithologic and geochemical changes that accompanied the progressive rise of the chemocline.

Modern Sedimentation on the Slope

Laminated, relatively organic-carbon-rich sediments presently are found at 250 m, but the surficial sediments (to 50 cm or more) at depths of 200 m and shallower are bioturbated and unlaminated. Although the pycnocline and particle maximum impinge on the slope between 135 m and 150 m in this region, anoxic conditions at the seafloor are not recorded in the sediments as undisturbed laminae except below 200 m. A well-developed organic-rich surface "fluff" layer was recovered at the 250 m station (Sta. 157, BC 78). Shell-rich surface layers, primarily composed of small specimens of Mytilus, occurred in all box cores taken at shallower depths, indicating sufficient oxygen at depths of 200 m or less for metabolism of benthic metazoans. In addition, sediment in all box cores from depths shallower than 250 m contains small-diameter, open, vertical worm burrows that extend to 10 cm depth or less. Live worms were recovered in sieved samples of the upper 5 cm of sediment from these shallow-water box cores.

A reddish-brown oxic layer also occurs at the top of each of the cores taken from depths shallower than 225 m; the thickness of this layer decreases with increasing water depth. At the 200 m station (Sta. 151; BC 73), the reddish surface layer is only 0.5 cm thick and is underlain by greenish-gray, burrow-mottled mud. No discrete manganese layer was observed in sediments beneath the surface, but abundant disarticulated Mytilus shells at the sediment-water interface were found encrusted by brownish-black to orange-brown ferromanganese coatings. The same is true of the 150 m station (Sta. 151; BC 74) where the oxidized layer was at least 10-15 cm thick. The box core slab from 135 m depth (Sta. 155; BC 76) recovered over 60 cm of oxidized, burrowed, reddish-brown to

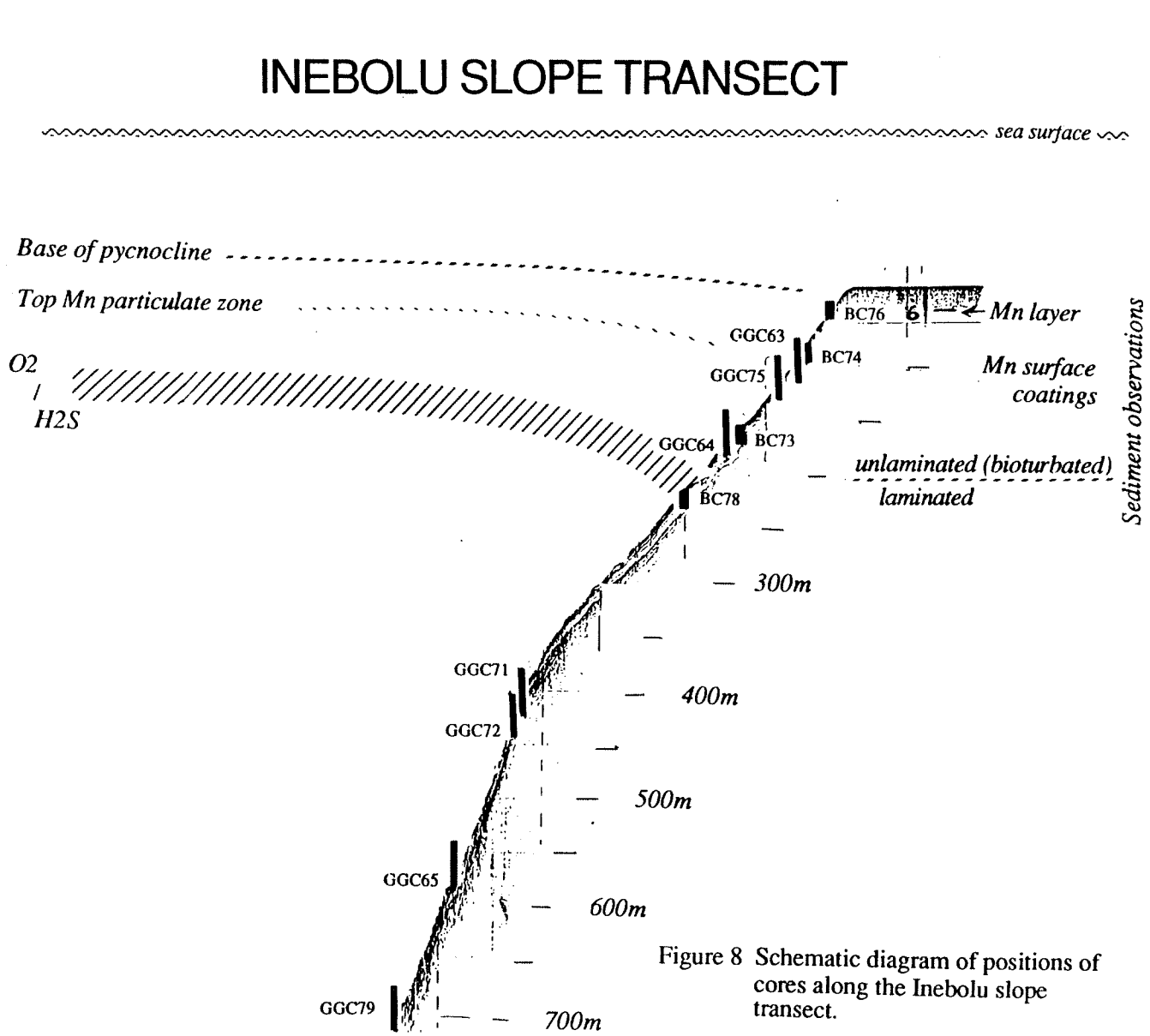

Figure 8 Schematic diagram of positions of cores along the Inebolu slope transect.

Figure 9: Generalized lithology of sediment in GGC 71.

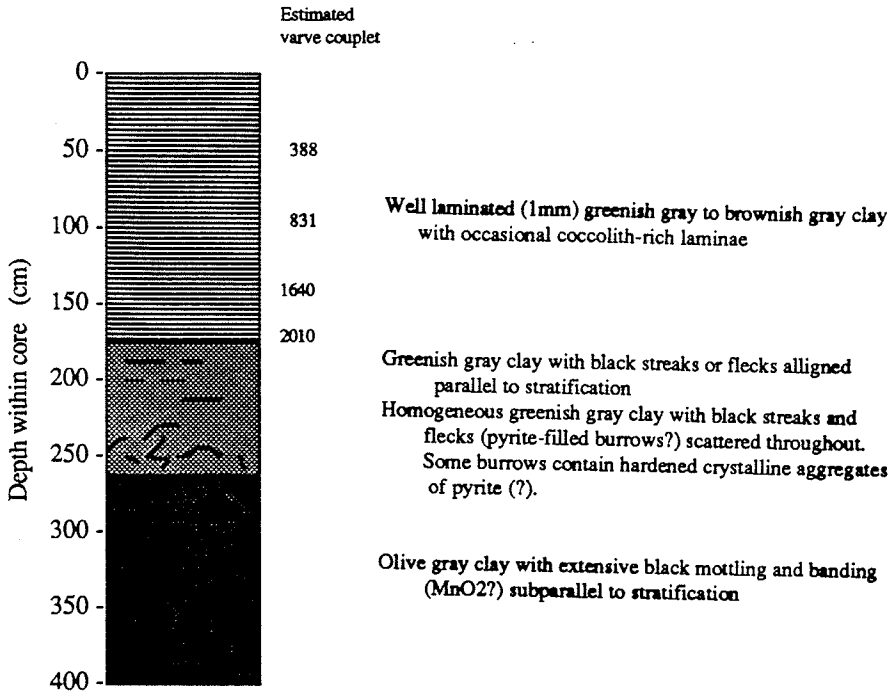

Figure 10: Rise of the O2/H2S interface as a function of time (modified from Glenn and Arthur, 1985).

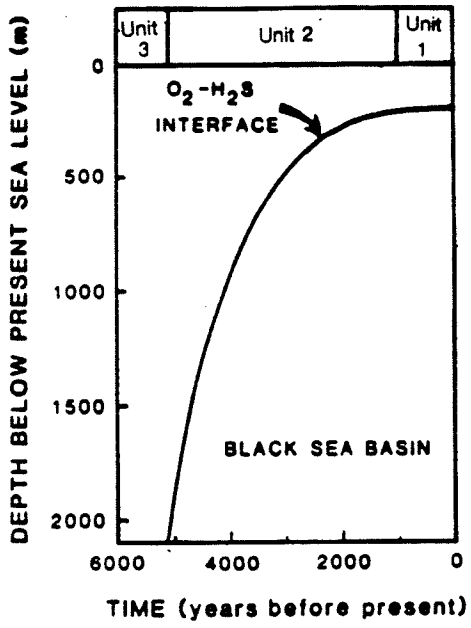

reddish-olive mud, with a 1.0 cm thick black Mn-layer at about 2-3 cm below the sediment-water interface. No Mn-layers were observed deeper in any of the box core slabs.

History of the Development of Anoxia

The extruded and split gravity core (GGC 71; 411 m water depth) allowed us to estimate the time at which the oxic/anoxic interface rose to approximately 400 m and above in this part of the Black Sea. Greenish-gray, thinly laminated sediment occurs in the upper 170 cm of the core (Fig. 9). The base of this laminated sequence is interpreted as marking the onset of anoxia above the seafloor at the 411 m site; the complete elimination of dissolved oxygen inhibited benthic metazoan activity, thus preserving the record of seasonality of production of organic components and flux of detrital clay minerals. The varves are typically millimeter to submillimeter laminae couplets consisting of a thin, dark, presumably "organic" lamina and a thicker greenish-gray clay lamina. The basal 10 cm of the laminated sequence in GGC 71 has laminae that are calcium-carbonate rich. Post-cruise microscopic examination will determine whether these are coccolithophorid-bearing laminae equivalent to the basal part of Unit 1 or some other form of carbonate that indicates inorganic carbonate precipitation and a preservation event at the onset of anoxic conditions on the slope. Assuming that the core top was recovered intact and that each laminae couplet represents one year of deposition, preliminary varve counts were made on the GGC 71 record. We obtained an estimated 2,040 years B.P. for the timing of development of anoxia at this depth on the slope. This age is older than the age estimated for the base of Unit 1 in the deep basin (1,600 years B.P. or less; Degens et al., 1978) and suggests that the initiation of anoxia at 400 m occurred during the latter part of sapropel (Unit 2) deposition.

This 2,040 years B.P. age contrasts with an estimate of 4,000-6,000 years B.P. based on ^{14}C data for the first appearance of varved, sapropelic sediments given by Calvert et al. (1987) for the development of the sapropel at an eastern basin slope site (R/V Atlantis II Sta. 1470, 1969) at 906 m depth. Degens et al. (1978), on the other hand, suggested an age of 2,800 years B.P. for the rise of the O_2/H_2S interface to a depth of 470 m on the slope in the western Black Sea on the basis of varve counting. Thus, there is reasonable agreement between two preliminary studies of varved sequences at about 400 m on the slope from different parts of the basin. We would expect an older age for the rise of the O_2/H_2S interface at the 906 m site studied by Calvert et al. (1987). A simple model that illustrates the rise of the O_2/H_2S interface was constructed by Glenn and Arthur (1985; after Deuser, 1974) using available age constraints on the initiation of anoxia in the deep basin and a "half life" model of the deep-water dissolved oxygen reservoir (Fig. 10). This model predicts inception of anoxia at 2,000 years B.P. on the slope at 400 m and at 3,800 years B.P. at 900 m depth.

We are certain that our post-cruise studies of the gravity cores from the three slope transects completed on R/V Knorr 134-8 will allow elucidation of the history of development of the O_2/H_2S interface in the Black Sea.

Manganese Mineralization at the O_2/H_2S interface

An interesting sidelight of the Inebolu slope transect was an opportunity to examine the accumulation of Mn-oxyhydroxides and the formation of incipient bedded manganese deposits (and other mobile transition metals) associated with the O_2/H_2S interface. The particle maximum associated with the pycnocline is, in part, attributed to particulate Mn formed at the redox boundary in the water column (see cruise report sections IV.E. and IV.F.). Degens and Stoffers (1976) predicted that metalliferous sediments should be formed at the O_2/H_2S interface. The sediments in our box cores, taken across the pycnocline and the O_2/H_2S interface contain Mn-coatings on shells at the surface, and the shallowest core (135 m) contained a thin Mn-rich layer 3 cm below the sediment-water interface, but no massive Mn-precipitation was noted. One of the reasons for this may be that modern sedimentation rates on the upper slope off Inebolu are high enough to maintain suboxic to anoxic conditions below the sediment-water interface, thereby allowing continual remobilization and upward migration of Mn. Mn-oxyhydroxide is then reprecipitated at the sediment-water interface as coatings on shell material, but much of it may be lost to the water column. Concentrations of shell debris were found mainly at the sediment/water interface, although some scattered shells and fragments occur deeper in the box cores. Dissolved and broken shells were recovered from greenish-gray mud in the lower parts of box cores and in GGC 71. The suboxic to marginally anoxic conditions in these sediments may promote dissolution of calcium carbonate because of the buildup of dissolved CO_2 without an accompanying increase in alkalinity.

The lower 2 meters of GGC 71 provide better support for the manganese mineralization concept (Fig. 9). Multiple dark sharp to diffuse bands, mottles and specks of Mn-oxides occur in greenish-gray to light reddish-brown mud. Pockets of concentration of crystalline Mn-oxide occur within some of the bands. The top of the Mn-rich zone occurs at about 30 cm below the base of the laminated interval. We suggest that the Mn-rich zone in GGC 71 represents the record of the rising pycnocline. Particulate Mn-oxides were precipitated from the water column at this time. The accumulation of Mn was augmented by upward diffusion and reprecipitation of Mn-oxides at or near the sediment/water interface from manganese reduced and remobilized at depth in the sediment. This interval was soon followed by suboxic and then anoxic conditions as the O_2/H_2S interface rose above the 400 m depth resulting in the preservation of varves.

V. B. TURBIDITES IN BLACK SEA SEDIMENTS

Y. Tosun Konuk, Muhammed Duman, Oya Algan,
and Tayfun Bilgic

Introduction

Black Sea turbidites pose many unsolved problems as to their origin, their exact extension, and the causes of their formation. As of today, several papers have been published dealing with the Black Sea turbidites. Due to the limited number of cores available so far, these papers, however, discussed mainly grain size and energy questions of a few individual turbidites.

Observations

The Holocene sediments of the Black Sea are subdivided into two units, the $CaCO_3$ bearing Unit 1, and the sapropelic and carbonate-free Unit 2. Both units contain turbidites of varying thickness (Fig. 1). Only a few of the recovered box cores did not contain turbidites (i.e., BC 17 and BC 47). Similar turbidite-free cores have also been described by Ross and Degens (1974).

Even though turbidites are a very common feature in the young sediments of the Black Sea (they may even play a more important role for the bulk sedimentation rate than the "normal" seasonal sedimentation recorded in the varved section), it has not been possible to trace a turbidite from one box core station to the next. Neither their thickness nor their color or grain size allows a classification of the encountered turbidites as yet. The number of turbidite layers at any one station is highly variable, excluding the definition of regions of high turbidite incidents at this stage of evaluation. Neighboring cores, like BC 34, BC 36, and BC 53 (Fig. 2) show very different numbers of turbidites, for example. This observation may point to very localized areas of origin and may even suggest quite low energy requirements for triggering a turbidite event.

Future turbidite research will have to focus on the following questions:

1) Is it possible to follow the horizontal extension of individual turbidites, and what is their lateral variance in thickness?

2) Can we define areas of high turbidite event probabilities?

3) What are the exact dates for these turbidites and can these dates be correlated with external, dated events like earthquakes, years of exceptionally heavy precipitation, rapid snow melts, or other climatic features?

Part of the answers may come from a detailed investigation of both the collected box and gravity cores. ^{14}C dating, investigation of clay and heavy minerals, and heavy metal concentrations are some of the tools to tackle the task.

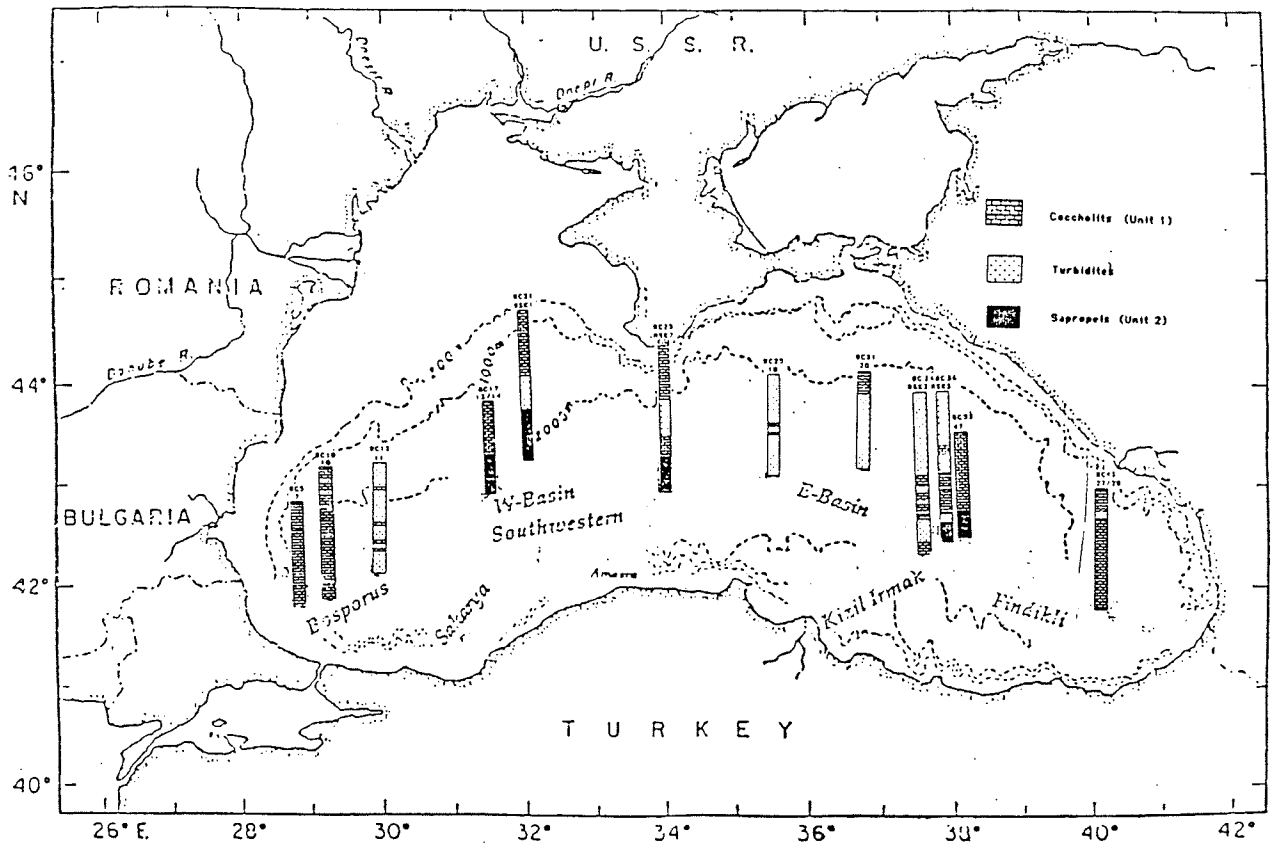

Fig. 1: Selected box core locations.

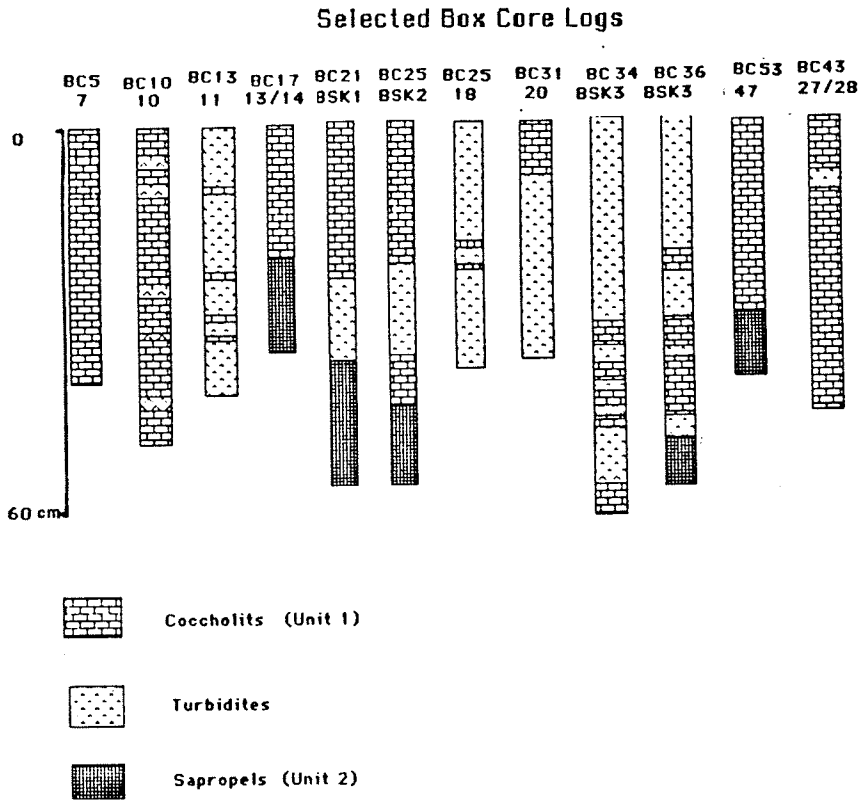

Fig. 2: Selected stratigraphic columns of box cores.

V. C. THE FIRST RECOVERY OF FLUFF LAYER FROM THE BLACK SEA BOTTOM; ONBOARD OBSERVATION

Susumu Honjo and James E. Broda

Introduction

A high sedimentation rate and a lack of bioturbation resulted in the preservation of the upper 50-100 cm of the recent sediments in the Black Sea (Ross and Degens, 1974). One of our objectives on this cruise was to recover a complete Unit 1 sequence (uppermost 30 cm; including the intact core top) to be able to correlate present-day water column fluxes with the most recent sedimentation in the Black Sea. The surface of Unit 1 was then to be examined to see if the hypothetical surface "fluff" layer does exist at the sediment/water interface. The first recovery of near-perfect water/sediment interface samples from the basin floor of the Black Sea using a Mark III box corer provided new and exciting discoveries and tentative explanations of the formation of varved sediments under the non-(animal)bioturbating, anaerobic deep ocean floor. In particular, the long-standing controversy over the existence and potential role of the "fluff layer" or benthic transition layer (Honjo et al., 1984) at the abyssal Black Sea, photographed by Vine (1984), is likely to be solved from results of this cruise.

Background

Recent studies on the vertical fluxes of particulate matter in the oceans indicate that energy and nutrients necessary for benthic metabolism are supplied by particles which settle with relatively high speed in the form of large collective masses, such as metazoan fecal pellets or so-called "marine snow" aggregates. Thus, the metabolic loss of labile matter within the abyssopelagic water column generally is not significant compared to the arrival rate at the benthic boundary (Honjo et al., 1984b). The surface productivity in the Black Sea is relatively large and aggregated particles should play a major role in the vertical sedimentation (e.g., V. Asper, cruise report section IV. H.). When such organic-rich settling particles are intercepted at the seafloor, they should accumulate at the sediment/water boundary (benthic boundary) for a period of time before the arrived material is consumed by benthic organisms unless the flux is equal or smaller than the rate of benthic consumption. These assumptions are only applicable in a non-erosional benthic environment; the anaerobic bottom of the abyssal Black Sea is all non-erosional except in areas of high turbidite deposition.

Objectives

The major questions were: How is the fluff material, if it exists, qualitatively and quantitatively related to the particle fluxes which were being measured by sediment traps in the Black Sea? Is there any difference between them in time and space? Without bioturbation, how is the organic matter in this fluff layer consumed at this boundary? The organic carbon content in Unit 1 (4%; Ross and Degens, 1974; Hay, 1988) is lower than in the water column particle flux collected with sediment traps previously in the southwestern Black Sea at mapsite BS. Then, what processes alter the newly arrived sediment, and who consumes, and at what rate, material on an anaerobic seafloor? Comparison of three critical components (settling particles, fluff, and underlying varved sediments) should provide answers for these important questions.

Successful recovery of an intact fluff layer - Methods

Between April 19 and April 29 evening, we deployed a Mark III box corer eight times with varying penetration speeds, and penetration depth adjustments, as well as with resisting plates attached in different configurations without success. All attempts resulted in considerable over-penetration through Unit 1 and part of Unit 2, except for one attempt which resulted in an almost-acceptable core which came up with a turbid water layer on top of the sediment.

In the early morning of April 30th at mapsite 47, (BC 53; 42°39.73N, 37°36.98E; see cruise report section III. Fig. 1 for location) at 2,154 m depth, the box core recovered a perfectly preserved water/sediment interface with a good part of Unit 1. This was the result of redistributing the resisting plates on the box corer. There was 8 cm of the water layer on top of the box core.

Onboard observations of the fluff layer - Results

1. The very water/sediment boundary observed in good box cores was covered by bacterial mats, with multiple colored scales with a diameter of one to a few centimeters and a thickness of half to one millimeter (Fig. 1). Most commonly, the water-facing surface of these individual scales were beige-colored to brownish-gray. Several scales on the 50x50 cm box core surface were conspicuous in being a brighter maroon or bluish-gray.

2. The vertical profile of the fluff showed several alternating laminae, relatively light and dark colored to charcoal grays, all within a few centimeters. The scales or mats were piled into the uppermost few millimeters but the scales gradually disappeared into the lower sediment. In the upper sediment, the dark laminae were generally thicker than the light colored laminae, but this relationship reversed in the lower part of the fluff layer.

3. The dark laminae became thinner with increasing depth and the light-colored laminae became paler or "bleached." Within a few centimeters downcore, the dark- and light-colored laminae became a couplet of a well-demarcated thin, black lamina and a relatively thick, white lamina. Thus, the transition from the fluff layer to the characteristic upper Unit 1 sequence appears to be continuous. There were several layers of darker and lighter laminae in the fluff layer.

4. We observed the relationship mentioned above in a few good box cores subsequently taken from the west, central, and eastern Black Sea at various depths. We believe that observations 1 through 3 were applicable to most of the anaerobic sea floor in the Black Sea.

Tentative explanation of fluff formation - Discussion

A full explanation of these shipboard observations on the benthic boundary layer and the implications on the formation of Unit 1 sequences must wait until relevant laboratory analysis are completed. Following is a preliminary interpretation, based on the onboard observations.

First, as suspected, vigorous benthic metabolic processes were displayed by the well-developed anaerobic bacteria mats at the water/sediment interface of the deep Black Sea. However, rates of bacteria production and metabolic consumption are not known and warrant further study. Second, it is suggested that a varved sequence is formed in several years from continuously supplied settling particles.

As previously published, the annual sequence of flux observed at a southwestern Black Sea site (Site BS) showed 3 sedimentary phases in terms of the variability of the constituents of the new sediment (Honjo et al., 1987). These sedimentary phases were not observed at a second sediment trap site further offshore (Site BSC). Site BSC is probably more characteristic of sedimentation in the abyssal Black Sea, since the sedimentation is not as influenced by direct input of particulate matter from rivers and shelf resuspension (Hay et al., in press). The particle flux in spring is controlled by diatom blooms whereas the particle flux during summer and fall is dominated by a bloom of the coccolithophorid species Emiliania huxleyi. The organic carbon flux at site BS is highest during summer/fall due a higher lithogenic component in the particle flux in winter/spring. At site BSC, the organic carbon flux is highest during the bloom periods.

The particulate matter of the sediment trap samples from the previous feasibility studies at site BS and BSC did not reveal any characteristic lighter or darker colors that would correspond to the light and dark laminae in the bottom sediment. Known at present is that the dark laminae contain mostly terrigenous matter while the light laminae contain mostly coccoliths (e.g. Ross and Degens, 1974; Hay, 1988). The high concentration of terrigenous matter in the black laminae is probably due

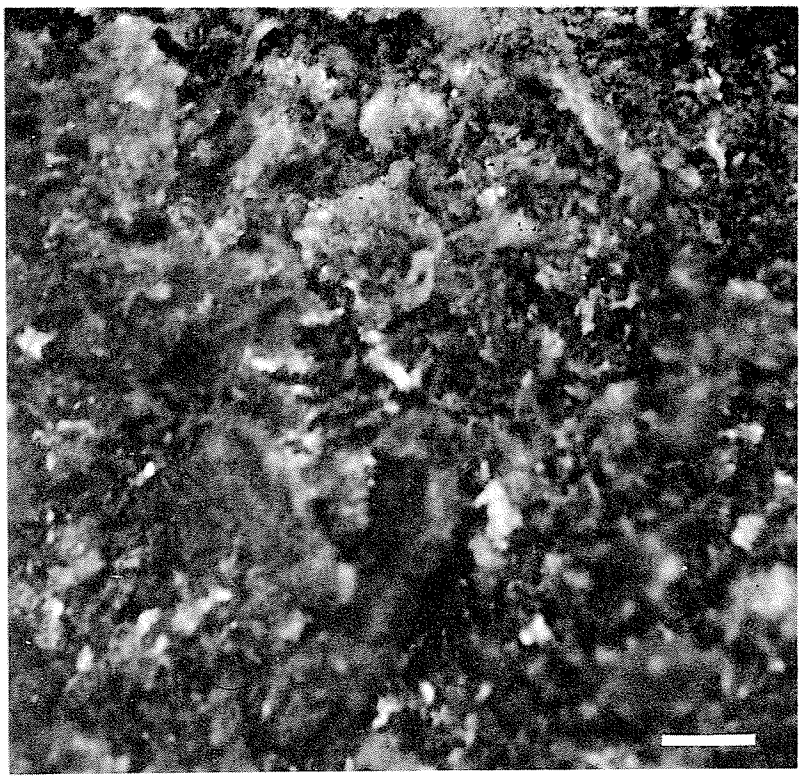

Figure 1. Photograph of well-preserved fluff layer in a box-core sample, taken through about 5 cm of water immediately after recovery.

to relative enrichment of terrigenous matter as a result of dissolution of biogenic silica after the spring bloom (Hay and Honjo, in press), making this lamina thinner and thinner near the sediment surface (Fig. 2). Organic constituents in the particle flux are consumed by metabolic consumption of the labile matter by anaerobic bacteria; however, organic carbon alone does not appear to have triggered the coloration of the dark laminae since organic carbon is deposited during all blooms (Honjo et al., 1987; Hay et al., in press). The cause for the coloration may instead be sought in biochemical processes on the basin floor related either 1) to the presence and subsequent dissolution of the biogenic silica, or 2) to biochemical processes that occur at the sediment/water interface temporally simultaneous with the high biogenic silica flux (spring). After completion of these processes, a thin well-defined black film substance remains, which may be a combination of refractory organic matter and iron-sulfur compounds. However, a better, scientifically-based solution of the intriguing question of the mechanism for the coloration of the black laminae certainly will have to await detailed biogeochemical analyses of the fluff layer in the laboratory.

Figure 2. Illustration of the tentative explanation of the formation of black-and-white couplets in the recent anaerobic sediments (Unit 1) in the abyssal part of the Black Sea basin.

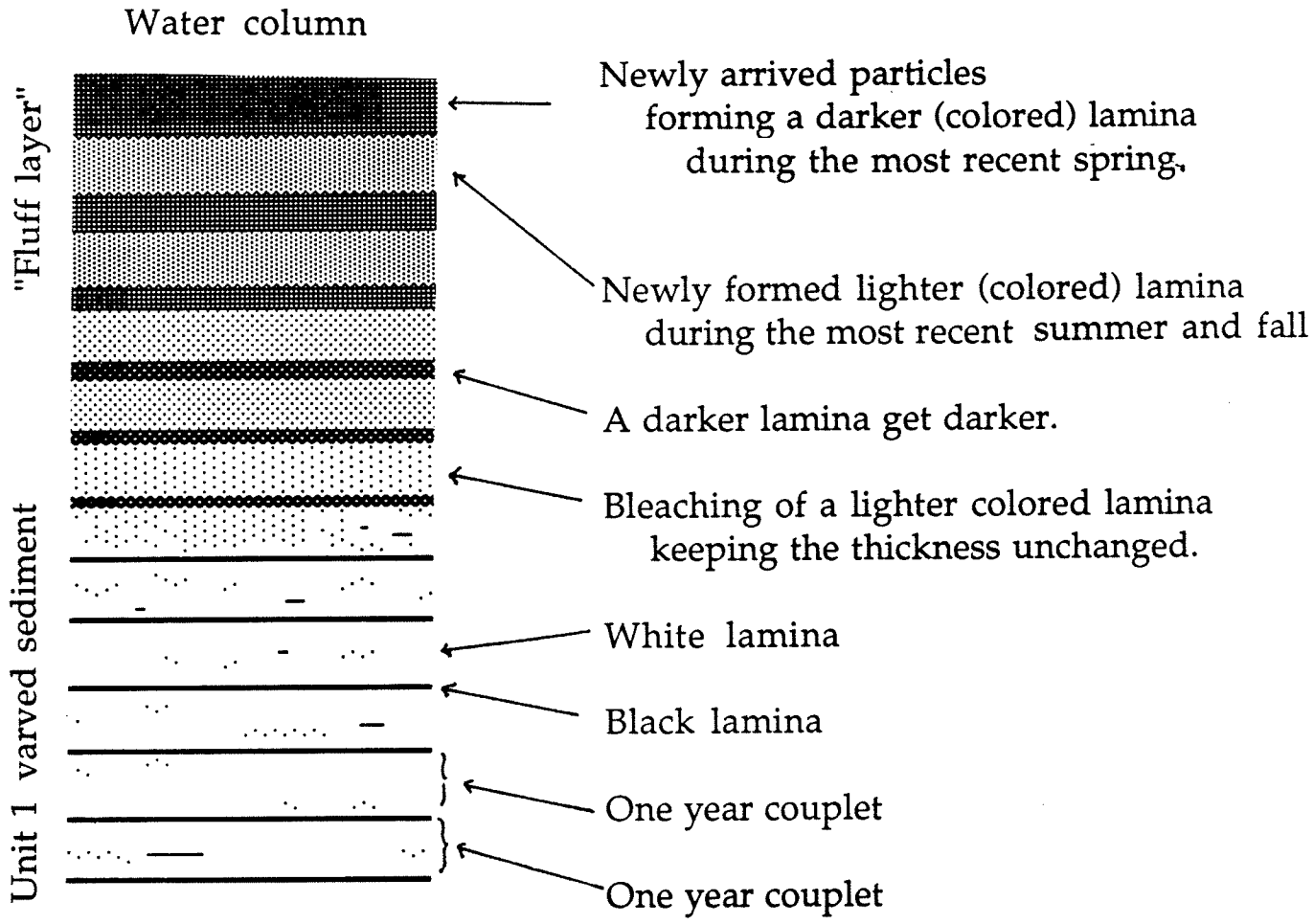

V. D. COMPOSITION OF SURFACE SEDIMENT

Cynthia H. Pilskaln

Introduction

Samples of the surface fluff material and the underlying top 1 1/2 cm of sediment were routinely collected from each box core in order to determine what types of particle aggregates were present (planktonic fecal pellets, etc.) and to complete a preliminary description of the surface sediment and fluff composition in terms of particle size, biogenic, and mineral components. Due to the lack of biological activity at the anoxic benthic boundary layer in the Black Sea, particle aggregates produced in the overlying water column, such as planktonic fecal pellets, should be present in the surface sediments, thus representing an important mechanism by which various biogeochemical components are delivered to the benthos and incorporated into the sediment record.

Methods

Approximately 100-200 cm^3 of the undisturbed fluff layer collected in the box cores were sampled with disposable 50 cm^3 syringes. Scrape samples amounting to 150-450 cm^3 of the upper 1 1/2 cm of surface sediment directly beneath the fluff layer were collected with a spatula. Half of each fluff and sediment sample was immediately fixed with 4% buffered formalin and placed in a refrigerated van (9°C) as archive samples. The other half of each sample collected was gently wet sieved using filtered sea water, with a number of duplicate samples being filtered with distilled water to check for any marked difference in the physical condition of the particulates when filtered with water of low ionic strength. All samples were sieved through plastic sieves fitted with disposable Nylon mesh of sizes 500 μm, 250 μm, 125 μm, and 63 μm. Following completion of the sieving process, the coarsest sediment fractions (> 500 μm and 500-250 μm) were examined in petri dishes with a hand lens (10x) and a light microscope (50x, 220x, and 475x magnification) for particulate identification. Smear-slides were also made for all size fractions and viewed under the microscope to assess composition. All sediment size fractions were fixed with 4% buffered formalin and stored in the refrigerated van following completion of the above procedures. The box cores from which samples were analyzed in the above manner during Leg 1 were: BC 10, 17, 21, 25, 31, 34, 43, 53, 55, and 58 (for locations, see Fig. 1, cruise report section V.A.).

Preliminary Results

The preliminary analysis of the Black Sea surface sediment composition provides some new and intriguing findings:

1) Intact planktonic fecal pellets form a major component of the larger than 500 μm fraction of the surface sediments in the Black Sea (Table 1). The rare occurrence of whole pellets in the fluff layer but their abundance in the sediment directly beneath this layer, indicates that they settle through the fluff layer to become incorporated into the surface sediments. This finding is significant in light of the fact that we do not find planktonic fecal pellets in the surface sediments of deep-sea, oxic benthic boundary layers due to the rapid remineralization of the organic-rich pellets by various micro- and macro-fauna at the sediment/water interface.

2) The fecal pellets collected in the surface sediments of the Black Sea are packed with coccoliths, suggesting that they represent a significant mode of vertical transfer of coccoliths from the water column to the sediments.

3) The common occurrence of coccolith flocs (0.1-2 mm in size) found in the coarse fraction of the fluff and in the top 1 1/2 cm of surface sediments (Table 1), and the abundance of 2-3 mm-sized, mucus-bound, lithogenic-rich flakes in the fluff layer, represent two other classes of large particulates besides planktonic fecal pellets which appear to play an important role in the flux of material in the Black Sea.

4) The presence of abundant opaline silica material in the surface sediments, in the form of diatom tests and silicoflagellate skeletons, has important implications for the remineralization rates of biogenic silica at the sediment/water interface. Such rates must be relatively high as we observe the nearly complete disappearance of opaline skeletal material within the first few centimeters of the Black Sea sediment record.

Table 1: Preliminary results of the composition of the surface sediment.

Key: E.A. = Extremely abundant
C = Common
R = Rare
N.O. = Not observed

Major sedimentary components

		Mucus-bound clay-rich flakes (2-3 mm)	Whole fecal pellets	Broken pellets/small organic aggregates	Coccolith flocs	Fish scales/bones	Large single centric diatoms	Silicoflagellates	Tintinnids	Single coccoliths	Individual clay grains
Fluff layer	> 500 µm	E.A.	R	C	E.A.	C	N.O.	N.O.	N.O.	N.O.	N.O.
	500-250 µm	N.O.	R	C	E.A.	R	N.O.	N.O.	N.O.	N.O.	N.O.
	250-125 µm	N.O.	R	C	C	N.O.	C	R	N.O.	N.O.	N.O.
	125-63 µm	N.O.	R	C	C	N.O.	C	R	N.O.	N.O.	C
	< 63 µm	N.O.	N.O.	N.O.	R	N.O.	R	N.O.	N.O.	E.A.	E.A.
Surface sediment	> 500 µm	N.O.	E.A.	C	C/E.A.	C	N.O.	N.O.	N.O.	N.O.	N.O.
	500-250 µm	N.O.	C	E.A.	C	R	R	N.O.	N.O.	N.O.	N.O.
	250-125 µm	N.O.	R	E.A.	C	N.O.	E.A.	R	N.O.	N.O.	R
	125-63 µm	N.O.	R	C	C	N.O.	E.A.	C	C	N.O.	C
	< 63 µm	N.O.	N.O.	N.O.	R	N.O.	R	N.O.	N.O.	E.A.	E.A.

V. E. POREWATER ANALYSIS

Gerd Liebezeit

Introduction

The chemical composition of marine sediments and their interstitial waters reflects a number of interconnected processes. These include source and time-related effects, as well as biological activity at the sediment/water interface and in the upper sediment layers. The resulting signal obtained from chemical analysis is hence the result of a complex array of interactions and therefore difficult to interpret in a straightforward way without additional information.

In the Black Sea, biological activity in the sediment is non-existent except for anaerobic bacterial metabolism. Furthermore, the high sedimentation rates prevent time-related processes from occurring. Thus, the chemical composition becomes largely controlled by the source function.

Method

A number of box cores were subsampled using an 8 cm i.d. perspex liner. Compaction of about 20-30% occurred during subsampling. This has been corrected in the data presented here assuming uniform compaction over the whole core length. Generally, 2 cm slices were analyzed. Sediment samples awaiting processing were stored and refrigerated in sealed PE bags. Interstitial water was obtained by squeezing (3.5 bar nitrogen overpresser, 0.45 µm cellulose acetate filters). To minimize a carryover between samples, the first few ml of each sample was discarded. Reactive and total dissolved phosphate (RDP, TDP) and silicic acid were determined onboard using standard nutrient methods. All samples were analyzed in triplicate whenever sample volume permitted.

The remaining samples were sealed in glass ampoules for future determinations of other components (chloride, fluoride, manganese, iron, dissolved organic carbon, amino acids, humic compounds).

Results and Preliminary Interpretation

1) In most box core profiles, silicic acid decreased with depth although some variability was observed (Figs. 1 and 2). Turbidite layers generally had considerably lower contents than varved sediments.

2) Both total dissolved phosphate (TDP) and reactive dissolved phosphate (RDP) were found to be highly variable in their profiles with no

apparent differences between varved and turbidite sequences. An overall general trend was not observed although tendencies towards either decreasing or increasing concentrations with depth could be seen.

3) The box core results are thus somewhat contrary to expectations. Since 2 cm slices were analyzed, the annual variability in input should have been averaged out, at least to a certain degree. Two possible explanations can be put forward: 1) dissolution of fish bone debris, and 2) formation of authigenic minerals or coatings.

4) Fish bones were encountered rather often in varved sediments. Dissolution of irregularly distributed specimens might well lead to the observed RDP profiles.

5) Mineral formation should lead to more uniform profiles unless it is controlled by other equally irregularly distributed components.

6) With the data at hand, no further interpretation of the depth profiles can be offered. Solid phase analyses of squeezed sediments for phosphorus compounds and biogenic opal have to be carried out to shed more light on the processes operating in modern Black Sea sediments.

7) In addition to box core subsamples, two gravity cores were sampled for porewater analysis. Sampling was either done in 5 cm slices or according to stratigraphy. GGC 66 was analyzed onboard (Fig. 2) whereas GGC 71 was sampled only.

8) Stratigraphic units are clearly discernible in silicic acid and RDP/TDP profiles of GGC 66. Especially in its lower part, presumably deposited under freshwater conditions, extremely low concentrations were found. Again, solid phase analysis has to be done before further interpretation can be made.

Figure 1: Silicic acid ($Si(OH)_4$ and phosphate analyses in porewater samples collected from box cores.

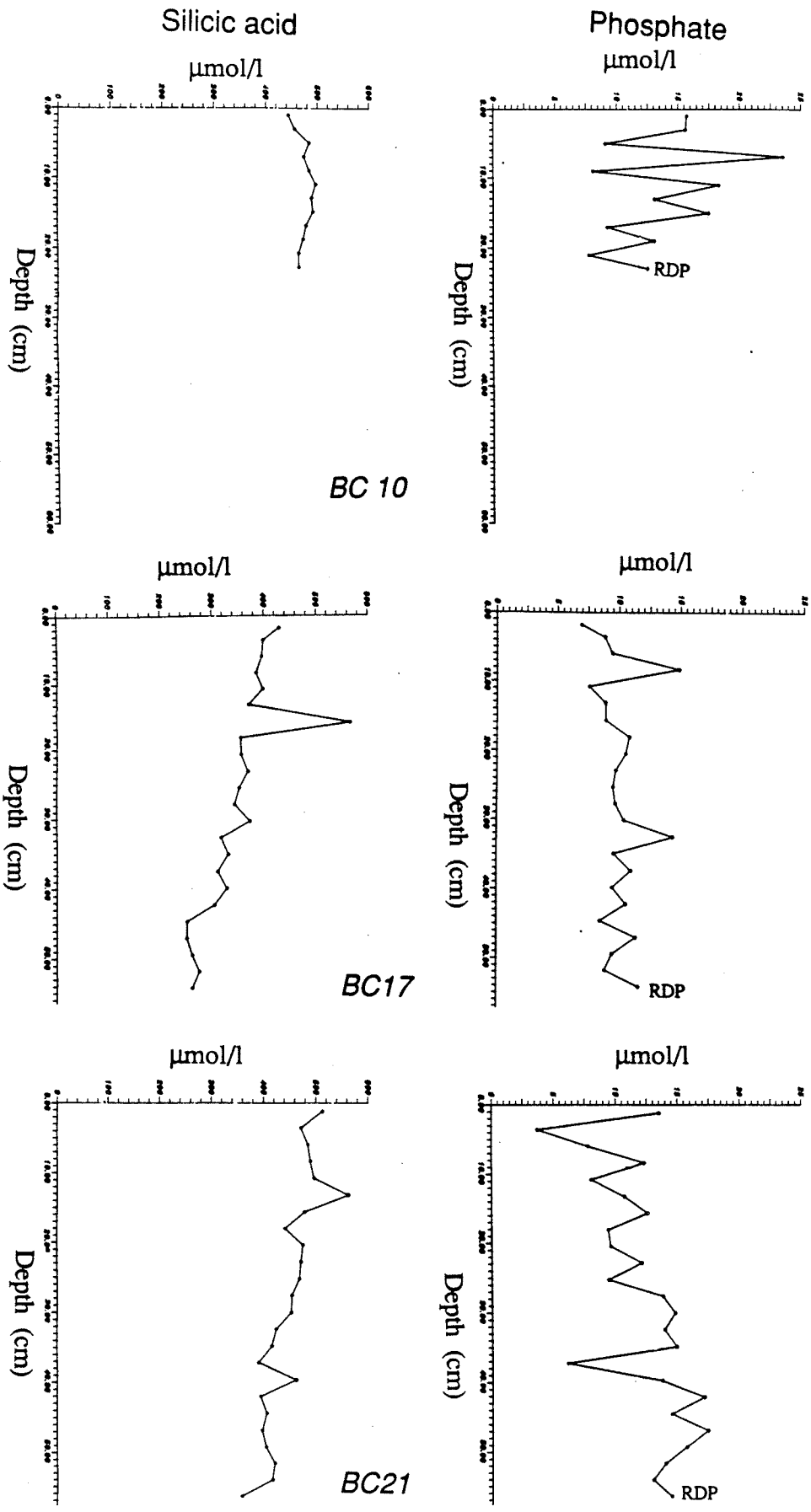

Figure 1: (cont.)

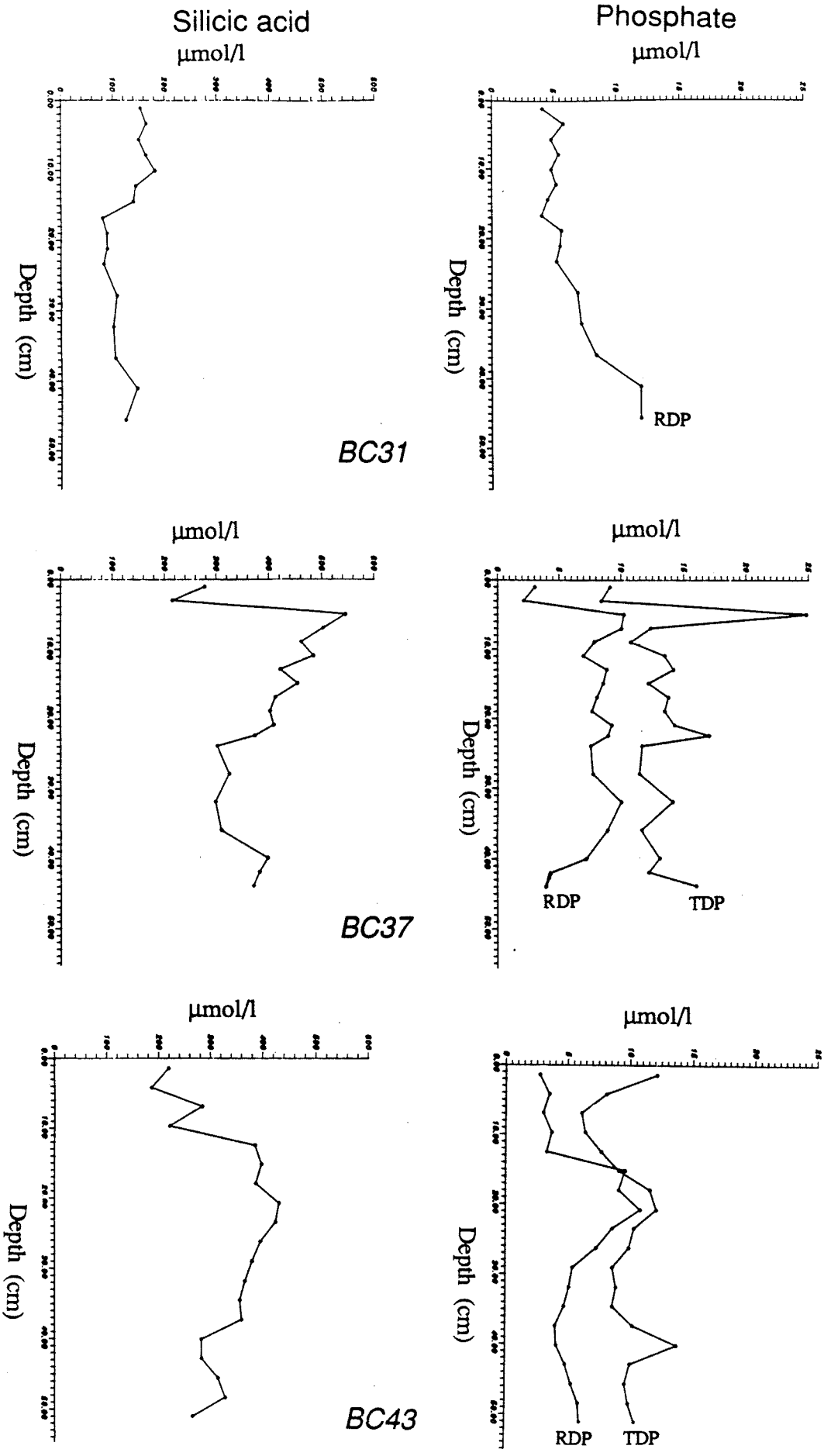

Figure 1: (cont.)

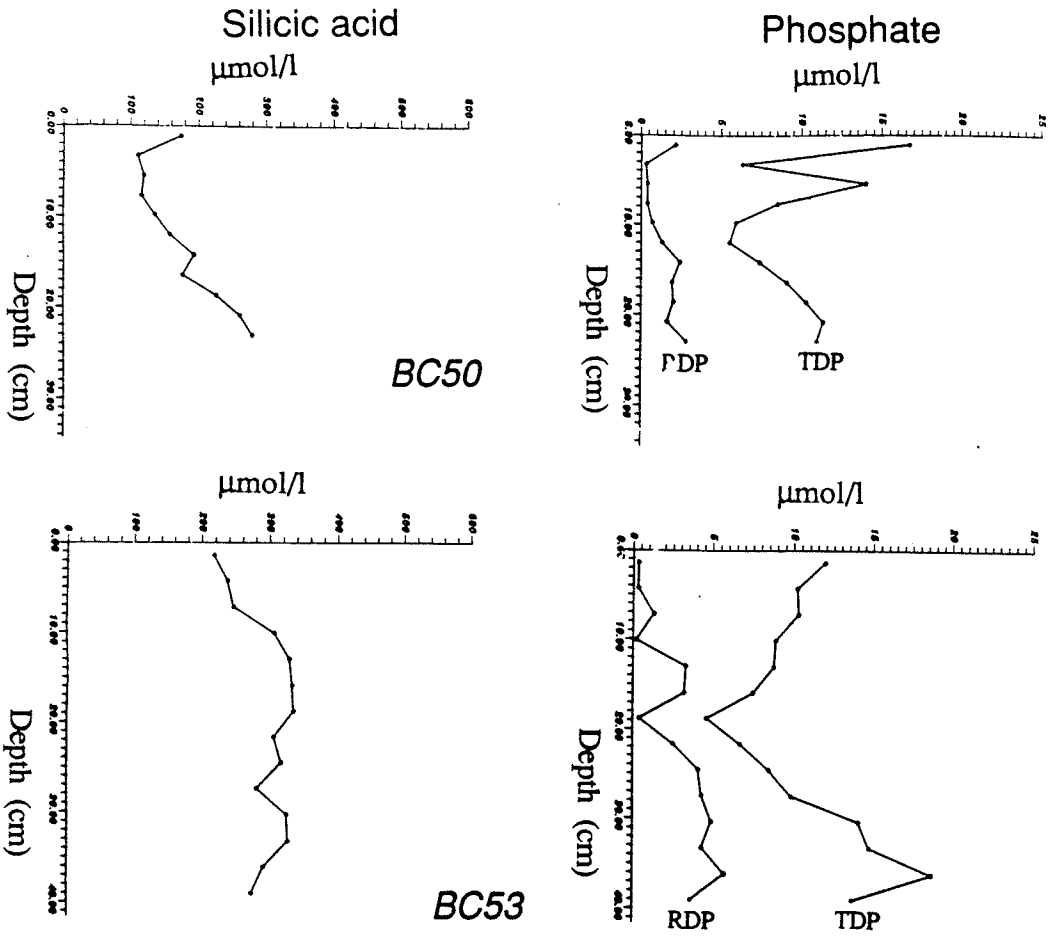

Figure 2: Silicic acid ($Si(OH)_4$ and phosphate analyses in porewater samples collected from gravity core GGC66.

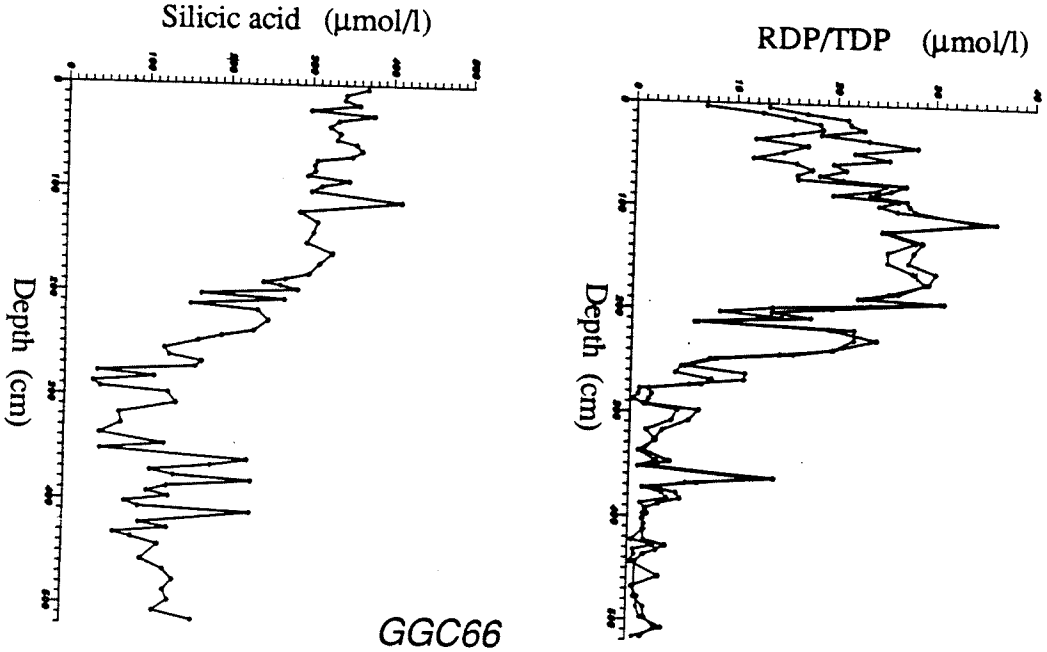

VI. REFERENCES

Anderson, R.Y. and D.W. Kirkland, 1966. Intrabasin varve correlation. GSA Bulletin, 27: 241-256.

Benli, H., 1987. Investigation of plankton distribution in the southern Black Sea and its effect on particle flux. In: Particle Flux in the Ocean, E.T. Degens, E. Izdar, and S. Honjo, editors, Mitteilungen des Geologisch-Palaeontologischen Institutes, Universität Hamburg, 62: 77-87.

Brewer, P.G. and D.W. Spencer, 1974. Distribution of some trace elements in the Black Sea and their flux between dissolved and particulate phases. In: Degens, E.T. and D.A. Ross, eds., 1974, The Black Sea - Geology, Chemistry, and Biology, Am. Assoc. Petr. Geol., Mem. 20: 137-143.

Briskin, M., J. Robins, W.R. Riedel, and R. Booker, 1986. Magnetic resonance imaging analyses of varved marine sedimentary records of the Gulf of California. Geophysical Research Letters, 13: 753-756.

Buesseler, K.O., H.D. Livingston, S. Honjo, B.J. Hay, S.J. Manganini, E.T. Degens, V. Ittekkot, E. Izdar, and T. Konuk, 1987. Chernobyl radionuclides in a Black Sea sediment trap: A preliminary report. Nature, 329: 825-828.

Bukry, D., 1974. Coccoliths as paleosalinity indicators - evidence from the Black Sea. In: Degens, E.T. and D.A. Ross, eds., 1974, The Black Sea - Geology, Chemistry, and Biology, Amer. Assoc. Petr. Geol., Mem. 20: 353-363.

Bukry, D., S.A. King, M.K. Horn, and F.T. Manheim, 1970. Geological significance of coccoliths in fine-grained carbonate bands of postglacial Black Sea sediments. Nature, 226: 1586-1587.

Calvert, S.E., J.S. Vogel, and J.R. Southon, 1987. Carbon accumulation rates and the origin of the Holocene sapropel in the Black Sea. Geology, 15: 918-921.

Degens, E.T. and D.A. Ross, eds., 1974. The Black Sea - Geology, Chemistry, and Biology. Amer. Assoc. Petr. Geol., Mem. 20, 633 pp.

Degens, E.T. and P. Stoffers, 1976. Stratified waters as a key to the past. Nature, 263: 22-26.

Degens, E.T., W. Michaelis, C. Garrasi, K. Mopper, S. Kempe, and V.A. Ittekkot, 1978. Warven-Chronologie und frühdiagenetische Umsetzungen organischer Substanzen holozäner Sedimente des Schwarzen Meeres. Neues Jahrbuch Geologisch-Palaeontologische Monatshefte, 5: 65-86.

Degens, E.T., V.A. Ittekkot, S. Kempe, V.L. Asper, and S.J. Manganini, 1984. Sedimentation mariner Schwebstoffe, untersucht mit Hilfe von Sedimentfallen. Unpublished progress report, Universität Hamburg, 30 pp.

Deuser, W.G., 1974. Evolution of anoxic conditions in the Black Sea during the Holocene. In: Degens, E.T. and D.A. Ross, eds., 1974, The Black Sea - Geology, Chemistry, and Biology, Amer. Assoc. Petr. Geol., Mem. 20: 133-136.

Finenko, Z.Z., 1967. Primary production in southern seas. In: Problems of Bio-oceanography, V.A. Vodianitskii, ed., Naukova dumka: 5-68 (Kiev, USSR).

Fonselius, S.H., 1974. Phosphorus in the Black Sea. In: Degens, E.T. and D.A. Ross, eds., 1974, The Black Sea - Geology, Chemistry, and Biology, Am. Assoc. Petr. Geol. Mem. 20: 144-150.

Glenn, C.R. and M.A. Arthur, 1985. Sedimentary and geochemical indicators of productivity and oxygen contents in modern and ancient basins: The Holocene Black Sea as the "type" anoxic basin. Chemical Geology, 48: 325-354.

Hay, B.J., 1987. Particle flux in the western Black Sea in the present and over the last 5000 years: Temporal variability sources, transport mechanisms. Ph.D. Thesis, WHOI-87-44, Joint Program, Massachusetts Institute of Technology/Woods Hole Oceanographic Institution, 201 pp.

Hay, B.J., 1988. Sediment accumulation in the central western Black Sea over the past 5100 years. Paleoceanography, 3(4) (in press).

Hay, B.J., and S. Honjo. Seasonal particle sources for varve formation in recent Black Sea sediments (submitted to Nature, 1988).

Hay, B.J., S. Honjo, S. Kempe, K.-C. Emeis, and T. Konuk. Interannual variability in particle fluxes in southwestern Black Sea at a nearshore and an offshore sediment trap site (submitted to Deep-Sea Research, 1988).

Honjo, S., 1980. Material fluxes and modes of sedimentation in the mesopelagic and bathypelagic zones. Journal of Marine Research, 38: 53-97.

Honjo, S., 1982. Seasonality and interaction of biogenic and lithogenic particulate flux at the Panama Basin. Science, 218: 883-884.

Honjo, S., K.W. Doherty, Y.C. Agrawal, and V.L. Asper, 1984a. Direct optical assessment of large amorphous aggregates (marine snow) in the deep ocean. Deep-Sea Research, 31: 67-76.

Honjo, S., S.J. Manganini, and J.J. Cole, 1984b. Sedimentation of biogenic matter in the deep ocean. Deep-Sea Research, 29: 609-625.

Honjo, S., B.J. Hay, S.J. Manganini, V.L. Asper, E.T. Degens, V.A. Ittekkot, E. Izdar, T. Konuk, and H.A. Benli, 1987. Seasonal cyclicity of lithogenic particle fluxes at a southern Black Sea sediment trap station. In: Particle flux in the Ocean, E.T. Degens, E. Izdar, and S. Honjo, eds., Mitteilungen des Geologisch-Palaeontologischen Institutes, Universität Hamburg, 62: 19-40.

Honjo, S., S.J. Manganini, V.L. Asper, B.J. Hay, and A.L. Karowe, 1988. Particle fluxes, south central Black Sea: 1982-1985 (Black Sea Sedimentation Data File, vol. 1). Woods Hole Oceanographic Institution Technical Report WHOI-88, and Piri Reis International Contribution Series Publ. No. 4, 106 pp. (in press).

Izdar, E., T. Konuk, V.A. Ittekkot, S. Kempe, and E.T. Degens, 1987. Particle flux in the Black Sea: Nature of the organic matter. In: Particle flux in the Ocean, E.T. Degens, E. Izdar, and S. Honjo, editors, Mitteilungen des Geologisch-Palaeontologischen Institutes, Universität Hamburg, 62: 1-18.

Lebedeva, L.P., and S.V. Vostokov, 1984. Studies of detritus formation processes in the Black Sea. Oceanology, 24: 258-263.

Morozova-Vodyanitskaya, 1948. Phytoplankton in the Black Sea. I. Phytoplankton in the Sevastopol area and survey of phytoplankton in the Black Sea. Sevastopol Biol. Station Trudy, 6: 39-172.

Müller, G., and P. Stoffers, 1974. Mineralogy and Petrology of Black Sea sediments.20: 200-248.

Nicholson, J.A.M., S. Honjo, B.J. Hay, R.W. Howarth, and J.C. Cisne. Particulate fluxes of reduced sulfur, iron, and organic carbon in the Black Sea (Site BSC) using time-series sediment traps. Submitted to Deep-Sea Research.

Pyzik, G.K., 1968. Studies of phytoplankton in the Black Sea from 1953-1963. In: Biological Studies of the Black Sea, Nauka, Moskow, pp. 30-39 (in Russian).

Ross, D.A., E.T. Degens, and J. MacIlvaine, 1970. Black Sea: Recent sedimentary history. Nature, 170: 163-165.

Ross, D.A. and E.T. Degens, 1974. Recent sediments of the Black Sea. In: E.T. Degens and D.A. Ross, eds., The Black Sea - Geology, Chemistry, and Biology, Amer. Assoc. Petr. Geol. Mem. 20: 183-199.

Ross, D.A., Neprochnov, Y.P., et al., 1978. Initial Reports of the Deep Sea Drilling Project, v. 42, Part 2, Washington, D.C., U.S. Government Printing Offices.

Roukhiyainen, M.I., 1975. On the seasonal dynamics of phytoplankton in the Black Sea. In: Biology of the Sea, Naukova dumka, Kiev: 3-15 (in Russian).

Shimkus, K.M. and E.S. Trimonis, 1974. Modern sedimentation in the Black Sea. In: The Black Sea - Geology, Chemistry, and Biology, E.T. Degens and D.A. Ross, eds., Amer. Assoc. of Petr. Geol. Mem. 20: 249-278.

Sorokin, Yu.I., 1982. The Black Sea. In: B.H. Ketchum, ed., Estuaries and Enclosed Seas, Ecosystems of the World, 26: 253-292, Elsevier Sci. Publ., New York.

Tambiev, S.B., 1987. New data on the constituents and chemical composition of the suspended and freely sinking particulate matter in the Black Sea waters. In: Particle flux in the Ocean, E.T. Degens, E. Izdar, and S. Honjo, eds., Mitteilungen des Geologisch-Palaeontologischen Institutes, Universität Hamburg, 62: 41-54.

Vine, A.C., 1974. Bottom Photographs of Black Sea. In: Degens, E.T. and D.A. Ross, eds., 1974, The Black Sea - Geology, Chemistry, and Biology, Amer. Assoc. Petr. Geol. Mem. 20: 338-346.

VII. LIST OF PARTICIPANTS

R/V Knorr, Cruise 134, Leg 8
April 16 to May 7, 1988

Algan, Oya
Atakoy 3, Kisim 06/2
Bakirkoy, Istanbul, Turkey
Tel.: 90 (57) 28798

Arthur, Michael, Dr., Co-Chief Scientist
Graduate School of Oceanography
University of Rhode Island
Narragansett, Rhode Island 02882
Tel.: (401) 792-6867

Asper, Vernon, Dr.
Center for Marine Sciences
University of Southern Mississippi
Building 1105, NSTL, MS 39529 USA
Tel.: (601) 688-3178
Telemail: USM.CMS

Benli, Huseyin, Dr.
Inst. of Marine Science & Technology
Dokuz Eylül University
Konak, Izmir, Turkey
Tel.: 90 (51) 254 4328

Bilgic, Tayfun
General Directorate of Mineral
Research and Exploration (MTA)
Geological Department
Balgat, Ankara, Turkey
Tel.: 90 (4) 223 4255, ext. 433
(Home): 90 (4) 319 2738

Briskin, Madeleine, Dr.
Department of Geology
University of Cincinnati
Cincinnati, Ohio 45221 USA
Tel.: (513) 475-3732

Broda, James
Woods Hole Oceanographic Institution
Woods Hole, Massachusetts 02543 USA
Tel.: (508) 548-1400, ext. 2513
Telemail: WHOI.GEOL.GEOPH

Dean, Walter, Dr.
Office of Energy and Marine Geology
Branch of Sedimentary Processes
U.S. Geological Survey
P.O. Box 25046, Denver, CO 80225 USA
Tel., (303) 236-1644

Degens, Egon, T., Dr. (Izmir to
Geol.-Paleonto. Inst. Istanbul)
University of Hamburg
Bundesstrasse 55
D-2000 Hamburg 13, FRG
Tel.: 49 (40) 4123-4992
Telemail: S.KEMPE

Derman, A. Sami
Turkish Petroleum Corp.
Madafaa Cad. No. 22/9
Bakanliklar, Ankara, Turkey
Tel.: 90 (4) 117 9160, ext. 593
(Home) 90 (4) 180 1775

Diercks, R. Arne
Geol.-Paleont. Institute
University of Hamburg
Bundesstrasse 55
D-2000 Hamburg 13, FRG
Tel.: 49 40 4123-5234
Telemail: S.KEMPE

Duman, Muhammed
Inst. of Marine Science & Technology
Dokuz Eylül University
Konak, Izmir, Turkey
Tel.: 90 (51) 254 4328

Gagnon, Alan
Woods Hole Oceanographic Institution
Woods Hole, Massachusetts 02543 USA
Tel.: (508) 548-1400, ext. 2513
Telemail: WHOI.GEOL.GEOPH

Hay, Bernward, Dr., Coordinator
Woods Hole Oceanographic Institution
Woods Hole, Massachusetts 02543 USA
Tel.: (508) 548-1400, ext. 2588
Telemail: S.HONJO

Honjo, Susumu, Dr., Chief Scientist
Woods Hole Oceanographic Institution
Woods Hole, Massachusetts 02543 USA
Tel.: (508) 548-1400, ext. 2589
Telemail: S.HONJO

Izdar, Erol, Dr. (Izmir to Istanbul)
Inst. of Marine Science & Technology
Dokuz Eylül University
Konak, Izmir, Turkey
Tel.: 90 (51) 254 4338

Kempe, Stephan, Dr.
Geol.-Paleont. Institute
University of Hamburg
Bundesstrasse 55
D-2000 Hamburg 13
Tel.: 49 (40) 4123 5234
Telemail: S.KEMPE

Konuk, Y. Tosun, Dr.
Inst. of Marine Science & Technology
Dokuz Eylül University
Konak, Izmir, Turkey
Tel.: 90 (51) 254328

Liebezeit, Gerd, Dr.
Geol.-Paleont. Institute
University of Hamburg
Bundesstrasse 55
D-2000 Hamburg 13, FRG
Tel.: 49 (40) 4123 5235
Telemail: S.KEMPE

Lobsiger, Urich, Dr. (Izmir to Istanbul)
Lobsiger Associates, Inc.
1127 Barrington St. (P.O. Box 3008 S)
Halifax, Nova Scotia, Canada B3J 3G6
Tel.: (902) 429-0283

Neff, Eric D.
Graduate School of Oceanography
University of Rhode Island
Narragansett, Rhode Island 02882 USA
Tel.: (401) 792-6867

Nicholson, Jo Ann
Department of Geology
Cornell University
Ithica, New York 14853 USA
Tel.: (607) 255-3698

Pilskaln, Cynthia H., Dr.
Monterey Bay Aquarium Research
Institute (MBARI)
160 Central Avenue
Pacific Grove, CA 93950 USA
Tel.: (408) 647-3719
Telemail: C.PILSKALN

Realander, Michael
University of Washington
School of Oceanography
Marine Science Buildign WB-10
Seattle, Washington 98125
Tel.: (206) 543-5186
Telemail: J.MURRAY

Woodward, Bonnie L.
Woods Hole Oceanographic Institution
Woods Hole, Massachusetts 02543 USA
Tel.: (508) 548-1400, ext. 2824
Telemail: S.HONJO

DOCUMENT LIBRARY

August 9, 1988

Distribution List for Technical Report Exchange

Attn: Stella Sanchez-Wade
Documents Section
Scripps Institution of Oceanography
Library, Mail Code C-075C
La Jolla, CA 92093

Hancock Library of Biology &
Oceanography
Alan Hancock Laboratory
University of Southern California
University Park
Los Angeles, CA 90089-0371

Gifts & Exchanges
Library
Bedford Institute of Oceanography
P.O. Box 1006
Dartmouth, NS, B2Y 4A2, CANADA

Office of the International
Ice Patrol
c/o Coast Guard R & D Center
Avery Point
Groton, CT 06340

Library
Physical Oceanographic Laboratory
Nova University
8000 N. Ocean Drive
Dania, FL 33304

NOAA/EDIS Miami Library Center
4301 Rickenbacker Causeway
Miami, FL 33149

Library
Skidaway Institute of Oceanography
P.O. Box 13687
Savannah, GA 31416

Institute of Geophysics
University of Hawaii
Library Room 252
2525 Correa Road
Honolulu, HI 96822

Library
Chesapeake Bay Institute
4800 Atwell Road
Shady Side, MD 20876

MIT Libraries
Serial Journal Room 14E-210
Cambridge, MA 02139

Director, Ralph M. Parsons Laboratory
Room 48-311
MIT
Cambridge, MA 02139

Marine Resources Information Center
Building E38-320
MIT
Cambridge, MA 02139

Library
Lamont-Doherty Geological
Observatory
Colombia University
Palisades, NY 10964

Library
Serials Department
Oregon State University
Corvallis, OR 97331

Pell Marine Science Library
University of Rhode Island
Narragansett Bay Campus
Narragansett, RI 02882

Working Collection
Texas A&M University
Dept. of Oceanography
College Station, TX 77843

Library
Virginia Institute of Marine Science
Gloucester Point, VA 23062

Fisheries-Oceanography Library
151 Oceanography Teaching Bldg.
University of Washington
Seattle, WA 98195

Library
R.S.M.A.S.
University of Miami
4600 Rickenbacker Causeway
Miami, FL 33149

Maury Oceanographic Library
Naval Oceanographic Office
Bay St. Louis
NSTL, MS 39522-5001

Marine Sciences Collection
Mayaguez Campus Library
University of Puerto Rico
Mayagues, Puerto Rico 00708

50272-101

REPORT DOCUMENTATION PAGE	1. REPORT NO. WHOI-88-35	2.	3. Recipient's Accession No.

4. Title and Subtitle

Temporal and Spatial Variability in Sedimentation in the Black Sea: Cruise Report R/V *Knorr* 134-8, Black Sea Leg 1, April 16 - May 7, 1988

5. Report Date: September 1988

6.

7. Author(s)

S. Honjo, B.J. Hay, and members of the scientific shipboard party

8. Performing Organization Rept. No.: WHOI-88-35

9. Performing Organization Name and Address

The Woods Hole Oceanographic Institution
Woods Hole, Massachusetts 02543

10. Project/Task/Work Unit No.

11. Contract(C) or Grant(G) No.
(C)
(G)

12. Sponsoring Organization Name and Address

The National Science Foundation

13. Type of Report & Period Covered: Technical Report

14.

15. Supplementary Notes

This report should be cited as: Woods Hole Oceanog. Inst. Tech. Rept., WHOI-88-35, and Piri Reis International Contr. Ser. #6.

16. Abstract (Limit: 200 words)

This document represents the cruise report of the highly successful Leg 1 of the R/V *Knorr* cruise to the Black Sea (Cruise 134-8) as a joint Turkish-American Oceanographic Expedition (Izmir to Istanbul, April 16 to May 7, 1988).

The focus of Leg 1 was to study the biogeochemical variability in sedimentation in the present and throughout the anoxic history of the Black Sea with high spatial and temporal resolution. In particular, this study involved the integrated study of water column fluxes (sediment traps, suspended sediment investigations, etc.), benthic boundary layer ("fluff layer"), and laminated bottom sediments (box cores, giant gravity cores). Highlights of the cruise included the collection of 62 giant gravity cores, and 30 box cores with perfectly laminated sediment and, for the first time ever, with the intact fluff layer. Three moorings with time-series sediment traps were deployed in the abyssal regions of the eastern, central, and western Black Sea to collect continuous samples over a time period of about 1 year and 3 months.

Summarized in the cruise report are logistics of the cruise, sample collections and descriptions, and preliminary discussions of observations and first measurements.

17. Document Analysis a. Descriptors

1. Black Sea
2. particle flux
3. laminated sediments

b. Identifiers/Open-Ended Terms

c. COSATI Field/Group

18. Availability Statement	19. Security Class (This Report)	21. No. of Pages
Approved for publication; distribution unlimited.	UNCLASSIFIED	156
	20. Security Class (This Page)	22. Price

(See ANSI-Z39.18) *See Instructions on Reverse*

OPTIONAL FORM 272 (4-77)
(Formerly NTIS-35)
Department of Commerce